creative commons
COMMONS DEED

저작자표시-비영리-변경금지 2.0 대한민국

이용자는 아래의 조건을 따르는 경우에 한하여 자유롭게

- 이 저작물을 복제, 배포, 전송, 전시, 공연 및 방송할 수 있습니다.

다음과 같은 조건을 따라야 합니다:

저작자표시. 귀하는 원저작자를 표시하여야 합니다.

비영리. 귀하는 이 저작물을 영리 목적으로 이용할 수 없습니다.

변경금지. 귀하는 이 저작물을 개작, 변형 또는 가공할 수 없습니다.

- 귀하는, 이 저작물의 재이용이나 배포의 경우, 이 저작물에 적용된 이용허락조건을 명확하게 나타내어야 합니다.
- 저작권자로부터 별도의 허가를 받으면 이러한 조건들은 적용되지 않습니다.

저작권법에 따른 이용자의 권리는 위의 내용에 의하여 영향을 받지 않습니다.

이것은 이용허락규약(Legal Code)을 이해하기 쉽게 요약한 것입니다.

Disclaimer

dCollection

이학박사학위논문

단자엽 식물에서의 브라시노스테로이드 생합성 및 신호전달 유전자의 기능 분석

Characterization of novel genes in brassinosteroid biosynthesis and signaling pathways in monocotyledonous plants

2017년 8월

서울대학교 대학원

생명과학부

Claudia Andrea Corvalán Bustos

ABSTRACT

Characterization of novel proteins in brassinosteroid biosynthesis and signaling pathways in monocotyledonous plants

Claudia Andrea Corvalán Bustos

Department of Biological Sciences

Graduate School

Seoul National University

Brassinosteroids (BRs) are growth-promoting hormones in plants that play important roles in plant architecture, and as a consequence plant yield, a subject of great agronomic interest. Components and mechanisms of BR responses have been elucidated mainly using the model dicotyledonous plant *Arabidopsis thaliana*, but interesting differences with monocotyledonous plants have been revealed after the increasing use of *Oryza sativa* (rice) for the study of BRs in grasses. These differences prompt the study of BRs directly in monocots and thus the development

of genomic resources and search for new tools. I joined the quest to find new ways to elucidate BR responses by studying plants with agronomic interest such as rice or model plants more closely related to cereal grasses. I first characterize the use of Propiconazole (Pcz) as a BR inhibitor for the use in field or large-scale experiments needed in monocots. Pcz treatments succeed to mimic BR-deficient mutant phenotypes on various monocot plants (i.e. maize, rice and Brachypodium), proving that its use was feasible. Using Pcz and available genomic and genetic tools I characterized the general response to BRs of the model grass *Brachypodium distachyon* and found several homologs genes from the BR signal (i.e. *BIN2*) and BR biosynthetic (i.e. *DWF4*, *CPD* and *BR6OX2*) pathways. Likewise, I used Pcz to screen a T-DNA mutant population in rice aimed to find new components of the BR response. From the screened lines, I further analyzed the denominate *propiconazole-resistant 1* (*pzr1-D*) which presented various BR-related phenotypes such as increase sensitivity to BR and grain yield when compared with wild-type plants. The gene affected by the mutation is likely to be a rice ortholog of Arabidopsis DPb, a transcription factor which dimerizes with E2F and together control transcription of proteins involved in cell division. The increment of PZR1 transcript levels by the T-DNA activation-tagging in *pzr1-D* mutants and PZR1 overexpressing lines produce more number of tiller, panicles, and panicle branches, all resulting in increased grain number compared with wild type. Plant phenotypes along with whole-transcriptome analysis present evidence that cell cycle and brassinosteroid signal may be linked through PZR1. Finally, as another tool for the study of BRs-related processes I developed and demonstrated the use of a specific

antibody anti BZR1, a key transcription factor and positive regulator of the BR signal. Anti-BZR1 antibody is able to detect active dephosphorylated and inactive phosphorylated forms of BZR1 in Arabidopsis and orthologs in rice, Setaria and Sorghum. In future, this antibody may be used to elucidate mechanisms in which the BZR1 is involved, specifically regarding its interaction with other proteins and the cross-talk between different plant signaling pathways.

Keyword: brassinosteroids, monocotyledonous, plant architecture, plant yield, cell cycle

Student Number: 2010-24008

TABLE OF CONTENTS

ABSTRACT…… i

CONTENTS……... iv

ABBREVIATION…… vii

LIST OF FIGURES…….. x

LIST OF TABLES…….. xiii

Chapter 1. General Introduction…….. 1

1-1. Brassinosteroids are growth-promoting hormones…… 2

1-2. Arabidopsis and brassinosteroids……... 4

1-3. Monocot plants and brassinosteroids……. 10

1-4. Brassinosteroids effects in monocot plants architecture…….. 19

1-5. Brassinosteroids and Regulation of the Cell Cycle…….. 24

1-6. BRASSINAZOLE-RESISTANT 1 (BZR1) as a key component of BR signaling pathway…….. 31

FIGURES AND TABLES……... 32

Chapter 2. Propiconazole Is a Specific and Accessible Brassinosteroid (BR) Biosynthesis Inhibitor for *Arabidopsis* and Maize…… 37

ABSTRACT…… 39

INTRODUCTION……... 40

MATERIALS AND METHODS…… 44

RESULTS ……... 48

DISCUSSION…….. 55

FIGURES AND TABLES……... 63

SUPPLEMENTAL INFORMATION……. 77

Chapter 3. Identification of Brassinosteroid Genes in *Brachypodium distachyon*…….. 79

ABSTRACT…… 81

INTRODUCTION……... 83

MATERIALS AND METHODS…… 86

RESULTS…… 90

DISCUSSION…….. 96

FIGURES AND TABLES……... 102

SUPPLEMENTAL INFORMATION……... 109

Chapter 4. The Rice DP Family Protein Defines a Novel Signaling Pathway in Brassinosteroid-Mediated Cell Division Processes……. 114

ABSTRACT…….. 115

INTRODUCTION……. 117

MATERIALS AND METHODS…….. 122

RESULTS…….. 130

DISCUSSION…… 140

FIGURES AND TABLES……. 147

SUPPLEMENTAL INFORMATION……... 165

Chapter 5. Analysis of Anti-BZR1 Antibody Reveals the Roles BES1 in Maintaining the BZR1 Levels in Arabidopsis……. 193

ABSTRACT…….. 195

INTRODUCTION……. 196

MATERIALS AND METHODS…….. 200

RESULTS…….. 205

DISCUSSION…… 211

FIGURES AND TABLES……. 216

SUPPLEMENTAL INFORMATION……... 222

REFERENCES……... 226

ABSTRACT IN KOREAN.....……... 241

ABBREVIATIONS

24-MC: 24-methylenecholesterol

3-DT: 3-dehydroteasterone

6-deoxo3DT: 3-dehydro-6-deoxoteasterone

6-deoxo3DT: 3-dehydro-6-deoxoteasterone

6-deoxoCS: 6-deoxocastasterone

6-deoxoTE: 6-deoxoteasterone

6-deoxoTY: 6-deoxotyphasterol

6-deoxoTY: 6-deoxotyphasterol

BAK1: BRI1-ASSOCIATED RECEPTOR

BEE: BR ENHANCED EXPRESSION

BES1: bri1-EMS SUPPRESSOR 1

bHLH: basic helix-loop-helix

BIN2: BRASSINOSTEROID INSENSITIVE 2

BKI1: BRI1-KINASE INHIBITOR 1

BL: brassinolide

BRD1: BRASSINOSTEROID-DEFICIENT DWARF 1

BRD2: BRASSINOSTEROID-DEFICIENT DWARF 2

BRI1: BRASSINOSTEROID-INSENSITIVE 1

Brz: brassinazole

BSKs: BRASSINOSTEROID SIGNALING KINASES

BSU1: *bri1*-SUPPRESSOR 1

BU1: BRASSINOSTEROID UPREGULATED 1

BZR1: BRASSINAZOLE RESISTANT 1

bzr1-1D: Arabidopsis brassinazole resistant1-1D

CDC2b: CYCLE-DEPENDENT KINASE 2b

CDK: CYCLIN-DEPENDENT KINASES

CPD: CONSTITUTIVE PHOTOMORPHOGENESIS AND DWARFISM

CR: campesterol

CS: castasterone

CYC D: D-type cyclin

CYC U: U-type cyclin

CYP450: cytochrome P450-type monooxygenases

D1: DWARF 1

D11: DWARF 11

DCL3: Dicer-like 3

Dicot: dicotyledonous

DP: E2F DIMERIZATION PARTNER

DS: dolichosterone

DTL: DWARF AND LOW-TILLERING

DWF4: DWARF 4

GA: gibberellin

GSK3: Glycogen Synthase Kinase-3

HBI1: HOMOLOG OF BEE2 INTERACTING WITH IBH1

HLH: helix-loop-helix

IBH1: ILI1-BINDING bHLH

ILI1: INCREASED LEAF INCLINATION 1

KRP: Kip-related proteins

LIC: TILLER ANGLE INCREASED CONTROLLER

Monocot: monocotyledonous

MDP1: MADS-DOMAIN-CONTAINING PROTEIN 1

PP2A: PROTEIN PHOSPHATASE 2A

PRE: PACLOBUTRAZOL-RESISTANT

QC: quiescent center

RGA1: RICE HETEROTRIMERIC G PROTEIN α SUBUNIT 1

ROT3: ROTUNDIFOLIA 3

TF: transcription factors

TE: teasterone

TY: typhasterol

TUD1: TAIHU DWARF 1

RAVL1: RAV-LIKE 1

RB: retinoblastoma

LAC1: LACCASE-LIKE PROTEIN 1

SG1: SHORT GRAIN 1

LIST OF FIGURES

Chapter 1:

Figure 1-1. Structure of brassinolide and the roles of brassinosteroids in plant development.

Figure 1-2. Representation of the BR biosynthetic pathway.

Figure 1-3. BR signaling pathways in Arabidopsis and rice.

Chapter 2:

Figure 2-1. Chemical structures of brassinazole, propiconazole, paclobutrazole, and uniconazole.

Figure 2-2. Responses of *Arabidopsis* seedlings to inhibitor treatments and BL Complementation.

Figure 2-3. Pcz specificity towards BR biosynthesis inhibition.

Figure 2-4. Sensitivity of *Arabidopsis* wild type, BR biosynthetic mutant *dwf7-1*, and signaling mutant *bri1-5* to Pcz and Brz.

Figure 2-5. Resistance of *dwf4-1* to Pcz and Brz.

Figure 2-6. Pcz impact on the expression of BR- and GA-related genes.

Figure 2-7. Tissue-specific response of dark and light grown W22 seedlings to Pcz and Ucz.

Figure 2-8. Impact of the genetic diversity on the tissue specific sensitivity towards Pcz and Ucz.

Figure 2-9. Influence of the genetic variation on the BR sensitivity in maize root.

Chapter 3:

Figure 3-1. Brachypodium seedlings exhibit dose-dependent dwarfism in response to propiconazole treatment.

Figure 3-2. Brachypodium leaf width and distance between veins are affected by Pcz.

Figure 3-3. BdBIN2 shows conserved motifs with other GSK3/SHAGGY-like kinase proteins.

Figure 3-4. Feedback regulation of Brachypodium BR biosynthetic genes after Pcz treatments.

Figure 3-5. Phenotypes of the *BdDWF4ox* and *BdBIN2ox* transgenic lines, suggesting the involvement of *BdDWF4* in BR biosynthesis and *BdBIN2* in responses, respectively.

Figure 3-6. *BRI1* homolog in *Brachypodium* fails to rescue the phenotypes of the BR-insensitive mutant *bri1-5*.

Chapter 4:

Figure 4-1. Propiconazole effects in rice seedlings.

Figure 4-2. Propiconazole resistance of *pzr1*-D mutant seedlings.

Figure 4-3. Phenotypes of adult plants.

Figure 4-4. Lamina inclination of wild-type and mutant seedlings.

Figure 4-5. BR sensitivity of *pzr1*-D and wildtype.

Figure 4-6. Activation-tagging T-DNA insertion in *PZR1*.

Figure 4-7. Phenotype resulting from *PZR1* overexpression in rice.

Figure 4-8. Phenotype resulting from *PZR1* overexpression in Arabidopsis.

Figure 4-9. Phylogenetic analysis of PZR1.

Figure 4-10. Expression pattern in rice tissues of seedlings and adult plants.

Figure 4-11. Morphology of calli derived from mutant and wild-type seeds.

Figure 4-12. Microscopic analysis of wildtype and pzr1-D mutant.

Figure 4-13. Enriched GO terms of DEGs in dark and DEGs in light.

Figure 4-14. Enriched GO terms of DEGs in dark and light.

Chapter 5:

Figure 5-1. Anti-BZR1 detects phosphorylated and dephosphorylated forms of BZR1 in Arabidopsis BZR1-HA overexpressing lines.

Figure 5-2. Anti-BZR1 detects changes in phosphorylation statutes and mainly recognizes BZR1 in Arabidopsis.

Figure 5-3. Anti-BZR1 detects BZR1 orthologs in three different monocot plants.

LIST OF TABLES

Chapter 1:

Table 1-1. Components of the BR signaling in Arabidopsis and rice.

Chapter 5:

Table 5-1. List of the signature peptides derived from BZR1 protein, as identified by ESI-Q-TOF.

Chapter 1. General Introduction

1-1. Brassinosteroids are growth-promoting hormones

Plant hormones play a crucial role in controlling physiological processes, and thus plants grow and develop in response to environmental factors. Steroid-derived hormones can be found in plant and animal kingdoms, and a four ring core of cholesterol generally forms part in their structure (Bishop et al. 2002; Marcinkowska et al. 2002) (Figure 1-1A). Brassinosteroids (BRs) are plant polyhydroxylated steroids which function as growth-promoting hormones. They have been related to many developmental and physiological processes in plants, including vascular differentiation, stem and root elongation, reproductive development, seedling photomorphogenesis, senescence and flowering timing, and stress responses (Figure 1-1B). Mutant plants, hence defective in BR synthesis or perception, display characteristic phenotypes such as short stature, round, curled leaves, short petioles, and reduce fertility (Clouse et al. 1996; Fujioka et al. 1997; Choe et al. 1998). The BR-biosynthetic and signaling pathways have been well studied in *Arabidopsis thaliana*, the model for dicotyledonous plants. A family of enzymes belonging to Cytochrome P450s mediates most of steps involved in BR biosynthesis, and characterization of mutants defective in these enzymes contributed to the understanding of BR biology (Kwon et al. 2005; Chung et al. 2013). Genetic, genomic, and proteomic approaches stablished components and mechanisms of the BR signaling pathway, which involves receptor kinases, protein-protein interactions with protein kinases, phosphatases, 14-3-3 proteins, and nuclear transcription factors.

Along this chapter, important advances in the BRs study are overview with more focus in the recent regulatory mechanisms, its applications and uses as a tool to modify growth of important crops. Right after, a comparison of the BR components and mechanisms studied to date in rice (*Oryza sativa*) and Arabidopsis plants is presented to understand the degree of conservation between monocotyledonous and dicotyledonous plants.

1-2. Arabidopsis and brassinosteroids

The small flowering plant *Arabidopsis thaliana* is the most popular model organism in plant biology. Not only its small size, but short life cycle, elevated number of seeds, relatively small genome size, and low cost and requirements for its culture are some of the characteristics that made Arabidopsis the most used model worldwide. Thus, is not surprising that most of the knowledge that we have accumulated to date about BRs biosynthesis, signaling and control have been made in Arabidopsis.

For long we have known that steroid-derivate compounds play important roles as hormones in the animal kingdom, but the study of the effects of sterols in plants doesn't exceed 40 years yet since their discovery in 1979 (Grove et al. 1979). To date many processes in the plant are now known to be controlled by brassinosteroids. The characterization of mutants in Arabidopsis revealed that BR-deficient and BR-insensitive plants display many growth defects such as dwarfism, delayed flowering, reduced fertility or sterility, dark-green rounded leaves and photomorphogenesis (light-mediated development) in darkness. In consequence, BRs have been related to a wide range of developmental processes such as cell elongation, responses to light, vascular differentiation, senescence timing and stress responses (Figure 1-1B).

1-2.1. Brassinosteroid biosynthesis and regulation in Arabidopsis

Unlike other plant hormones, no active transport of BRs over long distances within the plant have been observed. Consequently, BR accumulation and action in tissues

seems to depend exclusively on local biosynthesis and inactivation, both stringently regulated, primarily at the transcriptional level. (Hayat et al. 2003; Symons et al. 2008; Hategan et al. 2011). Brassinosteroid biosynthetic enzymes catalyze the conversion of plant steroids to BR precursors through oxidation and reduction reactions that add oxygenated functions to the A and B ring cores of cholesterol (Figure 1-1A). Thanks to chemical analyses and the discovery and characterization of dwarf mutants a lot about BR biosynthetic pathway; biosynthetic genes and the conversion steps, has been elucidated. To date more than 50 BR analogs have been identified. It was stablished that the physiologically most important possess 28 carbons (C_{28}), from which castasterone (CS) is the most widely distributed, followed by brassinolide (BL) which happens to be also the most biologically active BR derivate (Fujioka et al. 2003). C_{28} BRs are synthesized via multiple oxidative reactions using campesterol (CR) as precursor. Most of these oxidations are performed by cytochrome P450-type monooxygenases (hereafter CYP450s) belonging to the closely related CYP85 and CYP90 families. CYP450s transfer electrons from NADPH or NADH to a substrate (Hategan et al. 2011). BR biosynthetic pathway is far from being linear. It functions more like a metabolic network since BR-biosynthetic P450s enzymes, i.e. DWF4/CYP90B1 and CPD/CYP90A1, can act on multiple, structurally-related substrates depending on their availability (Chung et al. 2013). Figure 1-2 summarized the confirmed enzymes, BR intermediates and three major pathways of the BR biosynthetic network. Missing enzymes in the BR synthetic pathway include enzymes mediating C-2 hydroxylation to convert 6-deoxotyphasterol (6-deoxoTY) into 6-

deoxocastasterone (6-deoxoCS) and typhasterol (TY) into castasterone (CS). A candidate C-2 hydroxylase, CYP92A6, was found in *Pisum sativum* (Kang et al. 2001), but no homologs have been found in Arabidopsis or other plants. In addition, the enzyme catalyzing C-3 reduction to convert 3-dehydro-6-deoxoteasterone (6-deoxo3DT) to 6-deoxotyphasterol (6-deoxoTY) is missing too (red arrows in the Figure 1-2).

Regulation of BR biosynthesis is achieve by two major mechanisms; transcriptional modulation of the BR biosynthetic enzymes and by deactivation of bioactive hormone. Today we know that BRs regulate their own biosynthesis by negative feedback regulation of the BR biosynthetic genes. For instance, mRNA transcripts of *DWARF 4* (*DWF4*) accumulate in BR-deficient mutants or after application of the BR inhibitor brassinazole (Brz). Conversely, mRNA levels decrease upon treatment with BL. Other BR biosynthetic genes like *CONSTITUTIVE PHOTOMORPHOGENESIS AND DWARFISM* (*CPD*), *ROTUNDIFOLIA 3* (*ROT3*) and *CYP85A* behave similar.

Less is known about mechanism of BRs inactivation, but probably conjugation reaction and not catabolic breakdown is responsible for the rapid decrease of active BRs (Kim et al. 2010). These reactions include glycosylation or acylation of hydroxyl groups and additional hydroxylation among others (Hategan et al. 2011).

1-2.2. Brassinosteroid signaling in Arabidopsis

The study of brassinosteroid signal transduction in Arabidopsis allows us now to be acquired with the steps and players of the signal cascade from the membrane

receptor to the transcription factors in the nucleus. BR is perceived by the cell-surface receptor BRASSINOSTEROID-INSENSITIVE 1 (BRI1) which also interact with the co-receptor kinase BRI1-ASSOCIATED RECEPTOR (BAK1). As a result of this interaction, these kinase receptors trans-phosphorylate and fully activate each other. In the absence of BR, the interaction of BRI1 with BRI1-KINASE INHIBITOR 1 (BKI1) interfere in its interaction with BAK1, thus BKI1 acts as a negative regulator of BRI1 function (Li et al. 2002; Wang et al. 2006; Wang et al. 2008; Kim et al. 2010). The binding of BR to BRI1 marks the start of the signal, and downstream substrates of BRI1 kinase, identified as BRASSINOSTEROID SIGNALING KINASES (BSKs), continue the sequence of events downstream. Phosphorylated BSKs can interact and activate bri1-SUPPRESSOR 1 (BSU1), a protein phosphatase that regulates one of the majors components in the BR signaling, the negative regulator BRASSINOSTEROID INSENSITIVE 2 (BIN2) (Kim et al. 2009; Kim et al. 2010; Yang et al. 2011). BIN2 encodes a protein kinase similar to mammalian Glycogen Synthase Kinase-3 (GSK3), who usually play roles as negative regulator in various signaling pathways by phosphorylating other components and leading them to proteosomal-dependent degradation. In case of BR signaling, the substrates of BIN2 are two transcriptional factors (TFs); BRASSINAZOLE RESISTANT 1 (BZR1) and bri1-EMS SUPPRESSOR 1 (BES1) which are positive regulators of the BR pathway that directly command BR-responsive gene expression. When BIN2 is active, it phosphorylates and inactivate BZR1 and BES1 (Wang et al. 2002; Yin et al. 2002; He et al. 2005). Therefore, for the BR signaling to be transmitted, the inactivation

of BIN2 is a key step. When BR upstream signal from receptor kinases and BKSs activates BSU1 phosphatase, it de-phosphorylates BIN2 that inactivates and targets it for proteosomal degradation (Li et al. 2007; Peng et al. 2008). Other regulators of the BR signaling are 14-3-3 proteins and PROTEIN PHOSPHATASE 2A (PP2A), negative and positive regulators respectively. Although the mechanism of action of 14-3-3 proteins is not completely unravel, their interaction retains phosphorylated forms of BZR1 and BES1 in the cytosol, keeping them inactive (Gampala et al. 2007). Alternatively, the discovery of PP2A a few years ago finally disclosed the protein phosphatase behind the dephosphorylation, and consequent reactivation, of BZR1 and BES1 (Tang et al. 2011).

Besides BZR1 and BES1, helix-loop-helix and basic helix-loop-helix (HLH/bHLH) transcription factors were identified to mediate in the BR-regulated gene expression. The first TFs of this class described to be required for full BR response are the three redundant proteins denominated BEE1, BEE2 and BEE3, in where BEE stands for BR ENHANCED EXPRESSION. But their induction was triggered not just by BR but also other plant hormones (Friedrichsen et al. 2002). Similarly, the balance among three antagonizing HLH/bHLH factors named PACLOBUTRAZOL-RESISTANT (PRE), IBH1 and HBI, controls cell elongation as a module which works downstream of not just BR but other hormonal and environmental signals as well. PRE homologs, including PRE1 and its homolog in rice INCREASED LEAF INCLINATION 1 (ILI1), induce cell elongation by interacting antagonistically with ILI1-BINDING bHLH (IBH1) (Zhang et al. 2009). Conversely, IBH1 interacts with bHLH factor HOMOLOG OF BEE2

INTERACTING WITH IBH1 (HBI1), and inhibits HBI1 DNA-binding activity. Thus PRE1/ILI1 inactivate the inhibitory effects of IBH1 towards the positive regulator of cell expansion HBI1 (Zhang et al. 2009; Bai et al. 2012; Bai et al. 2012).

A scheme with the principal components and interactions of the BR signaling in Arabidopsis is presented in the Figure 1-3 (left panel).

1-3. Monocot plants and brassinosteroids

In contrast with the broad knowledge on BRs in dicot plants, by the studies in *A. thaliana*, little is known on the molecular function of BRs in monocotyledonous (hereafter referred as monocots). Just few dwarf BR-deficient mutants have been found in rice, maize and more recently in *B. distachyon*. This lack of tools and genomic resources to have access to new mutants limits the studies to the characterization of just a few BR-deficient or –insensitive mutants found so far. Besides, an alternative to mutants is the use of transgenic plants, but plant transformation protocols for crop plants usually requires callus transformation and regeneration steps that difficult the process and extend the time requirements (Bevan et al. 2010).

Among monocots, BR action mechanisms have been more studied in *Oryza sativa* (rice), a major crop that has been used extensively as a model plant for monocots. Although growth conditions for rice are highly demanding and its generation time is quite long for a model plant, the rice genome sequence is available (International Rice Genome Sequencing 2005) and lot of effort has been made into generation of several mutant populations for study (Jeong et al. 2002; Jeong et al. 2006; Wan et al. 2009). The access to all these new genomic resources, afforded to find some Arabidopsis orthologs of biosynthetic genes and counterparts of BR signal pathway. The identification of orthologs in BR processes indicated that the mechanisms may be somehow conserved between monocots and Arabidopsis (Hong et al. 2005; Tanabe et al. 2005; Sakamoto et al. 2006).

1-3.1. Brassinosteroid biosynthesis in monocot plants

As shown in the previous part, almost the complete network of proteins involved along with subtracts and products, was identified in *A. thaliana* (Hategan et al. 2011; Chung et al. 2013). In contrast, just few BR-deficient mutants have been found in rice or other monocots. Like in Arabidopsis, monocot mutants with BR deficiency shows dwarfism and abnormal skotomorphogenesis. In addition, monocots display some interesting traits such as erect leaves, shortening of the second internode, and reduce tiller number among others. To date, *dwarf/brd1*, *d2*, *d11*, *brd2* and *dwarf4* rice mutants have been identified. Rice *BR-deficient dwarf 1* (*brd1*), possesses deficient C-6 oxidase activity, a function of the cytochrome P450 CYP85A family (Hong et al. 2002). The dwarf mutant, *ebisu dwarf* (*d2*) is defective in a gene encoding for cytochrome CYP90D2 that first was reported to catalyze C-3 oxidation steps in rice, like from 6-deoxoteasterone (6-deoxoTE) to 3-dehydro-6-deoxoteasterone (6-deoxo3DT) and from teasterone (TE) to 3-dehydroteasterone (3-DT) (Hong et al. 2003; Li et al. 2013). The *D11* gene, found to be defective in the *dwarf 11* (*d11*) mutant, encodes a novel CYP450 (CYP724B1) with high homology to *A. thaliana* enzymes involved in BR biosynthesis and showed to function in the early C-3 reduction to supply 6-deoxoTY and TY (Tanabe et al. 2005). The characterization of the *brassinosteroid-deficient dwarf 2* (*brd2*) mutant pointed *BRD2* as the homolog gene to *A. thaliana DIM/DWARF 1* in charge of C-24 reduction for the conversion of 24-methylenecholesterol (24-MC) to campesterol (CR) (Hong et al. 2005). The *osdwarf4-1* mutant with BR-deficient-like phenotypes revealed that *OsDWARF 4*

encodes a cytochrome P450 CYP90B2 that functions in C-22 hydroxylation steps in BR biosynthesis. Thus, *OsDWARF4* is a homolog of *A. thaliana DWARF4*, which encodes CYP90B1 (Sakamoto et al. 2006). Other studies of CYP450s involved in BR biosynthesis include two examples in maize (*Zea mays*) and one in *Brachypodium distachion*. In case of maize, two publications described first *ZmDWF1* and then *ZmDWF4*. In both cases, the homolog genes were found by an *in silico* analysis using *Arabidopsis* and rice DWF1 for *ZmDWF1* study, and just *Arabidopsis* DWF4 for *ZmDWF4*. Gene function was study by analysis of transgenic maize plants or overexpressing maize genes in *Arabidopsis* respectively (Tao et al. 2004; Liu et al. 2007). The case of Brachypodium was the study of *BdBRD1* gene that was found by the characterization of *bdbrd1-1,* a T-DNA insertion mutant. The *bdbrd1-1* mutant showed severe dwarfism, twisted leaves and late flowering phenotypes that were at least partially rescued by treatments with the BR derivate 24-epicastasterone (Xu et al. 2015).

Despite similarities between synthetic pathway in dicot and monocots, especially in the intermediates and products, some combine studies including phylogenetic relationships between *A. thaliana* and rice CYP450s revealed some differences. Initially, just one *DWF4* homolog was identified in the rice genome by *in silico* tools. However, later studies showed that *D11,* which showed high homology with *A. thaliana CYP724A1*, was also related to *OsDWF4*. Hence, apparently in rice CYP90B2/OsDWF4 and CYP724B1/D11, function redundantly in C-22 hydroxylation. While *D11* seems to be essential to maintain active BR levels for normal shoot elongation and flower developing, *OsDWF4* contributes

only with additional BRs required for leaf inclination but not for flower or grain development (Sakamoto et al. 2006). An uncommon BR compound, dolichosterone (DS), has been also describe to be an active BR in rice. DS, which normally is not detected in plants, accumulates in *brd2* mutant where CR production is impaired. This uncommon BR was demonstrated to be active in rice since its application enhances lamina angle and is even able to rescue the phenotype of other severe dwarf mutants such as *brd1* (Hong et al. 2005). One more difference, and the most critical, among dicot and rice pathway is the end product of the BR biosynthetic pathway. In *A. thaliana*, CYP85A2 mediates the synthesis of BL, the end product and most active BR in these plants. Nevertheless, in rice plants, no detectable BL levels has been found and no CYP85A2 homolog enzyme has been characterized yet. Apparently, monocot plants have only one copy of *CYP85A* in the genome and castasterone (CS) is likely to be the end product (Kim et al. 2008).

1-3.2. Brassinosteroid signaling pathway in monocot plants

Although many plant traits seem to be controlled by BR-related genes, the gene network controlling these processes is still limited in monocot plants (Divi et al. 2009; Zhang et al. 2014). Some orthologs to Arabidopsis genes in the BR signaling pathway have been found, such as the receptor BRI1 and its co-receptor BAK1, named OsBRI1 (or D61) and OsBAK1 respectively (Yamamuro et al. 2000; Nakamura et al. 2006; Li et al. 2009; Zhao et al. 2013). The rice dwarf mutant *d61*, was the first identified from the BR signaling. Mapping of *d61* locus showed that its short stature and less sensitivity to BL phenotypes were the result from the genetic lesion in BRI1 ortholog gene (Yamamuro et al. 2000; Nakamura et al.

2006). Two homologs of BIN2, the major negative regulator of BR signaling, were identified as GSK3/SHAGGY-like kinase 1 and 2 (OsGSK1 and OsGSK2), in where OsGSK2 is more likely to be rice the counterpart of Arabidopsis BIN2 (Koh et al. 2007; Tong et al. 2012; Tong et al. 2012). Finally, searching for homologous to BZR1 and BES1 in the rice genome resulted in the finding of OsBZR1, which showed 53% sequence identity with the Arabidopsis counterparts. Suppression of this gene leaded to dwarfism, erect leaves and reduce sensitivity to BR. In the same work it was also shown the interaction between OsBZR1 and 14-3-3 proteins, showing conserved functions of these genes in the BR signal transduction in rice and Arabidopsis (Sakamoto 2006; Bai et al. 2007; Kim et al. 2010; Zhao et al. 2013). Another module than seems to be at least partially conserved between Arabidopsis and rice is the one composed of HLH transcription factors.

It was mentioned before that HLH proteins have been shown to interact with TFs and play critical roles in the BR and other hormone signals in Arabidopsis (Friedrichsen et al. 2002; Zhang et al. 2009). Particularly in rice, INCREASED LEAF INCLINATION 1 (ILI1) was presented as a homolog of PRE1, an HLH protein from the PRE family with functions in the BR signaling in Arabidopsis. Overexpression of *ILI1* resulted in pronounced leaf inclination in rice plants, which is a typical BR-related phenotype. Using *ILI1* as a bait, the interacting protein ILI1-BINDING bHLH (IBH1) was found, which according to the opposite phenotypes seemed to be *ILI1* antagonist. ILI1 and its Arabidopsis homolog PRE1 interact with rice and Arabidopsis IBH1 proteins, which also evidences a conservation of this mechanism in both model plants (Zhang et al. 2009).

1-3.3. Rice specific brassinosteroid signaling components

Despite the list of homolog genes in rice has been increasing, especially the last few years, still many genes with the functions of *PP2A*, *BSK*s and *BSU1* have not been found (Zhang et al. 2014). More interestingly, other components with not known orthologs in Arabidopsis has been identified in rice too, which indicates existence of specific BR functions in monocots and/or some degree of function redundancy. Some examples of these components are DWARF AND LOW-TILLERING (DLT) and TILLER ANGLE INCREASED CONTROLLER (LIC), which act downstream of OsBRI1 and OsGSK2 to positive and negative regulate rice BR signaling respectively (Tong et al. 2009; Zhang et al. 2012). DLT was found through mutant screening in where *dlt* displayed BR-related phenotypes such as compact stature, dark-green erect leaves, late flowering, and reduced tillering number. DLT overexpression was able to recover BL insensitivity of *d61* mutants and it was shown to interact and be a target of OsGSK2 phosphorylation (Tong et al. 2009; Tong et al. 2012). LIC1 in the other hand, encodes a novel CCCH-type zinc finger protein which is also OsGSK2 target. Gain-of-function *lic-1* mutation and *LIC* overexpression lines showed phenotypes associated with BR-deficiency or -insensitivity such as erect leaves. In contrast, *LIC* antisense lines showed hypersensitivity response to BR in lamina bending assays. Therefore, like OsBZR1, LIC also showed to be target of GSK3-like kinases in the BR signaling pathway, but playing opposite roles. In fact, LIC and OsBZR1 can regulate each other transcription by direct binding to their promoter regions, and function antagonistically in the regulation of downstream genes. While BZR1 is known as a

positive regulator of BR signal in rice and Arabidopsis, LIC is a novel module that may repress BZR1 transcription to attenuate the BR signaling pathway in rice (Zhang et al. 2012; Zhang et al. 2014).

Aside from OsBZR1, and rice specific DLT and LIC transcription factors, another novel component functioning downstream in the BR signaling was identified as well, the BRASSINOSTEROID UPREGULATED 1 (BU1) (Tanaka et al. 2009). BU1 is the first rice-specific bHLH transcription factor regulating BR signaling identified so far. Genetic and morphologic data evidences that BU1 is a positive regulator of the BR response. Rice plants overexpressing BU1 showed enhanced bending of the lamina joint, increased grain size, and resistance to Brz (Tanaka et al. 2009).

Another DNA-binding protein mediating the rice BR signaling pathway is RAV-LIKE 1 (RAVL1). Two mutant allele *ravl1-1* and *ravl1-2* were identified as semi dwarf with dark-green leaves and weak responses to BL in lamina inclination assays. All these phenotypes evidenced a possible relation with the BR signaling, that was later reported to work in the regulation of genes from both, the BR-signaling and -biosynthetic pathways. RAVL1 possesses a B3 DNA binding domain that was shown to directly bind to promoters of BR receptor *BRI1* and BR biosynthetic genes *D2*, *D11* and *BRD1* to activate their transcription. It was also demonstrated that unlike BZR1-mediated regulation of BR biosynthetic genes, RAVL1-mediated activation is not subject to BR feedback regulation. Moreover the studies about the relationship between RAVL1 and BZR1 over common targets (i.e. *BRD1*) showed that suppression of BZR1 was epistatic to activation of

RAVL1. Taken together, RAVL1 functions to apparently maintain the basal activity of the BR genes to ensure basal levels of brassinosteroids (Je et al. 2010; Je et al. 2010).

Screening of rice brassinolide-regulated genes resulted in the isolation and functional characterization of *MADS-DOMAIN-CONTAINING PROTEIN 1* (*OsMDP1*). *MDP1* transcription was upregulated by darkness and suppressed by BL treatments and *MDP1*-deficient plants showed abnormal elongation of primary roots and coleoptiles, and enhanced lamina joint inclination, all BR-related responses, indicating that this gene could be acting as a negative regulator of the BR signaling in rice (Duan et al. 2006).

Another example of rice novel proteins in BR signal is the U3 ubiquitin ligase TAIHU DWARF 1 (TUD1). Mutant *tud1* were characterized as dwarf plants with impaired patterns of internode elongation and short, erect and dark-green leaves, all suggesting that TUD1 was involved in a BR pathway. Studies revealed that TUD1 interacts genetically and physically with DWARF 1 (D1), also named RICE HETEROTRIMERIC G PROTEIN α SUBUNIT 1 (OsRGA1), a heterotrimeric G protein subunit involved in gibberellin (GA) and BR responses but in an alternative pathway independent of BRI1 (Wang et al. 2006; Oki et al. 2009). G-protein elements normally mediate signaling responses between surface receptors and downstream effectors, and in this case D1 along with TUD1 were revealed to regulate BR-mediated growth and development in rice (Hu et al. 2013; Zhang et al. 2014).

Finally, one of the most recent reports about a novel BR signaling component in rice is another G protein, named OsPRA2 (Zhang et al. 2016). OsPRA2 co-localizes with OsBRI1 and inhibits BRI1 kinase activity and BAK1 interaction. Moreover OsPRA2 is able to control activation pattern of BZR1 modulating BZR1 phosphorylation/dephosphorylation pattern. In *OsPRA2* overexpressing plants BZR1 remains in its inactive phosphorylated form, while phosphorylation level of BZR1 decreased in transgenic plants with suppressed expression of *OsPRA2*. Thus OsPRA2 in another novel negative regulator of OsBZR1 and OsBRI1 that plays important roles in the fine-tuning of the BR responses in rice (Zhang et al. 2016). Figure 1-3 and Table 1-1 resume the rice components of the BR signaling identified so far along with their Arabidopsis homologs.

1-4. Brassinosteroids effects in monocot plants architecture

Plant architecture refers to plant height, leaf erectness, tiller number and panicle number and morphology. All these aspects in plant determine at the end biomass and grain yield (Divi et al. 2009). Because of the effects of brassinosteroids in plant growth, a lot of testing of exogenous application of BR to a variety of species have been tested with some beneficial results, however, the high cost of synthetic BRs makes this practice hard to use in agriculture. For this reason, the manipulation of genes involved in the synthesis of BRs to modulate endogenous levels, as well as the sensitivity of plants to BRs by affecting genes involved in BR perception and response was seen as a great alternative for the use in agriculture (Yang et al. 2008).

1-4.1. Plant height

Most off the BR-deficient or -insensitive plants present dwarf or semi dwarf phenotypes with specific pattern of internode elongation. Usually, the second internode is shortened, whereas other internodes are almost not affected. This kind of phenotype was denominate dm-type dwarfism (Hong et al. 2004). In the called 'green revolution', high-yielding rice and wheat varieties were achieve by the use of dm-type semi dwarf plants. The reduction in plant height led to improve harvest index which is defined as the grain: straw ratio. Smaller plants with less tiller but no effects in the grain size or weight allowed denser planting and thus increase yield. A typical dm-type dwarfism can be found in weak alleles in *BRI1* mutants

such as *d61* and also in BR biosynthetic mutants *d2* and *d11* (Yamamuro et al. 2000; Hong et al. 2003; Tanabe et al. 2005).

1-4.2. Leaf angle

Leaf angle of plants is not just related with dense planting, but also an aspect which has been shown to affect photosynthesis. Erect leaves allow greater penetration of light to the lower leaves of the plant, increasing their photosynthetic capacity (Murchie et al. 1999; Sakamoto et al. 2006). Many examples of brassinosteroid and its importance in leaf angle was already shown. As a general rule, BR-deficient or insensitive mutants present more erect leaves while mutants with increase amount of BRs or more sensitive to BR present increase leaf angle. The leaf angle is very dependent of BR, reason why the 'lamina bending assay' is the most used bioassay to test plant response to BRs and/or BRs concentration (Wada et al. 1984). One example of the manipulation of BRs and leaf angle is the *osdwarf4-1* mutant. In this case, the disruption of *OsDWARF4* gene produced semi-dwarf plants with more erect leaves that were grown under conditions of dense planting, which resulted in increased biomass and yield (Sakamoto 2006; Sakamoto et al. 2006). Other examples of erect leaves used to increase yield potential has been shown in the BR receptor mutant *d61*, and BR-deficient mutants *d2* and *brd1* (Morinaka et al. 2006; Zhang et al. 2014). The BR signaling module composed by HLH/bHLH transcription factors ILI1 and IBH1 has been proposed as good candidates for manipulation in yield-increase breeding programs for their importance determining leaf angle of the plant (Zhang et al. 2009; Zhang et al. 2014).

1-4.3. Tiller number

The number of tiller per plant will determine the panicle number and thus grain yield at the end. Usually tiller number and height are traits negatively related; dwarf plants generally present more tillers. Unfortunately, no much is known about this process and data is a little contradictory. While most of the BR dwarf mutants present increase tiller number, there are some exceptions. First, rice plants expressing maize or Arabidopsis versions of DWF4 only in stems, leaves and roots produced more tillers and more seeds than wild-type plants (Wu et al. 2008). Also *dwarf and low- tillering* (*dlt*) mutant presents an exception by itself. As it name defines, *dlt* mutant shows both semi-dwarf and fewer tiller phenotypes along with dark-green and erect leaves. Due to its unique phenotype, the study of this gene could provide insights into the relation between height and tillering and the mechanisms controlling both traits. In addition to BL responses, DLT seems to also involve in tillering and has been proposed that DLT could be controlling rice tillering by repression of some BR biosynthetic genes while it is regulated at protein level by GSK2 and at transcriptional level by BZR1. In mutants with deficient BR signal or biosynthesis BZR1 action is neutralized by BIN2, leading to increase expression of DLT and tiller formation. High expression of DLT in *d2* and *d11* mutants support this hypothesis (Tong et al. 2009).

1-4.4. Grain size and yield

Several examples of changes in the seed size have been reported in BR-related mutants. One of the first reports was presented in Arabidopsis, were the ectopic overexpression of *DWF4* resulted in an increase in the total number of branches,

seed yield and size (Choe et al. 2001). A similar case of ectopic overexpression of DWF4 was reported in maize (Liu et al. 2007). In rice, examples of increase grain size related with BR responses have been reported in plants overexpressing HLH family of transcription factors *ILI1* and *BU1* (Tanaka et al. 2009; Zhang et al. 2009). In the opposite case, *d11* showed small-grain phenotypes as well as other BR-deficient mutants *d2* and *brd1*, who show reduction of length and width of the seeds respect to their wild types (Hong et al. 2002; Hong et al. 2003; Tanabe et al. 2005). The dominant mutant *short grain 1* (sg1) was identified as well as dwarf mutant with short grains and dark-green erect leaves (Nakagawa et al. 2012).

More recent cases of BR modulation toward increase grain size or yield is the study of microRNA OsmiR397. This miRNA is expressed in seeds and its overexpression causes increase number of branches and grains per main panicle, greater grain size and thus enhanced yield by downregulating its target gene, the laccase-like protein *OsLAC*. In this study, *OsLAC* was showed to be involved in the brassinosteroid pathway, more specifically in brassinosteroid sensitivity of the plants by enhancing BR signaling, but not BR accumulation that leads to increase grain yield (Zhang et al. 2013). Other case of genes related with BR homeostasis and agronomical traits is the rice Dicer-like 3 homolog OsDCL3a, a primarily responsible for 24-nt small interfering RNAs (siRNA) processing. A reduction in *OsDCL3* expression, thus OsDCL3a-dependent 24-nt siRNAs, causes impair regulation of a broad set of genes, particularly in genes involved in GA and BR homeostasis. Thus *OsDCL3a* impairment causes dwarfism, large flag leaf angle

and reduction in number of secondary branches by affecting genes involved in BR and GA mechanisms(Wei et al. 2014).

1-5. Brassinosteroids and Regulation of the Cell Cycle

Most plants can produce new organs throughout lifespan continually, in contrast to animals that typically develop them once. This feature of plants require a strict balance in cell division and differentiation. Plants also possess cell wall, and because their inability to move, their adaptation to environment depends uniquely on their growth. All these special features may be the reason why regulation of cell cycle in plants is so important, demonstrated for example on a higher number of regulatory members compared to the animal cell cycle (Scofield et al. 2014). So, as a fundamental event in plant growth, the relationship between cell division control along with hormonal and environmental signals is important to understand.

Plants with defects in either BR signal or synthesis, exhibit a distinctive dwarf phenotype with stunted shoots and small, dark-green, round leaves. Plant growth can be determined by cell proliferation, expansion of individual cells or both, but morphology of BR mutants is attributed mainly to decrease in cell elongation (Kauschmann et al. 1996; Szekeres et al. 1996; Azpiroz et al. 1998; Choe et al. 1999; Yoshizumi et al. 1999; He et al. 2003; Kwon et al. 2005). In agreement with this statement, genes related with cell growth and cell wall organization revealed to be targets of BZR1 and BES1 transcription factors, which are key factors in the BR response (Sun et al. 2010; Yu et al. 2011). However less evidences, and even contradictory results about BR involvement in cell cycle were initially reported. Addition of epi-brassinolide to carrot culture cells induced cell enlargement but decreased number of cells (Sala et al. 1985). Moreover expression

of arabidopsis *CDC2b* gene, a plant-specific cell cycle-dependent kinase-related gene, was shown to be induced by BR but was found to be involved in cell elongation rather than in cell division (Yoshizumi et al. 1999). But more evidences in favor of BR roles in cell cycle are being gathered, especially over the last years. In cell cultures from Col-0 and *det2*, defective in the early step of BR synthesis, BR could even substitute cytokinins in the culture media for normal cell division. In the same work the D-type cyclin *CycD3* transcription was shown to be upregulated by BR. These findings suggested that BR may promote cell division through *CycD3*. Moreover histological analysis of leaf using *det2* mutant along with *dwarf1* reported that cell number significantly decreases in these mutants, validating that BRs play a role not only regulating cell expansion, but also proliferation (Hu et al. 2000; Nakaya et al. 2002). Late findings include recent work from our research team in where callus derived from BR-deficient mutant *dwf7-1* display various characteristics attributable to slower cell division rates (Cheon et al. 2010). A study about leaf size using different transgenic lines also showed that increase in the cell number was predominantly responsible of leaf size enlargement when BR receptor BRI1 was overexpressed in arabidopsis plants (Gonzalez et al. 2010). Furthermore, two studies done in roots have shown important roles of BRs controlling meristem size through control of cell cycle progression and cell expansion (Gonzalez-Garcia et al. 2011; Hacham et al. 2011). In *bri1* mutants, short-root phenotype and small meristem size can be explained in part by reduced number of meristematic cells. BRI1 activity in the epidermis was demonstrated to be sufficient to control gene expression for normal cell

progression in the root meristem, although this signal is transmitted independently of the well-known BZR1 and BES1 pathway (Hacham et al. 2011). BR effects are dose dependent since not only BR deficiency can cause reduction in cell division rate, but so do enhanced BR signaling by continuous BL treatment or as in *bes1-D* gain-of-function mutation. In these cases high BR signal leads to premature exit from cell cycle that results in early differentiation, shortening meristem (Gonzalez-Garcia et al. 2011). Very similar results were found in leaves, where continuous BL treatment reduced the number of cells and promoted cell expansion and differentiation (Zhiponova et al. 2013). By genetic analysis it was also revealed involvement of other BR receptors aside of BRI1, BRL1 and BRL3, in the cellular dynamics of quiescent center (QC) cells. Also related with maintenance of QC cells, BR pathway controls expression of transcription factor ERF115 and BRAVO, which are a rate-limiting factor of QC division and a cell-specific repressor of QC division respectively (Fabregas et al. 2013; Heyman et al. 2013; Vilarrasa-Blasi et al. 2014). In contrast to all data emerging, the precise mechanisms underlying BR control in cell cycle is not known yet. Moreover these mechanisms seem to be more complex than expected, since apparently it requires optimal BR levels and specific targets in different tissues and phases. Thus where and when BRs control plant growth thought cell proliferation remains to be determined.–

1-5.1. BRs and cell cycle control in rice

The recent evidence reported of BRs altering cell-cycle progression is limited to Arabidopsis examples, and there is almost no reports of BRs involvement in cell

division in monocots. To date, the characterization of the T-DNA mutant *xiao* along with studies of a U-type cyclin in the control of leaf erectness are the only two evidences of the possible BR connection with cell cycle in rice (Jiang et al. 2012; Sun et al. 2015).

The *xiao* mutants display semi-dwarfism, erect leaves, short panicles and internodes and smaller seeds as many BR-deficient or -insensitive mutant plants. Longitudinal sections of the organs showed that *xiao* had significantly fewer cells than wild-type plants, with no distinguishable difference in cell size. *XIAO* is predicted to encode a LRR kinase, and the mutation in this gene was shown to reduce expression levels of BR-related genes such as *D11* and *DWARF4*. Impair expression of these genes resulted on reduce BR biosynthesis, which is reflected in the low levels of endogenous BR intermediates of *xiao* compared to wild-type plants. Furthermore, the expression of three BR signaling genes in rice (i.e. *LIC, OsMDP1* and *BU1*) is compromised in these mutants. Thus, as a LRR kinase, phosphorylation by XIAO may be involved on BR signaling and cell cycle and provide a link between these two processes. This is supported by the observation that *XIAO* is co-expressed with a number of genes involved in cell cycle (Jiang et al. 2012).

The study of the molecular mechanisms in the control of leaf erectness illustrates the more recent evidence of how BRs regulate cell proliferation in rice (Sun et al. 2015). In the study, it was demonstrated that leaf erectness depends on the abaxial sclerenchyma cell number in the lamina joints and that the

sclerenchyma cell proliferation is regulated by BR signaling components. BR-deficient or –insensitive mutants present more erect leaves and increase abaxial sclerenchyma cell layers. When finding for the possible link between the two processes, the group found an U-type cyclin, *CYC U4;1*, whose expression is enriched in tissues from lamina joint and it is regulated by direct binding of BES1 to its promoter region. Thus *CYC U4;1* acts as a downstream target of BR signaling to regulate leaf angle. Furthermore, BIN2 can interact and phosphorylate CYC U4;1 to promote its activity in cell cycle. Thus these data support the regulation mechanism of leaf erectness by BRs. When BR signaling is attenuated in the lamina joints, the active BIN2 can inhibit BES1 activity to release the inhibitory effect on *CYC U4;1* transcription, and at the same time can also phosphorylate CYC U4;1 protein to enhance its activity to accelerate abaxial sclerenchyma cell proliferation which results in erect leaves. In contrast, in the presence of BRs there is a decrease in the abaxial sclerenchyma cell number to enhance lamina inclination (Sun et al. 2015).

1-5.2. E2F Family in the Control of Cell Cycle

Cell cycle progression is regulated at two points; the transition from G_1-phase to S-phase and from G2-phase to M-phase and molecular players and mechanisms involved in this regulation are highly conserved among species. Particularly, the roles of cyclin-dependent kinases (CDKs), cyclins, Kip-related proteins (KRP), retinoblastoma (RB) proteins, transcription factor E2F (E2Fs) and E2F dimerization partners (DPs).

Usually, cyclins and CDKs act as complex at a precise time and drive the cell cycle progression by phosphorylating downstream target proteins. In the other hand, the conserved RB-E2F/DP pathway plays an important role in cell cycle control by regulating the transcription of the genes involved in the progression to the S phase from the G_1 phase. The DNA-binding activity of E2F can be stimulated by DP proteins, thus E2F/DP heterodimeric transcription factors (TFs) activate transcription of genes responsible of cell cycle control, initiation of replication, and enzymes required for DNA synthesis. E2F/DP pathway is well conserved in animals and plants.

In Arabidopsis, at least three *E2F* (*E2Fa*, *E2Fb*, and *E2Fc*) and two DP (*DPa* and *DPb*) has been identified (Magyar et al. 2000; Kosugi et al. 2002; Vandepoele et al. 2005). In rice, not much work has been done related with these genes, but a genome-wide analysis identified several core cell cycle genes, including four *E2Fs* (*OsE2F1*, *OsE2F2*, *OsE2F3*, and *OsE2F3*) and three *DPs* (*OsDP1*, *OsDP2* and *OsDP3*) in the model monocot (Guo et al. 2007). Nevertheless, expression analysis in the same work failed to detect two of the three DP genes transcripts, *OsDP2* (hereafter DPB or PZR1) and *OsDP3*, in different rice tissues.

In wheat, the isolation and characterization of a DP protein (TmDP) was reported in the early 2000s, and provided evidences that E2F/DP heterodimerization properties are conserved in plant and animals (Ramirez-Parra et al. 2000). DP proteins have a similar domain organization between species, which

includes a DNA binding and heterodimerization with E2F binding domains. TmDP from wheat was shown to associate with E2F from human and TmE2F, thus the molecular basis for the heterologous interaction between E2F and DP proteins is well conserved. Interestingly, although TmDP contains DNA binding domain, which is similar to E2Fs, TmDP alone cannot bind to DNA. On the contrary, TmE2F can bind to DNA alone, although with low affinity compared to E2F/DP heterodimer (Ramirez-Parra et al. 2000). The consensus DNA binding sequence of E2Fs has been identified as TTTCGCGC (Sekine et al. 1999; Magyar et al. 2000), and potential targets in plants has been identified by genome-wide studies (Vandepoele et al. 2005).

1-6. BRASSINAZOLE-RESISTANT 1 (BZR1) as a key component of BR signaling pathway

Transcription factor BZR1 has been identified as a key component of the BR signaling pathway along with its closest homolog BES1 (Wang et al. 2002; Yin et al. 2002; Kim et al. 2010). BRs, mainly through BZR1 and BES1, regulate a large number of genes involved in plant developmental and physiological processes (Kim et al. 2009; Sun et al. 2010). These transcription factors (TFs) are subject to post-transcriptional modifications and exists in two different forms, phosphorylated and dephosphorylated BZR1 and BES1. In ambient conditions BZR1 and BES1 exists mostly in phosphorylated forms (pBZR1 and pBES1) resulting from the activity of BIN2 kinase (Choe et al. 2002). Phosphorylated BZR1 and BES1 are recognized as inactive forms and are subject to degradation via 26S proteasome (He et al. 2002; Li et al. 2002). On the other hand, the presence of active BRs such as BL induces rapid dephosphorylation of these TFs, by PP2A activity and inactivation of BIN2. Dephosphorylated forms of BZR1 and BES1 can be observed in the nucleus where they are active and regulate their respective targets genes (Li et al. 2005; Yin et al. 2005; Ryu et al. 2007). In genome-wide studies BZR1 was shown to regulate around 80% of genes downstream of BRI1-mediated BR signal. Thus, BZR1 is a mayor regulator of the BR signaling pathway. This transcription factor can directly bind to genes involved in hormones biosynthetic pathways, or modulate expression level of key components of the other signaling pathways or even co-regulate common transcriptional targets along with others important TFs.

FIGURES AND TABLES

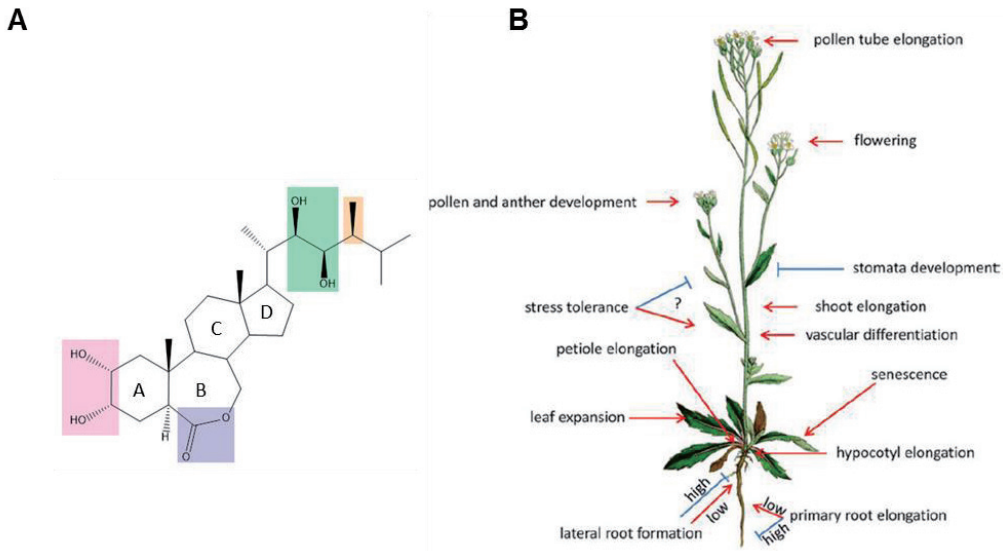

Figure 1-1. Structure of brassinolide and the roles of brassinosteroids in plant development. (**A**) Schematic representation of brassinolide in where four key functional groups in rings A and B and in the steroidal side chain are indicated by colored background. (**B**) A graphic representation of the roles of brassinosteroids in plant development. Red arrows indicate promotion of developmental process by BR while blue indicate inhibition. Low and high refers to low and high BR concentrations. Modified from Yang et al., 2011.

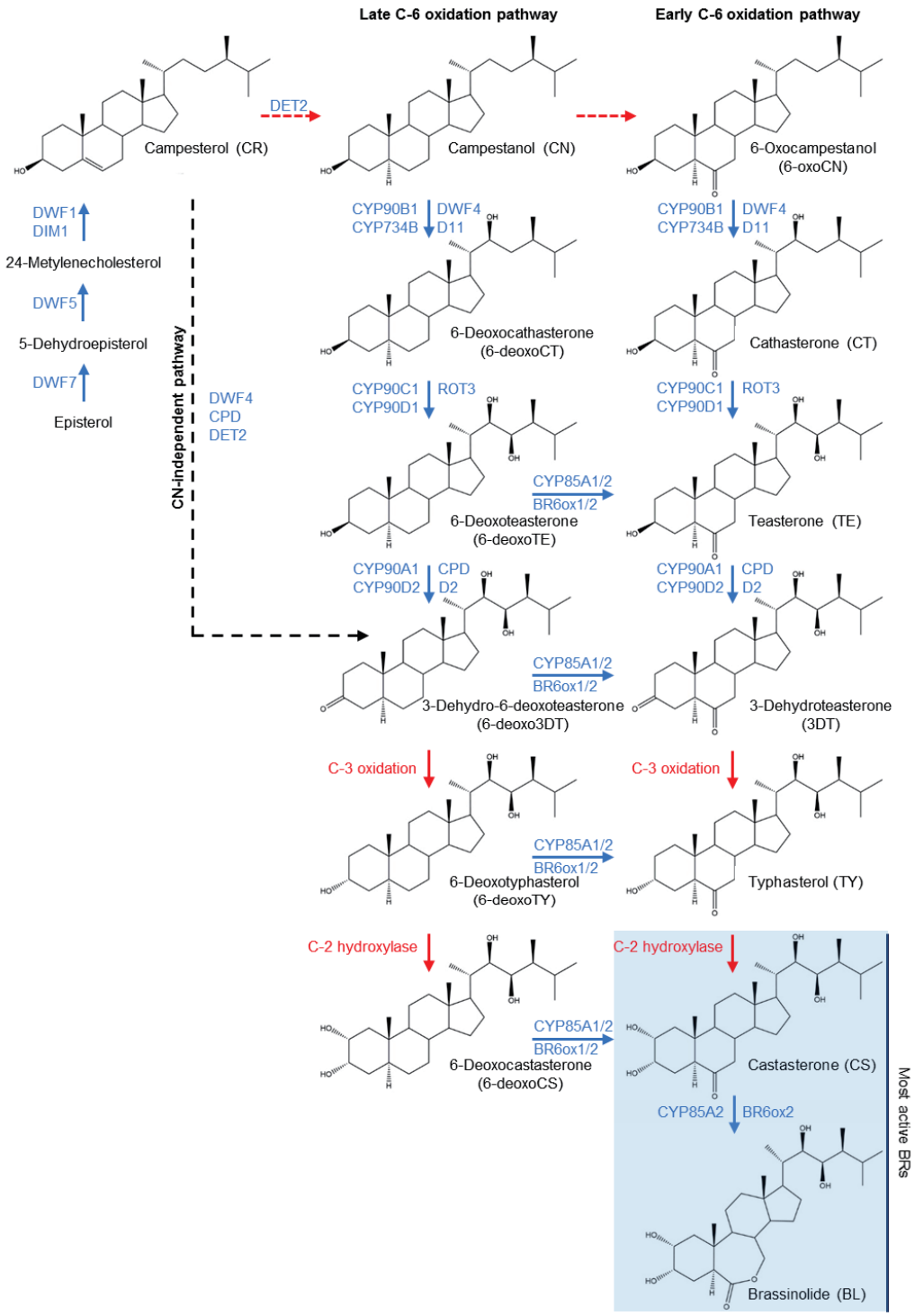
Late C-6 oxidation pathway
Early C-6 oxidation pathway
Campesterol (CR)
DET2
Campestanol (CN)
6-Oxocampestanol
(6-oxoCN)
DWF1
DIM1
24-Metylenecholesterol
DWF5
5-Dehydroepisterol
DWF7
Episterol
CN-independent pathway
DWF4
CPD
DET2
CYP90B1
CYP734B
DWF4
D11
6-Deoxocathasterone
(6-deoxoCT)
Cathasterone (CT)
CYP90C1
CYP90D1
ROT3
CYP85A1/2
BR6ox1/2
6-Deoxoteasterone
(6-deoxoTE)
Teasterone (TE)
CYP90A1
CYP90D2
CPD
D2
3-Dehydro-6-deoxoteasterone
(6-deoxo3DT)
3-Dehydroteasterone
(3DT)
C-3 oxidation
6-Deoxotyphasterol
(6-deoxoTY)
Typhasterol (TY)
C-2 hydroxylase
6-Deoxocastasterone
(6-deoxoCS)
Castasterone (CS)
CYP85A2
BR6ox2
Brassinolide (BL)
Most active BRs

Figure 1-2. Representation of the BR biosynthetic pathway. Solid arrows indicate single reactions, while dashed arrows multiple reactions. Red arrows highlight missing steps. Known enzymes performing the reactions are in blue and red names indicate unknown enzymes with known functions.

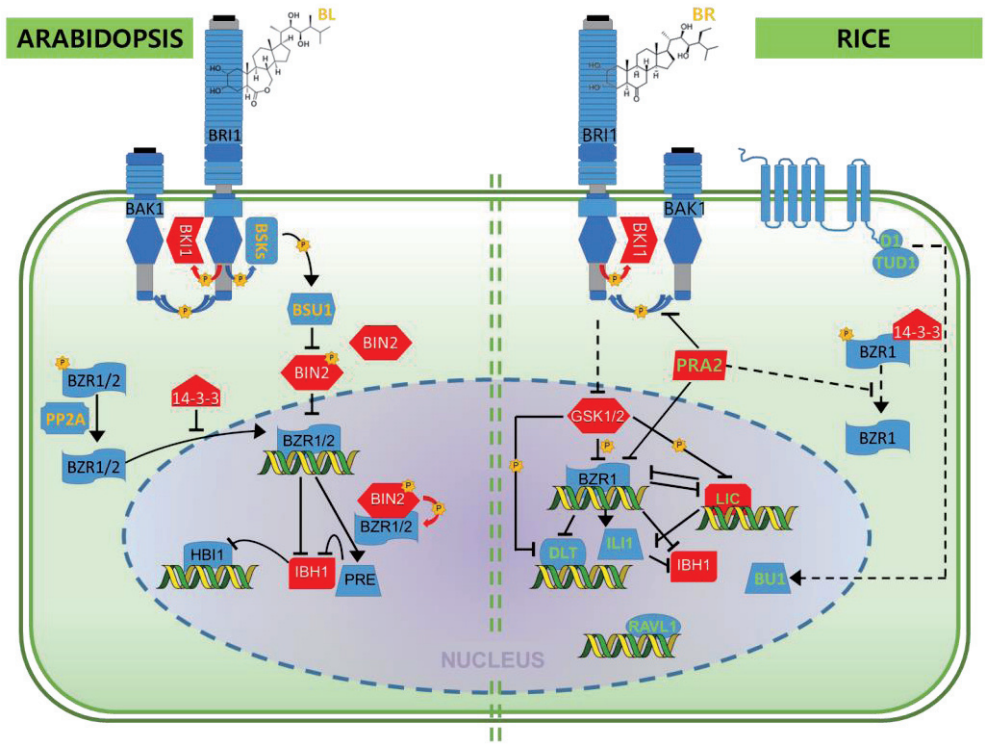

Figure 1-3. BR signaling pathways in Arabidopsis and rice. Comparison of Arabidopsis (left panel) and rice (right panel) components in the BR signaling pathway. Blue figures indicate positive regulators while figures in red present negative regulators of the BR signal. Names in yellow indicate proteins with not homolog genes found in rice. Names in green represent rice-specific modulators.

Table 1-1. Components of the BR signaling in Arabidopsis and rice.

Gene	Arabidopsis homologs	Description	Loss of function	Gain of function	References
	BSKs	Protein kinase			Tang *et al.* 2008
	BSU1	Protein phosphatase			Mora-Garcia *et al.* 2004
	PP2A	Protein phosphatase			Tang *et al.* 2011
14-3-3	*14-3-3*	14-3-3			Bai *et al.* 2007
BKI1	*BKI1*	Membrane-associated phosphoprotein			Wang *et al.* 2006
BU1	*PRE1, BEE1 BIM1*	bHLH transcription factor	erect leaves	enhanced lamina bending	Tanaka *et al.* 2009
D1/RGA1	*GPA1*	G-protein α subunit	dwarf, small seeds		Wang *et al.* 2006
DTL		GRAS family transcription factor	dark-green erect leaves, semi dwarf, less sensitivity to BR		Tong *et al.* 2009
IBH1	*AtIBH1*	bHLH transcription factor	enhanced lamina bending	erect leaves, dwarf	Zang *et al.* 2009
ILI1	*PRE1*	HLH transcription factor	erect leaves	enhanced lamina bending, enhanced BR response	Zang *et al.* 2009
LIC1		CCCH-type zinc finger protein	large leaves and tillering angles, dwarf	erect leaves and reduce BR sensitivity	Zang *et al.* 2012
OsBAK1	*BAK1*	LRR-kinase	dwarf, erect leaves, BR insensitivity	semi dwarf, enhanced lamina bending	Li *et al.* 2009
OSBRI1	*BRI1*	BR receptor	erect leaves, dwarf, BR insensitive		Yamamuro *et al.* 2000
OsBZR1	*OsBZR1/2*	Transcription factor	erect leaves, semi dwarf	enhanced lamina bending	Bai *et al.* 2007
OsGSK1	*BIN2*	GSK3-like kinase	enhanced BR response, enhanced stress tolerance	dwarf	Koh *et al.* 2007
OsGSK2	*BIN2*	GSK3-like kinase	enhanced lamina bending, long seeds and leaves	dwarf, dark-green leaves, fewer tillers.	Tong *et al.* 2012
OsMDP1		MADS box protein	enhanced BR response		Duan *et al.* 2006
PRA2		G-protein	large leaves, enhanced lamina bending	dwarf, small seeds, erect leaves	Zang *et al.* 2016
RAVL1		B3-like DNA binding protein	semi dwarf, dark-green leaves, reduce BR response	Enhanced BR response of the lamina	Je *et al.* 2010
TUD1		U-box E3 ubiquitin ligase	reduce BR sensitivity, dwarf, dark-green erect leaves		Hu *et al.* 2013

Chapter 2. Propiconazole Is a Specific and Accessible Brassinosteroid (BR) Biosynthesis Inhibitor for *Arabidopsis* and Maize

Propiconazole Is a Specific and Accessible Brassinosteroid (BR) Biosynthesis Inhibitor for *Arabidopsis* and Maize

Thomas Hartwig[1,+]., Claudia Corvalan[2,+]., Norman B. Best[1] , Joshua S. Budka[1] , Jia-Ying Zhu[3] , Sunghwa Choe[2,4]*, Burkhard Schulz[1] *

[1] Department of Horticulture and Landscape Architecture, Purdue University, West Lafayette, Indiana, United States of America

[2] School of Biological Sciences, College of Natural Sciences, Seoul National University, Seoul, Korea

[3] Department of Plant Biology, Carnegie Institution for Science, Stanford, California, United States of America

[4] Plant Genomics and Breeding Institute, Seoul National University, Seoul, Korea

+ Equal contribution

* Corresponding author:

Sunghwa Choe shchoe@snu.ac.kr

Burkhard Schulz bschulz@purdue.edu

Published May 9, 2012 in PLOS ONE. DOI: 10.1371/journal.pone.0036625

ABSTRACT

Brassinosteroids (BRs) are steroidal hormones that play pivotal roles during plant development. In addition to the characterization of BR deficient mutants, specific BR biosynthesis inhibitors played an essential role in the elucidation of BR function in plants. However, high costs and limited availability of common BR biosynthetic inhibitors constrain their key advantage as a species-independent tool to investigate BR function. We studied propiconazole (Pcz) as an alternative to the BR inhibitor brassinazole (Brz). Arabidopsis seedlings treated with Pcz phenocopied BR biosynthetic mutants. The steady state mRNA levels of BR, but not gibberellic acid (GA), regulated genes increased proportional to the concentrations of Pcz. Moreover, root inhibition and Pcz-induced expression of BR biosynthetic genes were rescued by 24epi-brassinolide, but not by GA_3 co-applications. Maize seedlings treated with Pcz showed impaired mesocotyl, coleoptile, and true leaf elongation. Interestingly, the genetic background strongly impacted the tissue specific sensitivity towards Pcz. Based on these findings we conclude that Pcz is a potent and specific inhibitor of BR biosynthesis and an alternative to Brz. The reduced cost and increased availability of Pcz, compared to Brz, opens new possibilities to study BR function in larger crop species.

INTRODUCTION

Brassinosteroids (BRs) are poly-hydroxylated steroidal hormones with profound effects on several physiological plant responses. They are involved in regulating cell elongation and division (Azpiroz et al. 1998; Cheon et al. 2010), vascular differentiation (Yamamoto et al. 1997; Fukuda 2004), photomorphogenesis (Neff et al. 1999; Song et al. 2009), leaf angle inclination (Wada et al. 1981; Wada et al. 1984), seed germination (Steber et al. 2001), stomata development (Kim et al. 2012), as well as suppression of leaf senescence and abscission (Iwahori et al. 1990). Radioactive tracer studies in cell cultures of *Catharanthus roseus* established the steps of the BR metabolic pathway (Fujioka et al. 2003). This work was complemented by the characterization of several BR-deficient mutants in Arabidopsis (Gachotte et al. 1995; Kauschmann et al. 1996; Li et al. 1996; Szekeres et al. 1996; Choe et al. 1998; Choe et al. 1999), as well as crops like tomato, pea, and rice (Clouse 2011). These studies showed that several steps of BR biosynthesis are mediated by cytochrome P450 monooxygenases (P450s) (Fujioka et al. 2003; Clouse 2011). Although the importance of BRs for agricultural crops such as sorghum (*Sorghum bicolor*) and maize (*Zea mays* L.) has been recognized (Hartwig et al. 2011), only a few null-mutations have been reported in these species (Hartwig et al. 2011; Makarevitch et al. 2012).

The field of chemical genomics greatly benefited from the use of chemical inhibitors/modifiers (Blackwell et al. 2003; Raikhel et al. 2005). Potent and specific biosynthesis inhibitors are useful tools to evaluate the functions of

endogenous substances, including phytohormones. Biosynthetic mutants and specific metabolic inhibitors displayed their effectiveness in mode of action studies of gibberellic acid (GA) and BRs (Rademacher 2000; Sekimata et al. 2002). Numerous triazole compounds have been shown to inhibit P450s, one of the largest and most ubiquitous group of plant enzymes that catalyze oxidative processes in life systems (Mizutani et al. 2010). Paclobutrazol (Pac) and uniconazole (Ucz) are two triazole plant growth regulators (Figure 2-1) that block sterol 14R-demethylation, phenocopy GA mutants, and reduce endogenous GA levels (Rademacher 2000). Both compounds inhibit P450 CYP701, which catalyzes an early step in GA biosynthesis (Rademacher 2000). Furthermore, Ucz also has been reported to slightly decrease the endogenous concentration of castasterone and inhibits BR-induced tracheary element differentiation (Iwasaki et al. 1991). These reports suggested that Ucz may also affects BR biosynthesis and later screens of structurally similar azoles led to the development of brassinazole (Brz) (Figure 2-1), the first specific BR biosynthetic inhibitor (Asami et al. 1999; Asami et al. 2000).

Brz's mode of action is to bind and block DWF4/CYP90B1. DWF4 is a P450 that mediates multiple rate-limiting C22 alpha-hydroxylations in the biosynthesis of BRs (Asami et al. 2001). *DWF4* expression is a target of regulation by both endogenous signals like auxin (Chung et al. 2011; Maharjan et al. 2011) and exogenous cues like temperature (Maharjan et al. 2011). Brz and its even more specific derivative Brz2001 (Sekimata et al. 2001) became invaluable

tools for BR research. Not only did they help to reveal the role of BRs in various plant species, they were also essential for the isolation and characterization of genes that function in BR signaling (Min et al. 1999; Vert et al. 2005; Kim et al. 2010). However, low accessibility and high costs associated with Brz/Brz2001 have limited their use in agricultural crops that often require large-scale applications. In this context, it would be beneficial to the research community to have access to potent, specific, and more cost efficient azole BR inhibitors in plants.

The triazole compound propiconazole (Pcz), 1-[[2-(2,4-dichlorophenyl)-4-propyl-1,3-dioxolan-2-yl]methyl]-1,2,4-triazole, (Figure 2-1) as a potent inhibitor of BR biosynthesis was first reported after examining its inhibitory effect on hypocotyl elongation of cress plants (*Lepidium sativum*). This inhibitory effect of Pcz was reversed by co-application with brassinolide. Based on the Pcz structure additional BR inhibitors, such as 2RS,4RS-1-[2-(4-trifluoromethylphenyl)-4-n-propyl-1,3-dioxolan-2-ylmethyl]-1H-1,2,4-triazole, were identified (Sekimata et al. 2002). On the other hand, Pcz has been commercially used as fungistat (BannerMaxx, Syngenta) against a broad range of phytopathogenic fungi. Its fungistatic mode of action is the same as that of Ucz and Pac; blocking of lanosterol 14R-demethylase (CYP51A1) (Wiggins et al. 1984; Yoshida et al. 1991). Pcz has also been studied extensively for its toxicity on plants, animals, humans, and the environment (Thorstensen et al. 2001; Li et al. 2013). Here we present a molecular genetic analysis of Pcz's effects on Arabidopsis and maize

seedlings. Our results indicate that Pcz is a potent and specific inhibitor of the BR metabolic pathway in plants.

MATERIALS AND METHODS

Plant materials and growth conditions

Seeds of *Arabidopsis thaliana* were surfaced-sterilized before being sprinkled on 0.8% agar-solidified media containing 0.5× Murashige and Skoog salts and 1% sucrose. After one day of stratification at 4°C, plates were transferred to a growth room and grown under a 16 h photoperiod. For the *bzr1-1D* experiments, seedlings were stratified for 48 h at 4°C, irradiated for 6 hours to promote germination and then transferred to a growth chamber and grown in the dark at 22°C.

Maize plants were grown under greenhouse conditions at 27°C (day) and 21°C (night). Unless indicated otherwise, plants were grown in coarse Vermiculite (SunGro Horticulture, Bellevue, WA and Perlite Vermiculite Packaging Industries, Inc., North Bloomfield, OH). Plants were fertilized with 200 ppm Miracle-Gro Excel (Scotts, Marysville, OH) adjusted to pH 6 following manufacturer recommendations.

Chemical treatments and morphological analysis

Seedlings of 3-day old Ws-2 wild type were transferred to agar-solidified media supplemented with Pcz (Banner Maxx, Syngenta, Greensboro, NC), Brz (gift from Shozo Fujioka, Riken, Japan) and Ucz (Consise, Fine Americas Inc., Walnut Creek, CA) alone or in combination with BL (Sigma Aldrich, St Louis, MO) or GA_3 (Gold Biotechnology, St. Louis, MO). Media plates were placed vertically to ease morphometric analysis of the root and each plate contained more than 10

seedlings. After 3 days of treatment, images were taken and the growth parameters were analyzed using ImageJ software. For treatments with Pcz and Brz of BR mutants (*dwf4-1*, *dwf7-1* and *bri1-5*) and its Ws-2 wild type, the seedlings were grown for 7 days on MS media before being transferred to the inhibitor-containing media. Measurements were done after 3 days of the treatment. *bzr1-1D* and its wild type Col-0 seedlings were grown in the dark on MS media containing Pcz or Brz for 7 days and hypocotyl lengths were measured.

For all treatment experiments in maize, seeds were sterilized for 7 min at 60°C in a water bath prior to planting and grown under greenhouse conditions. For de-etiolation assays, maize seeds were imbibed for 28 h in paper towels and soaked with distilled water containing indicated concentrations of Pcz or Ucz. They were then planted 10 cm deep in 15 cm wide pots with coarse Vermiculite, watered with identical concentrations of Pcz or Ucz, and grown for additional 7 d at 28°C and 90% humidity in the dark. Control plants were grown in the dark or light in the absence of Pcz or Ucz treatment. Plants were then harvested, photographed, and analyzed using ImageJ software. Mesocotyl length was determined from the root-shoot transition zone to the first node. Coleoptile and true leaf length was measured from the first node to the tip of the coleoptile or true leaves, respectively, whereas the length of the main root was used to determine root length.

For light grown Pcz experiments, W22 seeds were planted 5 cm deep in 24.5 cm wide pots with coarse Vermiculite and watered every fifth day. Pcz was added at indicated concentrations to the water solution. After 21 days plants were harvested,

photographed, and analyzed using ImageJ. Plant height was measured from the root-shoot transition zone to the highest leaf collar, whereas the length of the main root was used to determine root length.

RNA extraction and qRT-PCR detection of gene transcripts

Arabidopsis thaliana Ws-2 seeds were surface sterilized and stratified for 48 h at 4°C, followed by growth for 4 days at 100 µmol/m^2/sec, 16:8 h light/dark cycle at 25°C. The seedlings were then transferred into Erlenmeyer flasks prefilled with 50 ml ½ MS with 1% sucrose liquid media (pH 5.7) and were allowed to grow for 2 d at 100 rpm under the conditions described above. For the treatments, 500× stock solutions were made in 50% DMSO (0.1% final concentration) and 100 µl of each stock solution, or 50% DMSO for the mock treatment, were applied at the beginning of the light cycle on day 7. After 10 h at 100 rpm the seedlings were harvested and immediately frozen in liquid nitrogen.

Total RNA was isolated from seedlings, as described by Eggermont et al. (Eggermont et al. 1996). For qRT-PCR analysis, total RNA was pre-treated with DNase I (Invitrogen), and cDNA was synthesized using Reverse Transcriptase (Invitrogen). Ubiquitin conjugating enzyme 21 used as internal control was amplified with UBC21_FOR (300 nM) and UBC21_REV (300 nM). Gen-specific primers used were: DWF4_FOR1 (500 nM); DWF4_REV1 (500 nM); BR6ox2_FOR1 (300 nM) and BR6ox2_REV1 (300 nM); CPD_FOR1 (500 nM) and CPD_REV1 (500 nM); BAS1_FOR1 (1100 nM) and BAS1_REV1 (1100 nM); BZR1_FOR1 (300 nM) and BZR1_REV1 (300 nM); GA2ox1_FOR2 (500 nM)

and GA2ox1_REV2 (500 nM) as well as GA20ox1_FOR1 (500 nM) and GA20ox1_REV1 (500 nM). Primer sequences are listed in Table S2-1. All primers showed >90% efficiency at their indicated concentrations. qRT-PCRs were performed as described previously (Orlova et al. 2009; Hartwig et al. 2011) using the StepOnePlus instrument (Invitrogen). Each data point represents the average of three independent biological replicates (approximately 30 samples per replicate), with three technical replicates

Statistical analysis

The Microsoft Excel© add-in XL Toolbox (ver. 3.02 http://xltoolbox.sourceforge.net) was used to obtain all descriptive and comparative statistics. Analyses of variance (ANOVA) for sets of data groups were performed with "Multiple comparisons/Post-hoc" testing. Once a significant difference (p<0.05) was detected, "Post-hoc" tests, using the Holm-Sidak algorithm, were performed to test which of the possible multiple comparisons between the data groups were significant.

RESULTS

Arabidopsis seedlings treated with Pcz display dwarf phenotypes

To study Pcz's impact on Arabidopsis, we treated wild-type Ws-2 plants with Pcz concentrations ranging from 0.1 to 5 μM for 5 days. Cotyledons showed a reduction in size and epinatic growth responses with treatments of Pcz (Figure 2-2A and B). Subsequently, we evaluated the effect of Pcz on primary root length. The results showed a dose-dependent reduction of primary root growth, where 0.1 μM Pcz decreased the elongation by 20% and 5 μM Pcz by 54% compared to mock conditions (Figure 2-2A and C). No further significant decrease was observed at concentrations higher than 0.5 μM Pcz (Figure 2-2C).

We then evaluated the overall efficacy and specificity of Pcz compared to equal concentrations of Brz and Ucz. Wild-type Ws-2 plants treated with 1 μM Pcz or Brz for 4 days showed comparable reductions in root length of 38% and 41%, respectively (Figure 2-2D). In contrast, the impact of 1 μM Ucz on reduction of root length was significantly less with only a 25% decrease compared to mock treatments. We found a complementation of the phenotypes induced by 1 μM Pcz or Brz, but not 1 μM Ucz, with co-applications of 0.1 μM 24epi-brassinolide (BL), a bioactive epimer of brassinolide. Root length of plants co-treated with 1 μM Pcz plus 0.1 μM BL was not significantly different from mock treatments. On the contrary, the co-application of 1 μM Ucz and 0.1 μM BL showed no significant difference to treatments with 1 μM Ucz alone (Figure 2-2D). These results suggest

that Pcz and Brz have comparable efficacies in the inhibition of the BR biosynthetic pathway.

In some cases, triazole derivatives affect multiple targets; although usually to a varying extent (Min et al. 1999). To address whether Pcz inhibition is specific to the BR biosynthetic pathway or also affects P450 monooxgenases in GA biosynthesis, we compared co-applications of Pcz with BL or GA_3.
Again, *Arabidopsis* seedlings co-treated with Pcz and BL showed no difference in primary root length compared to mock conditions. In contrast, Pcz induced-inhibition of root length was not recovered by exogenous co-application of GA_3 (Figure 2-3A and C). We did find a slight increase (17%) in root length with the co-application of Pcz and GA_3relative to Pcz treatment, however, a similar increase (11%) was found for GA_3 application compared to mock. Taken together, the results indicate that the inhibition of root growth caused by Pcz is complemented by the co-application of BL, but not GA_3.

Arabidopsis brassinazole resistant1-1D (*bzr1-1D*) mutants carry a dominant gain of function mutation in the transcription factor and major component of BR signaling, *BZR1*, which results in a constitutive BR response even in the absence of BRs. Therefore, *bzr1-1D* mutants are sensitive indicators for BR inhibitor specificity (Wang et al. 2002). Wild-type (Col-0) plants treated with 2 µM Pcz showed a reduction in hypocotyl length of 83%, whereas *bzr1-1D* mutants exhibited only 4% shorter hypocotyls, compared to mock (Figure 2-3D and F). Although *bzr1-1D* plants were more resistant to Brz applications than wild type, 2

μM Brz did reduce the length of *bzr1-1D* hypocotyls by 37% compared to mock (Figure 2-3E and F).

BR biosynthesis mutants show reduced sensitivity towards Pcz

The azole ring of Brz binds to the heme prosthetic group of DWF4 (CYP90B1), the rate-limiting enzyme in BR biosynthesis, forming a coordination complex, which impairs DWF4 activity (Asami et al. 2001). Mutants already deficient in BR biosynthesis should thus show a reduced sensitivity towards BR biosynthetic inhibitors such as Brz and Pcz. We tested wild-type and *dwf7-1* seedlings with Pcz and compared their responses to Brz treatments (Figure 2-4). DWF7 catalyzes the conversion of episterol to 5-hydroepisterol upstream of DWF4 (Choe et al. 1999). Wild-type (Ws-2) plants treated with either 1 μM Pcz or Brz, or 10 μM Brz produced 46%, 37%, and 64% shorter roots compared to mock conditions, respectively (Figure 2-4A and F). Although *dwf7-1* showed a significant response to 1 μM Pcz and 10 μM Brz treatments, the relative reduction (25% and 30%, respectively) was still lower than Pcz/Brz treated Ws-2 (Figure 2-4B and G). *bri1-5*, a weak allele of the major BR receptor *BRASSINOSTEROID RESISTENT1* (*BRI1*), and wild type respond similarly to Brz, but not to BL treatment (Li et al. 2009; Belkhadir et al. 2010). This suggests that although *bri1-5* is affected in BR signal transduction, it still responds to changes in BR homeostasis. We found that Pcz and Brz, at equal concentrations, had similar effect on *bri1-5* and Ws-2 (Figure 2-4A, C, F and H).

Since DWF4 has been shown to be a direct target of Brz (Asami et al. 2001), which is structurally similar to Pcz (Figure 2-1), we also took a closer look at the effect of Pcz on *dwf4* mutants. Ws-2 plants again showed a decrease in root length upon Pcz or Brz treatment (Figure 2-5A and C), but *dwf4-1* mutants did not exhibit a significant reduction (Figure 2-5B and C).

Pcz specifically influences the expression of BR biosynthetic genes

Transcriptional feedback regulation of rate-limiting step enzymes is a critical mechanism to maintain hormone homeostasis (Kim et al. 2006). Since triazole derivatives can have multiple targets, we evaluated the expression levels of both BR (*DWF4*, *BR6ox2*, *CPD*, *BAS1* and *BZR1*) and GA (*GA20ox1* and *GA2ox1*) related genes, to further assess the specificity of Pcz.

Using quantitative real-time PCR (qRT-PCR) we found a dose-dependent induction of BR biosynthetic gene expression (*DWF4*, *BR6ox2*, and *CPD*) with increasing Pcz concentrations (Figure 2-6A). With the same treatment conditions the mRNA levels of *BAS1*, a gene involved in BR degradation (Neff et al. 1999), showed a downward trend (Figure 2-6B). BZR1, a key regulator of BR signaling, did not show relevant changes in its expression upon Pcz treatments. The GA biosynthesis gene *GA20ox1*, which is feedback regulated by endogenous GA levels (Rademacher 2000), also showed no increase in expression upon Pcz application (Figure 2-6B).

The Pcz-induced increase in mRNA accumulation of *DWF4* and *BR6ox2* and concomitant decrease in *BAS1* expression was offset by co-application of Pcz with BL, but not by Pcz with GA_3 (Figure 2-6C). Our results also showed an expected decrease in *DWF4* and *BR6ox2* expression upon BL and to a smaller extent *GA20ox1* upon GA_3 treatment ($p=0.06$) (Figure 2-6C and D). Together these findings suggest that Pcz specifically affects BR regulated genes and do not provide evidence for an inhibitory effect on GA biosynthesis.

Pcz induces dwarfism in dark and light grown maize inbred W22 seedlings

Studies on crop species such as sorghum, rice, and maize often require large amounts of growth media which limits the use of cost intensive inhibitors such as Brz. For that reason, we tested the effect of Pcz on both dark and light grown seedlings of the maize inbred line W22. A strong reduction of hypocotyl elongation is one of the most striking characteristics of the de-etiolation phenotype of dark grown *Arabidopsis* mutants deficient in BR biosynthesis. Compared to mock, W22 seedlings grown in the dark for 8 d in the presence of 0.5 to 30 µM Pcz showed decreased mesocotyl elongation ranging from 27% to 64%, respectively (Figure 2-7A and C). Ucz treatment of 0.5 to 30 µM reduced the length of the mesocotyl 25% to 73% (Figure 2-7C). Similar to the mesocotyl, the lengths of true leaves were reduced from 21% to 51% by Pcz and from 20% to 56% by Ucz, respectively (Figure 2-7D). Although both Pcz and Ucz treatment affected the coleoptile, the relative reduction in length was less pronounced than in mesocotyls and true leaves (Figure 2-7E). Surprisingly, the primary root of W22 seedlings showed significant

differences in sensitivity towards Pcz and Ucz. Pcz concentrations up to 30 μM had no significant effect on primary root length. In contrast, seedlings treated with equal or greater than 5 μM Ucz resulted in significantly shorter primary roots when compared to mock (Figure 2-7F), reaching a reduction of 73% at 30 μM.

Pcz treatment also induced dwarfism in light grown W22 seedlings. Plants treated with 0.2 to 5 μM Pcz decreased their overall height by 29% to 45%, respectively (Figure 2-7B and G). In addition to the dwarf stature, Pcz induced shorter leaves and resulted in a more overall compact appearance (Figure 2-7B). Interestingly, unlike in dark treatments, the primary root length of seedlings grown for 21 d in the light was reduced by 30% when treated with 5 μM Pcz relative to mock (Figure 2-7H).

The genetic background of maize influences tissue specific sensitivity to Pcz

Given the great diversity between maize inbred lines (Liu et al. 2003), we assessed whether the genetic background influences the effects of Pcz and Ucz on dark grown maize seedlings. Thus, we repeated the dark assay using 3 additional maize inbred lines: Mo20W, A619, and B73. The length of the four evaluated tissues (mesocotyl, true leaves, coleoptile, and primary root) showed significant differences between Mo20W, A619, and B73 even in the absence of Pcz or Ucz (Figure 2-8A and G). In addition, when treated with Pcz or Ucz we observed significant differences between the inbred lines in both their overall and tissue-specific sensitivity. In the presence of 1 or 10 μM Pcz the mesocotyl length of Mo20W was reduced by 57% and 56%, respectively, relative to mock treatment

(Figure 2-8A and D). Likewise, B73 treated with the same concentrations of Pcz exhibited 40% and 52% shorter mesocotyls, respectively (Figure 2-8C and D). However, in the case of A619, only 10 μM Pcz had a significant but smaller impact (35%) on mesocotyl elongation, relative to mock (Figure 2-8B and D). Comparable results were obtained for the response of true leaves to Pcz and Ucz treatments (Figure 2-8A, C and E).

The primary roots of Mo20W, A619, and B73 showed a significant reduction in length when treated with 1 or 10 μM Ucz (Figure 2-8A to C and G). Interestingly, Mo20W and B73 showed, in addition to the Ucz sensitivity, a decrease in primary root length when treated with 1 or 10 μM Pcz. The primary root length of A619 was reduced significantly only at 10 μM Pcz, but to a smaller extent than Mo20W and B73 (Figure 2-8A to C and G). The coleoptile was the only tissue evaluated with comparable responses to both Pcz and Ucz in all three inbred lines (Figure 2-8A to C and F).

To test whether the differences in Pcz efficacy are due to differences in BR response, we compared the effect of BL on root elongation between the maize inbreds. W22 and A619 plants treated with 20 μM BL exhibited the smallest relative reduction (37% and 44%, respectively) in root length (Figure 2-9). On the other hand, Mo20W and B73 inbreds treated with the same amount of BL had 67% and 60% shorter roots than mock, respectively (Figure 2-9). This result is consistent with our previous findings for Pcz sensitivity, and supports our hypothesis that genetic diversity influences BR responses in maize.

DISCUSSION

Phytohormone biosynthesis inhibitors allow the species-independent study of hormonal function during plant development. Inhibitor studies can also support the isolation and characterization of hormone deficient mutants without prior knowledge of the mutant phenotype. Pcz has previously been reported to impair the hypocotyl growth of cress seedlings and that this inhibition is reversible by the co-application of BL. Chemical modification of Pcz also revealed structural elements essential for its inhibitory properties (Sekimata et al. 2002). Pcz's high accessibility and economical aspects prompted us to conduct a comparative analysis with the established BR inhibitor Brz.

Pcz treatment of *Arabidopsis* seedlings produced typical BR-deficient phenotypes such as: epinastically growing and dark-green cotyledons, reduced hypocotyl length, and a significantly shorter primary root (Figure 2-2). Using root length as a reference we found that even relatively low Pcz levels of 0.5 µM resulted in strong inhibition (Figure 2-2). As shown in independent experiments, the impairment of root growth in *Arabidopsis* through Pcz treatment can essentially be restored to length of mock-treated seedlings by BL, but not GA_3 (Figure 2-3). The slight effect of GA_3 on root elongation was independent of Pcz treatment and may not indicate a recovery of Pcz inhibition. In contrast, BL treatment had a dramatic effect on root elongation in Pcz treated seedlings (Figure 2-3).

In the absence of BR, the transcription factor BZR1 and its homolog BZR2 (BES1) are phosphorylated by the GSK3/SHAGGY-like protein kinase BIN2 (He et al. 2002; Wang et al. 2002). Phosphorylation negates BZR1's DNA-binding capacity and increases its cytoplasmic retention by phosphopeptide-binding 14-3-3 proteins (Yin et al. 2002; Bai et al. 2007; Gampala et al. 2007). The dominant *bzr1-1D* mutation increases BZR1's dephosphorylation by the phosphatase PP2A (Tang et al. 2011). BZR1 therefore remains nuclear localized and stabilized even in the absence of BRs causing *bzr1-1D* plants to show a constitutive BR response (Wang et al. 2002; Tang et al. 2011). In contrast to wild type, *bzr1-1D* mutants showed only a minor inhibition of hypocotyl growth in the presence of Pcz (Figure 2-3). Current evidence in rice and cress suggests that Brz inhibits BR biosynthesis but also affects GA responses (Sekimata et al. 2001). We found that *bzr1-1D* plants were more sensitive to Brz than Pcz (Figure 2-3) which suggests that Pcz is more specific. This hypothesis is supported by our finding that roots co-treated with Brz and BL, but not with Pcz and BL, were significantly shorter than mock (Figure 2-2).

Ucz has been extensively studied as an inhibitor of GA biosynthesis (Rademacher 2000). Circumstantial evidence reported by Yokota et al. and Iwasaki and Shibaoka (Iwasaki et al. 1991) indicates that Ucz might also act as a demethylase inhibitor in BR biosynthesis. We observed shorter roots and hypocotyls of Ucz-treated *Arabidopsis* seedlings. Although Pcz- and Ucz-induced phenotypes were similar, co-application of Ucz and BL was not significantly

different to Ucz alone (Figure 2-2). Based on these analyses, Pcz-mediated suppression of root and hypocotyl elongation is likely the result of a specific inhibition of the BR biosynthetic pathway.

DWF7/STE1 is a Δ^7 sterol C-5 desaturase that converts avenasterol to dehydroavenasterol or episterol to 5-dehydroepisterol early in BR biosynthesis (Choe et al. 1999). Significant reduction of root elongation with Pcz treatment was found in wild type and to lesser extent also for *dwf7-1* seedlings, whereas roots of *dwf4-1* mutants did not exhibit a significant decrease (Figure 2-4, Figure 2-5). The BR metabolic pathway is likely non-linear, as downstream BR intermediates can be found in most monogenic BR biosynthetic mutants, including *dwf7-1* (Choe et al. 1999; Choe et al. 1999; Noguchi et al. 1999). Therefore, Pcz treatment may further reduce endogenous BR pools in *dwf7-1* mutants. Loss of function mutations in *DWF4* result in a more severe phenotype which could be the reason why no further reduction in root length was observed in *dwf4-1* upon Pcz treatment. Alternatively, since DWF4 could be the target of Pcz – like for Brz (Asami et al. 2001) – an additional inhibition of growth can not be expected in an already genetically disrupted *dwf4-1* mutant. From our findings we conclude that BR biosynthesis mutants show a reduced sensitivity towards Pcz.

Another line of evidence that Pcz is a specific and potent BR biosynthesis inhibitor comes from transcriptional analyses of BR and GA regulated genes in *Arabidopsis*. BR homeostasis relies on the feedback regulation of *DWF4* transcription (Kim et al. 2006). Thus, differences in *DWF4* expression

reflect even minor changes in BR biosynthesis. As expected, we found that BL treatment reduced the expression of *DWF4* and other BR-biosynthetic genes in wild type, whereas Pcz application resulted in a dose-dependent increase of *DWF4*, *CPD* and *BR6ox2* transcripts (Figure 2-6). The induction of *CPD* expression relative to *DWF4* and *BR6ox2* was lower upon Pcz application, however, *CPD* is primarily post-transcriptionally regulated (Belkhadir et al. 2010). The Pcz dependent induction of BR biosynthetic gene expression was offset by the co-application of BL similar to BL treated controls. With co-application of GA_3 this Pcz dependent induction was not reverted (Figure 2-6).

PHYB ACTIVATION TAGGED SUPPRESSOR1 (BAS1/CYP72B1) catalyzes the conversion and inactivation of BL to 26-Hydro-BL. Similar to DWF4, BAS1 is feedback regulated by endogenous BR levels (Neff et al. 1999). We observed that BAS1 expression was induced by BL application and repressed by Pcz treatment (Figure 2-6).The co-application of Pcz with BL, but not with GA_3, countered the effect of Pcz on *BAS1* repression.

GA_{20}-oxidases catalyze the sequential conversions of GA_{53} to GA_{20}, late in the GA biosynthetic pathway (Hedden et al. 1997). Similar to *DWF4*, *GA20ox*-metidated steps are flux determining (Xu et al. 1997; Coles et al. 1999) and their expression is under feedback regulation (Xu et al. 1999). Similar to the observations for BR-biosynthetic genes, *GA20ox1* expression appeared negatively regulated by GA_3 (Figure 2-6). However, mRNA levels of *GA20ox1* were not increased over a broad spectrum of Pcz concentrations (Figure 2-6). These findings

are corroborated by data from the Genevestigator database (Zimmermann et al. 2004), which also shows a regulation of GA20-oxidases by both GA and Pac, but not Pcz. The expression pattern of GA catabolic gene *GA2ox1* (Hedden et al. 1997) showed an expected induction upon GA_3 application, but did not display relevant differences with either Pcz or BL treatments (Figure 2-6). Interestingly, the GA-dependent increase in *GA2ox1* expression was impaired by simultaneous treatment with Pcz (Figure 2-6). Interpreting this result, we cannot exclude the possibility of a BR-dependent GA regulation of *GA2ox1* expression. Our data also showed an overlap in the expression patterns of *BAS1* and *GA20ox1* (Figure 2-6). Taken together these results do not provide evidence for a negative effect of Pcz on GA biosynthesis.

To investigate if Pcz responses found in *Arabidopsis* can be corroborated with monocot plants we chose maize, a member of the prominent grass family (*Poaceae*). This family, of close to 10,000 species, encompasses important genetic models like *Brachypodium distachyon* (Draper et al. 2001), as well as important food crops such as wheat, rice, and maize. Recently, we have shown that Pcz treatment of wild type maize phenocopies the BR deficient dwarf *nana plant1* (*na1*) and also that *na1* plants are more Pcz resistant than wild type or GA impaired mutants (Hartwig et al. 2011). Using comparative treatments of increasing Pcz or Ucz concentrations we found a strong decrease in the mesocotyl length of dark-grown W22 seedlings (Figure 2-7). Similar responses were detected for true leaves (Figure 2-7). In comparison, the response of coleoptiles towards

inhibitor treatments was less pronounced (Figure 2-7). This indicates either a tissue-specific sensitivity towards Pcz or different BR levels in coleoptiles. The coleoptile, whose main role is support of juvenile leaves during soil penetration, originates directly from the pro-embryo and not from the apical meristem like the true leaves. It is therefore possible that these tissues have different reception and signaling systems for BRs.

In contrast to the results obtained with *Arabidopsis* we discovered that W22 roots were resistant towards Pcz. While Ucz treated dark-grown roots of W22 showed drastically reduced elongation, no significant response was observed over a broad range of Pcz concentrations up to 30 µM (Figure 2-7). While light-grown maize seedlings are obligate heterotrophic until day 7, an equal balance between heterotrophic and autotrophically produced carbon is reached on day 10 for leaves, and day 13 to 14 for roots. The slight reduction (30%) in root length observed in light-grown seedlings may be explained by the fact that these plants were measured after the switch to autotrophy when most of their carbon comes from photosynthesis. The strong reduction in plant height and decrease in photosynthetically active leaf surface at 5 µM Pcz treatment suggests that the plants had a decreased capacity to produce photosynthates. On the other hand, we analyzed dark-grown plants during a phase when they received most nutrients from the endosperm. These results may allude to fundamental differences in the control of cell elongation between W22 and *Arabidopsis* roots.

Maize roots contain the enzymes for the late C-6 oxidation steps of BR biosynthesis (Kim et al. 2005). Our observation of differential Pcz resistance of W22 roots raised the question if this is a feature specific to W22 inbreds. We therefore tested the effect of genetic diversity in maize inbreds (Liu et al. 2003) towards Pcz response using the lines Mo20W, A619, and B73. Significant differences between these inbred lines in the length of four analyzed tissues were observed even under mock conditions. Furthermore, we found significant differences in tissue specific sensitivity towards Pcz and Ucz (Figure 2-8). In general, Mo20W showed the highest sensitivity and A619 the highest resistance towards both inhibitors. Concerning tissue-specific responses, the coleoptile was the only organ which showed an even response to both Pcz and Ucz treatment in Mo20W, A619, and B73. In contrast, Pcz sensitivity in the roots and true leaves ranged from resistant (A619) to highly susceptible (B73 and Mo20W). The degree of Pcz response in maize roots seems therefore dependent on the genetic background of the maize line. The data also indicates differential hormonal regulation of tissue growth in aerial organs of maize inbreds. In rice and wheat tissue culture, accumulation of Pcz against a concentration gradient has been reported. This indicates active uptake systems in these grass species. In *Monilinia fructicola*, the ABC transporter MfABC1 is induced upon Pcz treatment, which suggests a possible role for transporters of the ABC family (Schnabel et al. 2003) in Pcz uptake in plants and fungi (Verrier et al. 2008). Differences in either root uptake, *in planta* transport, and/or Pcz catabolism may be responsible for the observed variances between maize inbreds. Nonetheless, our results also indicated

a relation of Pcz- and BL-sensitivity between the inbred lines. Compared to Mo20W and B73, W22 and A619 plants exhibited a smaller inhibition of root elongation in the presence of either Pcz or higher concentrations of BL (Figure 2-8, Figure 2-9). We therefore conclude that the genetic diversity between these maize lines influences their response to BRs.

We presented independent lines of evidence which indicate that Pcz inhibits BR metabolism and induces BR deficiencies in both *Arabidopsis* and maize seedlings. *Arabidopsis* seedlings treated with Pcz phenocopied BR deficient mutants such as *dwf7* and *dwf4*. Similarly, Pcz-induced dwarf phenotypes were discovered in both light and dark grown maize seedlings. Growth responses towards Pcz and Ucz were not equally expressed in all measured tissues of maize. Tissue specific sensitivity of Pcz in the coleoptile, mesocotyl, true leaves, and primary roots alludes to differential BR biosynthesis and/or signal transduction for the different maize tissues. Genetic variation of maize inbred lines implies that genetic enhancers and suppressors play a key role in Pcz-induced physiological responses. We presented that Pcz is a potent alternative to the commonly used Brz with a comparable specificity and efficacy. In contrast to Brz/Brz2001, Pcz is easily accessible and the associated costs are much lower, allowing its use for large-scale chemical genomics and field testing.

FIGURES AND TABLES

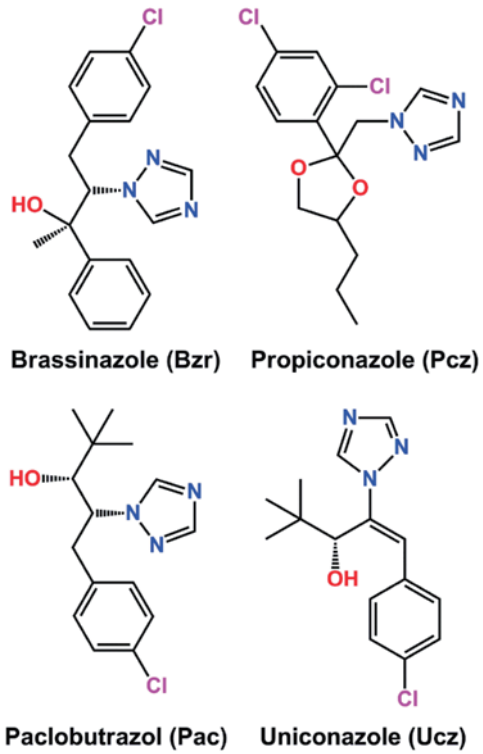

Figure 2-1. Chemical structures of brassinazole, propiconazole, paclobutrazole, and uniconazole. Structure elements critical for inhibitor activity have been color-coded: (blue) nitrogen atoms in the azole ring; (purple) chlorine atom(s) of the phenyl ring; and (red) either primary/secondary hydroxyl group or 1,3-dioxlane. Structures were drawn using the ChemBioDraw 12.0.2 software and structures were compared to the ChemACX 12.12.1 database.

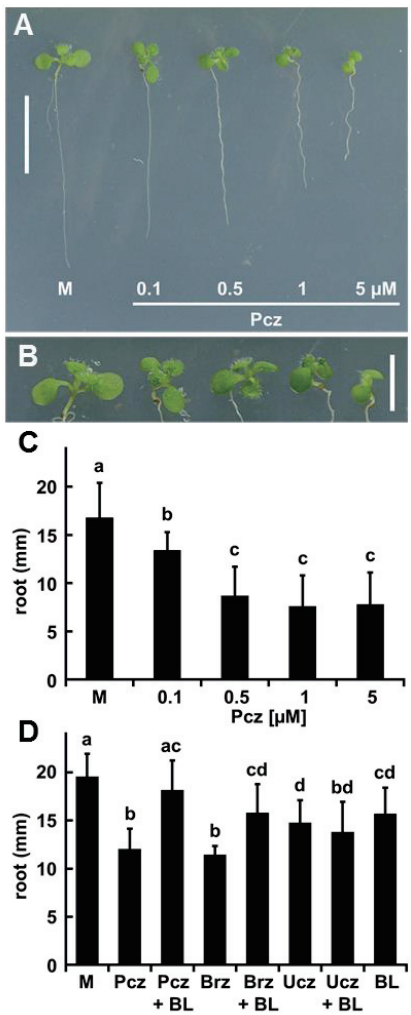

Figure 2-2. Responses of *Arabidopsis* seedlings to inhibitor treatments and BL Complementation. (**A–C**) 3-day old Ws-2 seedlings were transferred to ½ MS media containing 0, 0.1, 0.5, 1, or 5 µM of Pcz and incubated for 5 more days. (**A**) Seedlings at the end of treatment (5 d). (**B**) Close-up of the cotyledons and true leaves in the same order as (**A**). (**C**) Average root lengths at day 3 of treatment are illustrated (*n*>15). (**D**) 3-day old Ws-2 seedlings were transferred to ½ MS media

containing 1 μM of Pcz, Brz, Ucz, or co-applications of inhibitors (1 μM) with 0.1 μM BL or 0.1 μM BL alone and incubated for 4 more days. Average root lengths at the end of treatment (n>15). (**C–D**) Error bars represent standard deviation and lowercase letters indicate significant differences among treatments determined by "Post-hoc" test. Scale bar (**A**) 1 cm and (**B**) 0.5 cm.

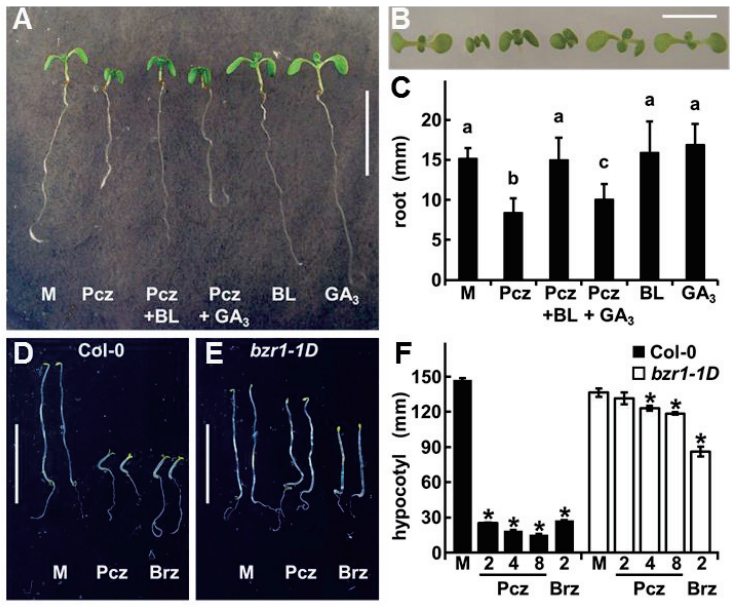

Figure 2-3. Pcz specificity towards BR biosynthesis inhibition. (**A–C**) 3-day old Ws-2 were transferred to ½ MS media containing either 1 µM Pcz, 0.1 µM BL, 10 µM GA_3, or co-applications of 1 µM Pcz with 0.1 µM BL or 10 µM GA_3 and grown for 3 more days. (**A**) Seedlings at the end of treatment. (**B**) Close-up of the cotyledons and true leaves in the same order as (**A**). (**C**) Average root lengths at day 3 of treatment (n>15). (**D–F**) Col-0 and *bzr1-1D* (Col-0) grown on ½ MS media in the dark for 7 days. (**D**) Col-0 or (**E**) *bzr1-1D* grown on medium with 2 µM Pcz or 2 µM Brz. (**F**) Hypocotyl lengths of Col-0 and *bzr1-1D* grown on medium with 2, 4, 8 µM Pcz or 2 µM Brz (n≥10). (**C**, **F**) Error bars represent standard deviation. (**C**) Lowercase letters indicate significant differences among treatments determined by "Post-hoc" test (p<0.05). (**F**) Asterisks indicate

significant difference to the respective mock determined by Student's *t*-test ($p<0.01$). Scale bar (**A**, **D**, **E**) 1 cm and (**B**) 0.5 cm.

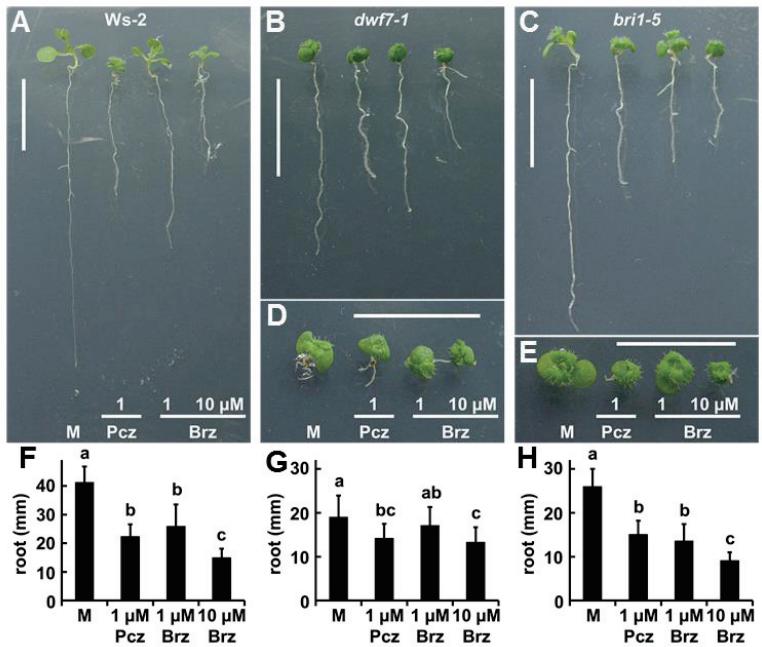

Figure 2-4. Sensitivity of *Arabidopsis* wild type, BR biosynthetic mutant *dwf7-1*, and signaling mutant *bri1-5* to Pcz and Brz. (**A**–**C**) Seedlings of (**A**) Ws-2, (**B**) the BR biosynthetic mutant *dwf7-1* (Ws-2), and (**C**) the BR signaling mutant *bri1-5* (Ws-2) grown on ½ MS media with either 1 µM Pcz or Brz or 10 µM Brz. (**D**–**E**) Close-up of the shoot apices harboring cotyledons and the first pair of true leaves of (**D**) *dwf7-1* and (**E**) *bri1-5*. (**F**–**H**) Average root lengths of (**F**) Ws-2, (**G**) *dwf7-1* and (**H**) *bri1-5* measured at the end of treatments (n>10). (**F**–**H**) Error bars represent standard deviation and lowercase letters indicate significant differences among treatments determined by "Post-hoc" test (p<0.05). Scale bar (**A**–**E**) 1 cm.

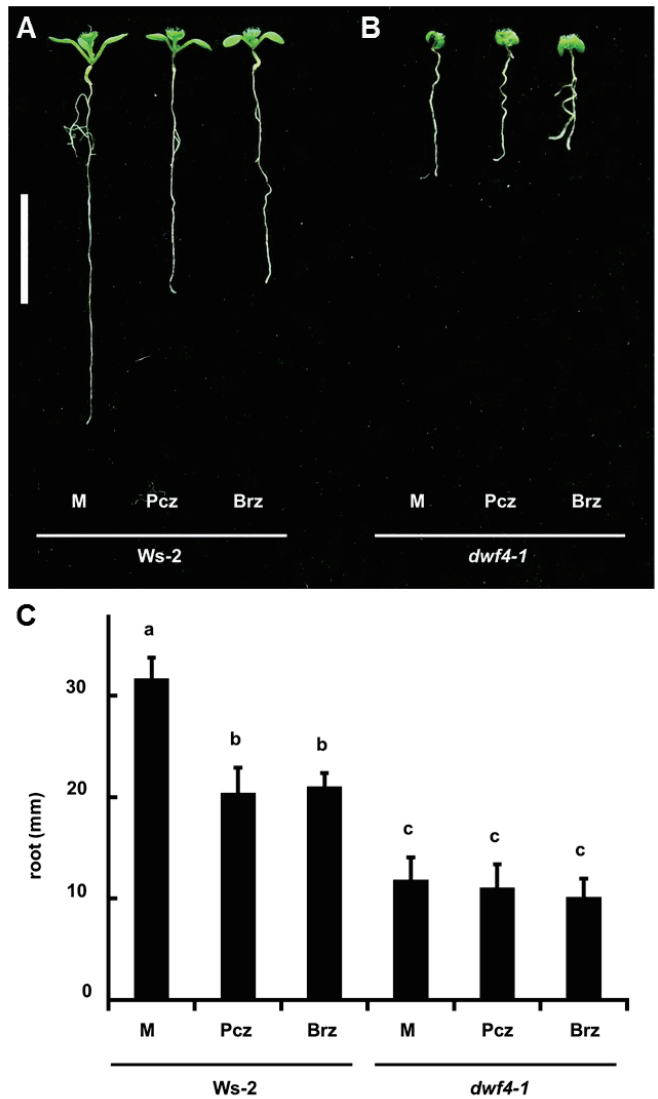

Figure 2-5. Resistance of *dwf4-1* to Pcz and Brz. (**A**–**B**) Seedlings of (**A**) Ws-2 and (**B**) *dwf4-1* grown on ½ MS media for 7 days, and then transferred to media containing 1 μM Pcz or Brz for 3 more days of growth. (**C**) Average root lengths of Ws-2 and *dwf4-1* measured at the end of treatments (n>10). Error bars represent

standard deviation and lowercase letters indicate significant differences among treatments determined by “Post-hoc” test ($p<0.05$). Scale bar (**A**–**B**) 1 cm.

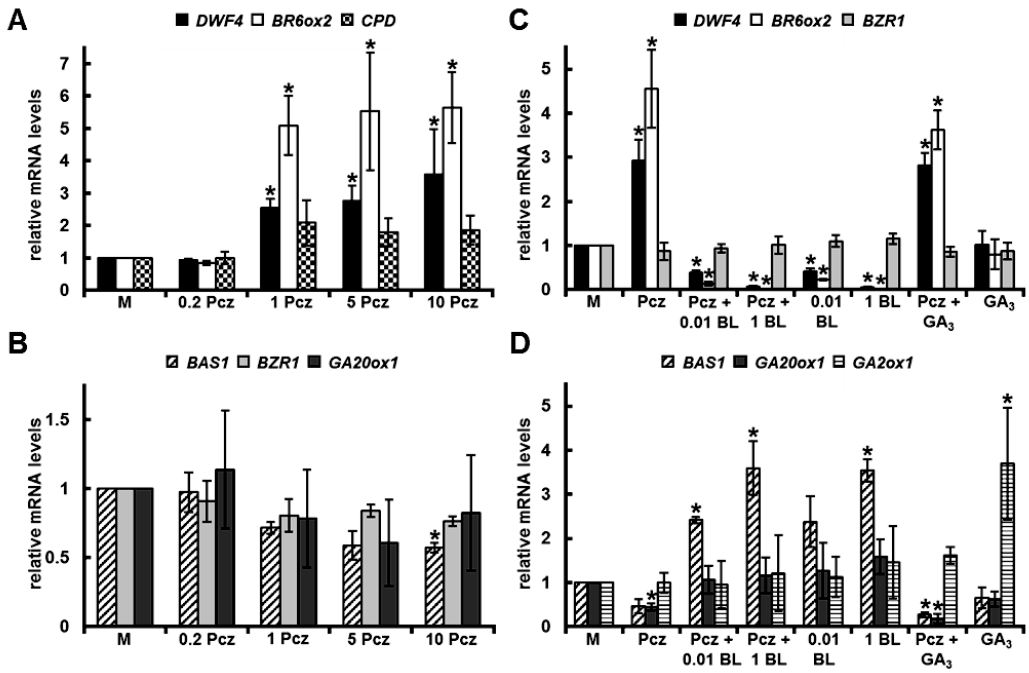

Figure 2-6. Pcz impact on the expression of BR- and GA-related genes. (**A**–**D**) Quantitative real-time PCR analysis of the transcript levels after treatment with 0.2, 1, 5 or 10 µM Pcz of (**A**) BR biosynthetic genes *DWF4*, *BR6ox2*, and *CPD* or (**B**) *BAS1*, *BZR1*, and *GA20ox1*, involved in BR degradation, BR signaling and GA biosynthesis, respectively. (**C**, **D**) Expression pattern of (**C**) BR biosynthesis and signaling or (**D**) BR degradation, GA biosynthesis and GA degradation (*GA2ox1*) genes measured after treatments with 1.5 µM Pcz, 0.01 or 1 µM BL, or 1 µM GA_3 or co-applications of Pcz (1.5 µM) with 0.01 or 1 µM BL or 1 µM GA_3. (**A**–**D**) Data points represent the average of three independent biological replicates with three technical replicates each. Error bars represent standard deviation. Asterisks indicate significant differences to the respective mock determined by Student's *t*-

test (p<0.05). Ubiquitin conjugating enzyme 21 (*UBC21*) was used as internal control.

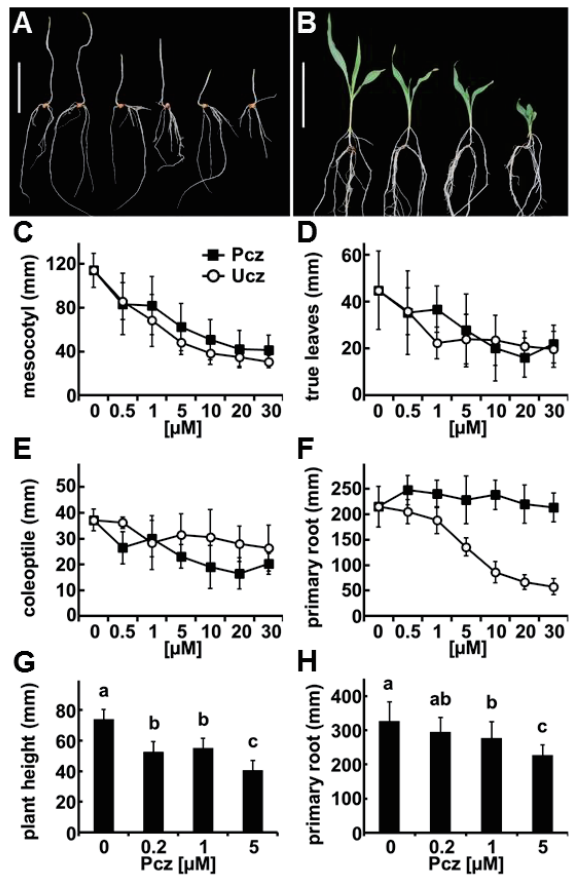

Figure 2-7. Tissue-specific response of dark and light grown W22 seedlings to Pcz and Ucz. (**A**) Maize seedlings grown for 8 d at 29°C in the dark treated with (left to right): 0 µM Pcz, 0 µM Ucz, 1 µM Pcz, 1 µM Ucz, 10 µM Pcz, and 10 µM Ucz, respectively. (**B**) W22 seedlings grown in the light for 3 weeks at concentrations of (left to right): 0, 0.2, 1, and 5 µM Pcz, respectively. (**C**–**F**) W22 seedlings grown for 8 d at 29°C in the dark with Pcz or Ucz at concentrations of 0, 0.5, 1, 5, 10, 20, or 30 µM. Lengths of the (**C**) mesocotyl, (**D**) true leaves, (**E**) coleoptile, and (**F**) primary root of W22 seedlings grown in the dark with indicated

concentrations of Pcz or Ucz (n>15). (**G–H**) Analysis of W22 maize seedlings grown in the light for 3 weeks at concentrations of 0, 0.2, 1, or 5 μM Pcz (Table S2-2). (**G**) Plant height and (**H**) primary root length was measured (n>15). Error bars represent standard deviation. (**C–H**) Statistical analysis determined by "Post-hoc" test is shown (**C–F**) in Table S2-1 and (**G–H**) indicated by lowercase letters (p<0.05). Scale bar (**A–B**) 10 cm.

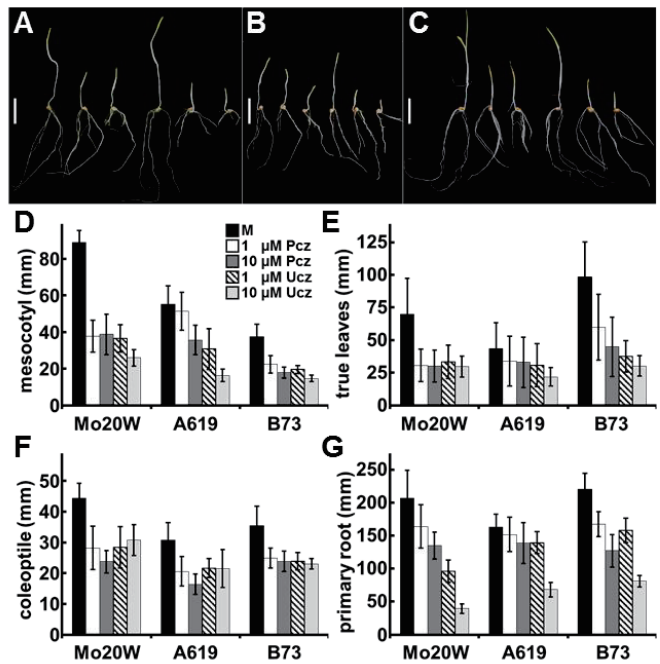

Figure 2-8. Impact of the genetic diversity on the tissue specific sensitivity towards Pcz and Ucz. (**A–C**) Maize inbred seedlings (**A**) Mo20W, (**B**) A619, and (**C**) B73 grown in vermiculite for 8 d at 29°C in the dark treated with (left to right): 0 µM Pcz, 1 µM Pcz, 10 µM Pcz, 0 µM Ucz, 1 µM Ucz, and 10 µM Ucz, respectively. (**D–G**) Length of the (**D**) mesocotyl, (**E**) true leaves, (**F**) coleoptile, and (**G**) primary root of Mo20W, A619, and B73 maize seedlings treated with 0 µM Pcz, 1 µM Pcz, 10 µM Pcz, 0 µM Ucz, 1 µM Ucz, or 10 µM Ucz, respectively (n>15). (**D–G**) Error bars represent standard deviation. Statistical analysis determined by t-test (p<0.05). Scale bar (**A–C**) 6 cm.

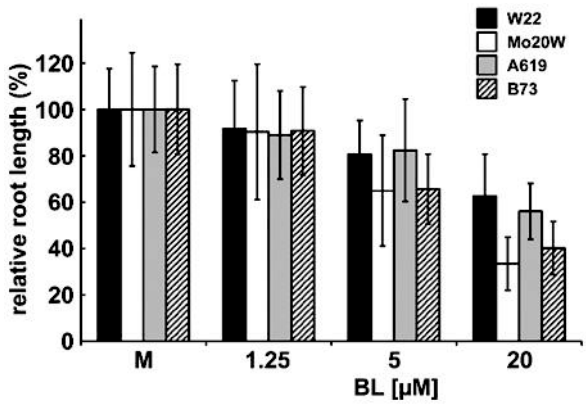

Figure 2-9. Influence of the genetic variation on the BR sensitivity in maize root. Maize inbred seedlings W22, Mo20W, A619, and B73 grown in vermiculite for 8 d at 29°C in the dark in the presence or absences of 1.25, 5, or 20 µM BL, respectively. Average length of the primary root measured at the end of treatment (n>15). Error bars represent standard deviation. Statistical analysis determined by t-test (p<0.05).

SUPPLEMENTAL INFORMATION

Table S2-1. List of primers.

Primer	Sequence (5' to 3')
CPD_FOR1	TTACCGCAAAGCCATCCAA
CPD_REV1	TCATCACCACCACCACCGTCAAC
DWF4_FOR1	GTTGGCCATTTCTTGGTGAAA
DWF4_REV1	TGGCGGTGTACGGTTTAAGA
GA20ox1_FOR1	GAAAATCAATGGCGCGCTCCAT
GA20ox1_REV1	CGGTGCAAGCAGCTCTTGTA
GA2ox1_FOR2	TGTCCCTCCCGATCACACTT
GA2ox1_REV2	ACGCTCTTGAACCTCCCATTT
BAS1_FOR1	CATGTGGCACGGAGCTTCTA
BAS1_REV1	CCGAGCTGGATTGAATTCGT
BZR1_FOR1	CAAACCCAAATGGCATGTCA
BZR1_REV1	CCAAATACCTGGACGAAGAAGAA
BR6ox2_FOR1	AACCGCTCACTCTCGACGAT
BR6ox2_REV1	CGTTGCCAATCTTGATGTCTCA
UBC21_FOR	CTGCGACTCAGGGAATCTTCTAA
UBC21_REV	TTGTGCCATTGAATTGAACCC

Table S2-2. Number of visible leaves and leaf collars of Pcz treated W22.

Treatment	No. of leaves	*p* value	No. of leaf collars	*p* value
Mock	4 ± 0.19		2.30 ± 0.46	
0.2 µM Pcz	4.08 ± 0.28	0.087	2 ± 0.51	0.026
1 µM Pcz	3.96 ± 0.2	0.939	1.83 ± 0.38	0.0003
5 µM Pcz	4 ± 0.41	0.433	1.69 ± 0.48	0.001

Chapter 3. Identification of Brassinosteroid Genes in *Brachypodium distachyon*

Identification of Brassinosteroid Genes in *Brachypodium distachyon*

Claudia Corvalán[1] and Sunghwa Choe[1,2,3,*]

[1] School of Biological Sciences, College of Natural Sciences, Seoul National University, Seoul 08826, Korea

[2] Convergence Research Lab for Plant Functional Products, Advanced Institutes of Convergence Technology, Suwon, Gyeonggi-do 16229, Korea

[3] Plant Genomics and Breeding Institute, Seoul National University, Seoul 08826, Korea

* Corresponding author:

Sunghwa Choe shchoe@snu.ac.kr

Published January 6, 2017 in BMC Plant Biology. DOI: 10.1186/s12870-016-0965-3

ABSTRACT

Brassinosteroids (BRs) are steroidal phytohormones that are involved in diverse physiological processes and affect many important traits, such as plant stature, stress tolerance, leaf angle, fertility, and grain filling. BR signaling and biosynthetic pathways have been studied in various plants, such as the model dicot *Arabidopsis thaliana*; however, relatively little is known about these pathways in monocots.

To characterize BR-related processes in the model grass *Brachypodium distachyon*, we studied the response of these plants to the specific BR biosynthesis inhibitor, propiconazole (Pcz). We found that treatments with Pcz produced a dwarf phenotype in *B. distachyon* seedlings, similar to that observed in Pcz-treated Arabidopsis plants and in characterized BR-deficient mutants. Through bioinformatics analysis, we identified a list of putative homologs of genes known to be involved in BR biosynthesis and signaling in Arabidopsis, such as *DWF4, BR6OX2, CPD, BRI1,* and *BIN2*. Evaluating the response of these genes to Pcz treatments revealed that candidates for *BdDWF4, BR6OX2* and*, CPD* were under feedback regulation. In addition, Arabidopsis plants heterologously expressing *BdDWF4* displayed tall statures and elongated petioles, as would be expected in plants with elevated levels of BRs. Moreover, heterologous expression of *BdBIN2* in Arabidopsis resulted in dwarfism, suggesting that BdBIN2 functions as a negative regulator of BR signaling. However, the dwarf phenotypes of Arabidopsis

bri1-5, a weak *BRI1* mutant allele, were not complemented by overexpression of *BdBRI1*, indicating that BdBRI1 and BRI1 are not functionally equivalent.

We identified components of the BR biosynthetic and signaling pathways in Brachypodium, and provided examples of both similarities and differences in the BR biology of these two plants. Our results suggest a framework for understanding BR biology in monocot crop plants such as *Zea mays* (maize) and *Oryza sativa* (rice).

INTRODUCTION

Brassinosteroids (BRs) are plant polyhydroxylated steroids that function as growth-promoting hormones. They have been implicated in many developmental and physiological processes in *Arabidopsis thaliana*, including vascular differentiation, stem and root elongation, reproductive development, photomorphogenesis, and stress responses. Hence, mutant plants defective in BR synthesis or perception display characteristic phenotypes such us short stature, round, curled leaves, short petioles, and reduce fertility (Clouse et al. 1996; Fujioka et al. 1997; Choe et al. 1998; Choe et al. 1999).

The BR-biosynthetic and signaling pathways have been well studied in *Arabidopsis thaliana*. A family of enzymes belonging to Cytochrome P450s mediates most of the steps of BR biosynthesis, and characterization of mutants defective in these enzymes contributed to the understanding of BR biology (Kwon et al. 2005; Chung et al. 2013). Various approaches have established the components and mechanisms of the BR signaling pathway; once BR binds to the receptor kinase, BRASSINOSTEROID-INSENSITIVE 1 (BRI1), transmits the signal to downstream genes, eventually leading to the repression or activation of BR responsive genes (Li et al. 2007; Kim et al. 2010).

It appears that BR signaling is conserved between monocotyledonous and dicotyledonous plants, as some counterparts of the Arabidopsis proteins are present in *Oryza sativa* (rice). For instance, orthologs of the receptor BRI1 and co-receptor

BRI1-ASSOCIATED RECEPTOR KINASE 1 (BAK1), named OsBRI1 and OsBAK1, respectively; two homologs of the negative regulator of the BR signaling protein BR INSENSITIVE 2 (BIN2), GSK3/SHAGGY-like kinase 1 and 2 (OsGSK1 and OsGSK2); and an ortholog of a major transcription factor in the BR transduction pathway BRASSINAZOLE RESISTANT 1 (OsBZR1) have been identified in rice (Sakamoto 2006; Kim et al. 2010; Tong et al. 2012; Tong et al. 2012).

Despite the similarities with dicot BR biology, some differences have been noted in monocots too. Brassinolide (BL), the most active form of BR and end product of BR synthesis in Arabidopsis, has not been detected in rice, where apparently castasterone (CS) seems to be the end product. Furthermore, no homolog of CYP85A2, which mediates BL synthesis, has been found in rice (Kim et al. 2008). In addition, components of BR signaling with no known orthologs in Arabidopsis have been identified in rice, indicating the existence of specific BR functions in monocots or some degree of functional redundancy. Examples of these components are DWARF AND LOW-TILLERING (DLT) and TILLER ANGLE INCREASED CONTROLLER (LIC), which act downstream of OsBRI1 and OsGSK2 to positively and negatively regulate rice BR signaling, respectively (Tong et al. 2009; Zhang et al. 2012), and the U3 ubiquitin ligase TAIHU DWARF 1 (TUD1), which interacts genetically and physically with D1/OsRGA, a heterotrimeric G protein subunit involved in gibberellin (GA) and BR responses (Hu et al. 2013).

Brachypodium distachyon (hereafter Brachypodium) is a relatively new model plant proposed for the study of grasses, since it has a short live cycle, is self-fertile, easy to grow, and is more closely related to Poaceae than is *A. thaliana* (Girin et al. 2014). However, little is known about phytohormones in *B. distachyon*. Only two dwarf mutants, with defects in the BRI1 receptor and a C-6 oxidase (BRASSINOSTEROID DEFICIENT DWARF 1; BRD1), have been characterized in this model plant (Thole et al. 2012; Xu et al. 2015).

In the present work, we used a specific BR biosynthesis inhibitor drug, propiconazole (Pcz) (Hartwig et al. 2012), to study BR action in Brachypodium and characterize orthologs of the BR-biosynthetic enzymes DWARF4, BR6ox2, and CPD. Furthermore, by heterologous complementation, we studied homologs of two important genes in the BR signaling pathway, the receptor BRI1 and the negative regulator BIN2. This work revealed important similarities and differences between the BR synthesis and signaling pathways in Arabidopsis and Brachypodium.

MATERIALS AND METHODS

Plant material and growth conditions

Brachypodium distachyon ecotype Bd21, a community standard diploid inbred line, was used in this research according to previous description in Hong et al. 2010 (Hong et al. 2010). Seeds were sterilized and germinated in water-soaked filter paper for 3 days before being transferred to soil. Plants were grown in growth room conditions at 22°C and a long-day (16 h light, 8 h dark) photoperiod. *Arabidopsis thaliana* wild-type Col-0 and Ws-2 ecotypes or mutant seeds (*gulliver3 - D* and *bri1-5*) were surface-sterilized before being sprinkled on agar-solidified MS (Murashige and Skoog) medium. After three day of stratification at 4°C, plates were transferred to a growth room and grown under long-day conditions at 22°C. After 10 days, seedlings were transferred to soil and maintained under the same conditions in a growth room.

Chemical treatments and morphometric analysis

For all treatments in Brachypodium, 3-day-old seedlings were transferred to coarse vermiculite soaked in the indicated concentrations of propiconazole solution or mock (DMSO) for control plants and grown for an additional 7 days. Seedlings were maintained in a growth room under normal long-day conditions, except for those grown under dark conditions, in which plates were covered with aluminum foil to mimic growth under total darkness. Plants were then harvested,

photographed, and analyzed using ImageJ software. Leaf length was measured from the root-shoot transition zone to the tip of the main leaf, whereas the length of the main root was used to determine root length. For leaf width, each leaf was measured in the exact middle to make an appropriate comparison. After measurements were taken, leaves were sectioned in the middle and cleared by washing in ethanol (EtOH) solutions. Sections were first washed in 90% EtOH at 37°C for 3 h. If necessary, the 90% solution was replaced to expedite clearing. Then sections were replaced in 50% solution for 5 minutes. Once the sections were cleared, they were placed overnight in 1% Safranin O diluted in 50% ethanol, to stain the veins a brilliant red color and facilitate observation under a microscope. A Primo Vert Inverted Microscope (Zeiss) was used to examine and image the samples, and then ImageJ software was used to calculate the total width and other parameters, such as distance between veins.

Identification of BR-related genes in Brachypodium

Using the UniProt server (http://www.uniprot.org/blast/), Arabidopsis and rice (*Oryza sativa*) BR-related genes were searched for in the Brachypodium genome by BLAST. For each search, query peptide sequences of well-known Arabidopsis proteins involved in BR signaling, including BRI1, BIN2, BSU1, and BZR1, and synthesis, including DWF4, CPD, and BR6OX2, were used. A multiple sequence alignment (MSA) was performed using the T-Coffee Multiple Sequence Alignment Server (http://tcoffee.crg.cat/) on the identified sequences with at least 40% identity and previously characterized proteins with equivalent functions in other plant

species. BoxShade software (http://embnet.vital-it.ch/software/BOX_form.html) was used to identify and visualize conserved sequences. A Neighbor-joining phylogenetic tree was built using the obtained MSA to illustrate the relatedness among known proteins and homolog candidates in *B. distachyon* and to select one for further characterization. A list of the BR-related proteins and candidates in *B. distachyon* used for the alignments and the MSAs can be found in supplemental information (Supplemental Table S3-1).

RT-PCR and quantitative real-time RT-PCR

For gene expression analysis, total RNA was prepared from Mock- or Pcz-treated *B. distachyon* seedlings using Trizol (Qiagen). RNA (2 μg) was reverse-transcribed using M-MLV enzyme (ELPIS), following the manufacturer's instructions, to synthesize cDNA, which was used as a template in PCR reactions. For semi-quantitative RT-PCR, the resulting cDNA samples were diluted (1:10) and equal amounts were used to amplify each gene. The level of gene expression was defined using *BdACT7* as a reference gene. Quantitative real-time RT-PCR detection was performed using the Applied Biosystems StepOne Real-Time PCR System and Power SYBR Green PCR Master Mix in combination with designed primers specific for *BdDWF4*, *BdBR6ox2,* and *BdCPD* (Supplemental Table S3-2). The reactions were performed in triplicate and the product was quantified by generating standard curves using serially diluted cDNA mix of all of the samples. Relative expression, representing fold change over the mock control, was normalized for each cDNA sample using *BdACT7* as internal control. As a negative control (NC)

we used distilled water in the same amount of the samples. In case of RT-PCR, the conditions were optimized until clear band of expected size was observed in the samples and no band was detected in the NC. In case of quantitative RT-PCR, NC was run in triplicate along with samples and normally gave us an undetermined C_T value or at least higher value than the most diluted sample from our standard curve to prove the accuracy and specificity of our primers in each run. Melting curves for each set of primers were also generated automatically by the StepOne Software (v2.3) from the Applied Biosystems system.

Cloning of *BdDWF4*, *BdBIN2,* and *BdBRI1*

To express *BdDWF4*, *BdBIN2,* and *BdBRI1* under the cauliflower mosaic virus 35S promoter (35S) in *A. thaliana,* RNA was extracted and cDNA was synthesized from Brachypodium 10-days-old seedlings and specific primers (Supplemental Table S3-2) were used to amplify full-length coding sequences (CDSs) of interest. PCR product was purified and cloned using the Invitrogen Gateway entry vector pENTR/SD/D-TOPO in combination with the destination pEarleyGate101(C-YFP-HA) vector. The constructs were transformed into Arabidopsis using conventional *Agrobacterium*-mediated techniques. For *35S::BdDWF4* and *35S::BdBIN2,* plants in the Col-0 background were used, whereas for *35S::BdBRI1,* the construct was introduced in *bri1-5* mutant background. Transgenic seedlings were selected on MS medium supplemented with 50 mg/L BASTA.

RESULTS

Brachypodium distachyon seedlings display BR-related phenotypes in response to propiconazole treatment

Since Brachypodium is a relatively new model plant, studies of processes and genes regulated by phytohormones in this organism are limited. The unavailability of Brachypodium BR-defective or -insensitive mutants made it challenging to determine if BR function is conserved across plant species. To study the mode of action of BRs and the factors involved in these processes, we first treated Brachypodium Bd21 seedlings with the BR-specific inhibitor Pcz in concentrations ranging from 1 to 50 μM for 7 days (Figure 3-1A to C). We observed a dose-response reduction of the total lengths of plants; 1 μM Pcz resulted in a ~13% reduction in length compared to mock conditions, whereas 50 μM, the greatest concentration tested, resulted in a ~60% reduction (Figure 3-1A). This reduction was especially severe in roots; the main root was reduced by 50% in plants treated with 20 μM Pcz relative to control plants, and by over 74% in those treated with 50 μM (Figure 3-1B). The Pcz-induced inhibitory effects were observed under both light and dark conditions (Supplemental Figure S3-1). In contrast to the effect on the overall length of the plant, leaf length was only reduced by ~25% under the strongest Pcz treatment (Supplemental Figure S3-2). To evaluate if Pcz had other effects on leaf morphology or the vascular system, we examined the leaf architecture in more detail, focusing on venation patterns, total number of veins, vein density, and distance between veins. Interestingly, we found that Pcz-treated

leaves were thicker and wider than those from plants grown under control conditions, but that the number of veins remained the same. As a consequence, the distance between veins is on average greater in the treated leaves, so vein density is reduced by Pcz treatment (Figure 3-2).

Identification of genes modulating BR response in Brachypodium

With the release of the whole genome sequence of *Brachypodium distachyon*, we were able to search for homologs that could participate in brassinosteroid biosynthesis or signaling in this species. We conducted a BLAST search of the Brachypodium database using the amino acid sequences of Arabidopsis proteins and then used multiple sequence alignment (MSA) and phylogenetic analysis to reduce the number of homolog candidates to one per protein for further evaluation. In the case of BIN2, the MSA and phylogenetic analysis were performed using Arabidopsis BIN2, BIN2-LIKE 1 (BIL1), and BIN2-LIKE 2 (BIL2) and also the rice homologs OsGSK1, OsGSK2, and OsSKetha. We also performed a second MSA, including *A. thaliana* BIN2, a GSK3 from human (P49841) and *D. melanogaster* (P18431), and rice *OsKetha* (Y13437) using the T-Coffee program to screen for conserved motifs. We observed that the kinase domain and the TREE domain, identified as being a putative Thr phosphorylation site by caseine kinase II and thus important for negative regulatory events, were also present in the Brachypodium homolog (Figure 3-3). Thus, we selected *Bradi2g48280*, *Bradi2g32620*, *Bradi2g36370*, *Bradi1g23550*, *Bradi1g69040*, *Bradi4g43110,* and

Bradi1g15030 as homologs of *BRI1*, *BIN2*, *BSU1*, *BZR1, DWF4*, *CPD,* and *BR6ox2,* respectively, for further characterization.

Brachypodium *DWF4*, *CPD,* and *BR6OX2* homologs are under feedback regulation

To verify that the genes identified by bioinformatics tools were in effect orthologs of BR biosynthetic genes in Brachypodium, we examined their transcripts levels in seedlings subjected to various Pcz treatments. To obtain a general sense of the gene expression response to the treatments, we performed semi-quantitative RT-PCR analysis on seedlings treated with three different concentrations of Pcz (10, 25, and 50 μM) along with mock. We noticed that the transcript levels of the three BR-related genes increased with increasing Pcz concentrations. The GA biosynthesis gene *GA20ox1* was used as a control for the Pcz treatment, to ensure that only BR-related genes were inhibited by the treatment (Figure 3-4A). After determining the conditions that produced a clear transcriptional response, we carried out a similar experiment using just mock and one Pcz concentration (50 μM) to analyze *BdDWF4*, *BdBR6ox2,* and *BdCPD* mRNA levels by quantitative real-time RT-PCR. For the first two genes, Pcz-treated seedlings exhibited a more than six-fold increase in expression with respect to the mock treatment, while *BdCPD* was only slightly upregulated (Figure 3-4B to D). Nonetheless all three candidate genes were found to be under negative feedback regulation, a characteristic of genes involved in BR biosynthesis. Normally, the expression of these genes is inhibited by the presence of BR and enhanced when BR levels are low such as under treatment with

inhibitors (i.e., a negative feedback mechanism regulates the activity of genes downstream of BR). Thus, *Bradi1g69040* (*BdDWF4*), *Bradi4g43110* (*BdCPD*), and *Bradi1g15030* (*BR6ox2*) may indeed be involved in BR biosynthesis in *Brachypodium distachyon*.

Overexpression of *BdDWF4* in *Arabidopsis thaliana* produce long and slender plants

To further evaluate the involvement of *BdDWF4* in BR responses, we introduced the full-length coding sequence of this gene into *A. thaliana* under the CaMV 35s promoter. From a total of 26 analyzed *BdDWF4* overexpressing lines (*BdDWF4ox*), half displayed an increase in plant height and had longer and narrower leaves than the wild-type control, Col-0 (Figure 3-5A). These characteristics are typical of brassinosteroid-overproducing mutant plants, such as *gulliver3 - D* (*gul3-D*), in which the increase in BR level is the result of activation tagging of *DWF4*. Analysis of the expression level in transgenic plants corroborated that degree of the phenotype is proportional to the levels of transcripts (Figure 3-5C). The results strongly suggest that *Bradi1g69040* plays a significant role in Brachypodium growth and development, probably by functioning in the BR biosynthetic pathway.

Overexpression of *BdBIN2* in Arabidopsis results in a stunted growth phenotype

We then overexpressed a candidate gene involved in BR signaling *BdBIN2,* in *A. thaliana* to study the effect of this gene on the phenotypes of the transgenic plants.

From a total of 32 analyzed lines, nearly 14% of the transgenic plants presented severe dwarf phenotypes, were unable to set flowers, and died after a few weeks (Figure 3-5B). These extreme dwarf plants presented the highest level of transcript accumulation (Figure 3-5D). Other *BdBIN2ox* lines showed milder phenotypes that were able to produce seeds but still exhibited a compact stature and smaller curled leaves compared with the wild type (Figure 3-5B). These findings insinuate that *Bradi2g32620* is a functional ortholog of BRIN2 in Brachypodium that operates as a negative regulator of the BR signaling pathway.

BdBRI1* overexpression does not revert the weak phenotype of *A. thaliana bri1-5

A search for *BRI1* in the Brachypodium genome yielded three candidate genes (Supplemental Table S3-1) that we arranged in a phylogenetic tree along with other BRI1 proteins described in various dicot (*A. thaliana*, pea (*Pisum sativum*), and tomato (*Lycopersicon esculentum*)) and monocot (rice (*Oryza sativa*) and barley (*Hordeum vulgare*)) plants. As a reference, we also used BRI1-LIKE proteins BRL1, BRL2, and BRL3 from Arabidopsis and rice. As shown in Figure 3-6A, we observed that the protein product of *Bradi2g48280* was in the same group as orthologs of BRI1 in monocots, and although it shares only ~53% amino acid sequence identity with AtBRI1, it shares more than 80% identity with amino acid sequences in its monocot counterparts. To test if *Bradi2g48280* (named BdBRI1 from now on) has the same functions as AtBRI1, we performed heterologous complementation experiments. Specifically, we examined if overexpression of

BdBRI1 was able to revert the dwarf phenotype of the BR-insensitive *bri1-5* mutant, which is a weak allele of *AtBRI1*. In a first experiment we obtained 13 independent lines, all exhibiting dwarf phenotypes similar to *bri1-5*. Similarly, in a second transformation we obtained another 21 transgenic lines resistant to the Basta which didn't show rescued phenotypes (Supplemental Figure S3-3A); *bri1-5/BdBRI1ox* lines were slightly taller than the *bri1-5* control, but were still dwarfed with abnormal leaf morphology (Figure 3-6B and C). These results indicate that although *Bradi2g48280* is likely a homolog of *Arabidopsis thaliana BRI1*, these two genes may have different structure and/or functions that make BdBRI1 incapable of operating as the BR receptor in Arabidopsis.

DISCUSSION

The use of knock-out and activation tagging mutants has facilitated the characterization of many important genes involved in phytohormone signaling and biosynthetic pathways. In the case of BRs, the characterization of dwarf mutants mainly in Arabidopsis has contributed to our current understanding of BR biology. However, few studies have evaluated BRs in Poaceae, and most advances in these crops have been made in rice and maize (Hartwig et al. 2011; Hartwig et al. 2012; Makarevitch et al. 2012; Zhang et al. 2014). The lack of BR-defective mutants is an obstacle in efforts to reveal BR functions in other model plants and at the time this work started, just one BR mutant had been identified in Brachypodium (Thole et al. 2012). Subsequently, one more mutant defective in BR biosynthesis has emerged (Xu et al. 2015).

In this report, we sought to contribute to the knowledge of BR biology using Brachypodium as a model plant by measuring the effects of a potent and specific BR inhibitor, Pcz. We demonstrated that Pcz treatments mimic the characteristic dwarf phenotypes of plants deficient in brassinosteroids and that the response is dose-dependent, similar to what was described for Arabidopsis and maize (Hartwig et al. 2012). Treatments with 50 μM Pcz caused severe phenotypes in seedlings, especially in the roots, where we observed a 75% decrease in length compared to the mock treatment, while the reduction in leaf length was almost 34%. The marked effect on roots may be due to the method used to apply Pcz. As we planted

the seedlings in vermiculite soil soaked with Pcz solution, the roots were in permanent and direct contact with Pcz, whereas the aerial tissue was not. Still, this method was able to cause not only a decrease in leaf length, but also other phenotypes in the leaves that were similar to the ones described in transgenic rice plants overexpressing the BR negative regulator BIN2 (Tong et al. 2012).

Although the Pcz-treated leaves initially seemed to develop relatively normally, they later curled, especially towards the top, and exhibited increased width and thickness compared to the mock treatments. Further analyses using cross-sections of leaves could reveal more about the possible effects of Pcz on venation pattern or cell organization in these tissues. Considering the phenotypes obtained using the chemical inhibitor in Brachypodium, we propose that Pcz treatments represent a powerful tool for studying BRs in this model plant. Pcz could be administered to investigate vascular and stomatal development, root growth, cell elongation, and meristematic cell maintenance, among other specific processes in which BR is known to play active roles (Fabregas et al. 2014; Singh et al. 2015).

The BR biosynthetic genes are primarily regulated at the transcriptional level, and this regulation is mainly mediated by the transcription factor BZR1, with supplemental regulation by other transcription factors. When BR signaling is activated, the dephosphorylated (i.e., active) form of BZR1 binds to the promotor sequence of BR synthetic genes to repress their transcription. This mechanism is known as negative feedback downregulation of BR biosynthetic genes (Kim et al. 2006; Chung et al. 2013). In this way, BL treatments reduce the expression of

DWF4, *CPD,* and *BR6ox2* while Pcz application has the opposite effect since it reduce BR levels (Hartwig et al. 2012). Considering this feedback regulation of the biosynthetic genes, we evaluated the transcript levels of our candidate BR-related genes *BdDWF4* (*Bradi1g69040*), *BdCPD* (*Bradi4g43110*), and *BdBR6ox* (*Bradi1g15030*) in seedlings subjected to Pcz treatment. We observed the Pcz-dependent induction of the three candidates tested, although the increase in *BdCPD* expression level was lower than that of the other two genes. However, a similar result was observed previously for Arabidopsis *CPD* upon Pcz application (Hartwig et al. 2012), possibly because another mechanism regulates the post-transcriptional level of *CPD*. Taken together, *BdDWF4*, *BdCPD,* and *BdBR6ox* are regulated by a feedback loop at the transcript level once BR levels decrease upon Pcz treatments, suggesting their possible role as enzymes involved in BR synthesis.

To date, many BR genes homologs to the ones characterized from *A. thaliana* have been identified in different monocot species and most of these works are based on the description of the phenotypes from mutant plants which in most of cases present dwarfism or other characteristic BR-related phenotypes. Nevertheless, not many of these studies examine the effects of the ectopic overexpression of these suggested homolog genes in Arabidopsis to examine if they fulfill similar roles to its dicot equivalent. Some exceptions are the overexpression of maize *DWF4* (*ZmDWF4*) and rice *GSK1*, one of the homologs of *BIN2*, in *Arabidopsis* (Koh et al. 2007; Liu et al. 2007). Ectopic overexpression of *ZmDWF4* generated Arabidopsis plants with longer petioles, narrower leaves, and increased size (Liu et

al. 2007), which is similar to the effects we obtained by overexpressing BdDWF4. This typical growth-promoting phenotype is also portrayed by transgenic plants overexpressing *AtDWF4* (Choe et al. 2001) and the gain-of-function mutant *gulliver3 - D/dwarf4 – D,* which we used as a control to compare the effects of our overexpression (Kim et al. 2013). In case of BIN2, opposite phenotypes are observed due to its role in modulating BZR1/BES1 degradation. Heterologous expression of the rice *BIN2* homolog *OsGSK1* in Arabidopsis resulted in plants that were barely one-third the height of control plants (Koh et al. 2007). Similarly, overexpression of *BdBIN2* affected plant height and other features in our experiments, but to a greater extent. This difference may be due to OsGSK1 having a minor role in BR signaling, since another homolog of BIN2 in rice, OsGSK2, seems to be a more prominent negative regulator that functions upstream of transcription factors such as OsBZR1, LIC, and DLT (Tong et al. 2012).

Homologs of the BR receptor BRI1 have been identified and studied in three monocot species to date, including rice, barley, and Brachypodium (Yamamuro et al. 2000; Chono et al. 2003; Nakamura et al. 2006; Feng et al. 2015). The functions of the BRI1 homolog in Brachypodium were revealed in studies of plants in which *BdBRI1* was silence by RNAi technology (Feng et al. 2015), while the homologs in the other two species were characterized using mutant plants. In addition to OsBRI1, BRI1-LIKE homologs (OsBRL1 and OsBRL3) have also been characterized in rice, and in both rice and barley different alleles of *BRI1* have been found in later works (Gruszka et al. 2011; Zhao et al. 2013). However, these

studies failed to determine if the monocot homologs of BRI1 are able to function as a BR receptor in dicot plants. This fact is indeed important, since the end product of BR synthesis and more active BR in monocots does not seem to be brassinolide, but castasterone. Thus, the structure of BRI1 remained to be compared in monocot and dicot plants (Kim et al. 2008). To do so, we first searched the Brachypodium genome for *BRI1* putative homologs. We found that *Bradi2g48280* likely functions as a BR receptor in Brachypodium (Feng et al. 2015); however, to test our hypothesis, we cloned the gene and heterologously expressed it in *A. thaliana bri1-5* mutant plants. To our surprise, the full-length coding sequence of *BdBRI1* was not able to rescue the dwarf phenotype of *bri1-5*, which is a weak allele of *bri1*. This was observed despite the plants were expressing the Brachypodium version of *BRI1* (Supplemental Figure S3-3B). Several transgenic lines showed a slight increase in total plant height, but still presented extremely curled leaves and defects in flowering and seed formation. As far as we know, this is the first time a monocot version of BRI1 has been expressed in *A. thaliana* to evaluate if complementation is possible. Our results represent an early step for comparing the functions and structures of BRI1 between dicot and monocot plants and thus broaden the understanding about BR response in crop plants. BRs have profound effects on several physiological responses such as plant size, fertility and leaves inclination, thus good biotechnological targets to manipulate plant architecture towards desirable agronomic traits. The identification and characterization of BR genes in Brachypodium along with the use of genetic engineering have the potential to

enhance crop yield in important crops and even the use of fertilizers could be potentially reduced with less negative environmental effects.

FIGURES AND TABLES

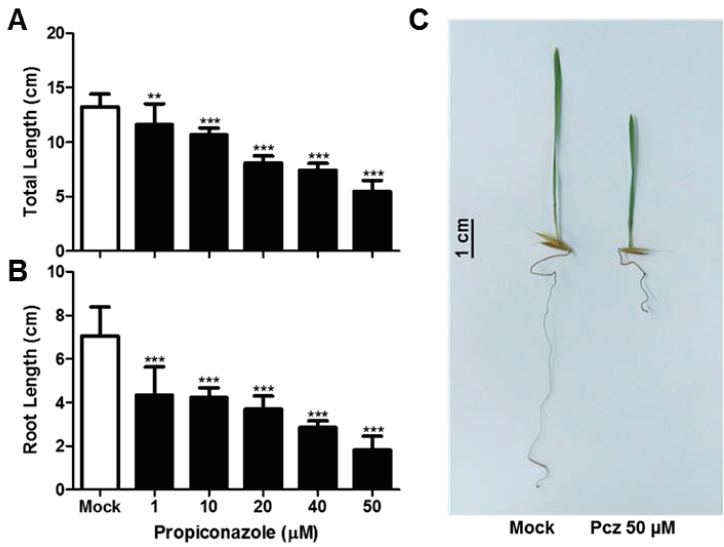

Figure 3-1. Brachypodium seedlings exhibit dose-dependent dwarfism in response to propiconazole treatment. (**A**) Total lengths of seedlings and (**B**) roots after 7 days of exposure to 0 (Mock) to 50 µM Pcz. (**C**) Morphology of 7-days-old seedlings subjected to the mock treatment and the strongest Pcz concentration tested. The graphs represent average value (n>10) and error bars standard deviation. Significant differences among treatments were determined by Student's *t*-test. **, P<0.001 and ***, P<0.0001.

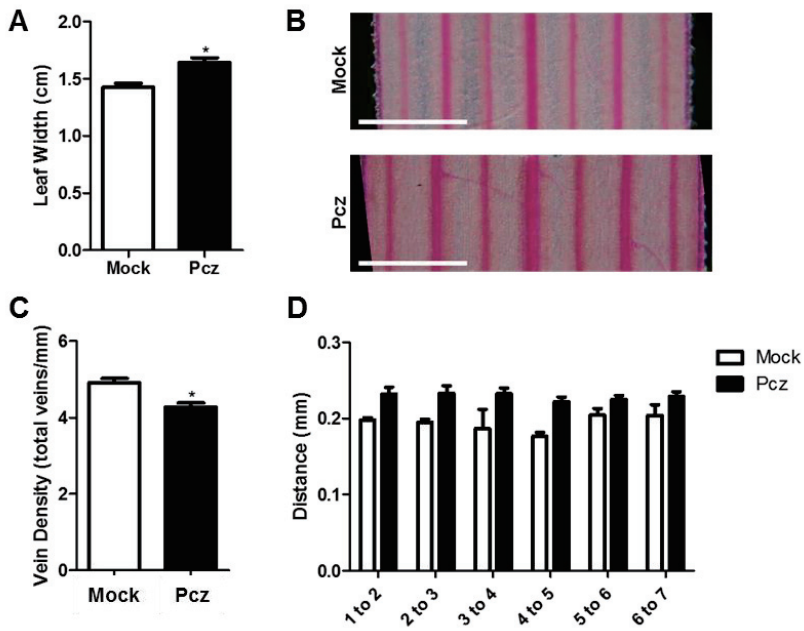

Figure 3-2. Brachypodium leaf width and distance between veins are affected by Pcz. (**A**) Leaves of seedlings undergoing mock or Pcz (50 μM) treatments were measured and dissected in the middle. (**B**) Safranin O-stained leaf sections were used to count and observe veins under the microscope. (**C**) The vein density values were obtained by dividing the total number of veins in the section by the width of the leaf. (**D**) The distance between veins was measured using ImageJ software. Scale bar = 0.5mm. The graphs represent average value (n>5) and error bars standard deviation. Significant differences among treatments were determined by Student's *t*-test. *, P<0.05.

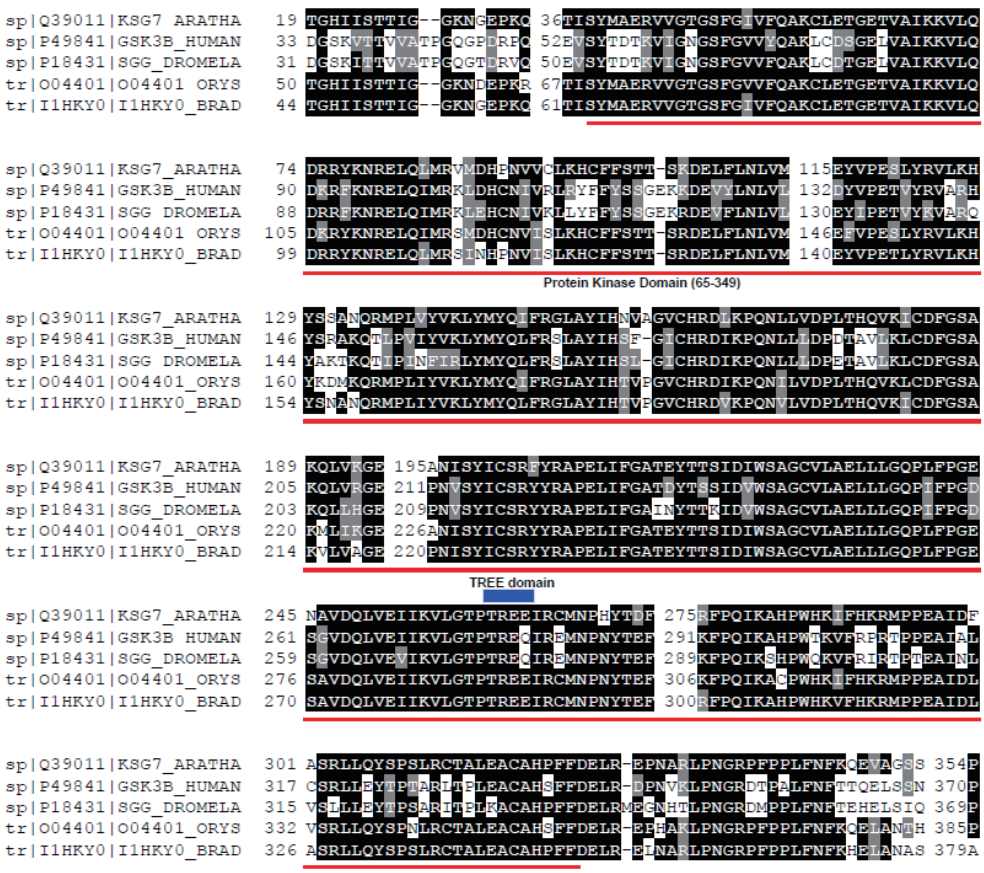

Figure 3-3. BdBIN2 shows conserved motifs with other GSK3/SHAGGY-like kinase proteins. Part of the multiple sequence alignment (MSA) of the BIN2 ortholog in Brachypodium (1HKY0) with AtBIN2 (Q39011) and a GSK3 homolog from human (P49841) and *D. melanogaster* (P18431). The conserved protein kinase domain is underlined in red and the TREE domain, which is well conserved in plants, is represented by a blue rectangle.

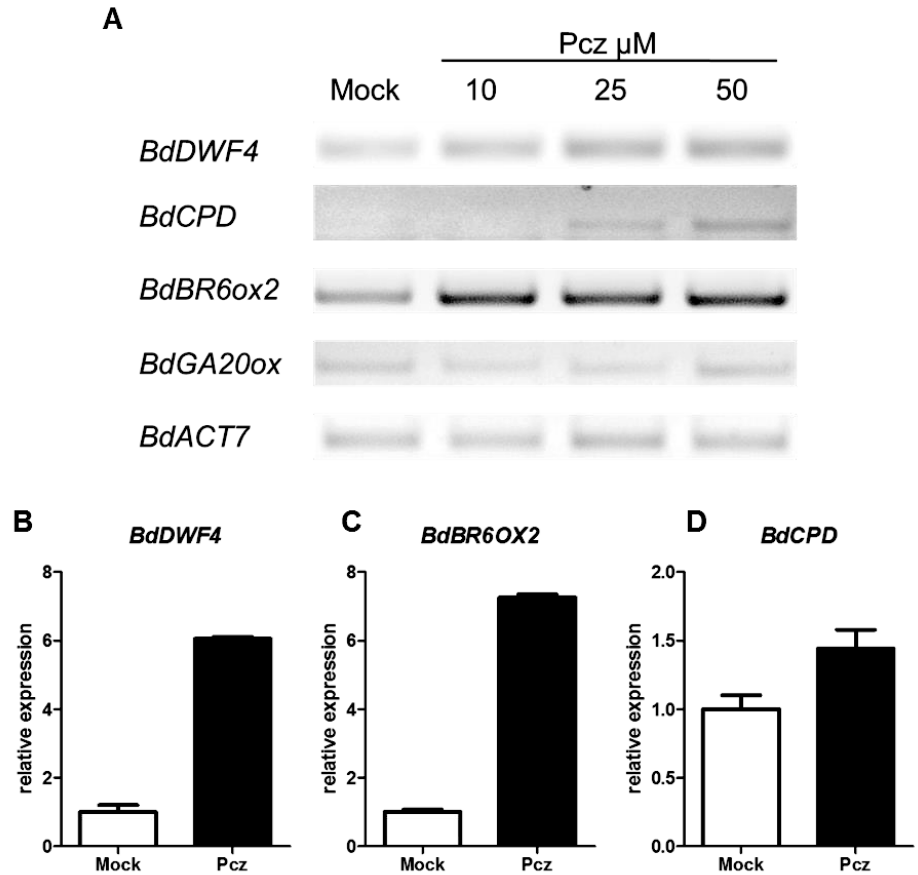

Figure 3-4. Feedback regulation of Brachypodium BR biosynthetic genes after Pcz treatments. (**A**) Semi-quantitative RT-PCR of putative BR biosynthetic genes *BdDWF4*, *BdBR6OX2,* and *BdCPD* and the GA biosynthetic gene *BdGA20ox* after treatment with the indicated concentrations of Pcz and a mock control. *BdACT7* is used as an internal loading control. (**B-D**) Quantitative real-time RT-PCR analysis evaluating the expression of the same genes under just mock or 50 µM Pcz.

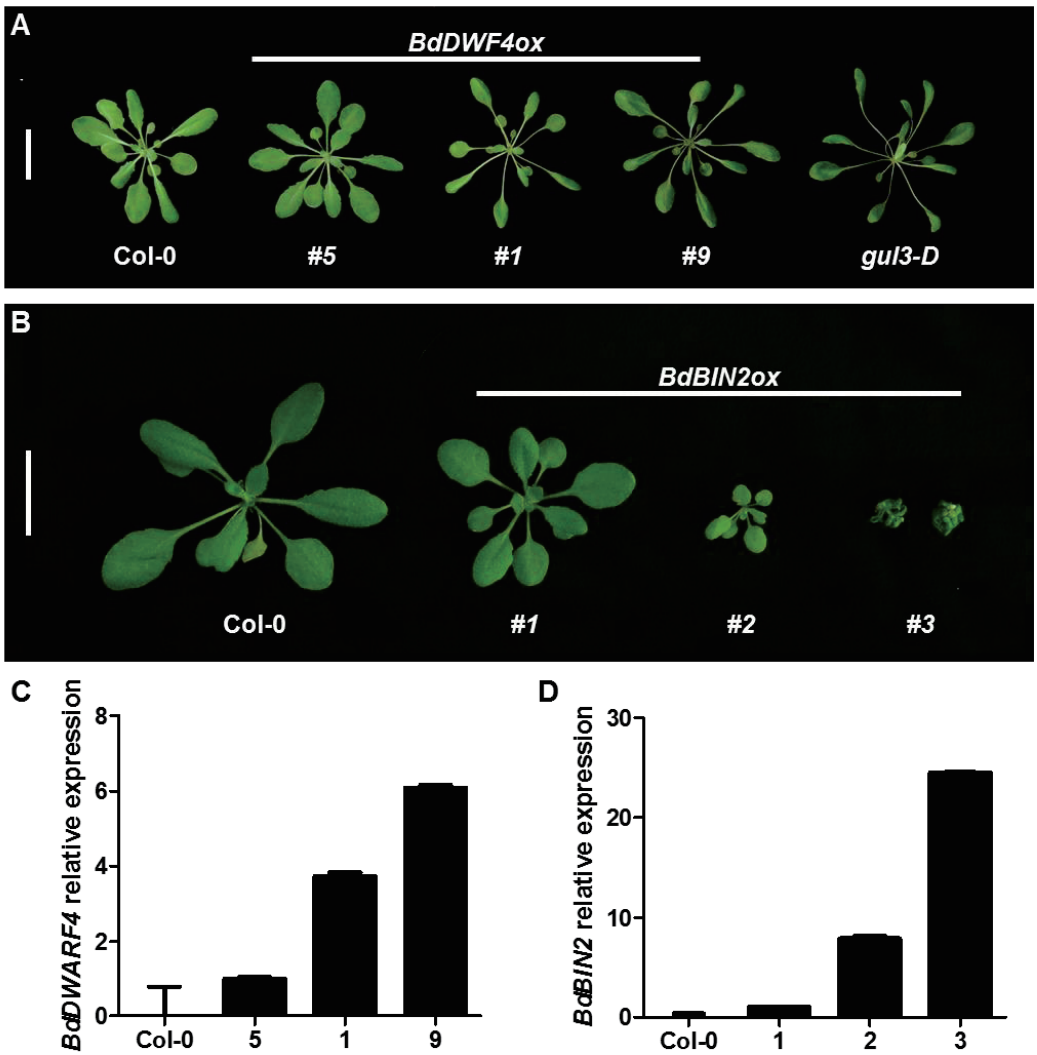

Figure 3-5. Phenotypes of the *BdDWF4ox* and *BdBIN2ox* transgenic lines, suggesting the involvement of *BdDWF4* in BR biosynthesis and *BdBIN2* in responses, respectively. (**A**) Morphology of three independent *BdDWF4* overexpression lines (#5, #1, and #9) along with wild type Col-0 and *gul3-D* BR overproducing mutant. (**B**) Phenotypes of the wild type Col-0 and *BdBIN2*

overexpressing lines. Line #2 represent mild phenotype, while #3 are examples of severe dwarfism. Scale bar = 2 cms. (C-D) Quantitative real-time analysis evaluating the heterologous expression of *BdDWF4* and *BdBIN2* respectively. Line #5 (**C**) and #1 (**D**) which don't show distinctive phenotype from wild type were used to compare expression of the rest of the lines. A*tUBQ10* was used as internal loading control.

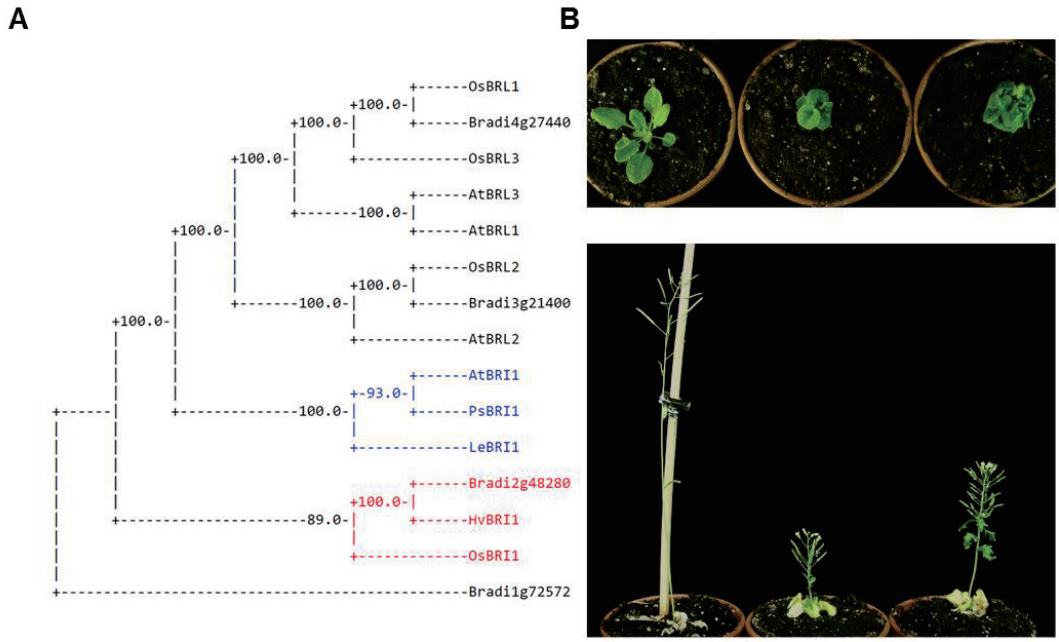

Figure 3-6. *BRI1* homolog in *Brachypodium* fails to rescue the phenotypes of the BR-insensitive mutant *bri1-5*. (A) Phylogenetic analysis showing Brachypodium BRI1 candidate proteins and BRI1 homologs in other species, including Arabidopsis, tomato, pea, rice, and barley. (B) Phenotypes of 3-week- or (C) 6-week-old WS-2 wild-type adult plants, the *bri1-5* mutant, and transgenic *bri1-5/BdBRI1ox* plants.

SUPPLEMENTAL INFORMATION

Figure S3-1. Brachypodium seedlings exhibit dwarfism in response to propiconazole treatment in dark. Morphology of 7-days-old seedlings subjected to the mock treatment and 50 μM Pcz.

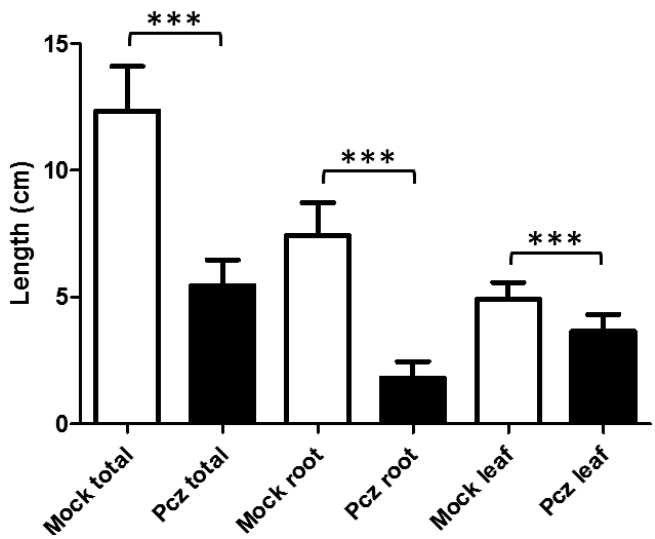

Figure S3-2. Propiconazole treatment reduces leaves and roots lengths in Brachypodium seedlings. Total lengths of seedlings, leaves and roots after 7 days of exposure to mock (white bars) or 50 μM Pcz (black bars). The graphs represent average value (n>10) and error bars standard deviation. Significant differences among treatments were determined by Student's *t*-test.***, P<0.0001.

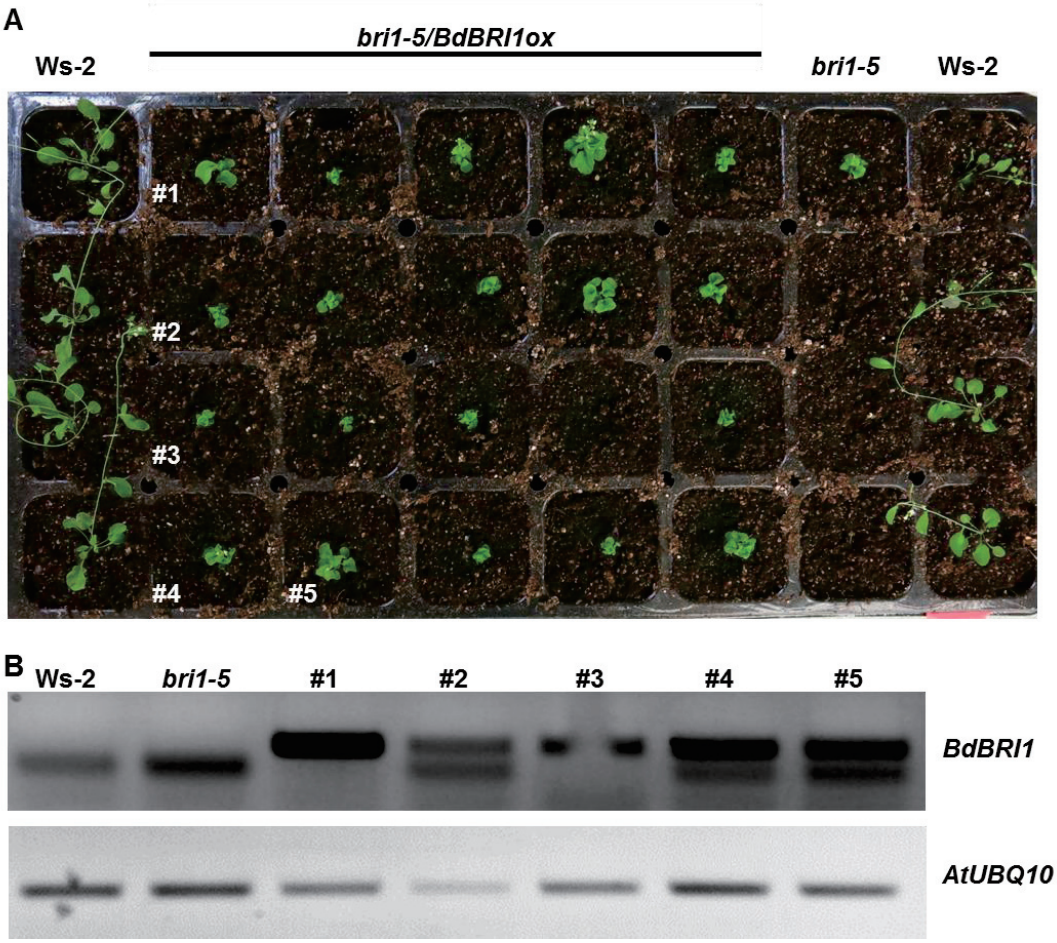

Figure S3-3. Phenotypes associated with *BdBRI1ox* lines and *BdBRI1* transcript accumulation. (A) Morphology of 5-week-old transgenic plants selected in Basta media along with Ws-2 wild type and *bri1-5* mutant as controls. (B) Expression of *BdBRI1* in five of the transgenic plants was confirmed through RT-PCR. *AtUBQ10* was used as an internal loading control.

Table S3-1. List of BR genes in *A. thaliana* and homolog candidates in Brachypodium.

		A.thaliana		*B. distachyon*				
Gene	**Description**	**Gene ID**	**Protein ID**	**Candidate Homologs**	**Candidate protein ID**	**Identity**	**Score**	**E-value**
BRI1	BR signaling (BR receptor)	*At4g39400*	O22476	*Bradi2g48280*	I1HQZ9	53.6%	2971	0.0
				Bradi4g27440	I1IP60	50.8%	2572	0.0
				Bradi3g21400	I1I325	45.6%	2122	0.0
BIN2	BR signaling (negative regulator)	*At4g18710*	Q39011	*Bradi2g32620*	I1HKY2	86.3%	1740	0.0
				Bradi2g06490	I1HKY0	89.0%	1731	0.0
				Bradi3g09067	I1HD48	82.5%	1611	0.0
BSU1	BR signaling (positive regulator)	*At1g03445*	Q9LR78	*Bradi2g36370*	I1HM01	51.6%	2183	0.0
				Bradi1g13710	I1GQ04	43.9%	1869	0.0
				Bradi4g01410	I1IGC2	37.5%	1399	8.30E-177
BZR1	BR signaling (positive regulator)	*At1g75080*	Q8S307	*Bradi1g23550*	I1GT13	52.5%	799	7.10E-102
				Bradi2g06400	I1HD37	41.0%	523	1.40E-60
				Bradi1g38180	I1GY36	40.8%	517	1.10E-59
DWF4 (CYP90B1)	BR biosynthesis	*At3g50660*	O64989	*Bradi1g69040*	I1H7R8	66.5%	1733	0.0
				Bradi5g12990	I1IYP5	42.4%	1035	6.50E-133
CPD (CYP90A1)	BR biosynthesis	*At5g05690*	Q42569	*Bradi4g43110*	I1IUJ6	62.2%	1415	0.0
				Bradi2g05980	I1HCZ1	41.2%	919	9.10E-116
BR6OX2 (CYP85A2)	BR biosynthesis	*At3g30180*	Q940V4	*Bradi1g15030*	I1GQE7	60.9%	1524	0.0

Table S3-2. Primers used in the research.

Gene	Locus ID	Direction	Sequence (5' to 3')	Size (bp)	Purpose
BdDWF4	*Bradi1g69040*	forward	**CACC**ATGGCCGCCATGATGGCGTCCATAACC	1521	cloning
		reverse	TATATCCACGGTCAAAACACTTTTCTCTTC		
BdBRI1	*Bradi2g48280*	forward	**CACC**ATGGATTCCTTGCGGGTGGCGATAGC	3369	cloning
		reverse	ATCCTTCTCTTCCTTGGCTTCCTTGAGG		
BdBIN2	*Bradi2g32620*	forward	**CACC**ATGGAGCAGACGGCGCCAGCGGCG	1215	cloning
		reverse	GCTCCCAGCATGGAAGAAGTTGAAGCCG		
BdACT 7	*Bradi4g41850*	forward	TCCTTTTCCAGCCATCTTTC	328	RT-PCR
		reverse	ATCGCTGGACCAGACTCATC		
BdDWF4	*Bradi1g69040*	forward	GCACCGGAAAGTAATTCGAG	331	RT-PCR
		reverse	CTTTGGAAAGTCCACGAAGG		
Bd85A2	*Bradi1g15030*	forward	ATGGCCTTGCTATCTGCACT	368	RT-PCR
		reverse	ACAGGTACTTGACCGCCATC		
BdCPD	*Bradi4g43110*	forward	TCAATCTCACCGTCAAGCAG	339	RT-PCR
		reverse	ACAGGCAGAAGTCCACCATC		
BdGA20ox	*Bradi2g24980*	forward	ACGGCTTCTTCCTGGTGAC	553	RT-PCR
		reverse	CGCGAAGAAGTCCCTGTAGT		
Bd85A2	*Bradi1g15030*	forward	AGCGGAAATTGCAACGTTCC	121	real-time RT-PCR
		reverse	AACTCGGATATGTAGCCCGTTG		
BdCPD	*Bradi4g43110*	forward	TTTCGCTTCATTCCGAGCTG	91	real-time RT-PCR
		reverse	TTTGTGGTTGCTCTGCCATC		
BdDWF4	*Bradi1g69040*	forward	AGATGGAAGGGCAATGCATC	125	real-time RT-PCR
		reverse	AGGTGGTGCAAAAAGATGGC		
BdBIN2	*Bradi2g32620*	forward	CAATAGATCTTGCTTCGCGG	146	real-time RT-PCR
		reverse	GTTGAATAGAGGTGGGAATGGG		
BdBRI1	*Bradi2g48280*	forward	TCTCTTTCAACCACTTCACCG	137	real-time RT-PCR
		reverse	GAGACTGGAGTTGGGATCTTG		
AtUBQ10	*AT4G05320*	forward	TCCAGGACAAGGAAGGTATTCC	205	real-time RT-PCR
		reverse	CCACCAAAGTTTTACATGAAACGAA		

Chapter 4. Activation Tagging of a Rice DP Family Gene in the *propiconazole resistant 1-D* Mutant Results in Alterations in Cell Division.

ABSTRACT

Brassinosteroids (BR) are known to regulate plant architecture and yield in rice. For this reason, genes involved in modulation of the BR response are recurrent targets of genetic manipulation to improve rice traits toward yield increase. Here we report an activation-tagging mutant with increased yield from a mutant screening using BR biosynthetic inhibitor propiconazole (Pcz). We identified *propiconazole resistant1-D* (*pzr1-D*) mutant which is resistant to the Pcz treatment and also presents various BR-related phenotypes such as semi-dwarfism, and increased number of tiller but increased sensitivity to BR. We revealed that these phenotypes are related to the transcriptional increase of a rice ortholog of Arabidopsis DPb gene positioned upstream of the T-DNA insertion in the mutants. DPb belongs to a family of transcription factor known to play important roles in cell division in animal and plants. Like its ortholog DPb, rice PZR1 is expressed differentially in rice organs and seems to play a role in cell division. Callus derived from *bzr1-D* seeds were significantly smaller and presented root-like structures in callus induction media, denoting unbalanced cell division and differentiation processes. Microscopy analysis also revealed differential number and size of cells from roots and leaves in mutant seedlings compared with wildtype. Moreover, transcriptome analysis between

wildtype and *pzr1*-D mutant also revealed differential expression of genes involved in cell-cycle regulation. Dominant mutants *pzr1-D* and transgenic plants overexpressing *PZR1* gene show increased number of tiller, panicles and branches in the panicles, all resulting in considerably increased yield compared to the control plants. These results support a role of the PZR1 in mediating BR-regulated cell division control in rice.

INTRODUCTION

Rice is an important cereal crop and at the same time a model plant for molecular research. Many efforts in rice studies have focused on the improvement of plant architecture, i.e. plant height, leaf erectness, tiller and panicle number and seed size, all aspects that determine yield. In the last years, significant progress have been made, especially by generating activation-tagging or knock-out mutants that can be analyzed by forward genetics. But although many factors involved in plant architecture have been identified, the studies are not complete or have not improved biomass and or yield significantly. Thus, the generation and characterization of more mutant populations may facilitate the identification of the related functional genes and associated genetic network that controls important aspects determining plant architecture.

Brassinosteroids (BRs) are known to affect plant architecture by controlling plant height, leaf erectness and seed size among other traits. Typical BR-deficient mutants in rice display dwarf phenotypes, dark-green, erected and shortened leaf sheaths in early vegetative stage (Clouse et al. 1996; Fujioka et al. 1997; Choe et al. 1998). After flowering, the height of plants reaches only ~ 40% of wild type, the internode elongation differs from wild type, panicles are malformed, and have reduced number of

branches and spikelets (Yamamuro et al. 2000; Hong et al. 2003; Tanabe et al. 2005; Hong et al. 2005; Sakamoto et al. 2006). The overexpression of biosynthetic genes or increase BR sensitivity result in contrasting phenotypes; plants having large stature, with increased number of flowers and seeds and more bent lamina from the vertical axis of the leaf towards the abaxial side (Divi et al. 2009). Like this, the manipulation of genes involved in the modulation of BR endogenous levels, or affecting plants sensitivity to BR have shown promise in agriculture (Yang et al. 2008). To date, one of the key BR biosynthetic genes, *DWF4*, has been manipulated in Arabidopsis, rice, tomato, *Brassica napus* and maize (Choe et al. 2001; Sakamoto 2006; Sakamoto et al. 2006; Liu et al. 2007; Li et al. 2016; Sahni et al. 2016). Similarly, studies in the BR receptor BRASSINOSTEROID INSENSITIVE 1 (BRI1) mutant *d61* in rice and *zmbri1*-RNAi plants in maize has been reported (Morinaka et al. 2006; Kir et al. 2015)**.** In these examples, the overexpression or disruption (gene knockout) of *DWF4* or *BRI1* resulted in beneficial impacts for the plant yield. Like those, other examples have been shown to affect plant architecture (Divi et al. 2009); thus the identification of novel mutants related with BR action is essential.

Brassinazole (Brz) is a commonly used chemical BR-biosynthetic inhibitor that has been useful in the identification of new components of the

BR-synthetic or signaling pathways (Asami et al. 1999; Asami et al. 2000; Sekimata et al. 2001; Wang et al. 2002). We decided to use a similar strategy to identify new factors related with the BR pathway and their downstream targets or partner in rice. However, Brz's high cost and difficult accessibility limits its use, making experiments with *Oriza sativa* (rice), or other monocot plants that often require large-scale experiments, difficult. On the other hand, a relatively new potent and specific BR inhibitor has been use in monocots studies, the triazole propiconazole (Pcz) (Corvalan et al. 2017). In contrast to the limitations of Brz, Pcz is a commercially used fungicide, thus is easily accessible and with inexpensive costs, allowing its use for large-scale chemical genomics and field testing. Pcz treatments produce typical BR-deficient phenotypes such as epinastically growing and dark-green cotyledons, and reduced hypocotyl and primary root lengths (Hartwig et al. 2012). Evidence using Pcz treatments in genetically disrupted *dwf4-1* mutant seedlings pointed that DWF4 is likely to be target of Pcz, like it is for Bzr (Asami et al. 2001; Hartwig et al. 2012).

For plants, as sessile organisms that respond to environment by growth, the regulation of cell cycle is particularly important. The progression of the cell cycle is regulated at two points; the transition from G_1-phase to S-phase and from G2-phase to M-phase. The E2F family of TFs

plays an important role by regulating the transcription of the genes involved in the progression to the S phase from the G_1 phase. The DNA-binding activity of E2F can be stimulated by Dimerization Partner (DP) proteins, thus E2F/DP heterodimeric TFs activate transcription of genes responsible of cell cycle control, initiation of replication, and enzymes required for DNA synthesis in S-phase (Kosugi et al. 2002). E2F/DP pathway is well conserved in animals and plants. In Arabidopsis, at least three *E2F* (*E2Fa*, *E2Fb*, and *E2Fc*) and two DP (*DPa* and *DPb*) have been identified along with their target genes (Magyar et al. 2000; Kosugi et al. 2002; Vandepoele et al. 2005). The only study about DPs in plants is a report in where the overexpression of *E2F* and *DPa* produced very dwarf Arabidopsis plants with curled leaves and cotyledons (De Veylder et al. 2002). In rice, a genome-wide analysis identified several core cell cycle genes, including four E2Fs and three DPs (*OsDP1*, *OsDP2* and *OsDP3*). However, just the transcripts of *DP1* were detected by RT-PCR while attempts to detect *DP2* and *DP3* failed in all the tested tissues (Guo et al. 2007).

In the current study, we screen a T-DNA activation-tagging mutant population using large-scale Pcz treatments. These mutants were developed using the pGA2715 vector with 35S enhancers, which can cause transcriptional activation of genes nearby the insertion, resulting in

dominant gain-of-function mutations (Jeong et al. 2002). Among seventeen propiconazole-resistant lines, we further analyzed the denominated *propiconazole-resistant 1* (*pzr1-D*) mutant, which presented increased yield when grown in field. Moreover, mutant plants presented several BR-characteristic phenotypes such as semi-dwarfism and larger numbers of tiller along with increased sensitivity in bioassays to measure BR response. Molecular characterization and phylogenetic analysis allowed us to determine that the insertion in *pzr1-D* produced activation-tagging of an ortholog of the Arabidopsis DPb transcription factor, with roles in the regulation of cell cycle. Dominant mutants and transgenic plants overexpressing *PZR1* gene show increase number of tiller, panicles and branches in the panicles, all resulting in considerable increased yield compared to the control plants. Our findings reveal a possible role of the PZR1 transcription factor in mediating BR-regulated cell division control in rice. These findings may serve as a basis for new molecular strategies that in combination with conventional breeding methods could help in the develop of plants that results in optimal phenotypes favoring yield without the need for conventional long-term breeding programs, and decrease the use of fertilizers and their negative environmental effects.

MATERIALS AND METHODS

Plant materials

Rice wild type and mutant plants used in this report belong to DongJin background. Our *pzr1-D* mutant and other screened lines proceed from a previously described library of activation-tagging lines (Jeong et al. 2002). Rice plants were grown under paddy field growth condition (2014 to 2015) or in greenhouse at 28 to 30°C. For plants in field, 3-weeks old seedlings were planted from the end of May to mid or end of October, time at which they were harvested and studied.

Arabidopsis wild-type Col-0 and transgenic lines were surfaced-sterilized before being sprinkled on 0.8% agar-solidified media containing 0.5x Murashige and Skoog (MS) salts and 1% sucrose. After 48 h stratification at 4°C in dark, plates were transferred to a growth room and grown under at 22°C and a 16 h light photoperiod. If needed, seedlings were transferred to soil after 10 days in MS media.

Chemical treatments and morphologic analysis

Rice seeds were sterilized for 30 min with sodium hypochlorite 50% and washed 4 to 5 times with water prior to planting. Before each treatments the seeds were germinated in filter paper soaked with water for 2 days. Just

germinated seeds with similar growth were used for treatments in where they were planted 1 cm deep. For Pcz treatments we use coarse vermiculite soil soaked with water supplemented with the indicated Pcz concentrations. We used Pcz 100 mM dissolved in DMSO as a working solution and DMSO alone was added to the water as control or mock condition. Plants were maintained in total dark or long-day light conditions as indicated in each experiment. After 7 days of treatment, images were taken and then growth parameters were measured from the images using ImageJ software. Total plant height was measured from the end of the root to the highest leaf, whereas the length of the main root was used to determine root length. Seed length and area were also calculated with ImageJ software from the digital pictures. All statistical data was calculated using GraphPad Prism 5 software. Significance was evaluated using Student's *t*-test.

Genomic DNA and genotyping

DNA extraction was performed using HiGene™ Genomic DNA Prep kit (BIOFACT) following manufacturer recommendations. Extracted DNA was quantified using Epoch™ Spectrophotometer System (BioTek) controlled with the Gen5 Data Analysis software interface. We used 50 ng of DNA template in two set of PCRs for genotyping. In one PCR we used specific primers for *LOC_Os03g05760* gene and the vicinities of the gene to amplify

the wild-type allele. Other PCR was performed using primer of left border of the T-DNA (pGA2715 LB) with gene specific primer to amplify the mutant allele in which T-DNA is inserted. This analysis allowed us to identify homozygous and heterozygous mutant plants for each line, as well as their segregating wild type. When line amplifies just wild type allele was considered segregating wild type (w/w), when just mutant allele amplified then homozygous (T/T). In cases of plants amplifying both, heterozygous for the insertion (w/T). The sequences of the primers used in the PCRs are specified in Supplemental Table S4-1.

Lamina-joint bending assay

Lamina bending bio assay was slightly modified from the version described by Wada et al. (Wada et al. 1984; Zhang et al. 2012). We sterilized and germinated seeds in filter paper and then transferred them to 0.5x MS media in where they were grown for other 7 days in dark conditions. We chose seedlings presenting uniform growth to cut off segments containing the second-leaf lamina joint. The segments were floated on distilled water for 24 h in dark to wash out chemical residues from plant that may alter the experiment and to ensure that all lamina angles of the samples were similar before the treatment. Once again we chose only uniform samples presenting similar angle degree to continue the treatment, in where this time the

segments were floated on distilled water containing indicated concentrations of brassinolide (BL). All the procedures including sectioning of the samples and transfer to the different solutions were performed in a dark room to avoid as much light as possible. The segments were incubated for 48 h in dark with the different treatments and then we photographed the samples to measure the angle between the lamina and the blade sheath using ImageJ software. All statistical data was calculated using GraphPad Prism 5 software and significance was evaluated using Student's t-test.

RNA isolation and gene expression analysis

Total RNA used for qRT-PCR analysis was isolated from rice or Arabidopsis tissues using RNeasy Plant kit (QIAGEN) following manufacturer's instructions. Using 2 μg of the RNA, cDNA was synthesized using M-MLV reverse transcriptase (ELPIS). qRT-PCR was run using the Applied Biosystems StepOne Real-Time PCR System and Power SYBR Green PCR Master Mix as previously described (Corvalan et al. 2017) using the primers listed in Supplemental Table S4-1. For Arabidopsis OX lines, gene expression data was normalized against OX line 8, which presented low expression of the transcript in RT-PCR studies. This is because *03g05760* is a rice gene and thus is not present in Col-0 control plants.

Phylogenetic analysis

Protein sequences showing similarity to PZR1 protein were retrieved using BLAST server on Phytozome website (https://phytozome.jgi.doe.gov/pz/portal.html). Protein sequences of Arabidopsis, rice, wheat and human proteins were obtained from the UniProt server (http://www.uniprot.org) and phylogenetic analysis was performed using Clustal Omega (http://www.ebi.ac.uk/Tools/msa/clustalo/) and BoxShade software (http://embnet.vital-it.ch/software/BOX_form.html) to identify and visualize conserved sequences. The resulting phylogenetic tree was generated using Neighbor-joining method (Clustal Omega) and to visualize and modified it we used Figtree program v1.4.3. A list of the proteins sequences used as an input in the servers can be found in Supplemental Table S4-2.

Cloning and plant transformation

For overexpression of rice *OsDPB/PZR1* under the cauliflower mosaic virus 35S promoter (35S) in rice and *A. thaliana,* we constructed the vectors as follows: RNA was extracted and cDNA was synthesized from 7-days old rice seedlings and specific primers (Supplemental Table S4-1.) were used to amplify full-length coding sequence (CDS) of interest. The obtained product of 696 bp corresponding to our gene of interest was purified and cloned into

the entry vector pENTR/SD/D-TOPO (Invitrogen). The clones in the entry vector were then cloned into the destination pEarleyGate101(C-YFP-HA) vector, which is compatible with the gateway system. For Arabidopsis transformation, *Agrobacterium* GV3101 strain was transformed with the vectors, and LBA4404 strain was used for rice. The constructs were transformed into plants using conventional *Agrobacterium*-mediated techniques and transgenic seedlings were selected on MS medium supplemented with 20 mg/L BASTA. BASTA-resistant and -sensitive plants were identified and chi-square test carried out to validate the data for 3:1 segregation for segregation analysis.

Callus induction

Rice seeds were sterilized and put in filter paper until completely dry. Twelve to eighteen seeds were germinated and culture on 2N6 media plates containing Duchefa's Chu(N6) powder (4 g L^{-1}), sucrose (30 g L^{-1}), L-proline (2.9 g L^{-1}), casein (0.3 g L^{-1}), myo-inositol (0.1 g L^{-1}), 2.4-D (2 mg L^{-1}) and phytagel (4 g L^{-1}) at pH adjusted to 5.8. Plates were placed in growth chamber in dark conditions at 32°C for the indicated days before being weighed and photographed for analysis with ImageJ software.

Microscopy

Root images were obtained using a Leica TCS SP9 confocal laser scanning microscope. Root samples were excised 1 cm above the root tip from 7-days-old seedlings and then submerged in propidium iodide (PI) solution 10 μg/mL for 3 minutes. Before observe the samples were rinsed two times in distilled water. Image were compiled and analyzed using LAS X software version 3.0.2. For cell counting and size determination, we considered cells inside a 60 μm^2 square drawn in the meristematic zone, 300 μm above from the root tip.

For the leaf images, a Primo Vert inverted microscope (Zeiss) was used along with ImageJ software for the measurements. Each leaf of 7-days-old seedlings was dissected in the middle, were the images were taken and used to compare between genotypes.

Transcriptome analysis and identification of DEGs between wildtype and pzr1-D mutant seedlings

Total RNA was extracted from seedlings using Trizol reagent following manufacturer's instructions. Treatments were performed in triplicate for seedlings of two genotypes, wildtype (WT) and *pzr1-D* (MUT) and were grown under light or total dark conditions. A total of 12 samples were prepared and subjected to quality inspection. From them, duplicates of each

treatment with the best purity value were used to construct sequencing libraries. Quality inspection, library preparation and raw data processing were conducted by a contracted service (THERAGEN ETEX, http://www.theragenetex.com/). Shortly, quality was assessed on an Agilent Bioanalyzer 2100 with RNA integrity number (RIN) greater than 7 (above 9 in most of the samples). Libraries were generated using UltraTM RNA Library Prep Kit for Illumina and were sequenced on an Illumina HiSeq 4000 system. Differentially expressed genes (DEGs) were identified in the samples as WT dark-vs- *pzr1-D* dark and WT light -vs- *pzr1-D* light. Expression levels of each gene was calculated using HTseq software and normalized, DEGs were screened as log2 (fold changes) ≥ 1 and corrected P-value (Q-value) ≤ 0.05. For gene ontology (GO) analysis, venn diagrams and promoter analysis, we used tools available online in http://pantherdb.org/, http://www.interactivenn.net/ and http://plantpan2.itps.ncku.edu.tw/gene_group.php?#multipromoters respectively.

RESULTS

Mutation by activation tagging confers resistance to BR inhibitor propiconazole

Previously, we reported a new potent and specific BR-inhibitor propiconazole (Pcz) and demonstrated its uses in maize and Brachypodium plants (Hartwig et al. 2012; Corvalan et al. 2017). In contrast to the high-priced and thus limited use of its counterpart Brz, Pcz allowed us to perform large-scale tests with very low costs to screen a T-DNA activation-tagging mutant population. These mutants were developed using transposable elements with 35S enhancers, the pGA2715 vector, which can cause transcriptional activation of genes nearby the insertion, resulting in dominant gain-of-function mutations (Jeong et al. 2002).

First, we studied the response of rice to the inhibitor to find the optimal conditions in where we could isolate Pcz-resistant mutants. As expected, Pcz affected rice growth and produced dwarfism in a dose-dependent manner (Supplemental Figure S4-1). We found that treatments of 30 μM Pcz reduced the total size of wild-type seedlings up to 47%, and the response of the root was even more severe, with 65% of inhibition (Figure 4-1A to B). To ensure that Pcz was effectively inhibiting BRs, we tested the expression levels of a key BR biosynthetic gene, *OsDWF4.* We observed

increase in *OsDWF4* mRNA abundance in plants treated with Pcz, which is in concordance with the negative feedback regulation of BR biosynthetic genes (Figure 4-1C). Thus, we expected that using this condition we could perform visible phenotypic screening for resistant seedlings reflected on their root and or leaf lengths.

We were able to find 17 lines from the activating-tagging mutant population presenting different degrees of resistance to the treatment and denominated them as PROPICONAZOLE RESISTANT (PZR) 1 to 17. Among these lines we isolated a dominant mutant, *pzr1-D* with visible resistant phenotype that co-segregated with the T-DNA insertion (Supplemental Figure S4-2). Root lengths of homozygous mutant seedlings with 30 μM Pcz were almost the same that under mock condition, contrary to wild type which presented 45% inhibition of root growth (Figure 4-2). Our Pcz treatment for the screening and confirmation were done under dark conditions, but similar results were obtained with treatments in normal light conditions (Supplemental Figure S4-3).

***PZR1* increase number of tiller, panicles and yield in rice**

We examined phenotypes of adult plants in field and under greenhouse conditions and observed that *pzr1-D* mutants presented increased yield when comparing with wild-type plants (Figure 4-3). Plant total weight was

increase in 33% compared with WT although their total height did not show significant differences (Figure 4-3A, B and E). Increase of weight can be explained for the elevated number of tiller in the mutants, as well as the increase in the number of panicles in each plant (Figure 4-3C, D and E). Seed weight per plant increased from 20 grams in WT to 50 grams in the mutants, which means a yield increase of around 40% (Figure 4-3G). We then studied the morphology of the panicles, and found that not just the number of panicles increased by the mutation, but the number of primary and secondary branches in each panicle was higher in *pzr1-D* (Figure 4-3F, H and I). Taking into consideration the results above, the higher weight of total seeds in the activation-tagging mutants is more likely due to increase in number of seeds in each plant more than by increase in the seed size. We studied seed size, area and weight and corroborated that mutant seeds are not significantly different from WT seeds. In fact they were slightly smaller than in the WT (Supplemental Figure S4-4).

Mutant plants present BR-sensitive phenotype in lamina-joint, root and coleoptile growth bioassays.

Considering that *pzr1-D* mutant was isolated as resistant to BR inhibitor we next proceed to evaluate our mutant response to exogenous brassinolide (BL). Rice leaf bending is known to be sensitive to active BRs, and this is

the basis under the well-known lamina-joint inclination bioassay to test BR response (Wada et al. 1981). We first noted that under normal growth conditions the bending angle of the leaf of *pzr1-D* seedlings is more than that of the wild-type plants (Figure 4-4A and B). In the lamina-join assay, we noticed than in the presence of BL the leaf angle increased dramatically in *pzr1-D* plants while wild-type plants presented a milder response (Figure 4-4C and D). We observed that when we increase the BL concentration, the difference in the angle response becomes more significant (Figure 4-4E). This suggest that our mutant may be more sensitive to exogenous BL than wild-type seedlings. To support this, we also tested the response of root and coleoptile growth of the seedlings upon BL treatment in dark conditions. In absence of BL, we found significant differences in root growth between *pzr1-D* and its wild type counterpart when growing in darkness (Figure 4-5A). Moreover, when media was supplemented with BL the inhibition of root growth in *pzr1-D* was more affected than in wildtype and the opposite was observed in coleoptile (Figure 4-5B and C). Thus, more sensitivity in mutant seedlings was confirmed by root inhibition and coleoptile elongation by BL.

Then we tested whether expression of *PZR1* was affected by BL levels by checking transcript levels following Pcz treatments in seedlings.

We found that PZR1 expression was down-regulated in plants subject to the treatment (Figure 4-5D).

PZR1 Activation-Tagging Confers the BR-Related Phenotypes

Previous analyzes of the activation-tagging mutant population (Jeong et al. 2002) revealed that a gene, *Os03g05760*, is located 1.8 kb downstream of the T-DNA insertion (Figure 4-6A). Thus we checked the expression level of *Os03g05760* and other two genes in the vicinities of the insertion (*Os03g05750* and *Os03g05770*). The expression level of *Os03g05760* in the mutant was about 10 times that in the wild-type. The expression of the other two genes remain at similar values with wild-type samples (Figure 4-6B). On this basis, increase in the *Os03g05760* mRNA levels appears to be responsible for the phenotypes in the *pzr1-D* mutant. We also examined the expression level of this gene in the heterozygous and segregating wild-type plants, and found that increase in the expression was in a dose-dependent manner in the mutants (Figure 4-6C). This along with the intermediate phenotypes that we found in the heterozygous plants, indicated us that our mutation was dominant, and therefore we designated it as *pzr1-D* (Supplemental Figure S4-2 and S4-5).

PZR1 Overexpression Causes Increment of Tiller Number in Rice and Lateral Roots in Arabidopsis

To confirm whether the observed phenotypes are caused by *PZR1* increased expression in the *pzr1-D* mutant, we transformed wild-type rice and Arabidopsis plants with an expression vector that drives *PZR1* CDS under CaMV 35S promoter. For rice plants we observed that, like in *pzr1-D*, tiller and panicle number is increase in lines which significantly overexpress *PZR1* such as #1, 2, 3, 9 and 10 (named OX 1-10) (Figure 4-7). Lines #13 and #16 present expression values that are not very different to wild-type conditions and present similar phenotype with DongJin plants.

For Arabidopsis *PZR1*-overexpressing plants (hereafter OX), we couldn't find any distinguish phenotype in adult plants. Yet seedlings with high expression levels of *PZR1* (i.e. OX 2, 3 and 5) showed increase lateral roots number, which can be attributed to DP roles in cell cycle (Figure 4-8 and Supplemental Figure S4-6).

PZR1 Encodes a Rice Homolog of DP Transcription Factor Responsible of Cell Cycle Control

Next we studied about the possible functions of *Os03g05760* gene. We screened Arabidopsis database using full-length protein sequence of the product of *Os03g05760* (Q84VA0), to look for orthologs genes. The highest

scores corresponded to two DP (Q9FNY2 and Q9FNY3) and three E2F (Q9FV71, Q9FV70 and F4ILT1) proteins, all from a family of transcription factors with roles in cell cycle. Plant DP proteins have been identified and studied in Arabidopsis and wheat (Magyar et al. 2000; Ramirez-Parra et al. 2000) and three possible DP orthologs in rice were found using genome-wide analysis (Guo et al. 2007). Phylogenetic analysis of PZR1 sequence along with known DP proteins in plant supported the fact that PZR1 is likely to be an ortholog of Arabidopsis DPb (Figure 4-9). We observed that a DNA-binding and heterodimerization domains are present in the PZR1 sequence, which support our hypothesis that this gene could be performing similar functions to its ortholog in Arabidopsis (Figure 4-9B).

To understand the functions of *PZR1* in rice, we investigated its expression pattern in rice tissues of seedlings and adult plants (Figure 4-10). We observed that expression of this gene was relatively low in plants, with lower expressions in root compared to aerial tissues (Figure 4-10B). Still we were able to detect the transcripts in all studied tissues in adult plants, in where we found that tissues from leaves presented the higher expression. This was even more obvious when we studied *PZR1* expression in *pzr1-D* mutants (Figure 4-10C).

Because of the possible roles in cell division of *PZR1* we studied callus initiation and morphology in WT and *pzr1-D*. Callus induced from mutant seeds were smaller than callus derived from WT seeds, and presented adventitious root formation (Figure 4-11A and B). When we supplemented callus induction media with Pcz they showed less sensitivity to the treatment. While Pcz-treated WT calli were almost half of the size of the calli growth in control conditions, there was no significant difference among Pcz-treated and no treated in *pzr1-D*-derived calli (Figure 4-11C and D).

Next we performed microscopic analysis of wildtype and mutant roots to analyze whether PZR1 affected cell number or size. Roots of *pzr1-D* contained more cells, most of which were smaller (Figure 4-12). Similarly, mutant leaves are wider compared to wildtype and present more but smaller cells (Supplemental Figure S4-7). Therefore, *PZR1* may play a role in regulation of cell cycle in rice.

To elucidate the possible molecular basis of the relation between BR and cell cycle processes through PZR1 we performed genome-wide transcriptome analysis between wild type and mutant *pzr1-D* seedlings. To avoid individual differences among plants, we sampled three to four seedlings per treatment and analysis were performed considering two

biological replicates. In total, and considering consistency in all the samples, were found 1141 differentially expressed genes (DEGs) among wild-type and mutant seedlings. From those, 678 genes were differentially expressed just under dark growing conditions, 229 when growing the seedlings in light and 234 were shown to be differentially expresses independent of the light treatment (Supplemental Figure S4-8A). We then identified DEGs that were up- or down-regulated in the mutants when compared to the wild type (Supplemental Figure S4-8B) and listed the twenty most significant differentially expressed genes in each condition (Supplemental Table S4-3 and S4-4). To try elucidate what those genes might have in common we performed gene ontology (G.O.) analysis to find significant enriched terms. Among the most abundant G.O. terms was cellular processes (GO:0009987), containing 202 DEGs. In cellular process, G.O. terms such as cell cycle (GO:0007049), cellular component movement (GO:0006928), chromosome segregation (GO:0007059) and cytokinesis (GO:0000910) were found enriched. Other found terms include cellular component organization (GO:0016043), cellular component organization or biogenesis (GO:0071840), kinase activity (GO:0016301), protein serine/threonine kinase activity (GO:004674), nucleic acid binding (GO:0003676) and nucleotide binding (0000166), all mostly involved with

cell cycle process and regulation (Figure 4-13 and 4-14). In fact we found that transcription of several known rice cell cycle genes were differentially expressed genes (DEGs) in *pzr1-D* compared with WT (Supplemental Table S4-5). Several GOs of catalytic activities (GO:0003824) and protein binding protein binding (GO:0005515) were enriched too (data not shown), so we tested if some of those genes were related with BR signaling or synthesis, but we could not find significant DEGs among the BR-related genes between wild type and the mutant (Supplemental Table S4-6).

Additionally, we examined the promoter sequences of the 80 top differentially expressed genes listed in Supplemental Tables S4-3 and S4-4 and found that 77 out of 80 contain E2F/DP consensus promoter binding sequence TTTC[CG]CGC (Vandepoele et al. 2005) (Supplemental Table S4-7). All results above suggest that *pzr1-D* mutation directly affects cell division, but further analysis are needed to clarify if BR regulates cell-cycle genes through PZR1.

DISCUSSION

The lack of information about BR processes in monocot plants motivated the development of new genetic tools and studies in the last few years. To date, several genes controlling rice architecture and yield have been found to relate to BR responses and many mutants have been identified with potential uses for agronomic improvement. Like other BR-related mutants in rice, the *pzr1-D* mutant displays semi dwarfism and increased number of tiller, two traits that are usually negatively related; dwarf plants generally present more tillers. But unlike to other BR mutants, the dwarfism in *pzr1-D* was not accompanied by a significant reduction of the seed size. On the contrary, seed size was almost not affected, while increased number of tiller resulted in increased number of panicles in the plant, all contributing to an increment of yield per plant.

In this study we were able to determine that the *pzr1-D* phenotype resulted from the activation of *PZR1*, a homolog to Arabidopsis DP transcription factor (Figure 4-6 and 4-9). DP is a dimerization partner of E2F transcription factor that stimulate DNA-binding to activate transcription of genes involved in progression to the S phase. Results showed that just as the increased transcript levels of *PZR1* in the T-DNA activation-tagging lines, *PZR1* overexpression in rice produced similar

phenotypes and yield increase (Figure 4-3 and 4-7). The E2F/DP heterodimer function is well conserved in animal and plant kingdoms, and phylogenetic analysis showed that the heterodimerization domain is well conserved in PZR1, a reason to believe that PZR1 is likely to be involved in cell cycle regulation in rice along with E2F just as its Arabidopsis homologs (Figure 4-9). Aside from the phylogenetic analysis other results support PZR1 function as a regulator of the cell cycle. First calli morphology was completely altered in *pzr1-D*-derived compared with wildtype-derived calli. Calli formed from *pzr1-D* seeds were smaller and presented root-like structures, thus the balance between cell division and cell differentiation was clearly altered in the mutant background (Fire 4-11). Second, number and size of cells in root and leaf is altered in the mutant compared with wildtype counterpart (Figure 4-12 and Supplemental Figure S4-7). Additionally, genome-wide transcriptome analysis revealed an association of PZR1 with a number of genes involved in cell-cycle regulation (Supplemental Table S4-5). Many GOs related with cellular processes were enriched in the DEGs between WT and *pzr1-D* (Figure 4-13 and 4-14). Still some data would be necessary to determine at which point the up regulation of *PZR1* is interrupting the normal cell cycle and differentiation progression. Interestingly, the analysis of the top DEGs promoter sequence determined

that almost all the differentially expressed genes have consensus E2F/DP binding sequence in their promotor, establishing once more that PZR1 may acting as Arabidopsis DP transcription factor (Supplemental Figure S4-9 and Table S4-7).

The dwarf phenotype observed in BR-deficient or -insensitive mutants is mainly caused by decreased cellular elongation, but also it has been reported that in some cases cell proliferation is altered as well (Kauschmann et al. 1996; Szekeres et al. 1996; Azpiroz et al. 1998; Choe et al. 1999; Yoshizumi et al. 1999; He et al. 2003; Kwon et al. 2005). Additional microscopic analysis of tissues from *pzr1-D* along with flow cytometric analysis could determine whether cell cycle processes are indeed affected in the mutant, and which molecular process are implicated. Previously, it was reported in Arabidopsis that the overexpression of *E2F* alone produced seedlings with enlarged cotyledons, but the overexpression of *E2F* and its partner *DP* together caused severe dwarfism. Similar to what we observed in *pzr1-D* mutant roots, cotyledon and roots sections of *E2F* and *DP* overexpressing lines contained more, but smaller cells compared with the wildtype and possess an enlarged nuclei, which is product of enhanced endoreduplication. The extra cells in the *E2F/DP* transgenic plants were explained as a result of prolongation of the proliferative phase of cell

cycle, delaying differentiation of the cells (De Veylder et al. 2002). In the other hand, the characteristic phenotype of *pzr1-D* callus may be a result of a shortening of the cell cycle and precocious progress toward differentiation (Figure 4-11). Anyhow, PZR1 transcription factor may be an important rate-limiting factors for cells to divide.

Interestingly, it was previously reported that the overexpression of *DP* factor alone did not cause any phenotype in Arabidopsis seedlings, and overexpression of just *E2F* resulted in shorter roots (De Veylder et al. 2002; Ramirez-Parra et al. 2004). But contrary to both results, the overexpression of rice version of *DP*, *PZR1*, in Arabidopsis produced seedlings with longer primary root and increment hair density and overall higher root biomass, another important agronomic trait related with drought resistance (Figure 4-8). The phenotypes produced by overexpression of *PZR1* in rice and Arabidopsis, and the fact that this phenotype is the opposite to the one described for overexpression of *E2F* transgenic plants, prompted us to think that rice PZR1 and Arabidopsis DP may not have totally overlapping functions, and PZR1 may have a different role aside of just being merely a dimer partner of E2F (Figure 4-7 and 4-8). Proteomic approaches, such as yeast-two-hybrid experiments, or co-purification of protein complexes might identify partners different from E2F that would provide clues to

elucidate other possible molecular functions or mechanisms of regulation of PZR1. Further molecular analysis could finally reveal BRs effect on PZR1 in wild-type and *pzr1-D* mutant too. Although *pzr1-D* displays various BR-related phenotypes and even confers Pcz resistance on the plants we are still far from fully understanding how PZR1 acts as an intermediate among BR signal and cell cycle. Is not clear whether cell cycle is affected in the mutant owing to an altered BR function, or whether BR regulates cell-cycle genes through PZR1. Seeing that *pzr1-D* mutation does not affect significantly the expression of BR-related genes (Supplemental Table S4-6), but present increased sensitivity to BRs and resistance to Pcz, we speculate that PZR1 could be regulating cell-cycle genes via mechanisms that occurs downstream in the response to BRs. It is well known that phosphorylation plays important roles in the BR signaling during the whole process involving BRI1, BAK1, BKSs, BIN2 and BZR1 (Kim and Wang, 2010; Tang et al., 2011; Ye et al., 2011 add cell cycle). Similarly, phosphorylation plays essential roles in cell-cycle control where cyclin-dependent kinases (CDKs) and cyclins form complexes that phosphorylate targets through progression of the cycle phases (Inze et al. 2006). The nature of PZR1 as cell-cycle regulator with kinase target motifs in its sequence (data not shown) led us to hypothesize that it could be target of phosphorylation by a

component of the BR cascade, which would mean a possible link between both processes. In the context of the BR signaling, one of the most important components is the protein kinase BIN2, or OsGSK2 in rice, which acts at different levels, even mediating different pathways (Kim et al. 2012; Khan et al. 2013). In fact, a recent example of BIN2-mediated cell-cycle regulation was described in rice, where BIN2 was shown to interact and phosphorylate an U-Type Cyclin, CYC U4;1 (Sun et al. 2015). The majority of known BIN2 and other GSK3 substrates contains a short consensus sequence S/TxxxS/T, where S/T corresponds to serine or threonine and x any other residues (Zhao et al. 2002). Conveniently, when checking PZR1 sequence two typical motifs, $T^{35}xxxS^{39}$ and $S^{77}T^{78}xxS^{81}$, were found, rising a possible hint about PZR1 regulation through OsGSK2.

Further research is needed to reveal the complete mechanisms associated with PZR1 and to fully understand *pzr1-D* phenotype. Nevertheless, it is clear that the DP pathway may be used to direct cell division in plants to allow yield and architecture to be adjusted. Since E2F and DP are well-conserved proteins, DP orthologs are most likely to exist in other cereals of agronomic importance. Therefore, similar approaches can be applied to other species through modulation of these homologous genes

to boost yield by increasing tiller and panicle numbers, or even increase drought resistance by amplification of both primary and lateral roots.

FIGURES AND TABLES

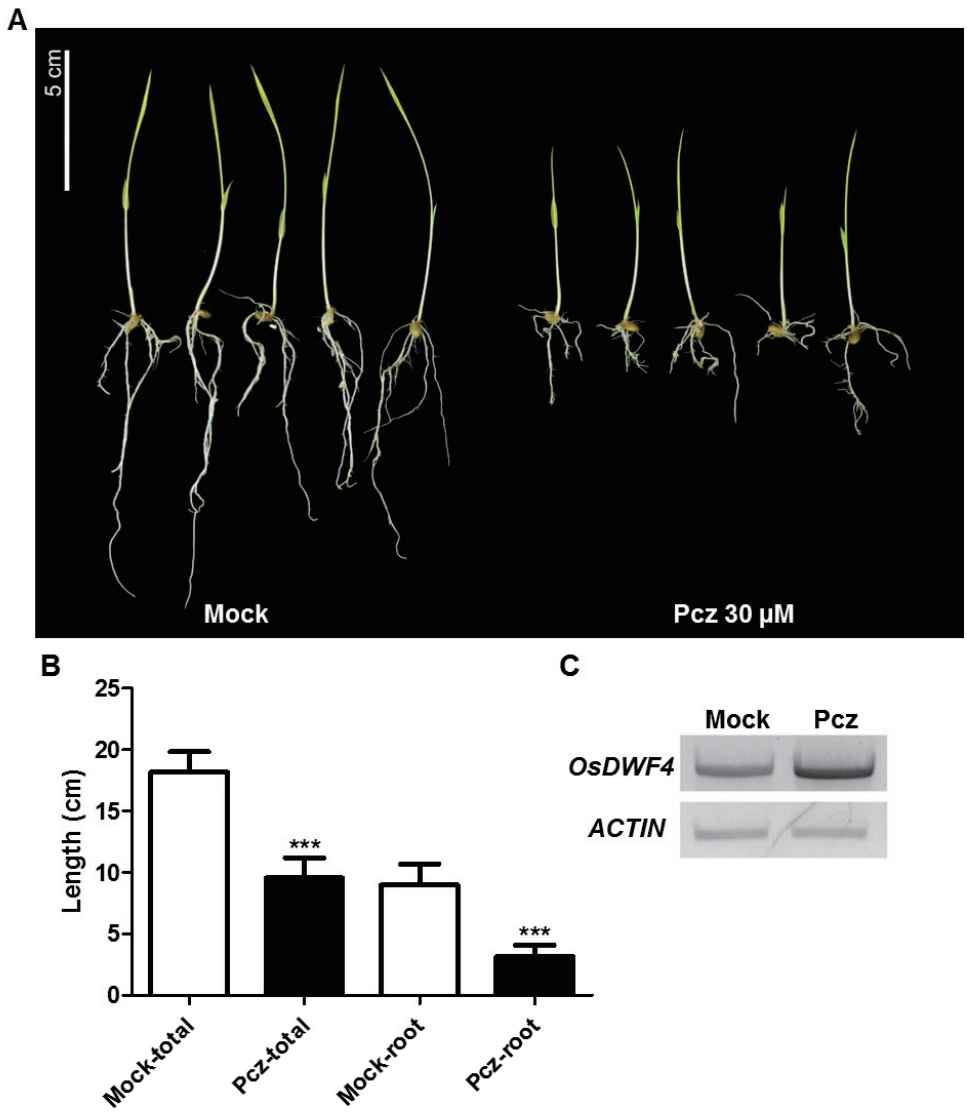

Figure 4-1. Propiconazole effects in rice seedlings. (**A**) Morphology of 10-days old rice seedlings under mock or 30 µM Pcz treatments in the dark. (**B**) Overall and root lengths of seedlings shown in panel A. Values represent average of at least 10

samples and error bars represent standard deviation. Significant differences among treatments were determined by Student's *t*-test. ***, P<0.0001. (**C**) Semi-quantitative RT-PCR comparing *DWF4* expression in mock and Pcz treatments. Actin was used as internal control.

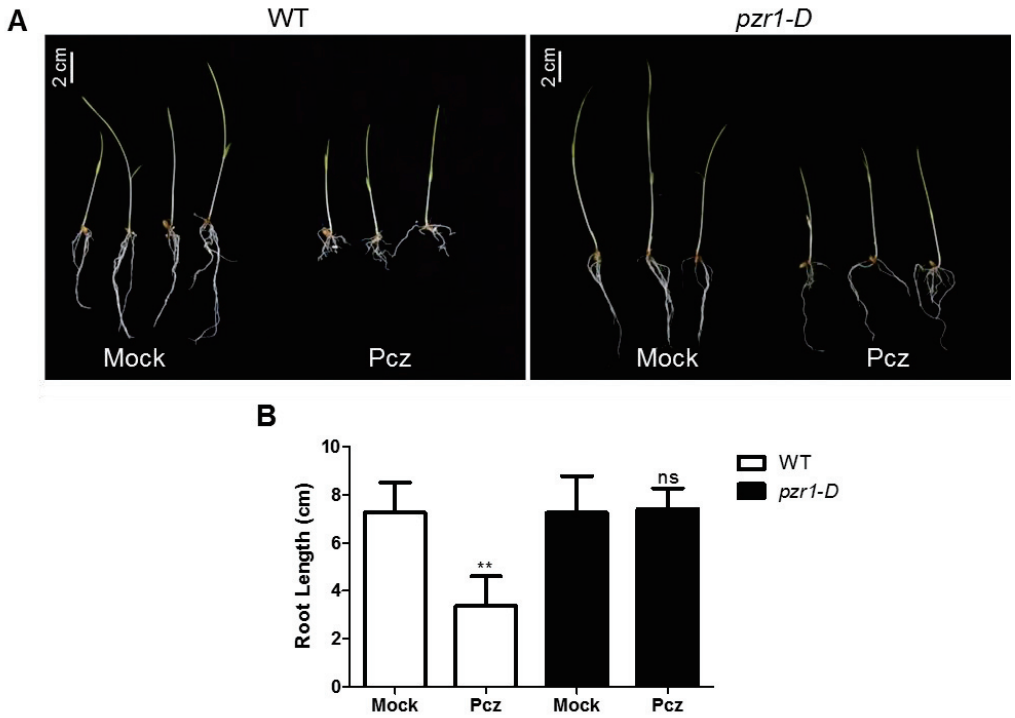

Figure 4-2. Propiconazole resistance of *pzr1*-D mutant seedlings. (**A**) Morphology of 10-days old rice wild-type and mutant seedlings under mock or 30 μM Pcz treatment conditions. (**B**) Root lengths of wild-type and *pzr1-D* seedlings under each treatment. Values represent average of 12 samples per treatment. Error bars represent standard deviation. Significant differences among treatments were determined by Student's *t*-test. **, P<0.001 and ns non-significant.

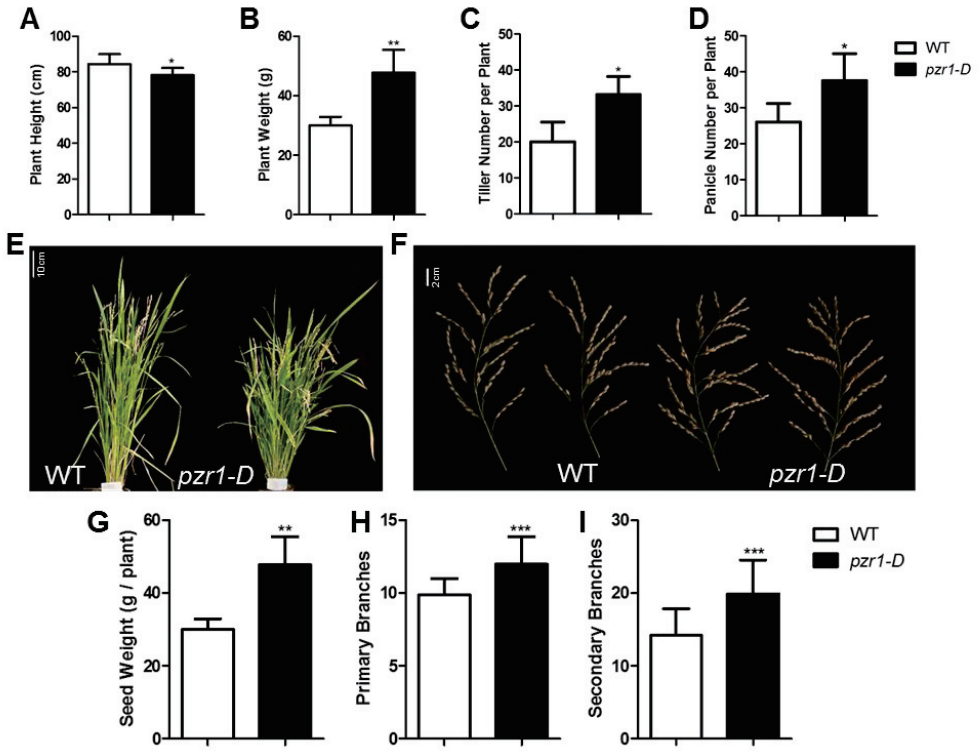

Figure 4-3. Phenotypes of adult plants. (**A**) Plant height, (**B**) plant weight, (**C**) tiller number and (**D**) number of panicles was graphed for wild type and *pzr1-D*. (**E**) Comparison of adult plants and (**F**) panicle morphology between wild type and mutant. Comparison of the (**G**) seeds weight per plant, (**H**) number of primary branches and (**I**) secondary branches. The graphs represent average value (n>7) and error bars represent standard deviation among samples. Significant differences among treatments were determined by Student's *t*-test. *, P<0.05; **, P<0.001 and ***, P<0.0001.

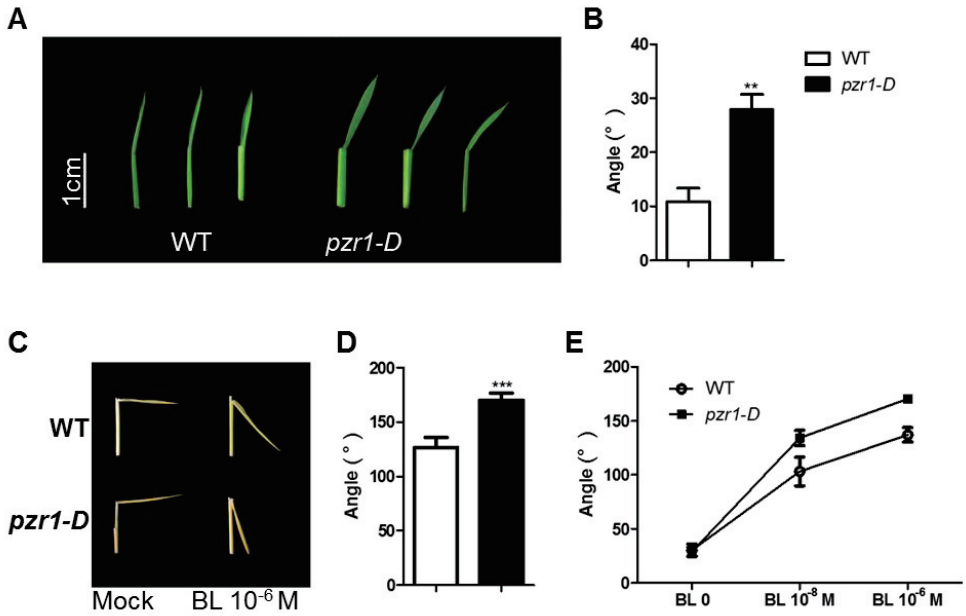

Figure 4-4. Lamina inclination of wild-type and mutant seedlings. (**A-B**) Inclination of the segment corresponding to the second leaf from wild type and mutant *pzr1-D*. (**C-E**) Lamina inclination bioassay performed with indicated concentrations of brassinolide (BL). The graphs represent average value (n=15) and error bars represent standard deviation among samples. Significant differences among treatments were determined by Student's *t*-test. **, P<0.001 and ***, P<0.0001.

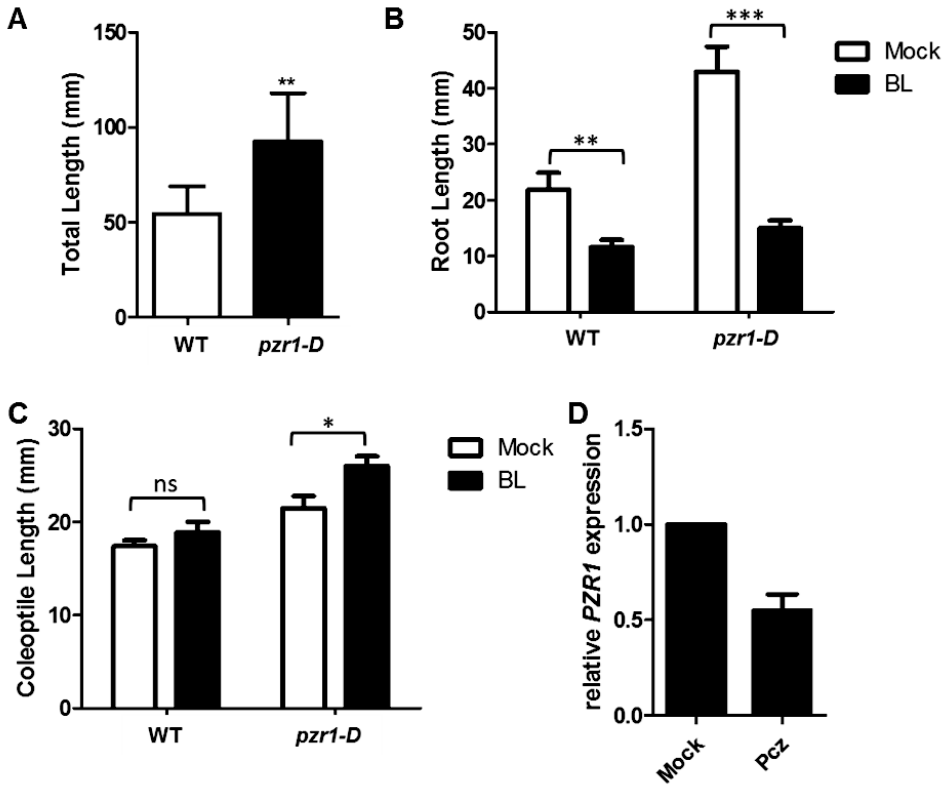

Figure 4-5. BR sensitivity of *pzr1*-D and wild type. (**A**) Effect of darkness in wild-type and *pzr1-D* seedlings. (**B**) BL sensitivity tested by root inhibition in the different genotypes in the presence of BL (1 μM) and in dark conditions. (**C**) Difference in coleoptile growth was measured as a result of BL and dark treatments to seedlings. (**D**) qRT-PCR to examine changes of *PZR1* transcript levels in WT after propiconazole (30μM) treatments. In all measurements, the bars represent average values (n>6). Standard deviation and significant differences are also shown. For significance ns stands for non-significant; *, P<0.05; **, P<0.001 and ***, P<0.0001.

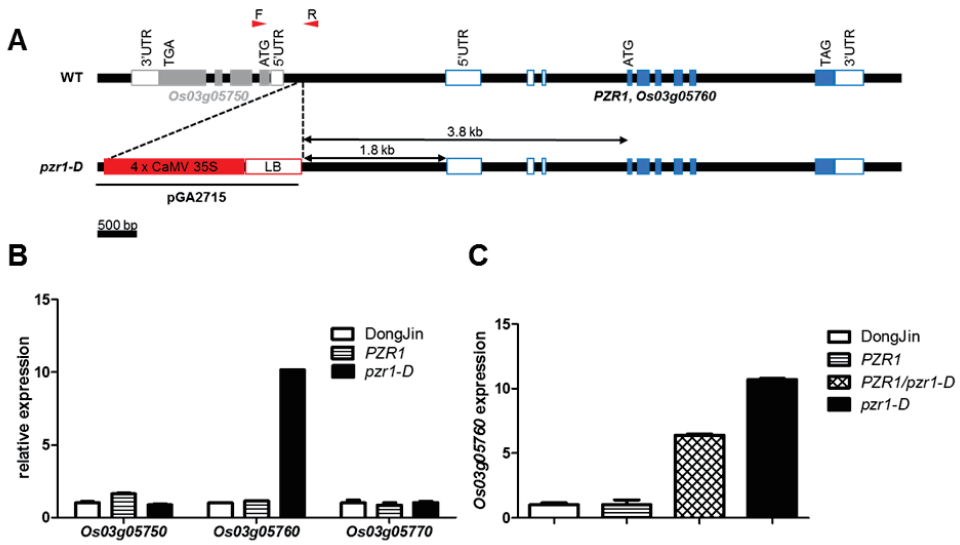

Figure 4-6. Activation-tagging T-DNA insertion in *PZR1*. (**A**) Schematic representation of *PZR1* wildtype (WT) and mutant (*pzr1-D)* alleles. Arrows indicate distance from the border of the insertion to the gene. White boxes represent 5' and 3' UTRs, exons are in blue boxes and introns are represented in black. Red arrowheads demark the position of forward and reverse primers used for genotyping. Grey boxes represent exons of the gene upstream *PZR1*. (**B**) qRT-PCR of three genes adjacent to the T-DNA insertion. (**C**) Transcription levels of *PZR1* in wild type (DongJin), segregating wild type (*PZR1*), heterozygous (PZR1/*pzr1-D*) and mutant (*pzr1-D*) genotypes. Graphs show data from a representative experiment out of three biological replicates performed.

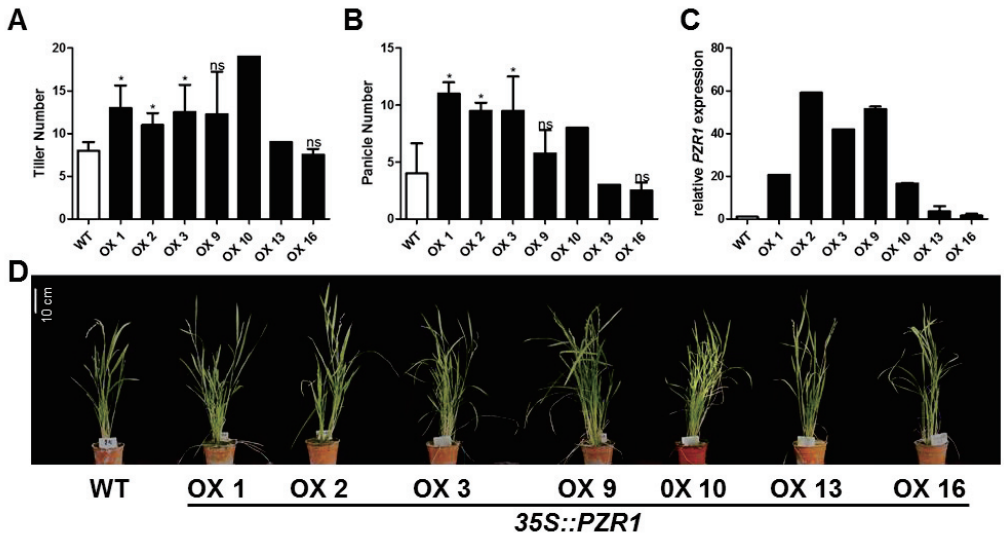

Figure 4-7. Phenotypes resulting from *PZR1* overexpression in rice. (**A**) Number of tiller, (**B**) number of panicles and (**C**) expression levels of *PZR1* in transgenic plants are compared with non-transformed plants. (**D**) Morphology of representative 1-month old plants from each line are show.

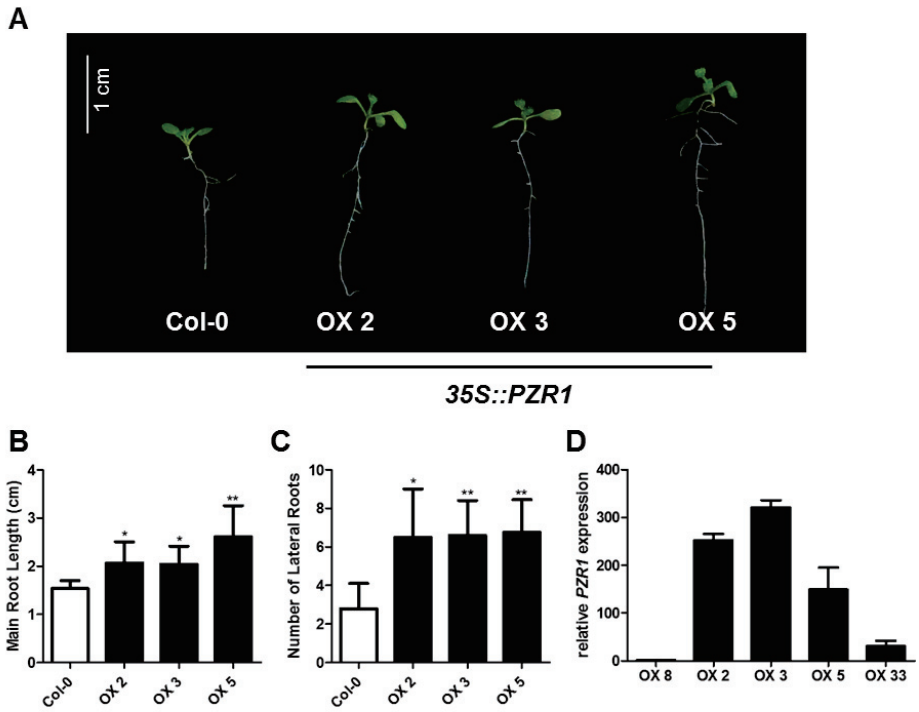

Figure 4-8. Phenotype resulting from *PZR1* overexpression in Arabidopsis. (**A**) Morphology of non-transformed Col-0 wild-type plant and representative seedlings of three independent transgenic lines. (**B**) The length of primary root, (**C**) number of lateral roots are graphed as the average value with n=10. (**C**) Expression levels of *PZR1* in transgenic plants are compared with transgenic line OX 8, which express *PZR1* but a low level. In the graphs, error bars represent standard deviation and the significant differences were determined by Student's *t*-test. *, P<0.05; **, P<0.001 and ***, P<0.0001.

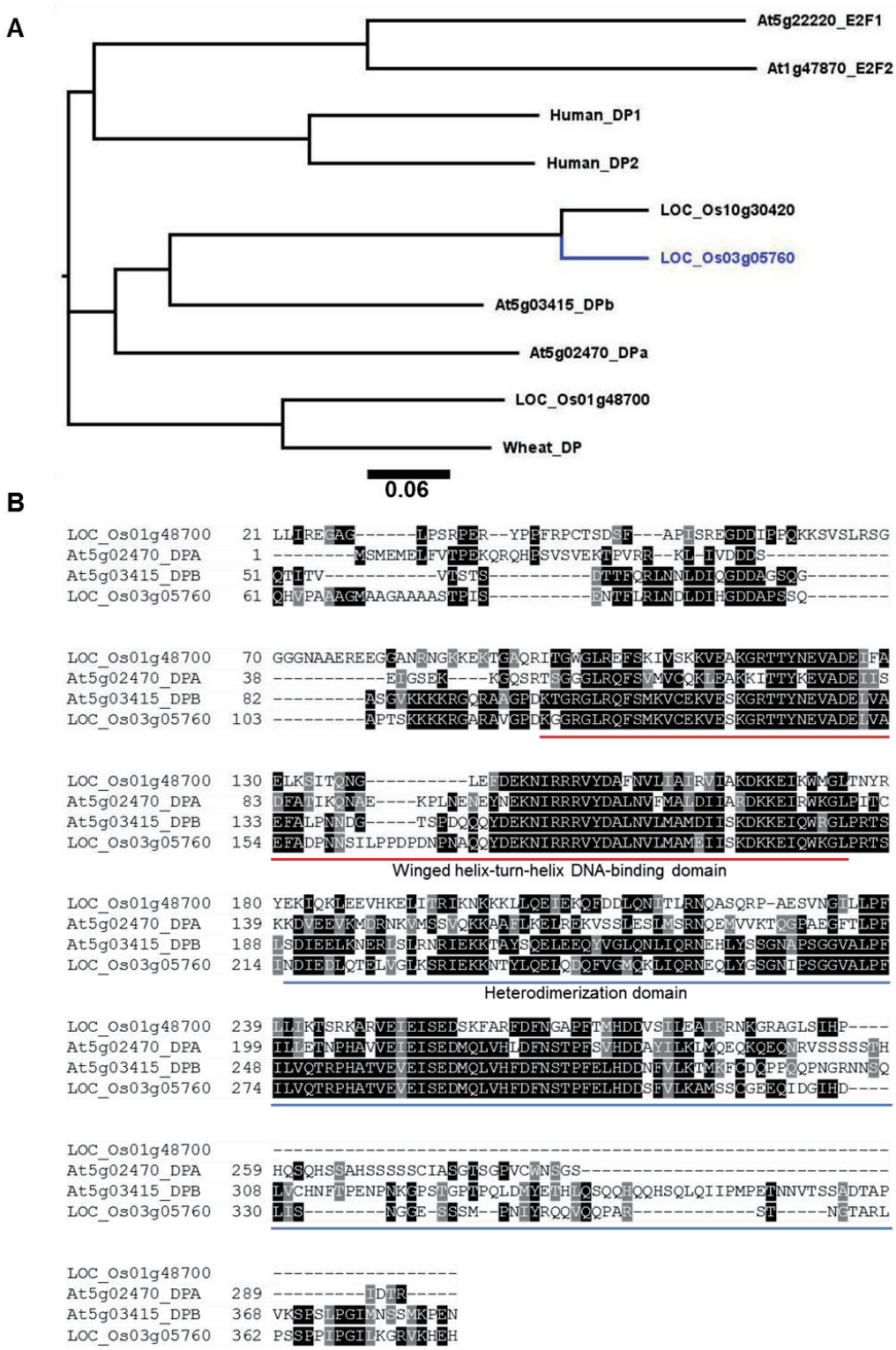
A
At5g22220_E2F1
At1g47870_E2F2
Human_DP1
Human_DP2
LOC_Os10g30420
LOC_Os03g05760
At5g03415_DPb
At5g02470_DPa
LOC_Os01g48700
Wheat_DP
0.06
B
LOC_Os01g48700 21 LLIREGAG------LPSRPER--YPEFRPCTSDSF---APISREGDDIPPQKKSVSLRSG
At5g02470_DPA 1 --------MSMEMELFVTPEKQRQHESVSVEKTPVRR--KL-IVDDDS----------
At5g03415_DPB 51 QITITV----------VTSTS----------DTTFQRLNNLDIQGDDAGSQG--------
LOC_Os03g05760 61 QHVPAAAGMAAGAAAASTPIS----------ENTFLRLNDLDIHGDDAPSSQ--------
LOC_Os01g48700 70 GGGNAAEREEGGANRNGKKEKTGAQRITGWGLREFSKIVSKKVEAKGRTTYNEVADEIFA
At5g02470_DPA 38 ----------EIGSEK-----KGQSRTSGGGLRQFSVMVCQKLEAKKITTYKEVADEIIS
At5g03415_DPB 82 ---------ASGVKKKKRGQRAAGPDKTGRGLRQFSMKVCEKVESKGRTTYNEVADELVA
LOC_Os03g05760 103 ---------APTSKKKKRGARAVGPDKGGRGLRQFSMKVCEKVESKGRTTYNEVADELVA
LOC_Os01g48700 130 ELKSITQNG----------LEFDEKNIRRRVYDAFNVLIAIRVIAKDKKEIKWMGLTNYR
At5g02470_DPA 83 DFAIIKQNAE----KPLNENEYNEKNIRRRVYDALNVFMALDIIARDKKEIRWKGLPITC
At5g03415_DPB 133 EFALPNNDG-----TSEDQQQYDEKNIRRRVYDALNVLMAMDIISKDKKEIQWRGLPRTS
LOC_Os03g05760 154 EFADPNNSILPPDPDNPNAQQYDEKNIRRRVYDALNVLMAMEIISKDKKEIQWKGLPRTS
Winged helix-turn-helix DNA-binding domain
LOC_Os01g48700 180 YEKIQKLEEVHKELIIRIKNKKKLLQEIEKQFDDLQNITLRNQASQRP-AESVNGILLPF
At5g02470_DPA 139 KKDVEEVKMDRNKVMSSVQKKAAFLKEIREKVSSLESLMSRNQEVVVKTQGEAEGFTLPF
At5g03415_DPB 188 LSDIEELKNERLSLRNRIEKKTAYSQELEEQYVGLQNLIQRNEHLYSSGNAPSGGVALPF
LOC_Os03g05760 214 INDIEDLQTELVGLKSRIEKKNTYLQEIQDQFVGMQKLIQRNEQLYGSGNIPSGGVALPF
Heterodimerization domain
LOC_Os01g48700 239 LLIKTSRKARVEIEISEDSKFARFDFNGAPFTMHDDVSIIEAIRRNKGRAGLSIHP----
At5g02470_DPA 199 ILLETNPHAVVEIEISEDMQLVHLDFNSTPFSVHDDAYILKLMQECKQEQNRVSSSSSIH
At5g03415_DPB 248 ILVQTRPHATVEVEISEDMQLVHFDFNSTPFELHDDNFVLKTMKFCDQPPQQPNGRNNSQ
LOC_Os03g05760 274 ILVQTRPHATVEVEISEDMQLVHFDFNSTPFELHDDSFVLKAMSSCGEEQIDGIHD----
LOC_Os01g48700 ----------
At5g02470_DPA 259 HQSQHSSAHSSSSSCIASGTSGPVCYNSGS----------
At5g03415_DPB 308 LVCHNFTPENPNKGPSTGPTPQLDMYEIHLQSQQHQQHSQLQIIPMPETNNVTSSADTAP
LOC_Os03g05760 330 LIS---------NGGE-SSSM--ENIYRQQVQQPAR----------ST-----NGTARL
LOC_Os01g48700 ----------
At5g02470_DPA 289 ---------IDTR-----
At5g03415_DPB 368 VKSESLPGILNSSMKPEN
LOC_Os03g05760 362 PSSEPIPGILKGRVKHEH

Figure 4-9. Phylogenetic analysis of PZR1. (**A**) Phylogenetic tree constructed with characterized DP proteins from human (UniProt protein ID Q14186 and Q14188), wheat (Q9FET1), Arabidopsis (Q9FNY2 and Q9FNY3) and the putative rice orthologs (Q84VA0, Q84VF4 and Q84VD5). (**B**) Multiple sequence alignment of Arabidopsis DP proteins and two rice putative orthologs. Sequence underlined in red delimits the DNA-binding domain while the underlines in blue the heterodimerization domain.

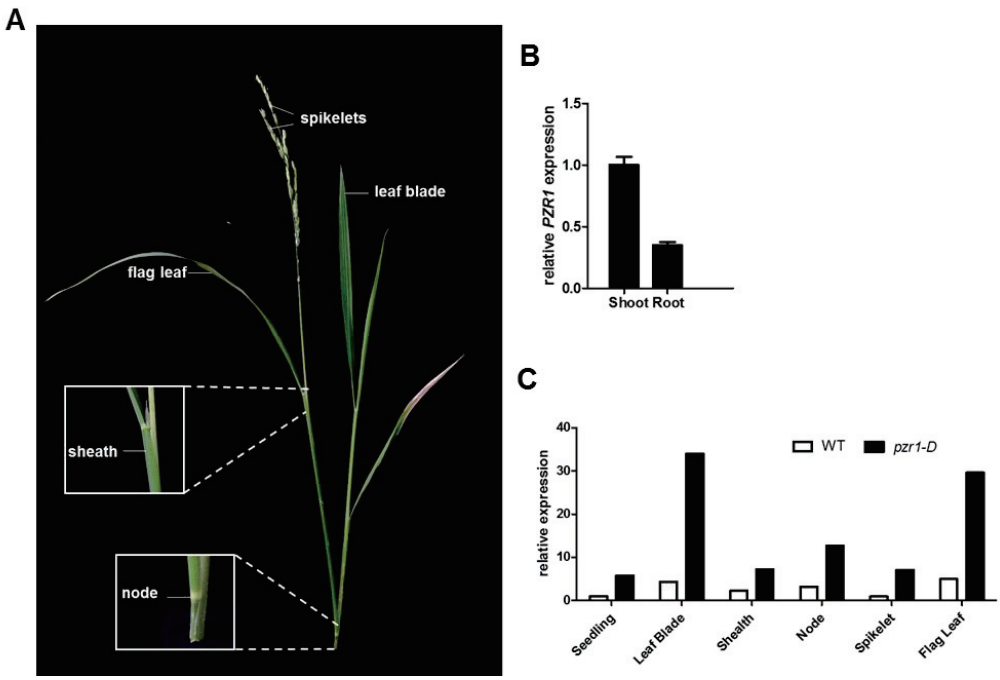

Figure 4-10. Expression pattern in rice tissues of seedlings and adult plants. (**A**) Morphology of adult rice plant showing different tissues studies including leaf blades, flag leaf, spikelets, sheath and node. (**B**) qRT-PCR comparing the expression of *PZR1* in roots and shoots from seedlings. (**C**) qRT-PCR comparing the expression of *PZR1* in 7-day-old seedlings and different tissues from adult plants.

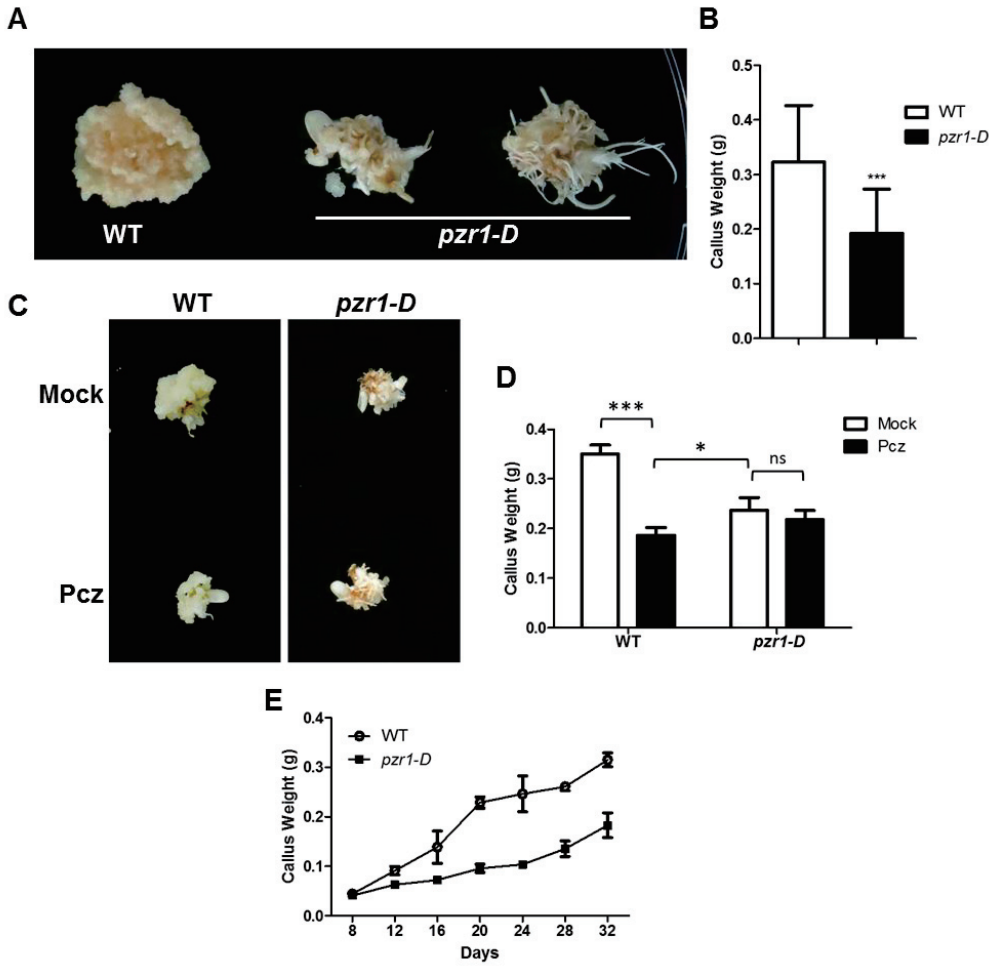

Figure 4-11. Morphology of calli derived from mutant and wild-type seeds. (**A-B**) Morphology and weight measure of calli derived from wild-type and from *pzr1-D*. (**C-D**) Morphology and weight comparison between wildtype and *pzr1-D* derived calli that were grown in callus induction media supplemented with Pcz. (**E**) Growth profile showing the effects of *pzr1-D* mutation in callus development. In the graphs, error bars represent standard deviation and the significant differences were determined by Student's *t*-test. *, P<0.05 and ***, P<0.0001.

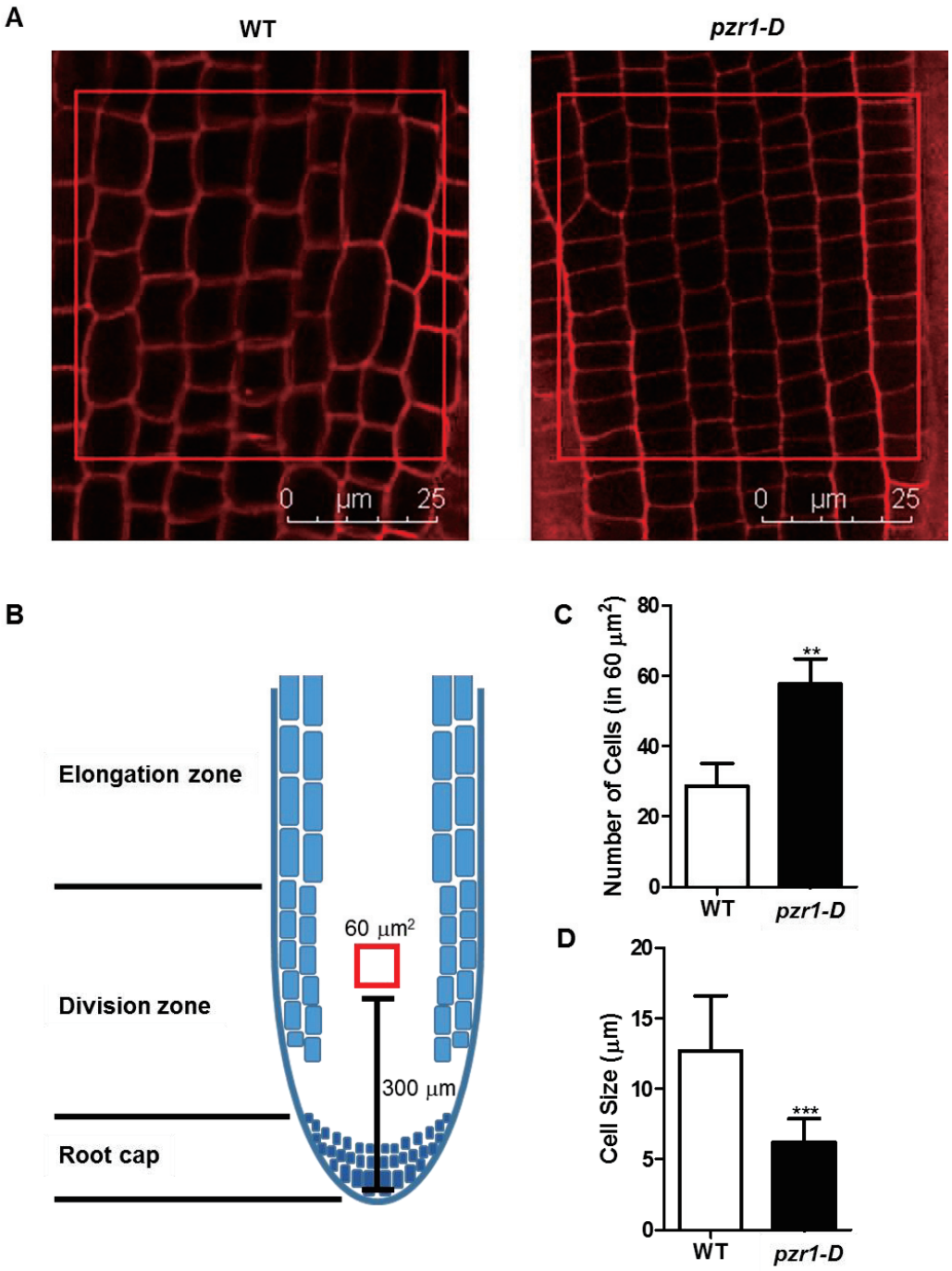
A
WT
pzr1-D
0 µm 25
0 µm 25
B
Elongation zone
Division zone
Root cap
60 µm²
300 µm
C
Number of Cells (In 60 µm²)
80
60
40
20
0
**
WT
pzr1-D
D
Cell Size (µm)
20
15
10
5
0
***
WT
pzr1-D

Figure 4-12. Microscopic analysis of wildtype and *pzr1-D* mutant. (**A**) Images show a section of meristematic zone of 7-day-old seedling PI-stained roots of wildtype and *pzr1-D*. (**B**) Schematic representation of the root. Red square (60 mm2) marks the point in where the image was taken and cells measured. (**C**)The number and (**D**) size of the cells contained in the square were count in four different samples for each genotype and the average values with standard deviation graphed. Significant differences were determined by Student's *t*-test. **, $P<0.001$ and ***, $P<0.0001$.

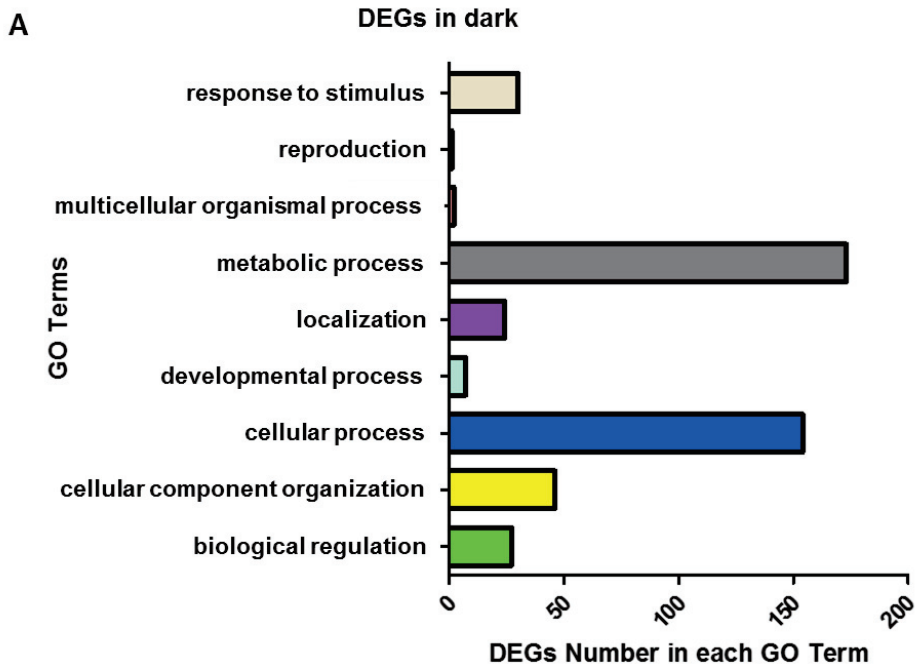
A
DEGs in dark
response to stimulus
reproduction
multicellular organismal process
metabolic process
localization
developmental process
cellular process
cellular component organization
biological regulation
GO Terms
0
50
100
150
200
DEGs Number in each GO Term

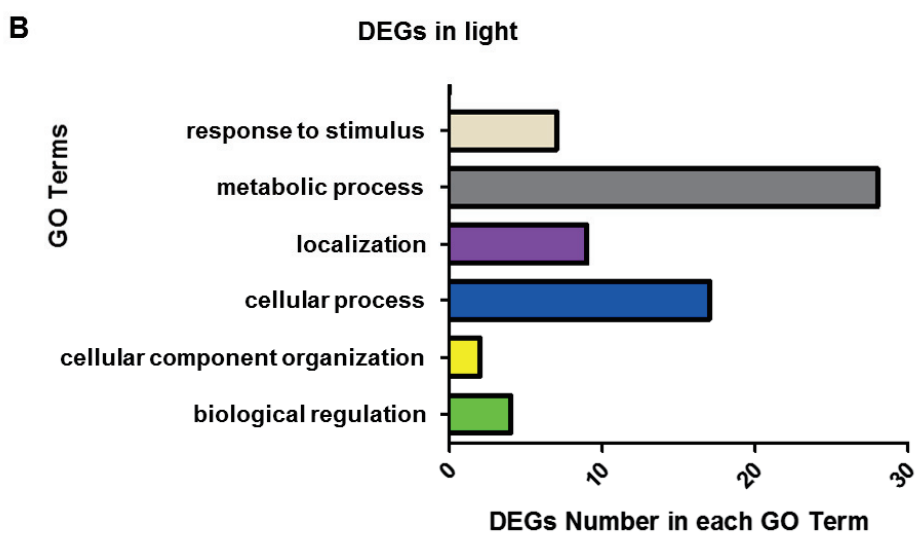
B
DEGs in light
response to stimulus
metabolic process
localization
cellular process
cellular component organization
biological regulation
GO Terms
0
10
20
30
DEGs Number in each GO Term

Figure 4-13. Enriched GO terms of DEGs in dark and DEGs in light. (**A**) List of GO terms of DEGs between wildtype and mutant when seedlings were maintained in dark or (**B)** light conditions.

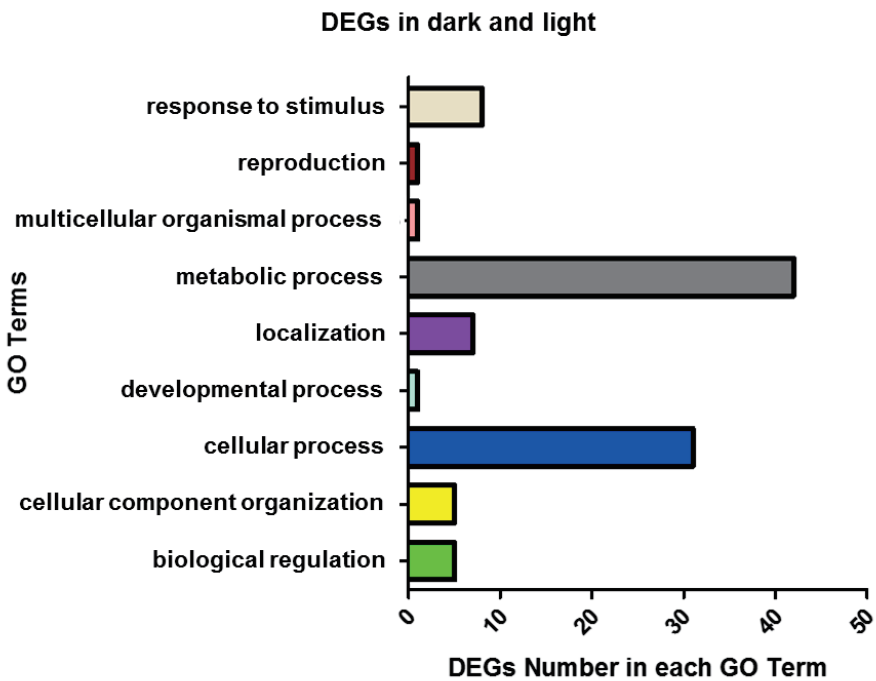

Figure 4-14. Enriched GO terms of DEGs in dark and light. List of GO terms of genes differentially expressed in both dark and light conditions.

SUPPLEMENTAL INFORMATION

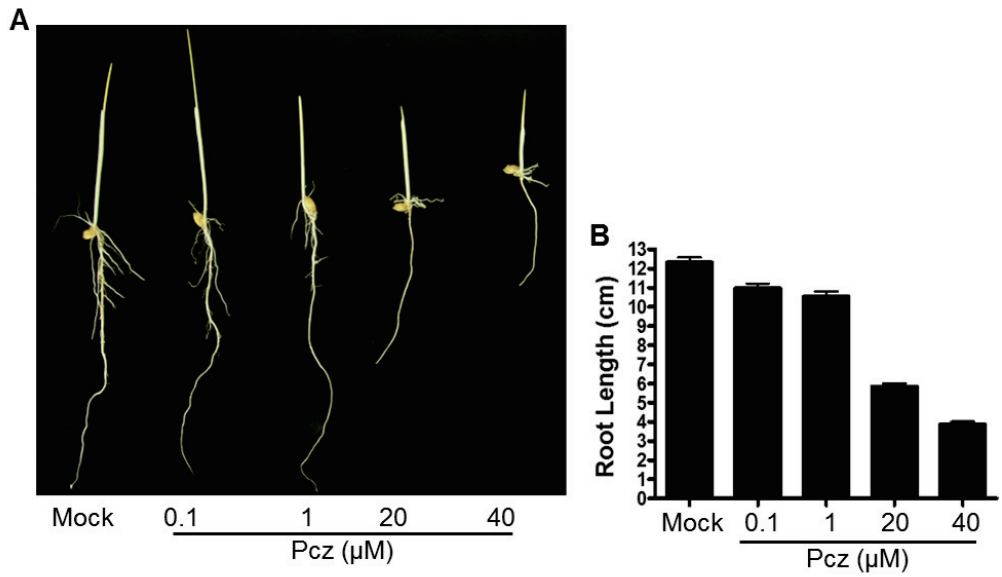

Figure S4-1. Dose response study of propiconazole effect in rice. (**A**) Morphology and (**B)** measurement of root lengths of plants after 10 days treatments with concentrations from 0 (Mock) to 40μM of BR inhibitor Pcz. Error bars represent standard deviation.

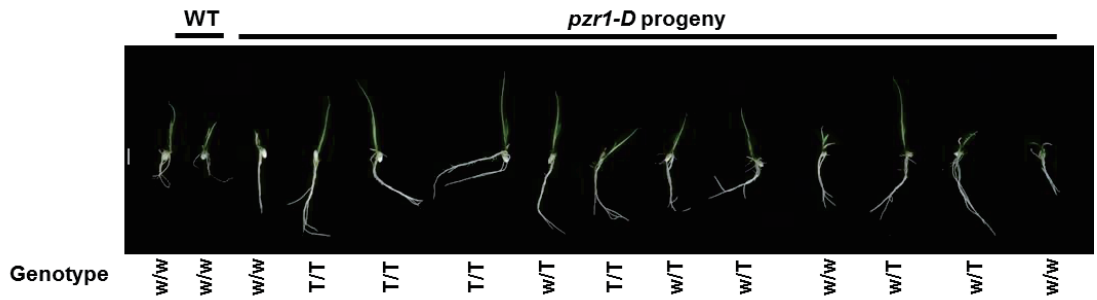

Figure S4-2. Propiconazole sensitivity of *pzr1-D* progeny. Morphology of 7-days old seedlings grown in Pcz-supplemented media. The different genotypes are represented as w/w for wildtype, T/T as mutant (T representing T-DNA) and w/T as heterozygous.

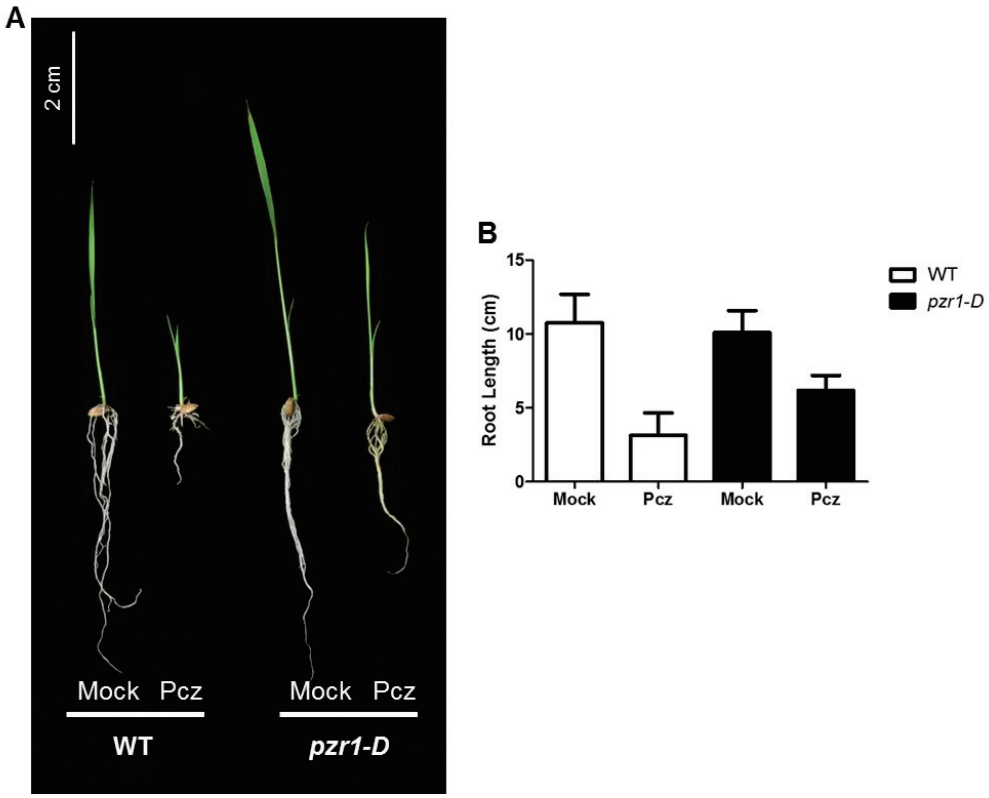

Figure S4-3. Propiconazole treatment effect in rice under light conditions. (**A**) Morphology and (**B**) measurement of root lengths of seedlings after 10 days treatments in media supplemented with 30 μM Pcz and grown under normal light conditions. In the graphs, error bars represent standard deviation.

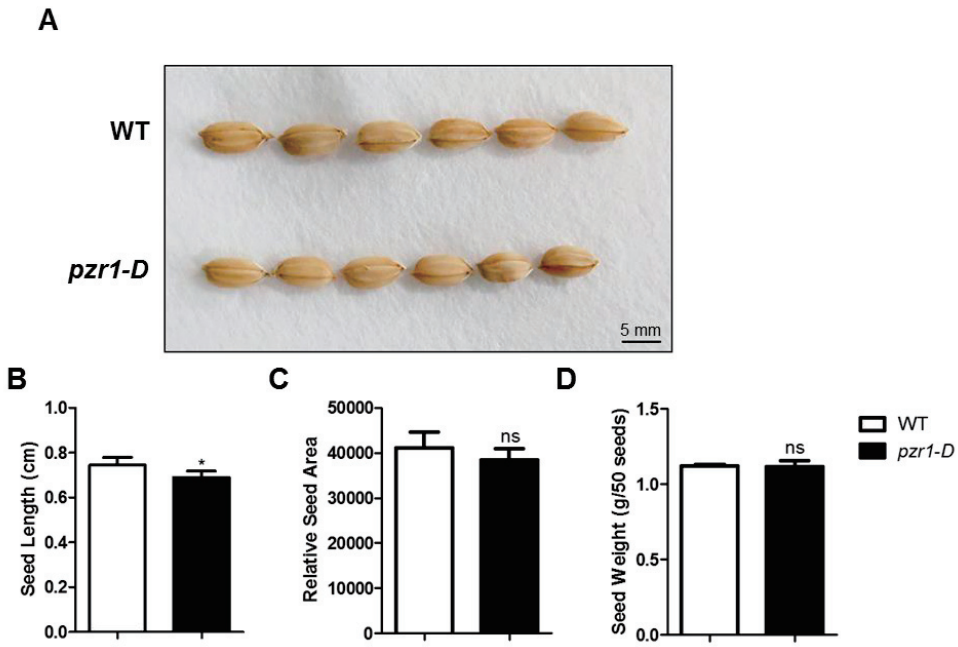

Figure S4-4. Study of *pzr1-D* seeds. (**A**) Wild type a mutant seeds were compared in relation to (**B**) seed length, (**C**) area and (**D**) weight. A total of 200 seeds per genotype were measured and the average was used to draw the graphs. Error bars represent standard deviation and the significant differences were determined by Student's *t*-test. *, P<0.05 and ns denote non-significant difference.

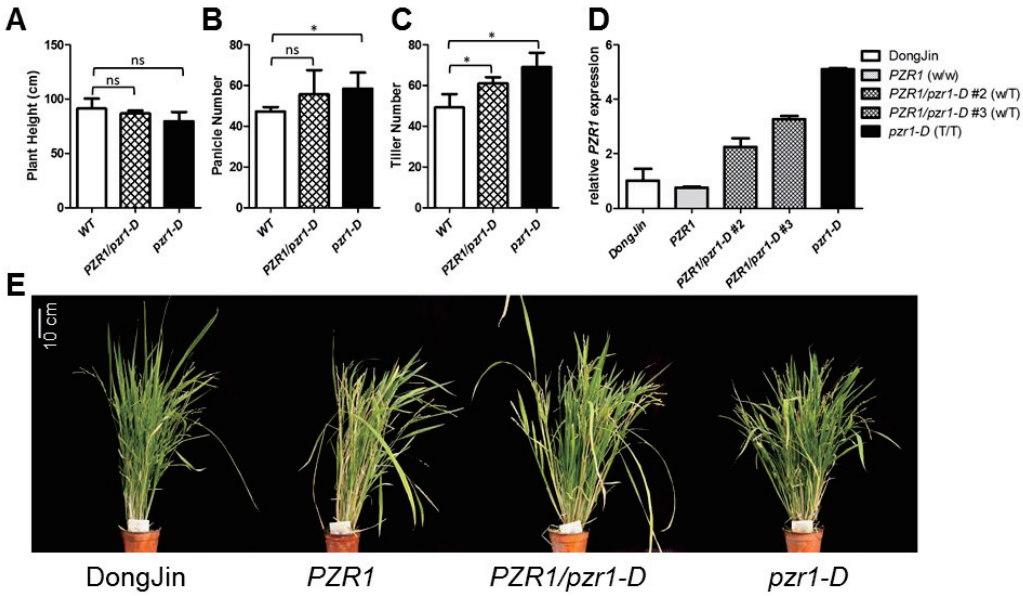

Figure S4-5. Expression levels and phenotypes of heterozygous plants. Graphs with measures of the different genotypes (wildtype DonJin, segregating wildtype, heterozygous *BZR1/pzr1*-D and homozygous mutant *pzr1-D*) comparing (**A**) plant height, (**B**) panicle number and (**C**) tiller number. (**D**) Shows the qRT-PCR data for each of the genotypes in relation with *PZR1* expression. (**F**) A representative plant of each genotype is presented.

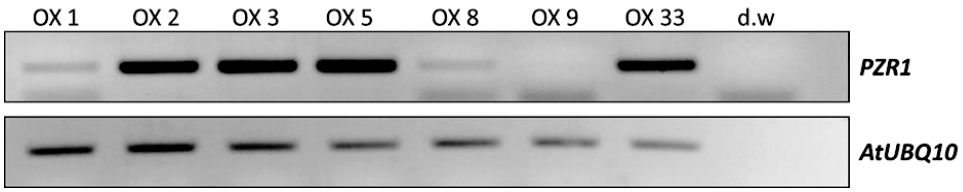

Figure S4-6. Semi-quantitative RT-PCR of Arabidopsis PZR1 overexpressing transgenic plants. RNA samples of independent transgenic lines were collected from seedlings to measure expression level of rice *PZR1*. Overexpressing lines OX 1 and OX 8 amplified the fragment corresponding to *PZR1* but a very low level. Arabidopsis *UBIQUITIN 10* was used as reference gene.

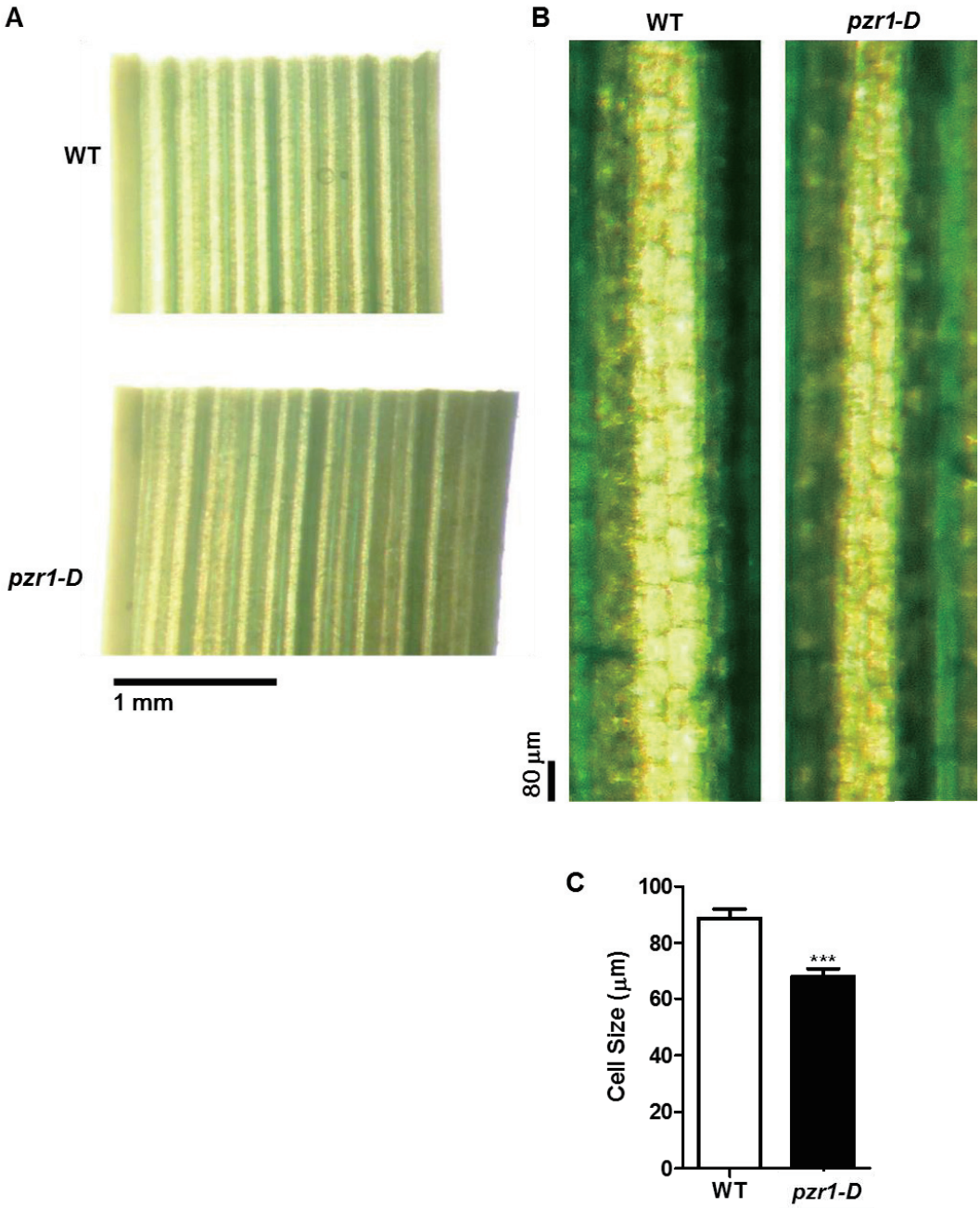

Figure S4-7. Microscopic analysis of leaves from wildtype and *pzr1-D* mutant seedlings. (**A**) Images of leaves from wildtype and mutant dissected in the middle observed with 10X magnification. (**B**) Images of samples observed with 20X

magnification and (**C**) used to measure cell size. Six slides with samples per genotype were measured and twenty to thirty cells were measure in each to obtain the average and standard deviation shown in graph. Significance was determined by Student's *t*-test. ***, P<0.0001.

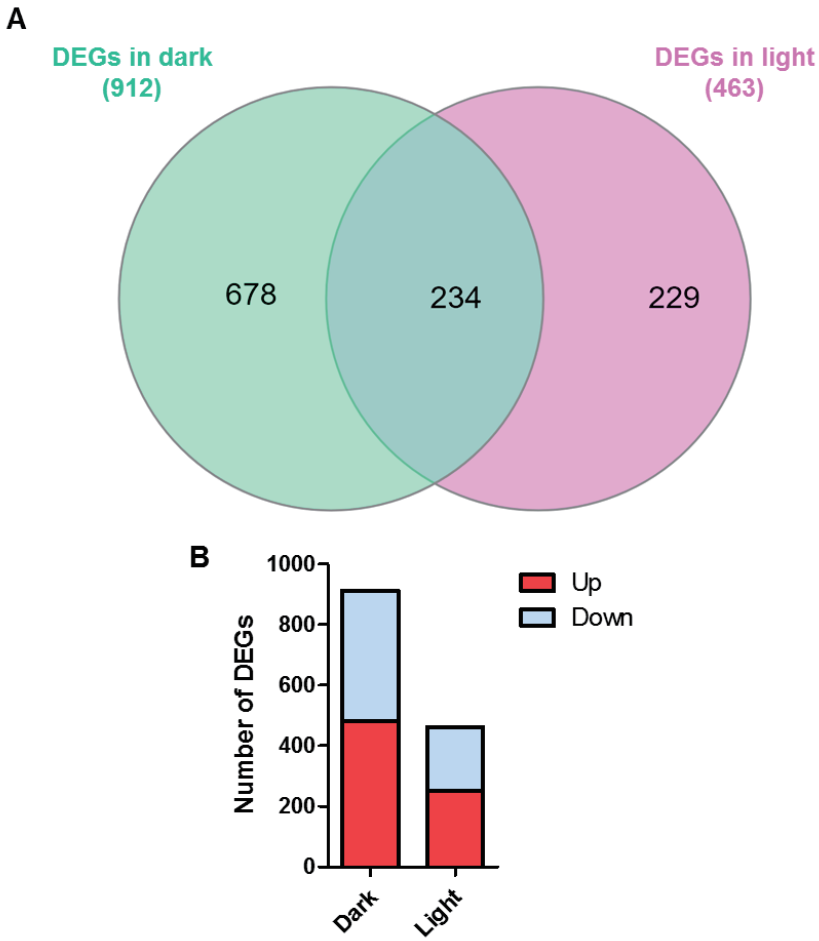

Figure S4-8. Venn diagram of DEGs between wildtype and mutants. (**A**) Considering the all the wildtype and mutant samples grown in dark or in light and in duplicate, 678 DEGs between wild type and mutant were found in dark, 229 DEGs were found in light and 234 genes are differentially expressed in both light conditions. (**B**) From the 678 DEGs in dark, 481 were up-regulated and 431 down-regulated. In light, 252 were found to be up- and 211 down-regulated.

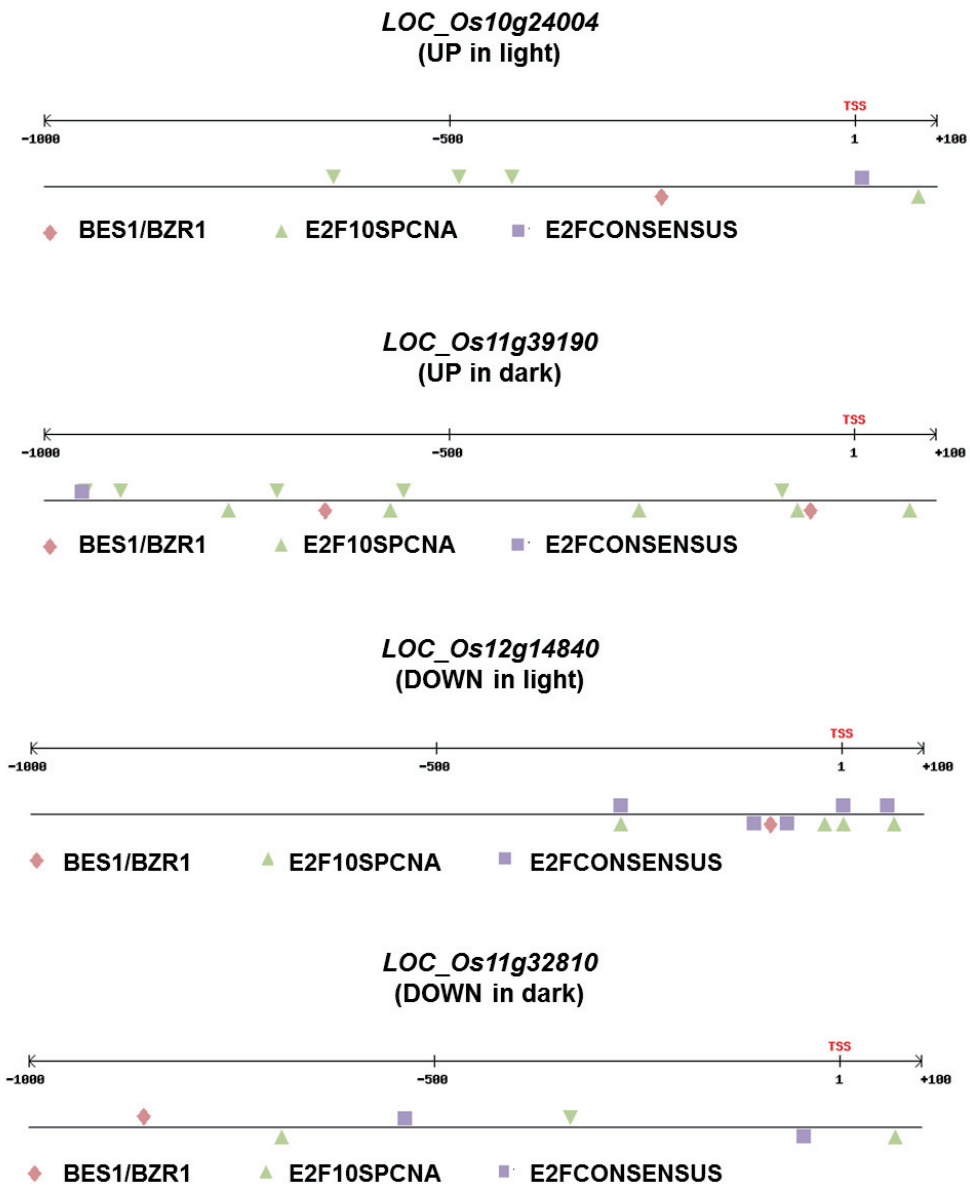

Figure S4-9. Promoter region of top DEGs. Schematic representation of four different genes promoter region and the location of two different E2F/DP and BZR1/BES1 consensus cis-acting elements.

Supplemental Table S4-1. Primers used in the research.

Gene	Locus ID	Direction	Sequence (5' to 3')	Size (bp)	Purpose
PZR1	*LOC_Os03g05760*	forward	**CACC** ATGAACTTGTTGCCGAATTTGC	693	cloning
		reverse	ATGCTCGTGCTTCACTCGC		
pGA2715 LB		forward	TTGGGATCCTCTAGAGTCGA		genotyping
OsDPB/PZR1	*LOC_Os03g05760*	forward	TGCGATCCCAGAGACAACCC	865	genotyping
		reverse	TGAGCCGTGGCCGCATAGAAA		
OsDPB/PZR1	*LOC_Os03g05760*	forward	AGCATTTTGCCACCAGATCC	149	real-time RT-PCR
		reverse	GCAACCCCTTCCACTGAATTTC		
03g05750	*LOC_Os03g05750*	forward	ACGAGAAGAAGAAGGACAAGGG	97	real-time RT-PCR
		reverse	TCGATGCTCTTGCCTTTGTC		
03g05770	*LOC_Os03g05770*	forward	TCCTCTTCCACGACTGCTTC	144	real-time RT-PCR
		reverse	CCAGCTCCGTCTTGATCTCG		
OsACTIN	*LOC_Os03g50885*	forward	GCGTGGACAAAGTTTTCAACCG	152	real-time RT-PCR
		reverse	TCTGGTACCCTCATCAGGCATC		
OsCPD	*LOC_Os11g04710*	forward	TTCTTCTCCATCCCCTTTCCTCTCGCCA	211	real-time RT-PCR
		reverse	TTCTTCTCCATCCCCTTTCCTCTCGCCA		
OsCYP85A1	*LOC_Os03g40540*	forward	GAGGTGGCTGGAGAAGAACAT	99	real-time RT-PCR
		reverse	AGGAAGTAGGCACCGTAGAAAT		
OsDWF4	*LOC_Os03g12660*	forward	TGGGCTCTGAAACAATCTAACCT	118	real-time RT-PCR
		reverse	CAAGGAAGAAGATGGCGAGG		
AtUBQ10	*At4g05320*	forward	TCCAGGACAAGGAAGGTATTCC	205	real-time RT-PCR
		reverse	CCACCAAAGTTTTACATGAAACGAA		

Supplemental Table S4-2. List of the proteins sequences for phylogenetic data.

Name	UniProt	Protein Sequence
Human DP1	Q14186	MAKDAGLIEANGELKVFIDQNLSPGKGVVSLVAVHPSTVNPLGKQLLPKTFGQSNVNIAQQVVI GTPQRPAASNTLVVGSPHTPSTHFASQNQPSDSSPWSAGKRNRKGEKNGKGLRHFSMKVCEKV QRKGTTSYNEVADELVAEFSAADNHILPNESAYDQKNIRRRVYDALNVLMAMNIISKEKKEIK WIGLPTNSAQECQNLEVERQRRLERIKQKQSQLQELILQQIAFKNLVQRNRHAEQQASRPPPPNS VIHLPFIIVNTSKKTVIDCSISNDKFEYLFNFDNTFEIHDDIEVLKRMGMACGLESGSCSAEDLKM ARSLVPKALEPYVTEMAQGTVGGVFITTAGSTSNGTRFSASDLTNGADGMLATSSNGSQYSGS RVETPVSYVGEDDEEDDDFNENDEDD
Human DP2	Q14188	MIISTPQRLTSSGSVLIGSPYTPAPAMVTQTHIAEATGWVPGDRKRARKFIDSDFSESKRSKKGD KNGKGLRHFSMKVCEKVQRKGTTSYNEVADELVSEFTNSNNHLAADSAYDQKNIRRRVYDAL NVLMAMNIISKEKKEIKWIGLPTNSAQECQNLEIEKQRRIERIKQKRAQLQELLLQQIAFKNLVQ RNRQNEQQNQGPPALNSTIQLPFIIINTSRKTVIDCSISSDKFEYLFNFDNTFEIHDDIEVLKRMGM SFGLESGKCSLEDLKLAKSLVPKALEGYITDISTGPSWLNQGLLLNSTQSVSNLDLTTGATLPQS SVNQGLCLDAEVALATGQFLAPNSHQSSSAASHCSESRGETPCSFNDEDEEDDEEDSSSPE
Wheat DP	Q9FET1	MAPPRGGAAAAATAALDLTGVHILEASSVPPLPERGGNAVQRKGAVDPDKDRKKEKAAAPRI TGWGLREYSKIVCEKVEAKGRTTYNEVADEIYSELKSMAHIGQGFDEKNIRRRVYDAFNVLIAL RVIAKEKKEIRWMGLSNYRYEKIKKLEEVRKELVNKIRNKKALLQEIEKQFDDLQNIKLRNQTL ESSAENVNGIRLPFVLVKTSRKARVEIEISDDSKFAHFEFNGAPFTLHDDLSILEGVRGNSIGKAG RATLH
At5g03415 DPB	Q9FNY2	MTTTGSNSNHNHHESNNNNNNPSTRSWGTAVSGQSVSTSGSMGSPSSRSEQTITVVTSTSDTTF QRLNNLDIQGDDAGSQGASGVKKKKRGQRAAGPDKTGRGLRQFSMKVCEKVESKGRTTYNE VADELVAEFALPNNDGTSPDQQQYDEKNIRRRVYDALNVLMAMDIISKDKKEIQWRGLPRTSL SDIEELKNERLSLRNRIEKKTAYSQELEEQYVGLQNLIQRNEHLYSSGNAPSGGVALPFILVQTR PHATVEVEISEDMQLVHFDFNSTPFELHDDNFVLKTMKFCDQPPQQPNGRNNSQLVCHNFTPE NPNKGPSTGPTPQLDMYETHLQSQQHQQHSQLQIIPMPETNNVTSSADTAPVKSPSLPGIMNSS MKPEN
At5g02470 DPA	Q9FNY3	MSMEMELFVTPEKQRQHPSVSVEKTPVRRKLIVDDDSEIGSEKKGQSRTSGGGLRQFSVMVCQ KLEAKKITTYKEVADEIISDFATIKQNAEKPLNENEYNEKNIRRRVYDALNVFMALDIIARDKKE IRWKGLPITCKKDVEEVKMDRNKVMSSVQKKAAFLKELREKVSSLESLMSRNQEMVVKTQGP AEGFTLPFILLETNPHAVVEIEISEDMQLVHLDFNSTPFSVHDDAYILKLMQEQKQEQNRVSSSS STHHQSQHSSAHSSSSSCIASGTSGPVCWNSGSIDTR
At5g22220 E2F1	Q9FV71	MSEEVPQQFPSSKRQLHPSLSSMKPPLVAPGEYHRFDAAETRGGGAVADQVVSDAIVIKSTLKR KTDLVNQIVEVNELNTGVLQTPVSGKGGKAKKTSRSAKSNKSGTLASGSNAGSPGNNFAQAGT CRYDSSLGLLTKKFINLIKQAEDGILDLNKAADTLEVQKRRIYDITNVLEGIGLIEKTLKNRIQW KGLDVSKPGETIESIANLQDEVQNLAAEEARLDDQIRESQERLTSLSEDENNKRLLFVTENDIKN LPCFQNKTLIAVKAPHGTTLEVPDPDEAGGYQRRYRIILRSTMGPIDVYLVSQFEESFEDIPQADE PSNVPDEPSNVPDVPSNLPSTSGLPENHDVSMPMKEESTERNMETQEVDDTQRVYSDIESHDFV DGIMKIVPPDLDMGVDYWFRSEVGEVSITDMWPDESGPDWNQMITFDQDHAGPSDNKILEQPQ TPSSPTPEESTATRSPTGS
At1g47870 E2F2	Q9FV70	MAATSNSGEDPTLSYHHRSPFRFELLQSISSSDPRYSSLTPSSTNRPFSVSQSLPNSQLSPLISPHW DDSYSQITQKVQKSRKNHRIQLGSIANMSGGESIDIAKVIVKQESSPQNVKRVYNKSKGGTKLL KAGKRMANGEVQNGGLNGASINCRYDSSLGLLTKKFVKLIQEAEDGTLDLNYCAVVLEVQKR RIYDITNVLEGIGLIEKTTKNHIRWKGADNLGQKDLGDQISRLKSEVESMQSEESRLDDLIRERQ EALRSLEEDDYCRRYMFMTEEDITSLPRFQNQTLLAIKAPTASYIEVPDPDEMSFPQQYRMVIRS RMGPIDVYLLSKYKGDSAETSDKLGNESDQKAPVGVDTPSLKIVTSDTDLKADYWFESDAEVS LTDLWSNFNS
LOC_Os03g05760	Q84VA0	MNLLPNLQIPITAFCHQIRIIPMQQQYDEKNIRRRVYDALNVLMAMEIISKDKKEIQWKGLPRTSI NDIEDLQTELVGLKSRIEKKNTYLQELQDQFVGMQKLIQRNEQLYGSGNIPSGGVALPFILVQTR PHATVEVEISEDMQLVHFDFNSTPFELHDDSFVLKAMSSCGEEQIDGIHDLISNGGESSSMPNIY RQQVQQPARSTNGTARLPSSPPIPGILKGRVKHEH
LOC_Os01g48700	Q84VF4	MAPPCGDAAAAASAAPGLANLLIREGAGLPSRPERYPPFRPCTSDSFAPISREGDDIPPQKKSVS LRSGGGGNAAEREEGGANRNGKKEKTGAQRITGWGLREFSKIVSKKVEAKGRTTYNEVADEIF AELKSITQNGLEFDEKNIRRRVYDAFNVLIAIRVIAKDKKEIKWMGLTNYRYEKIQKLEEVHKE LITRIKNKKKLLQEIEKQFDDLQNITLRNQASQRPAESVNGILLPFLLIKTSRKARVEIEISEDSKF ARFDFNGAPFTMHDDVSILEAIRRNKGRAGLSIHP
LOC_Os10g30420	Q84VD5	MVSGAAHSASTSGGGGGSEGSPTGRAAPGMQGGGSAATPAASASASTPASETTVARRLDGLDI QGDDAPSSQPATSKKKKRGPGTRATGPDKGGRGLRQFSMKVCEKVESKGRTTYNEVADELVA EFADPNNNFASPDPDNPNTPQFDEKNIRRRVYDALNVLMAMDIISKDKKEIQWKGLPRTSMSD VEELKTEIIGLKGRIDKKNAYLQELEDQFVGLQNLAQRNEQLYGSGNAPSGGVALPFILVQTRP HATVEVEISEDMQLVHFDFNSTPFELHDDSFVLKALGFSGKEPDDTQAWVGNGGECSTTPIYHQ SPQVARPNGVRLPTSPPIPGILKGRVKHEH

Supplemental Table S4-3. List of top twenty most significant differentially expressed genes (DEGs) in *pzr1-D* compared with WT in light.

GeneAcc	Description	Value WT	Value *pzr1-D*	log2 (FoldChange)	q-value
		UP-regulated genes			
OS11G0549665		0	117	inf	0.00421916
OS10G0381601		0	84.5	inf	0.00421916
OS11G0573100		0	39	inf	0.00421916
OS11G0549675		0	34.4	inf	0.00421916
OS11G0549680		0	27.1	inf	0.00421916
OS11G0639300		0	26.6	inf	0.00421916
OS01G0146101		0	17.9	inf	0.00421916
OS03G0629800		0	13.9	inf	0.00421916
OS11G0636050		0	11.3	inf	0.00421916
OS07G0159200		0	10	inf	0.00421916
OS12G0100100	RNA recognition motif family protein	0	9.99	inf	0.00421916
OS11G0606400	NB-ARC domain containing protein	0.0586	7.56	7.01	0.0462538
OS03G0223301	-	0.884	68.3	6.27	0.00421916
OS07G0486000		0.254	13.8	5.77	0.00421916
OS02G0129000	-	0.114	5.89	5.69	0.00421916
OS11G0540600		0.512	17.3	5.08	0.00421916

OS07G0531900		0.325	10	4.95	0.00421916
OS12G0431300		2.55	68.2	4.74	0.00421916
OS03G0576200	Potassium transporter 21	0.152	3.7	4.6	0.0310093
OS08G0203350		5.4	131	4.6	0.00421916
OS11G0562100		0.399	8.86	4.47	0.00421916
		DOWN-regulated genes			
OS11G0701700	-	79.4	0	-inf	0.00421916
OS12G0222650	-	75.6	0	-inf	0.00421916
OS12G0172150		72.7	0	-inf	0.00421916
OS12G0257450	-	36.3	0	-inf	0.00421916
OS12G0247700	Mannose-specific jacalin-related lectin	26.9	0	-inf	0.00421916
OS12G0222300		24.5	0	-inf	0.00421916
OS12G0255200	Staphylococcal nucleaseue family protein	21.7	0	-inf	0.00421916
OS12G0250900		19.7	0	-inf	0.00421916
OS12G0254400	-	16.3	0	-inf	0.00421916
OS10G0175500	-	12.7	0	-inf	0.00421916
OS05G0202800	Metallothionein-like protein 3B	123	2.24	-5.78	0.00421916
OS11G0518900		13.3	0.267	-5.63	0.00421916
OS08G0255500		8.2	0.166	-5.62	0.00421916
OS11G0689800	-	25.2	0.524	-5.59	0.00421916
OS07G0543500	Putative BLE2 protein	5.24	0.181	-4.86	0.00421916
OS12G0209800		24.8	1.25	-4.31	0.00421916

OS11G0255300	Cysteine endopeptidase; Cysteine proteinase-rice; Thiol protease SEN102, putative	22.7	1.22	-4.22	0.00421916
OS12G0211500		6.86	0.407	-4.08	0.00421916
OS06G0254300		163	9.63	-4.08	0.00421916
OS11G0134300	Similar to Serine/threonine kinase.	16.9	1.03	-4.04	0.00421916

Supplemental Table S4-4. List of top twenty most significant differentially expressed genes (DEGs) in *pzr1-D* compared with WT in dark.

GeneAcc	Description	Value WT	Value *pzr1-D*	log2 (FoldChange)	q-value
		UP-regulated genes			
OS09G0467700	-	0	32.6	inf	0.003138
OS01G0146101	-	0	20.9	inf	0.003138
OS01G0148100	-	0	13.8	inf	0.003138
OS07G0187001	-	0	12	inf	0.003138
OS11G0640300	Leucine Rich Repeat family protein, expressed	0	8.52	inf	0.003138
OS12G0257400	-	0	7.45	inf	0.003138
OS07G0159200	-	0	7.43	inf	0.003138
OS01G0845950	-	0	7.03	inf	0.003138
OS11G0691100	-	0	5.9	inf	0.003138
OS07G0153150	-	0.239	68.4	8.16	0.003138
OS11G0605100	NB-ARC domain containing protein	0.0808	11.8	7.18	0.005711
OS03G0223301	-	0.506	68.2	7.08	0.003138
OS08G0367300	-	0.0699	7.11	6.67	0.019729
OS11G0618700	-	0.11	9.56	6.44	0.005711
OS07G0162450	-	0.541	44.8	6.37	0.003138

OS02G0129000	-	0.113	8.92	6.3	0.003138
OS03G0299700	-	1.61	123	6.25	0.003138
OS11G0549680	-	0.407	26.1	6	0.003138
OS07G0486000	-	0.252	15.8	5.97	0.003138
OS11G0569800	Receptor kinase, putative, expressed	0.196	11.2	5.83	0.003138
	-	**DOWN-regulated genes**			
OS12G0250900	-	20.9	0.522	-5.33	0.003138
OS12G0406000	-	6.36	0.18	-5.14	0.003138
OS11G0696600	-	26.1	0.763	-5.09	0.003138
OS11G0532600	-	5.49	0.17	-5.01	0.010306
OS01G0520180	-	81.5	2.56	-4.99	0.003138
OS07G0297400	-	93.3	2.98	-4.97	0.003138
OS07G0535200	-	6.74	0.245	-4.78	0.003138
OS12G0425800	-	56.2	2.1	-4.74	0.003138
OS11G0685200	-	7.46	0.304	-4.62	0.003138
OS12G0204600	NB-ARC domain containing protein	6.52	0.265	-4.62	0.003138
OS12G0239300	-	281	12.1	-4.53	0.003138
OS07G0677100	Peroxidase	40.3	1.79	-4.5	0.003138
OS07G0103000	-	15.1	0.67	-4.49	0.010306
OS05G0414400	-	6.21	0.312	-4.32	0.003138
OS11G0693800	-	18.2	0.953	-4.25	0.003138
OS05G0369900	-	8.11	0.475	-4.09	0.003138

OS11G0687100	Von Willebrand factor type A domain containing protein, expressed	41	2.49	-4.04	0.003138
OS12G0425500	-	3.73	0.227	-4.04	0.003138
OS08G0255500	-	6.59	0.416	-3.99	0.003138
OS11G0689800	-	16.1	1.18	-3.77	0.003138

Supplemental Table S4-5. List of known rice cell cycle genes differentially expressed genes (DEGs) in *pzr1-D* compared with WT.

Common Name	Description	Sample	Value in WT	Value in *pzr1-D*	log2 (FoldChange)
OsRAA1	Flowering-promoting factor 1-like protein 1	WT vs *pzr1-D* in dark	6.625	19.519	1.559
		WT vs *pzr1-D* in light	5.698	16.287	1.515
CycB1;1	Cyclin-B1-1	WT vs *pzr1-D* in dark	65.441	39.659	-0.723
		WT vs *pzr1-D* in light	21.389	22.576	0.078
Psd1	Similar to Lipid transfer protein.	WT vs *pzr1-D* in dark	649.943	336.993	-0.948
		WT vs *pzr1-D* in light	192.136	278.211	0.534
CDKB;1	Similar to Cyclin-dependent kinase B1-1	WT vs *pzr1-D* in dark	25.206	15.539	-0.698
		WT vs *pzr1-D* in light	13.253	11.259	-0.235
CycT1;3	Cyclin-dependent kinase A-2	WT vs *pzr1-D* in dark	18.959	12.393	-0.613
		WT vs *pzr1-D* in light	9.255	8.796	-0.073
CDKG;1	Cyclin-dependent kinase G-1	WT vs *pzr1-D* in dark	18.775	32.877	0.808
		WT vs *pzr1-D* in light	39.671	40.669	0.036
PCNA	Proliferating cell nuclear antigen	WT vs *pzr1-D* in dark	129.495	68.486	-0.919
		WT vs *pzr1-D* in light	37.115	45.642	0.298
CKS1	Cyclin-dependent kinases regulatory subunit 1	WT vs *pzr1-D* in dark	49.949	31.799	-0.651
		WT vs *pzr1-D* in light	36.218	35.047	-0.047
CDKG;2	Cyclin-dependent kinase G-2	WT vs *pzr1-D* in dark	17.678	24.627	0.478

		WT vs *pzr1-D* in light	28.401	24.079	-0.238
CycB2;1	Cyclin-B2-1	WT vs *pzr1-D* in dark	24.121	15.741	-0.616
		WT vs *pzr1-D* in light	8.909	8.037	-0.149
CycU1;1	Cyclin-P1-1	WT vs *pzr1-D* in dark	0.497	1.333	1.424
		WT vs *pzr1-D* in light	4.273	8.237	0.947
CycD2;2	Similar to Cyclin-D3-1	WT vs *pzr1-D* in dark	10.231	6.013	-0.767
		WT vs *pzr1-D* in light	5.588	5.224	-0.097
CycB2;2	Cyclin-B2-2	WT vs *pzr1-D* in dark	46.6	27.177	-0.778
		WT vs *pzr1-D* in light	13.102	14.476	0.144
CycD6;1	Cyclin-D6-1	WT vs *pzr1-D* in dark	1.046	0.29	-1.849
		WT vs *pzr1-D* in light	0.257	0.373	0.537
CycD2;1	Cyclin-D2-2	WT vs *pzr1-D* in dark	17.749	9.653	-0.879
		WT vs *pzr1-D* in light	6.29	6.813	0.115
CDKB2;1	Cyclin-dependent kinase B2-1	WT vs *pzr1-D* in dark	58.09	34.057	-0.77
		WT vs *pzr1-D* in light	24.909	26.196	0.073
CDKB;2	Cyclin-dependent kinase B2-1	WT vs *pzr1-D* in dark	58.09	34.057	-0.77
		WT vs *pzr1-D* in light	24.909	26.196	0.073
CycA3;2	Cyclin-A3-2	WT vs *pzr1-D* in dark	9.151	5.852	-0.645
		WT vs *pzr1-D* in light	3.704	4.441	0.262

Supplemental Table S4-6. Transcription analysis of BR-related genes between wild type and mutant samples.

Common name	Locus	GeneAcc	Sample	log_2 (FoldChange)	p-value	q-value (FDR)
BRD2	*LOC_Os10g25780*	OS10G0397400	WT vs *pzr1-D* in dark	-0.767	0.02015	0.24208
			WT vs *pzr1-D* in light	0.071	0.87925	0.998836
			WT in light vs WT in dark	-1.136	0.0052	0.0343
			pzr1-D in light vs *pzr1-D* in dark	-0.297	0.44305	0.757683
BU1	*LOC_Os06g12210*	OS06G0226500	WT vs *pzr1-D* in dark	-0.677	0.0252	0.273259
			WT vs *pzr1-D* in light	0.455	0.3027	0.998836
			WT in light vs WT in dark	-0.674	0.08085	0.232747
			pzr1-D in light vs *pzr1-D* in dark	0.457	0.1989	0.508703
CPD	*LOC_Os11g04710*	OS11G0143200	WT vs *pzr1-D* in dark	-0.013	0.97135	0.993398
			WT vs *pzr1-D* in light	-0.17	0.6949	0.998836
			WT in light vs WT in dark	1.083	0.00945	0.052762
			pzr1-D in light vs *pzr1-D* in dark	0.928	0.01575	0.09921
CYU U4	*LOC_Os10g41430*	OS10G0563900	WT vs *pzr1-D* in dark	-0.182	0.52235	0.90231
			WT vs *pzr1-D* in light	0.524	0.2296	0.998836
			WT in light vs WT in dark	-0.734	0.05655	0.183027
			pzr1-D in light vs *pzr1-D* in dark	-0.025	0.9398	0.979809
D1/RGA1	*LOC_Os05g26890*	OS05G0333200	WT vs *pzr1-D* in dark	-0.227	0.3371	0.795016

			WT vs *pzr1-D* in light	-0.154	0.6375	0.998836
			WT in light vs WT in dark	-0.183	0.51775	0.726889
			pzr1-D in light vs *pzr1-D* in dark	-0.116	0.66355	0.890237
D11	*LOC_Os04g39430*	OS04G0469800	WT vs *pzr1-D* in dark	-0.175	0.52285	0.902546
			WT vs *pzr1-D* in light	-0.016	0.9689	0.998836
			WT in light vs WT in dark	0.067	0.8424	0.924814
			pzr1-D in light vs *pzr1-D* in dark	0.222	0.4932	0.79573
D2	*LOC_Os01g10040*	OS01G0197100	WT vs *pzr1-D* in dark	0.291	0.7683	0.96754
			WT vs *pzr1-D* in light	0.031	0.9806	0.998836
			WT in light vs WT in dark	0.188	0.8881	0.947621
			pzr1-D in light vs *pzr1-D* in dark	-0.067	0.96015	0.986463
DET2	*LOC_Os01g63260*	OS01G0851600	WT vs *pzr1-D* in dark	0.274	0.3618	0.8125
			WT vs *pzr1-D* in light	0.269	0.5872	0.998836
			WT in light vs WT in dark	-0.969	0.02075	0.092117
			pzr1-D in light vs *pzr1-D* in dark	-0.972	0.0126	0.084386
DLT	*LOC_Os06g03710*	OS06G0127800	WT vs *pzr1-D* in dark	-0.721	0.0047	0.102712
			WT vs *pzr1-D* in light	0.196	0.63245	0.998836
			WT in light vs WT in dark	-1.266	0.00085	0.00883
			pzr1-D in light vs *pzr1-D* in dark	-0.343	0.2811	0.605619
CYP85A1	*LOC_Os03g40540*	OS03G0602300	WT vs *pzr1-D* in dark	0.226	0.38615	0.830562
			WT vs *pzr1-D* in light	-0.027	0.9415	0.998836

			WT in light vs WT in dark	-0.167	0.62115	0.80088
			pzr1-D in light vs *pzr1-D* in dark	-0.422	0.1663	0.462462
DWF4	*LOC_Os03g12660*	OS03G0227700	WT vs *pzr1-D* in dark	0.447	0.1126	0.544227
			WT vs *pzr1-D* in light	0.234	0.55495	0.998836
			WT in light vs WT in dark	0.047	0.89705	0.952183
			pzr1-D in light vs *pzr1-D* in dark	-0.167	0.60415	0.862559
IBH1	*LOC_Os04g56500*	OS04G0660100	WT vs *pzr1-D* in dark	-0.009	0.97315	0.9935
			WT vs *pzr1-D* in light	0.068	0.85085	0.998836
			WT in light vs WT in dark	0.375	0.26225	0.487693
			pzr1-D in light vs *pzr1-D* in dark	0.45	0.14605	0.430993
ILI1	*LOC_Os04g54900*	OS04G0641700	WT vs *pzr1-D* in dark	-0.261	0.6042	0.929166
			WT vs *pzr1-D* in light	1.315	0.0868	0.998836
			WT in light vs WT in dark	-1.247	0.0619	0.194385
			pzr1-D in light vs *pzr1-D* in dark	0.325	0.5662	0.840967
LIC1	*LOC_Os06g49080*	OS06G0704300	WT vs *pzr1-D* in dark	-0.047	0.85305	0.978932
			WT vs *pzr1-D* in light	-0.242	0.45305	0.998836
			WT in light vs WT in dark	0.397	0.1889	0.402623
			pzr1-D in light vs *pzr1-D* in dark	0.198	0.499	0.799138
OsBAK1	*LOC_Os08g07760*	OS08G0174700	WT vs *pzr1-D* in dark	-0.05	0.83425	0.975002
			WT vs *pzr1-D* in light	-0.254	0.4136	0.998836
			WT in light vs WT in dark	-0.504	0.0767	0.22431

			pzr1-D in light vs *pzr1-D* in dark	-0.711	0.0087	0.064254
OsBRI1	*LOC_Os01g52050*	OS01G0718300	WT vs *pzr1-D* in dark	0.278	0.28905	0.75793
			WT vs *pzr1-D* in light	-0.156	0.6211	0.998836
			WT in light vs WT in dark	-0.444	0.1338	0.323951
			pzr1-D in light vs *pzr1-D* in dark	-0.878	0.00255	0.02502
OsBZR1	*LOC_Os07g39220*	OS07G0580500	WT vs *pzr1-D* in dark	-0.226	0.34045	0.796928
			WT vs *pzr1-D* in light	0.254	0.44625	0.998836
			WT in light vs WT in dark	-0.488	0.10615	0.280178
			pzr1-D in light vs *pzr1-D* in dark	-0.002	0.9948	0.997341
OsGSK1	*LOC_Os01g10840*	OS01G0205700	WT vs *pzr1-D* in dark	-0.12	0.6127	0.931796
			WT vs *pzr1-D* in light	-0.142	0.664	0.998836
			WT in light vs WT in dark	-0.358	0.22325	0.446406
			pzr1-D in light vs *pzr1-D* in dark	-0.382	0.1653	0.460797
OsGSK2	*LOC_Os05g11730*	OS05G0207500	WT vs *pzr1-D* in dark	0.058	0.8343	0.975002
			WT vs *pzr1-D* in light	-0.067	0.8588	0.998836
			WT in light vs WT in dark	-0.376	0.2785	0.505574
			pzr1-D in light vs *pzr1-D* in dark	-0.502	0.1198	0.382493
OsMDP1	*LOC_Os03g08754*	OS03G0186600	WT vs *pzr1-D* in dark	0.04	0.86645	0.980023
			WT vs *pzr1-D* in light	0.012	0.9706	0.998836
			WT in light vs WT in dark	0.115	0.6913	0.844294
			pzr1-D in light vs *pzr1-D* in dark	0.086	0.7557	0.926652

OsPRA2	*LOC_Os06g50060*	OS06G0714600	WT vs *pzr1-D* in dark	0.365	0.656	0.945298
			WT vs *pzr1-D* in light	0.533	0.76375	0.998836
			WT in light vs WT in dark	-1.503	0.4234	0.651072
			pzr1-D in light vs *pzr1-D* in dark	-1.334	0.33945	0.668891
OsXTR1	*LOC_Os11g33270*	Os11g0539200	WT vs *pzr1-D* in dark	-2.603	0.00005	0.00314
			WT vs *pzr1-D* in light	-1.364	0.00105	0.060394
			WT in light vs WT in dark	-2.655	0.00005	0.00091
			pzr1-D in light vs *pzr1-D* in dark	-1.414	0.00005	0
RAVL1	*LOC_Os04g49230*	OS04G0581400	WT vs *pzr1-D* in dark	0.255	1	1
			WT vs *pzr1-D* in light	-0.176	1	1
			WT in light vs WT in dark	-0.143	1	1
			pzr1-D in light vs *pzr1-D* in dark	-0.567	1	1
ROT3	*LOC_Os05g11130*	OS05G0200400	WT vs *pzr1-D* in dark	0.473	0.10085	0.521772
			WT vs *pzr1-D* in light	0.089	0.79985	0.998836
			WT in light vs WT in dark	0.971	0.00625	0.03931
			pzr1-D in light vs *pzr1-D* in dark	0.587	0.0646	0.26055
TUD1	*LOC_Os03g13010*	OS03G0232600	WT vs *pzr1-D* in dark	-0.115	0.6304	0.935969
			WT vs *pzr1-D* in light	-0.006	0.9827	0.998836
			WT in light vs WT in dark	-0.032	0.91115	0.95901
			pzr1-D in light vs *pzr1-D* in dark	0.077	0.7686	0.931037
XIAO	*LOC_Os04g48760*	OS04G0576900	WT vs *pzr1-D* in dark	-0.487	0.0404	0.346875

WT vs *pzr1-D* in light	-0.301	0.40065	0.998836
WT in light vs WT in dark	-0.652	0.03895	0.142059
pzr1-D in light vs *pzr1-D* in dark	-0.459	0.1058	0.353747

Supplemental Table S4-7. Transcription Factor Binding Sites (TFBS) occurrence in promoters of top most significant differentially expressed genes (DEGs) in *pzr1-D* compared with WT.

UP-REGULATED GENES

TFBS ID	TFBS Name	Support	Binding Site Sequence
TF_MOTIF_SEQ_0343	ANAERO1CONSENSUS	90.9	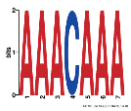
TF_MOTIF_SEQ_0372	ACGTOSGLUB1	90.9	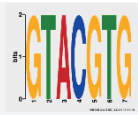
TF_MOTIF_SEQ_0458	E2FCONSENSUS	93.9	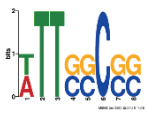
TF_MOTIF_SEQ_0429	E2F1OSPCNA	97	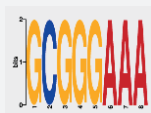
TF_MOTIF_SEQ_0259	CGACGOSAMY3	100	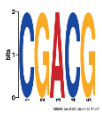
TF_MOTIF_SEQ_0274	BIHD1OS	100	
TF_MOTIF_SEQ_0321	GT1CONSENSUS	100	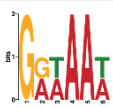
TF_MOTIF_SEQ_0425	SITEIOSPCNA	100	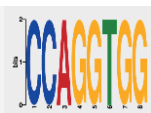

DOWN-REGULATED GENES			
TFBS ID	**TFBS Name**	**Support**	**Binding Site Sequence**
TF_MOTIF_SEQ_0389	TATABOXOSPAL	94.4	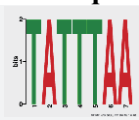
TF_MOTIF_SEQ_0343	ANAERO1CONSENSUS	91.7	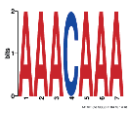
TF_MOTIF_SEQ_0425	SITEIOSPCNA	97.2	
TF_MOTIF_SEQ_0458	E2FCONSENSUS	97.2	
TF_MOTIF_SEQ_0344	AACACOREOSGLUB1	97.2	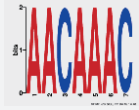
TF_MOTIF_SEQ_0429	E2F1OSPCNA	100	
TF_MOTIF_SEQ_0259	CGACGOSAMY3	100	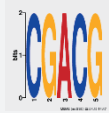
TF_MOTIF_SEQ_0274	BIHD1OS	100	
TF_MOTIF_SEQ_0321	GT1CONSENSUS	100	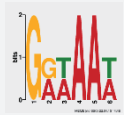

Chapter 5. Analysis of Anti-BZR1 Antibody Reveals the Roles BES1 in Maintaining the BZR1 Levels in Arabidopsis

Analysis of anti-BZR1 antibody reveals the roles BES1 in maintaining the BZR1 levels in Arabidopsis

Yu Jeong Jeong[1,+], Claudia Corvalán[1,+], Soon Il Kwon[2], and Sunghwa Choe[1,2,3,*]

[1] School of Biological Sciences, College of Natural Sciences, Seoul National University, Seoul 151-747, Korea

[2] Convergence Research Center for Functional Plant Products, Advanced Institutes of Convergence Technology, 864-1 Iui-dong, Yeongtong-gu, Suwon-si, Gyeonggi-do 443-270, Korea

[3] Plant Genomics and Breeding Institute, Seoul National University, Seoul 151-921, Korea

[+] Equal contribution

*Corresponding author: Sunghwa Choe shchoe@snu.ac.kr

Published March 15, 2015 in Journal of Plant Biology. DOI: 10.1007/s12374-014-0289-5

ABSTRACT

The transcription factor brassinazole-resistant 1 (BZR1) is a key component and positive regulator of the brassinosteroid (BR) signaling pathway. In this study, we report the cloning, expression, and purification of BZR1 for preparation of rabbit antibody against BZR1. The full-length coding sequence of BZR1 was cloned into the pET28a cloning vector and expressed in Escherichia coli to produce recombinant His-tagged BZR1. Using affinity chromatography with Ni-NTA beads under denaturing conditions, we were able to purify an approximately 38-kD recombinant His-BZR1 fusion protein, which was used to raise antiserum against BZR1. The antibody titer and sensitivity were evaluated by indirect ELISA and immunoblot. Furthermore, the antibody was used to detect protein from extracts derived from plant tissues, and was able to detect three major forms of BZR1 in Arabidopsis plants as well as in other three monocot species rice, Setaria viridis and sorghum. The produced anti-BZR1 antibody will be instrumental in determining the molecular mechanisms underlying BZR1 activity. Thus, we believe that our antibody represents a powerful tool for analyzing the role of BZR1 in plant physiology and characterizing the crosstalk between proteins in signaling cascades involving BZR1 in dicot and monocot plants.

INTRODUCTION

Brassinosteroids (BRs) are growth-promoting plant steroid hormones and BR signaling pathways are present in every plant system examined to date (Cheon et al. 2013). The transcription factor (TF) brassinazole-resistant 1 (BZR1) has been identified as a key component of the BR signaling pathway along with its closest homolog bri1-EMS- suppressor (BES1), also known as BZR2 (Wang et al. 2002; Yin et al. 2002; Kim et al. 2010; Kim et al. 2014). BRs, mainly through BZR1 and BES1, regulate a large number of genes involved in plant developmental and physiological processes (Kim et al. 2009; Sun et al. 2010; Chung et al. 2013). BR binding to the cell surface receptor kinase BR insensitive 1 (BRI1) initiates a well-defined signal transduction pathway that leads to the activation of the BR-responsive TFs, BZR1 and BES1 (Vert et al. 2005). These TFs are subject to post-transcriptional modifications and exist in two different forms, phosphorylated and dephosphorylated. In ambient conditions, BZR1 and BES1 exist mostly in phosphorylated forms (pBZR1 and pBES1), due the activity of BR insensitive 2 (BIN2) kinase (Choe et al. 2002; Li et al. 2002). Phosphorylated BZR1 and BES1 are recognized as inactive forms that can be found in the cytoplasm and are subject to degradation via the 26S proteasome pathway (He et al. 2002; Li et al. 2002).

The presence of active BRs, such as brassinolide (BL), induces the rapid dephosphorylation of these TFs, by a protein phosphatase 2A (PP2A) and the inactivation of BIN2. Dephosphorylated forms of BZR1 and BES1 can be observed

in the nucleus, where they are active and regulate their respective targets genes (Li et al. 2005; Yin et al. 2005; Ryu et al. 2007). The identification of BZR1 and BES1 targets by microarray analysis and similar techniques, and the analysis of these data suggest that these TFs regulate additional transcription factors to control directly or indirectly the large number of BR-responsive genes (Kim et al. 2010; Sun et al. 2010; Yu et al. 2011; Kim et al. 2014). In genome-wide studies, BZR1 was shown to regulate directly around one-quarter of the BR-responsive genes and around 80% of genes downstream of the BRI1-mediated BR signal (Sun et al. 2010). Thus, BZR1 is a major regulator of the BR signaling pathway.

Previous studies also demonstrated crosstalk between BRs and other hormones and environmental signaling pathways by way of BZR1 (Kim et al. 2012; Kim et al. 2013). The BZR1 TF can directly bind to genes involved in hormone biosynthetic pathways, modulate the expression level of key components of other signaling pathways, or even co-regulate common transcriptional targets along with other important TFs. For instance, the role of BZR1 as a molecular mediator of crosstalk between light and BR signaling pathways has been studied at different levels. BZR1 was demonstrated to regulate components of the light perception pathways, such as phytochrome B (PHYB) photoreceptors and phytochrome-interacting factor 3 (PIF3) (Kim et al. 2014; Kim et al. 2014). In addition, the BZR1 targets also include targets of key TFs of the phytochrome signaling pathway, such as long hypocotyl 5 (HY5), phytochrome-interacting factor 4 (PIF4), and PIF3-like 5 (PIL5) (Sun et al. 2010; Bai et al. 2012).

Moreover, functional studies confirmed that BZR1 and PIF4 form a complex that controls cell elongation and photomorphogenesis in response to environmental and BR signals (Maharjan et al. 2011; Oh et al. 2012). Despite this broad understanding of the BR signaling pathway, many of the molecular mechanisms underlying the crosstalk between hormonal or other environmental signaling pathways remain unknown, and there is much interest in determining how these networks are established, maintained, and fine-tuned. Because BZR1 is an important element in BR response pathways, we believe that its interaction with or regulation by other proteins is essential for understanding the connection between BR and established developmental processes or plant responses.

Prompted by the usefulness of anti-BES1 allowing detection of the modulation of BES1 phosphorylation status by other components (Mora-Garcia et al. 2004) and its use in the isolation of BES1-bound DNA in chromatin immunoprecipitation experiments (Yu et al. 2008; Yu et al. 2011), we believed that the development of an anti-BZR1 antibody could be used to observe the presence of BZR1 and the change in phosphorylation status (and thus BZR1 activity) in different tissues of Arabidopsis or under different conditions, and thereby contribute to understanding of the BR response pathway, which is still poorly understood at the molecular level. In this study, we introduced the full-length cDNA of Arabidopsis BZR1 into a vector, expressed a His-fusion of this gene in E. coli, purified the resulting His-tagged protein using affinity chromatography, and used this recombinant protein to develop an anti-BZR1 serum. Furthermore, we

determined the optimal concentration of the developed antibody for detection of BZR1 and evaluated its efficiency and specificity.

MATERIALS AND METHODS

Plant Material and Growth Conditions

Arabidopsis thaliana ecotypes Col and En-2 were used as wild type for treatments and protein extraction. Transgenic lines overexpressing *BZR1* (Ryu et al. 2007), *bzr1-1D*, and *bes1-1* (SALK_098634) are in the Col ecotype (He et al. 2005) and the *bes1-1D* allele is in the En-2 background. Seeds were sterilized as previously reported (Kim et al. 2012), and then germinated in 0.5x MS (Duchefa) with 1% sucrose under long-day conditions (16 h light/8 h dark). For rice (*Oriza sativa*), setaria (*Setaria viridis*) and sorghum (*Sorghum bicolor*) the seeds were first imbibed in water for 24 h, then de-husked and surface sterilized using 50% commercial Clorox solution. After 5 washing steps with sterile water, the seeds were sown in 0.8% agar media containing DMSO or 50 μM of brassinosteroid inhibitor propiconazole (Pcz). Seeds were first kept in dark and 4°C for 3 d after which seeds were placed in growth room conditions to let germinate in dark. Once germinated, seedlings were kept under long-day conditions.

Plasmid Construction

Total RNA was isolated from 10-day-old wild-type (Col) seedlings using Trizol Reagent (Sigma). Two micrograms of total RNA was reverse-transcribed (Fermentas), and used as a template to amplify the BZR1 coding sequence. The forward primer (5'-**CAT ATG** ATG ACT TCG GAT GGA GCT AC-3') was synthesized to include an *NdeI* site (shown in bold) and the reverse primer (5'-

GAA TTC TCA ACC ACG AGC CTT CC-3') an *EcoRI* site (shown in bold). Ligation of BZR1 fragment and pET28a vector was performed using T4 DNA ligase (Promega) and transformed into *E. coli* strains BL21(DE3), BL21(DE3)pLysS, and BL21(DE3)RIPL.

His-BZR1 Fusion Protein Expression in E. coli and Purification

For expression tests, 1 liter LB was inoculated with 1 mL of fresh overnight culture and grown at 37°C until an absorbance of 0.5-0.6 at 600 nm was reached. BZR1 expression was induced by adding IPTG to a final concentration of 1 mM to the culture medium and the culture was maintained for 4 h at 37°C and shaking at 200 rpm. After induction, cells were centrifuged (5000 rpm for 20 minutes) and the precipitated cells were either resuspended in lysis buffer A (20 mM Tris, 10 mM NaCl, pH 8) or in buffer B (50 mM NaH_2PO_4, 300 mM NaCl, pH 8). Samples were then electrophoresed on 10% SDS-PAGE (sodium dodecyl sulfate polyacrylamide gel electrophoresis) gels that were subsequently stained using CBB R-250 (Coomassie Brilliant Blue G-250). For BZR1 purification, a Ni-NTA agarose bead matrix was used for affinity chromatography. The pellet of the induced BL21(DE3)RIPL culture was resuspended in denaturing conditions using lysis buffer D (50 mM NaH_2PO_4, 300 mM NaCl, 8 M urea, pH 8) and supernatant was mixed with Ni-NTA agarose beads for 60 minutes at 4°C under gentle shaking. Flow-through was collected and the column was washed two times with wash buffer (50 mM NaH_2PO_4, 300 mM NaCl, 8 M urea, 20 mM imidazole, pH 8). The washed fractions were also collected, and finally the protein bound in the resin was rescued

using elution buffer (50 mM NaH_2PO_4, 300 mM NaCl, 8 M urea, 100 or 250 mM imidazole, pH 8). Each fraction was analyzed on a 10% SDS-PAGE gel. Finally, the total yield of proteins was calculated, and the concentration of the eluted target protein was determined by comparison with known concentrations of BSA separated on a 12% SDS-PAGE gel.

Protein Analysis

Purified protein was loaded on 12% SDS-PAGE gels and stained with Coomassie Brilliant Blue (CBB). The target protein was excised from the gel and the fragment was immersed in purified water and sonicated. Gel staining, washing and digestion steps were done according to (Yang et al. 2013). After digestion, the peptide solution was collected for protein identification by peptide mass fingerprinting (PMF) using ESI-Q-TOF analysis. PMS was performed by comparing the masses of identical peptides to those in the NCBI protein database using the MASCOT search engine (http://www.matrixscience.com).

Production of Antibodies against BZR1 and Titer Determination

Rabbits were injected with target protein and the antibody was purified by a contracted service (AbClon), and the antiserum titer was determined using indirect ELISA. Briefly, polystyrene plate wells were covered with 100-300 ng of antigen (BZR1) in sodium carbonate (Na_2CO_3) buffer (50 mM Na_2CO_3, pH 9.6, with 0.02% NaN_3). After overnight incubation at 4°C, unbound proteins were removed from plates by washing 3 times with phosphate-buffered saline (PBS)-Tween buffer (PBS containing 0.05% Tween-20). For blocking, 2% skim milk in 1X PBS

was added to each well and the samples were incubated for 1 h at room temperature. Afterward, wells were washed one more time with PBST buffer before the reaction for the serum titer test was initiated. Serial dilutions of pre-immune serum and test serum of 1:100, 1:1000, 1:5000, 1:10000, 1:50000, and 1:100000 were made in the antigen-coated plates using PBS. The reaction was incubated for 2 h at 37°C and then washed 3 times with PBS-T. Secondary antibody conjugated to horseradish peroxidase (Rabbit IgG-HRP) was added to the well, at a dilution of 1:10000, and allowed to bind for 1 h at 37°C, followed by a round of 3 wash steps with PBST. Finally, for colorimetric HRP-based ELISA detection, 3,3′,5,5′-tetramethylbenzidine (TMB) ELISA substrate (Abcam) was added, the reaction was stopped after blue color formation using stop solution (Abcam), and the absorbance was read at 450 nm. The results were expressed as the mean absorbance value of two independent tests. To determine whether the reaction in some point was positive or negative, the differences between the serum and antiserum values were analyzed for significant differences ($p<0.05$) applying Student's *t*-test. The cut-off value was determined as the mean of the OD values plus 2 fold the standard deviation in reactions using the negative serum or pre-immune serum (Frey et al. 1998).

Protein Extraction and Immunoblot Analysis of the BZR1 protein

Protein extraction and gel blot analyses were performed in at least biological triplicate, following the procedures described previously (Kim et al. 2014). Basically, Arabidopsis protein was extracted from the tissues of 5-day-old seedlings grown on

MS agar-solidified media and treated for 1 h in MS liquid media containing 1 μM BL. For monocot plants, protein extracts derive from 5-day-old dark-grown seedling. Protein amount was measured using Bradford solution, and desired amounts of total protein from Arabidopsis, rice, setaria, sorghum seedlings or serial dilutions of purified BZR1 were loaded onto a 10 or 12 % SDS-PAGE gel, subjected to electrophoresis, and transferred to a polyvinylidene difluoride membrane (PVDF; Millipore) for detection with antibody. Aside from the BZR1 antibody, anti-actin (MP Biomedicals) or anti-tubulin (Sigma) was also used (1:5000 and 1:3000 respectively) as a loading controls. Membranes were then visualized by chemi-luminescence (GE Healthcare).

Quantitative RT-PCR analysis

Quantitative RT-PCR was performed in 96-well plates (Applied Biosystems) using a commercial qPCR kit (Kapabiosystems) as previously described previously (Kim et al. 2014). The reactions were performed in triplicate. The relative mRNA levels represent fold change over the control. Oligonucleotide sequences of used primers are BZR1-F:CAGAGCCCTCTTTCATCAGC and BZR1-R:AGGAATGCCACCATTTCTGA. UBQ10-F:CCACCAAAGTTTT ACATGAAACGAA and UBQ10-R:TCCAGGACAAGGAAGGTATTCC

RESULTS

BZR1 Expression Levels in E. coli and Purification Using Ni-NTA Resin

To obtain a His-tagged fusion construct of Arabidopsis BZR1, we cloned the cDNA of Arabidopsis *BZR1* into the pET28a vector (see Materials and Methods), and produced the pET28a-BZR1 plasmid. This plasmid was introduced into three different *E. coli* strains (i.e., BL21(DE3), BL21(DE3)pLysS, and BL21(DE3)RIPL) to test the expression of target protein under different conditions. His-BZR1, with an expected molecular of 38 kD, was obtained from whole cell lysate only in the recombinant *E. coli* strain BL21 (DE3) RIPL (Figure S5-1A lanes 10 to 13). In contrast, His-BZR1 was almost undetectable in the other two host strains (Figure S5-1A lanes 2 to 9). Binding to Ni-NTA resin and purification were performed under denaturing conditions, which included 8 M urea in the lysis, washing, and elution buffers (Figure S5-1B). Protein fractions were obtained from a two-step purification method where the proteins from the flow-through and wash of the first purification step were used as the input of the second purification step (lanes 5 and 6 in Figure S5-1C). Because the eluates of the first and second purification steps included nonspecific bands, we decided to concentrate these eluates separately. We named BZR1 1A to a purer concentrate and BZR1 1B to a concentrate that includes some non-specific bands. The yield of recombinant BZR1 in the BZR1 1A and BZR1 1B concentrates was 5.4 mg and 15 mg, respectively. Thus, we successfully expressed and purified a 38-kD recombinant His-BZR1 protein in the *E. coli* strain BL21(DE3)RIPL using Ni-NTA resin and denaturing conditions.

Analysis of Purified Recombinant Protein and Titer Determination

The identity of the induced and purified recombinant protein was determined by ESI-Q-TOF analysis (Figure S5-2A and Table 5-I). The list of 18 peptides obtained after trypsin digestion of His-BZR1 protein is listed in Table I, and a comparison using the MASCOT program revealed that these peptides show good alignment with the BZR1 protein. Overall, the peptides covered 65% of the BZR1 amino acid sequence (NCBI BLAST; gi|6651069), thereby confirming that the purified protein was indeed BZR1 (Figure S5-2A).

The purified anti-BZR1 antibody titer was evaluated by indirect ELISA using a fixed amount of BZR1 antigen and a serial dilution of the antibody serum (from 1:100 to 1:100000). The results were expressed as absorbance values (OD_{450}), and are shown in a dose-response graph made using the mean values of two independent tests (Figure S5-2B). The first four dilutions were found to be significantly different from the pre-immune value ($p<0.05$; Student's *t*-test), whereas the 1:50000 and 1:100000 dilutions were not (*p*-values of 0.149 and 0.356, respectively). Considering this result, a dilution of 1:10000 was found to be optimal for BZR1 detection. Moreover, the antibody capacity to bind to its target at a concentration of 1:10000 was further tested by an immunoblot analysis using dilutions (1 ng to 1 µg) of His-BZR1 (Figure S5-2C). Since the sample containing 1 ng yielded a relatively weak band, we concluded that the sensitivity of the anti-BZR1 (1:10000) allowed for detection of samples containing concentrations of above 1 ng of BZR1.

Anti-BZR1 Detects Phosphorylated and Dephosphorylated Forms of BZR1 in Arabidopsis Plant Tissues

In Arabidopsis, the BR signaling pathway starts with the binding of BL to its receptor, which produces downstream events that include a shift in BZR1 phosphorylation status and subcellular localization (Ryu et al. 2007). The disappearance of the phosphorylated BZR1 (pBZR1) forms and the ratio of pBZR1 to dephosphorylated (dBZR1) forms are used as a read-out of the BR signaling status. It is thus important to test whether the anti-BZR1 antibody is able to detect both the phosphorylated and dephosphorylated forms of BZR1. To this end, we thus used transgenic lines overexpressing BZR1 protein (BZR1-HA) to test the antibody against dilutions of total protein extracts (Figure 5-1A) and to monitor the pattern of BZR1 after BL treatments (Figure 5-1B). Immunoblot analysis showed that our anti-BZR1 antibody detected both the phosphorylated and dephosphorylated forms of BZR1 in the original (1x) and 5- (5x) or 10-times (10x) diluted samples (Figure 5-1A). Additionally, we observed that the pBZR1 form becomes less abundant immediately after BL treatment (Figure 5-1B). Our results also showed a continued decrease in pBZR1 until 20 min (Figure 1-1B). We also observed the dephosphorylated BZR1 form at all-time points examined; however, the intensity of this signal did not vary dramatically after BL treatments as we expected (Figure 5-1B).

Next, we tested the ability of anti-BZR1 to bind to endogenous BZR1 protein in different genetic backgrounds, (Figure 5-2A and B). Similarly to what we observed in the overexpression lines, the amount of dBZR1 did not vary among

samples, whereas that of pBZR1 decreased after BL treatment in most of them. One exception was observed in the *bzr1-1D* background, in which dBZR1 was abundant both in the presence and absence of BL treatment (Figure 5-1B and A).

Since the BZR1 protein exhibits 88% amino acid sequence identity with BES1 (Yin et al. 2002), we tested the possibility that anti-BZR1 cross-reacts with and detects BES1 as well (Figure 5-2B). For this analysis, we used the *bes1-1D* dominant mutant, which displays a constitutive BR response and accumulation of BES1 in the nucleus, in a similar manner as its *bzr1-1D* counterpart does for BZR1 (Mora-Garcia et al. 2004). Our immunoblot assay using the anti-BZR1 antibody did not show a distinctive pattern in *bes1-1D* in comparison with its wild type background En-2, which suggested that anti-BZR1 mainly recognizes BZR1 (Figure 5-2B). Nonetheless, the *bes1-1* knock-out mutant didn't show same expected pattern of its wild type counterpart Col-0, which leaded us to check *BZR1* expression in this mutant background (Figure 5-2C). We found that mRNA levels of *BZR1* decrease significantly in *bes1-1* mutant, which may at least partially explain the weaker detection. Finally, we compared the BZR1 pattern in wild type and transgenic BZR1-HA overexpression lines under BL treatments using anti-BZR1 and anti-HA antibodies (Figure 5-2D). Our antibody detected HA-tagged BZR1 in a similar pattern with the one obtained using anti-HA, although other bands, most probably corresponding to non-tagged or native BZR1 protein, were observed in the membrane. Using this transgenic line we also were able to observe the change in dBZR1 form after BL treatment, which is maybe due to the increase amount of all

BZR1 forms in these transgenic lines. In summary, we demonstrated that our anti-BZR1 antibody recognizes both the pBZR1 and dBZR1 forms in protein extracts from plant tissues.

Anti-BZR1 Detects BZR1 Orthologs in Plant Tissues of Monocot Plants

Previous studies provided strong evidence of a conserved function of BZR1 in Arabidopsis and rice OsBZR1 (Os07g39220) in BR responses (Bai et al. 2007). Both proteins share near 53% of overall sequence identity, with higher homology in domains of important function. Because of this conservation, we tested if our antibody was able to detect BZR1 orthologs in rice and other monocots. To observe possible phosphorylation changes in BZR1 protein we tested protein extracts from rice, setaria and sorghum seedlings that were used for western blot and subject to hybridation with anti-BZR1 antibody (Figure 5-3A and B). The expected size of proteins was identified using full-length Arabidopsis BZR1 protein sequence against grass family genomes using phytozome BLAST tool (http://www.phytozome.net/). The highest amino acid sequence identity with BZR1 included the previously characterized OsBZR1 (Bai et al. 2007), *Setaria italica* Si030508m and *Sorghum bicolor* Sb02g037500 with expected protein size of 31.91 kD, 34.49 kD and 35.27 kD respectively. In all cases we detected bands near the expected sizes, although the signal was weaker compared with Arabidopsis, especially in setaria and sorghum where dephosphorylated forms were barely detected even loading more than double quantity of total protein. Using seedlings of different plant species we observed a heterogeneous affinity of BZR1 antibody towards BZR1 orthologs, were elevated

concentrations of total protein is required for detection. Compared with Arabidopsis, double or more quantity of protein was needed for rice, setaria and sorghum to detect BZR1 in the same membrane using antibody dilution of 1:10000. When same amount of total protein was tested, no detection was observed in setaria or sorghum and just weak pBZR1 protein was observed in rice (data not shown). To confirm the amount of loaded protein we tested the membrane using anti-α-tubulin (Figure 5-3A), anti-actin (data not shown) and and ponceau staining (Figure 5-3B). Nevertheless, the variety of species in the same membrane represents a difficulty in comparisons since pattern varies from one to the other species. Anti-α-tubulin antibody seems to be a good option with the exception of setaria that present a minimal reaction to this antibody compared with its counterparts. Lastly, our immunoblot analysis showed detection of high molecular weight proteins that don't match with the expected size of BZR1 in Arabidopsis or its orthologs in monocot plants. Further experiments are needed to conclude if they correspond to other forms of BZR1 or non-specific binding of the antibody

DISCUSSION

In this report, we defined the optimal conditions for inducing the expression of recombinant BZR1 and purifying this protein from an *E. coli* system for the production of anti-BZR1 antibody. Of the three different *E. coli* strains tested, His-BZR1 was only induced when the BL21(DE3)RIPL strain served as a host. This can be explained by the presence of 17 rare codons, i.e., 14 total single rare Arg codons and 3 tandem rare Arg codon double repeats, in the BZR1 sequence (http://nihserver.mbi.ucla.edu/RACC/) that are infrequently used by *E. coli*. Although *E. coli* systems have been used extensively to produce recombinant proteins, they have some limitations, including toxicity and degradation of the target protein and difficulty in expressing genes with codons rarely used in bacteria. This subset of codons are rarely used by *E. coli*, and thus correspond to rare tRNAs (Kleber-Janke et al. 2000); however, BL21-CodonPlus (DE3)RIPL competent cells contain extra copies of argU, ileY, and leuW as well as proL tRNA genes to overcome this obstacle (Schenk et al. 1995). Therefore, we concluded that BL21(DE3)RIPL host cells were the optimal strain for producing BZR1 recombinant protein.

Once we had identified a bacterial strain in which the BZR protein could be expressed, it was important to test the solubility of the expressed protein and then to purify it. Although a longer induction period at a lower temperature, i.e., overnight at 30°C or lower temperature, is generally recommended to obtain

soluble protein, induction at 37°C for 4 h showed better results. Expression under this condition yielded more protein and the resulting protein did not accumulate in inclusion bodies. Furthermore, the constitution of the lysis buffer affected our ability to detect BZR1 in the pellet or supernatant. The composition of the buffer was also important for the efficient binding of His-BZR1 protein to the Ni-NTA column during purification, since this binding was possible only under denaturing conditions. This may be due to the fact that the tag may be blocked or hidden by the assembled form of the protein, or make it physically difficult for the tagged protein to bind to the resin. However, in the presence of a strong denaturant, such as urea, the His tag can be completely exposed, facilitating its binding to the Ni-NTA column. Though binding to the resin was confirmed, we still detected lot of protein in the flow-through and wash fractions. For this reason, we performed a second purification step in which we used the flow-through and wash fractions of the first step as input to increase yield.

We demonstrated that the anti-BZR1 antibody developed here was able to detect BZR1 expressed in *E. coli* and also in total protein extracts from plant tissues. Furthermore, our anti-BZR1 antibody bound to both the phosphorylated and dephosphorylated forms of BZR1 and the observed phosphorylation patterns observed by immunoblot analysis correlated with previous descriptions. When BR signaling is not activated or in absence of BL treatments, pBZR1, which is the inactive form of BZR1 and is mainly present in the cytoplasm, accumulated (He et al. 2002; Yin et al. 2005; Ryu et al. 2007; Tang et al. 2011). In our immunoblot

analysis, we observed that pBZR1 accumulated under normal conditions not only in BZR1-overexpressing lines, but also in the wild type and various mutant backgrounds. Conversely, when seedlings were treated with BL, we observed a decrease in the amount of pBZR1 compared with mock treatments, which is an expected consequence of activation of BR signaling. Recently, our group demonstrated that a similar reduction in pBZR1 occurs under dark treatments (Kim et al. 2014). In that work, our anti-BZR1 antibody was used to detect the changes in the phosphorylation profile of the BZR1 transcription factor under different light regimes. Although anti-BZR1 was able to detect changes in pBZR1, we did not detect prominent changes in the amount of native dBZR1 even after many replicates of the experiment and under different durations of BL treatments. Just using BZR1-HA overexpression lines we were able to detect differences in dBZR1 form, which may be due to relatively high expressions of all forms of BZR1 in these lines, which make easier the detection of changes in the pattern after chemical treatment. We therefore concluded that our antibody is able to detect changes in both, phosphorylated and dephosphorylated form of BZR1. The phosphorylation pattern displayed by *bzr1-1D* was very distinctive from the other genetic backgrounds tested, but is in agreement with its constitutive BR response phenotype. The dominant mutation in *bzr1-1D* is caused by an amino acid change (Pro234 to Leu) in the PEST domain of the protein which stabilizes BZR1 protein (Wang et al. 2002; He et al. 2005; Li et al. 2005). The PEST domain is known for mediating proteolytic degradation, thus disruption of this motif may abolish

degradation, which explains the high levels of BZR1 forms in this mutant compared with its wild type counterpart (He et al. 2005), but doesn't explain the high levels of active form of BZR1 or dBZR1. The distinctive pattern showed by *bzr1-1D* differs from the pattern of simple BZR1 overexpression because it shows high levels of dBZR1, and this characteristic can be also related with the PEST domain. In case of BZR1/BES1 proteins, this domain was demonstrated to function as well as a PP2A binding site, thus increase levels of dBZR1 form could be due to increase phosphorylation by PP2A (Tang et al. 2011). In contrast, the phosphorylation pattern of BZR1 observed in the *bes1-1D* allele didn't differ from that in its wild-type counterpart, except for a slight reduction in pBZR1, which may be an effect of its constitutive BR response. Based on the finding that anti-BZR1 did not show increased binding in *bes1-1D,* which accumulates BES1 (Yin et al. 2002), we concluded that our antibody preferentially detects BZR1. To rule out the possibility that anti-BZR1 cross-reacts with BES1 the study of this antibody in *BZR1* knock-out lines would be very informative; however, no such mutant has been reported to date. As an alternative, we tested in the *bes1-1* background*,* a *BES1* knock out mutant (He et al. 2005), in where we expected no differences with the wild type. Surprisingly, BZR1 detection was weaker in *bes1-1*, opening a possibility of cross-reaction with BES1. However, BES1 as an important transcription factor in BR signalizing could be involved in BZR1 transcription, reason why we tested *BZR1* mRNA levels in the *bes1-1* mutant. In concordance with our immunoblot, a general decrease in BZR1 detection (e.g. decrease of BZR1

protein) can be explained by an important reduction of *BZR1* mRNA levels compared to wild type.

In conclusion, we report the production and characterization of an anti-BZR1 antibody. It was previously shown that our anti-BZR1 antibody (Kim et al. 2014) was extremely useful in studies related to BR signaling, since BZR1 is a key component of this signaling pathway. In future, this antibody may be used to elucidate mechanisms in which the BZR1 transcription factor is involved, specifically regarding its interaction with other proteins and the cross-talk between different plant signaling pathways. Importantly, this antibody may be used to analyze BR signaling pathways in understudied plants, because the protein sequences of BZR1 are well conserved as we demonstrate by the BZR antibody binding not just in Arabidopsis but other model plant species. Although the amount of protein or antibody required should be tested case by case for an optimal result in the detection.

FIGURES AND TABLES

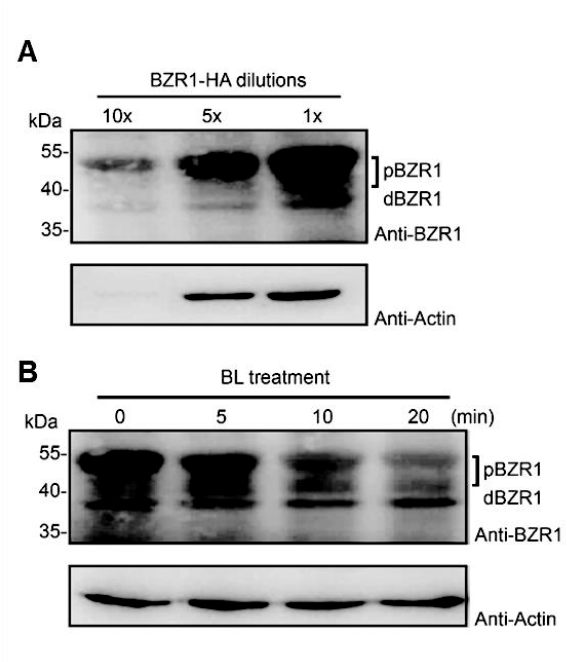

Figure 5-1. Anti-BZR1 detects phosphorylated and dephosphorylated forms of BZR1 in Arabidopsis BZR1-HA overexpressing lines. (**A-B**) Immunoblot analysis of BR-induced phosphorylation changes using the anti-BZR1 antibody. Immunoblot experiments showing phosphorylated (pBZR1) and dephosphorylated (dBZR1) forms of BZR1 in dilutions of total protein extracts obtained from transgenic plants overexpressing BZR1-HA (**A**) in the absence or presence (**B**) of BL treatment. The dilution factors are indicated as well as the duration of BL treatments.

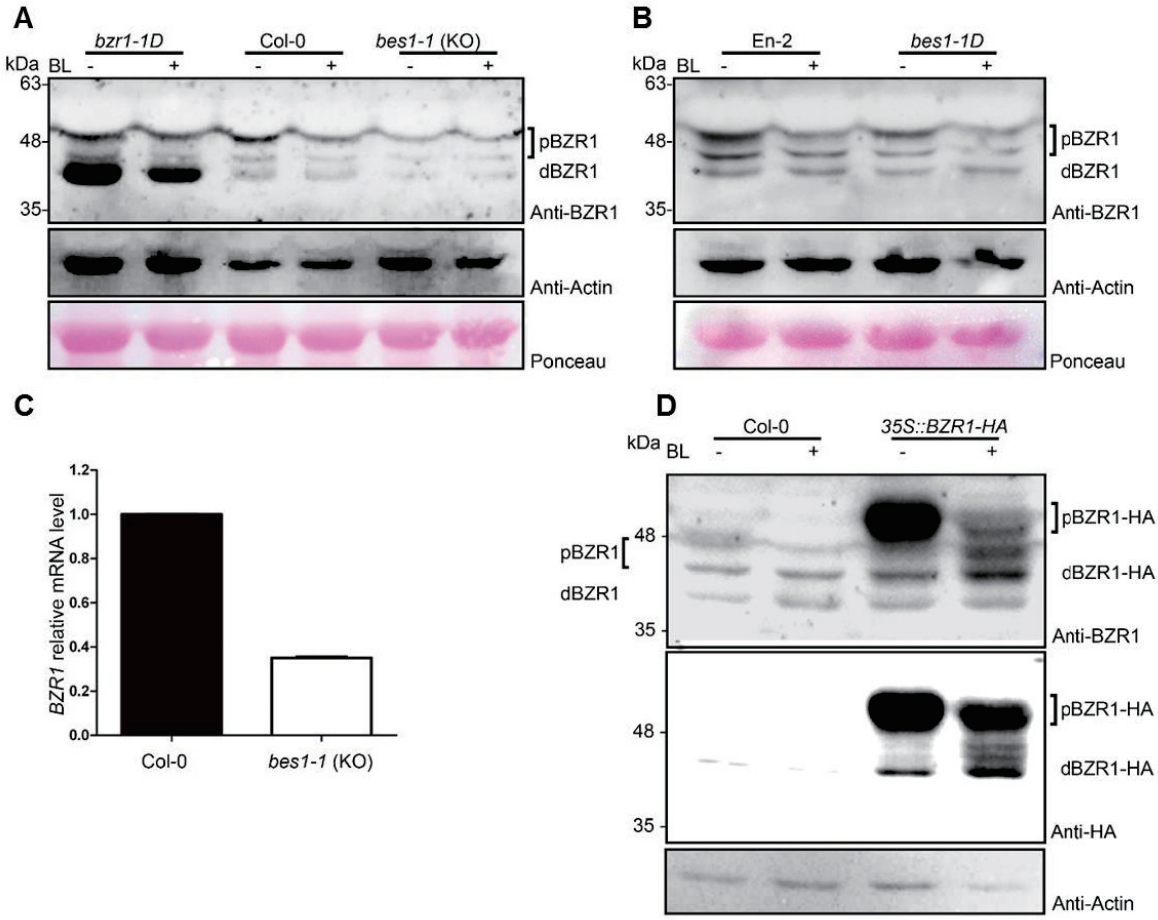

Figure 5-2. Anti-BZR1 detects changes in phosphorylation statutes and mainly recognizes BZR1 in Arabidopsis. (**A-B**) Immunoblot analysis of BL-treated *bzr1-1D*, *bes1-1,* and *bes1-1D* mutants and their respective wild type backgrounds, Col and En-2. All membranes were probed with anti-BZR1 antibody (upper panels). As loading control, we used actin detection (middle panels) and ponceau s staining (bottom panels). (**C**) Quantitative RT–PCR (qRT–PCR) analyses of *BZR1* mRNA expression in *bes1-1* knock-out mutant and wild type backgrounds. The mRNA

levels were normalized to UBQ10 and bars show mean +/- S.D. (**D**) Comparison of the BZR1 pattern in wild type and transgenic BZR1-HA overexpression lines under BL treatments. Same membrane was first detected using our rabbit anti-BZR1 and then using rat anti-HA antibodies. The membrane was finally detected using anti-actin as a loading control.

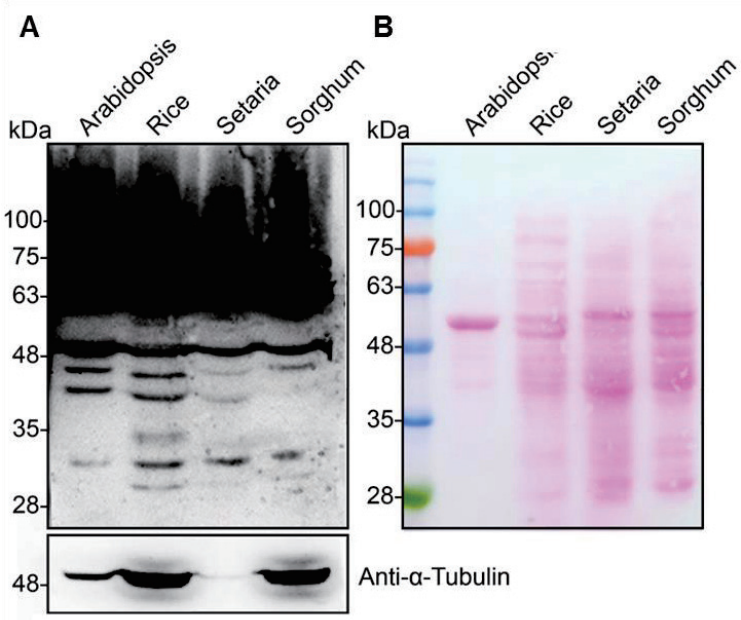

Figure 5-3. Anti-BZR1 detects BZR1 orthologs in three different monocot plants. (**A-B**) SDS-PAGE and Immunoblot analysis with anti-BZR1 using Arabidopsis and other three plant species. (**A**) After transferred to a membrane, immunoblotting was performed using our anti-BZR1. For Arabidopsis, 20µg of protein was loaded and 50µg were tested for all three monocot samples and (**B**) ponceau staining of membrane previous to the use of anti-BZR1 antibody was used to verify the amount of proteins loaded into the gel. Expected size for setaria BZR1 is 34.49 kD, 31.91 kD for rice and 35.27 kD for sorghum. Alternatively, the membrane was immunoblotted a second time using animal Anti-α-Tubulin (Sigma) as a loading control too (**A**, bottom panel).

Table 5-1. List of the signature peptides derived from BZR1 protein, as identified by ESI-Q-TOF.

Peak No	Sequence Position	Measures (m/z)	Charged	Measures (expected)	Measures (calculated)	Missed cleavage site(s)	Delta mass	Signature peptide
1	018-043	1154.3859	2	2306.7573	2306.0379	0	0.7194	RGSHMMTSDGATSTSAAAAAAAAAAARR
2	068-073	722.505	1	721.4977	721.4122	0	0.0855	KIYTGLRA
3	074-082	1005.915	1	1004.9077	1005.4767	0	-0.569	RAQGDYNLPKH
4	083-109	1035.8989	3	3104.6748	3106.4123	1	-1.7375	KHCDNNEVLKALCVEAGWVVEEDGTTYRK
5	092-109	1028.4094	2	2054.8043	2053.9414	0	0.8628	KALCVEAGWVVEEDGTTYRK
6	092-110	728.5479	3	2182.6218	2182.0364	1	0.5854	KALCVEAGWVVEEDGTTYRKG
7	111-125	765.6894	2	1529.3643	1528.7667	0	0.5976	KGCKPLPGEIAGTSSRV
8	163-178	1857.76	1	1856.7527	1856.8515	0	-0.0988	RGEPNNNMSSTFFPFLRN
9	163-190	1013.5156	3	3037.5248	3037.4603	1	0.0646	RGEPNNNMSSTFFPFLRNGGIPSSLPSLRI
10	179-190	1198.059	1	1197.0517	1196.6513	0	0.4004	RNGGIPSSLPSLRI
11	191-207	1757.573	1	1756.5657	1756.8665	0	-0.3008	RISNSCPVTPPVSSPTSKN
12	208-220	1494.163	1	1493.1557	1492.8038	0	0.352	KNPKPLPNWESIAKQ
13	221-249	1594.9194	2	3187.8243	3189.5011	1	-1.6768	KQSMAIAKQSMASFNYPFYAVSAPASPTHRH
14	228-249	816.0532	3	2445.1378	2445.1059	0	0.0319	KQSMASFNYPFYAVSAPASPTHRH
15	250-279	1148.9472	3	3443.8198	3443.5	0	0.3198	RHQFHTPATIPECDESDSSTVDSGHWISFQKF

16	325-337	1605.6	1	1604.5927	1604.7583	0	-0.1655	KFENSQVKPWEGERI
17	338-354	929.4224	2	1856.8303	1856.8825	0	-0.0522	RIHDVGMEDLELTLGNGKA
18	338-356	690.3702	3	2068.0888	2068.0258	1	0.063	RIHDVGMEDLELTLGNGKARG

SUPPLEMENTAL INFORMATION

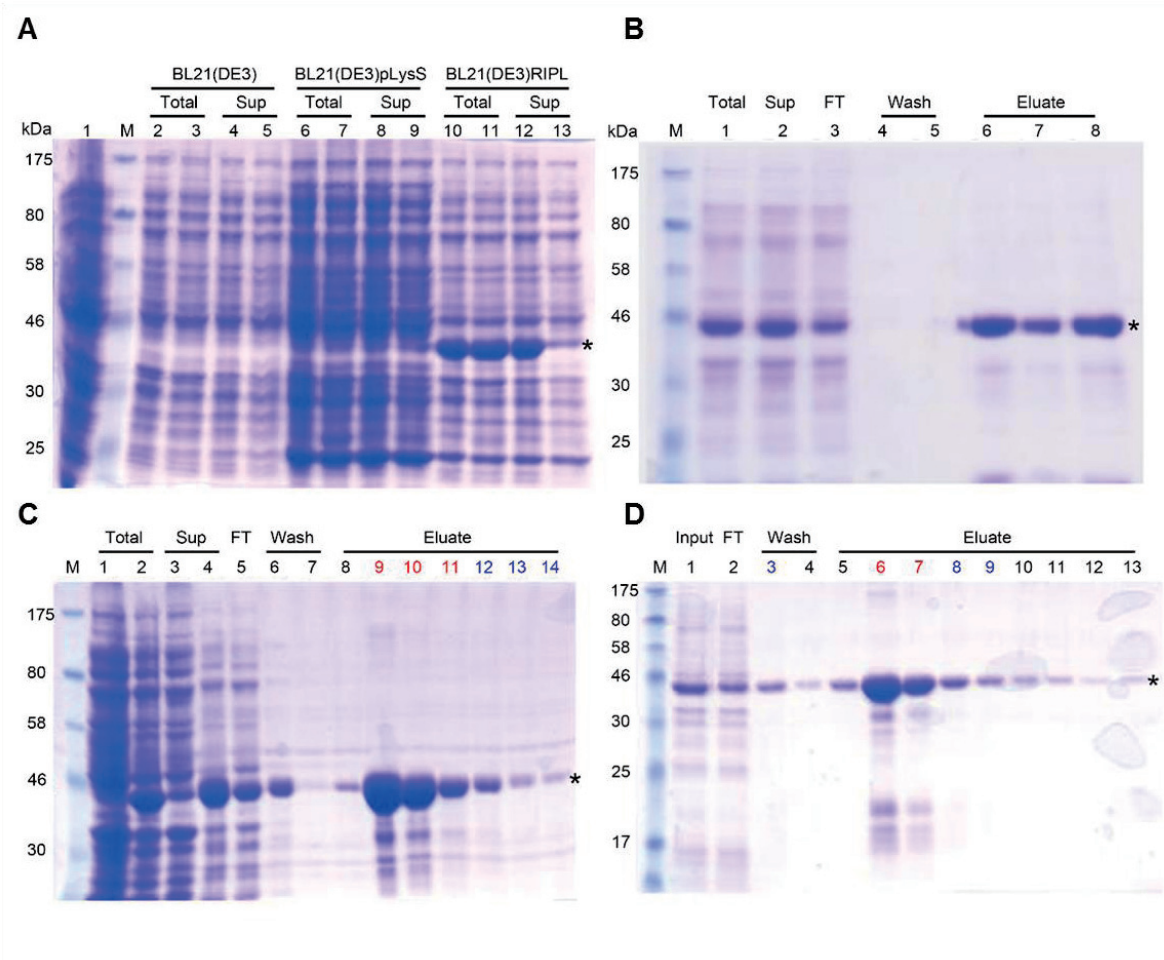

Figure S5-1. Expression and purification of recombinant His-BZR1 protein. (**A-D**) Expression patterns and elution profiles of recombinant BZR1 protein as shown in an SDS-PAGE gel stained with Coomassie Brilliant Blue. (**A**) Expression of recombinant His-BZR1 protein (asterisk) in three different *E. coli* strains – BL21(DE3), BL21(DE3)pLysS, and BL21(DE3)RIPL – all harboring the pET28a-

BZR1 plasmid. Lane 1, before IPTG induction; lane M, protein marker; and lanes 2-13, after 4 h of IPTG induction at 37°C. Total and Sup correspond to total protein extract after lysis (both supernatant and pellet) and supernatant, respectively. Supernatant from lines 4, 8 and 12 were obtained using lysis buffer A, while supernatant from lines 5, 9 and 13 were obtained using lysis buffer B (**B**) Ni-NTA binding test under denaturing conditions. Lane M, marker; lane 1, total protein suspended in urea-containing buffer; lane 2, urea supernatant; 3, flow-through; lanes 4-5, wash; lanes 6-8, eluate. (**C and D**) His-BZR1 purification steps. For the gel shown in (**C**); lane M, protein marker; lane 1 uninduced cell total lysate; lane 2, induced cell total lysate; lane 3, induced cell supernatant; lane 4, urea supernatant; lane 5, flow-through; lane 6 and 7, wash; and lanes 8 to 14, eluate. (**D**) Second purification lanes 5 to 13, eluate. The asterisks indicate the His-BZR1 protein.

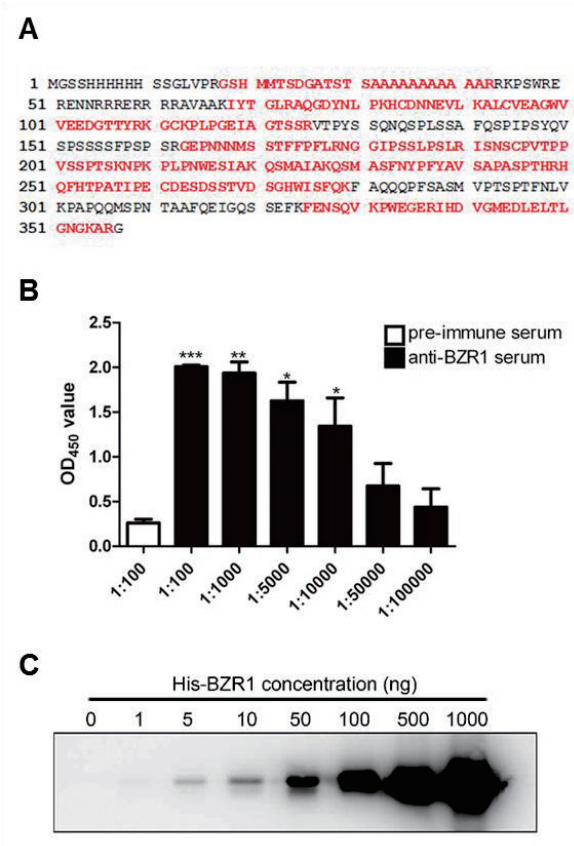

Figure S5-2. **Identity of the His-BZR1 protein and maximum sensitivity of the anti-BZR1 antibody.** (**A**) Matched peptides shown in bold red letters in the full amino acid sequence of *Arabidopsis thaliana* BZR1 protein after analysis with MASCOT (**B**) Determination of the antibody titer by indirect ELISA. A fixed amount of 200 ng His-BZR1 was combined with dilutions of 1:100 to 1:100000 of anti-BZR1 serum. As a negative control, a 1:100 dilution of pre-immune serum was used. Data are mean values with standard deviations. Statistically significant differences were evaluated using Student's *t*-test (*p<0.05; **p<0.003, and

***p<0.001). (**C**) Immunoblot analysis showing the detection of various dilutions of His-BZR1 with the anti-BZR1 antibody used at a dilution of 1:10000.

REFERENCES

Asami T, Min YK, Nagata N, Yamagishi K, Takatsuto S, Fujioka S, Murofushi N, Yamaguchi I, Yoshida S (2000) Characterization of brassinazole, a triazole-type brassinosteroid biosynthesis inhibitor. Plant Physiol 123: 93-100

Asami T, Mizutani M, Fujioka S, Goda H, Min YK, Shimada Y, Nakano T, Takatsuto S, Matsuyama T, Nagata N, Sakata K, Yoshida S (2001) Selective interaction of triazole derivatives with DWF4, a cytochrome P450 monooxygenase of the brassinosteroid biosynthetic pathway, correlates with brassinosteroid deficiency in planta. J Biol Chem 276: 25687-25691

Asami T, Yoshida S (1999) Brassinosteroid biosynthesis inhibitors. Trends Plant Sci 4: 348-353

Azpiroz R, Wu Y, LoCascio JC, Feldmann KA (1998) An Arabidopsis brassinosteroid-dependent mutant is blocked in cell elongation. Plant Cell 10: 219-230

Bai MY, Fan M, Oh E, Wang ZY (2012) A triple helix-loop-helix/basic helix-loop-helix cascade controls cell elongation downstream of multiple hormonal and environmental signaling pathways in Arabidopsis. Plant Cell 24: 4917-4929

Bai MY, Shang JX, Oh E, Fan M, Bai Y, Zentella R, Sun TP, Wang ZY (2012) Brassinosteroid, gibberellin and phytochrome impinge on a common transcription module in Arabidopsis. Nat Cell Biol 14: 810-817

Bai MY, Zhang LY, Gampala SS, Zhu SW, Song WY, Chong K, Wang ZY (2007) Functions of OsBZR1 and 14-3-3 proteins in brassinosteroid signaling in rice. Proc Natl Acad Sci U S A 104: 13839-13844

Belkhadir Y, Durbak A, Wierzba M, Schmitz RJ, Aguirre A, Michel R, Rowe S, Fujioka S, Tax FE (2010) Intragenic suppression of a trafficking-defective brassinosteroid receptor mutant in Arabidopsis. Genetics 185: 1283-1296

Bevan MW, Garvin DF, Vogel JP (2010) Brachypodium distachyon genomics for sustainable food and fuel production. Curr Opin Biotechnol 21: 211-217

Bishop GJ, Koncz C (2002) Brassinosteroids and plant steroid hormone signaling. Plant Cell 14 Suppl: S97-110

Blackwell HE, Zhao Y (2003) Chemical genetic approaches to plant biology. Plant Physiol 133: 448-455

Cheon J, Fujioka S, Dilkes BP, Choe S (2013) Brassinosteroids regulate plant growth through distinct signaling pathways in Selaginella and Arabidopsis. PLoS One 8: e81938

Cheon J, Park SY, Schulz B, Choe S (2010) Arabidopsis brassinosteroid biosynthetic mutant dwarf7-1 exhibits slower rates of cell division and shoot induction. BMC Plant Biol 10: 270

Choe S, Dilkes BP, Fujioka S, Takatsuto S, Sakurai A, Feldmann KA (1998) The DWF4 gene of Arabidopsis encodes a cytochrome P450 that mediates multiple 22alpha-hydroxylation steps in brassinosteroid biosynthesis. Plant Cell 10: 231-243

Choe S, Dilkes BP, Gregory BD, Ross AS, Yuan H, Noguchi T, Fujioka S, Takatsuto S, Tanaka A, Yoshida S, Tax FE, Feldmann KA (1999) The Arabidopsis dwarf1 mutant is defective in the conversion of 24-methylenecholesterol to campesterol in brassinosteroid biosynthesis. Plant Physiology 119: 897-907

Choe S, Fujioka S, Noguchi T, Takatsuto S, Yoshida S, Feldmann KA (2001) Overexpression of DWARF4 in the brassinosteroid biosynthetic pathway results in increased vegetative growth and seed yield in Arabidopsis. Plant J 26: 573-582

Choe S, Noguchi T, Fujioka S, Takatsuto S, Tissier CP, Gregory BD, Ross AS, Tanaka A, Yoshida S, Tax FE, Feldmann KA (1999) The Arabidopsis dwf7/ste1 mutant is defective in the delta7 sterol C-5 desaturation step leading to brassinosteroid biosynthesis. Plant Cell 11: 207-221

Choe S, Schmitz RJ, Fujioka S, Takatsuto S, Lee MO, Yoshida S, Feldmann KA, Tax FE (2002) Arabidopsis brassinosteroid-insensitive *dwarf12* mutants are semidominant and defective in a glycogen synthase kinase 3b-like kinase. Plant Physiol 130: 1506-1515

Chono M, Honda I, Zeniya H, Yoneyama K, Saisho D, Takeda K, Takatsuto S, Hoshino T, Watanabe Y (2003) A semidwarf phenotype of barley uzu results from a nucleotide substitution in the gene encoding a putative brassinosteroid receptor. Plant Physiol 133: 1209-1219

Chung Y, Choe S (2013) The Regulation of Brassinosteroid Biosynthesis in Arabidopsis. Crit Rev Plant Sci 32: 396-410

Chung Y, Maharjan PM, Lee O, Fujioka S, Jang S, Kim B, Takatsuto S, Tsujimoto M, Kim H, Cho S, Park T, Cho H, Hwang I, Choe S (2011) Auxin stimulates DWARF4 expression and brassinosteroid biosynthesis in Arabidopsis. Plant J 66: 564-578

Clouse SD (2011) Brassinosteroids. Arabidopsis Book 9: e0151

Clouse SD, Langford M, McMorris TC (1996) A brassinosteroid-insensitive mutant in Arabidopsis thaliana exhibits multiple defects in growth and development. Plant Physiol 111: 671-678

Coles JP, Phillips AL, Croker SJ, Garcia-Lepe R, Lewis MJ, Hedden P (1999) Modification of gibberellin production and plant development in Arabidopsis by sense and antisense expression of gibberellin 20-oxidase genes. Plant J 17: 547-556

Corvalan C, Choe S (2017) Identification of brassinosteroid genes in Brachypodium distachyon. BMC Plant Biol 17: 5

De Veylder L, Beeckman T, Beemster GT, de Almeida Engler J, Ormenese S, Maes S, Naudts M, Van Der Schueren E, Jacqmard A, Engler G, Inze D (2002) Control of proliferation, endoreduplication and differentiation by the Arabidopsis E2Fa-DPa transcription factor. EMBO J 21: 1360-1368

Divi UK, Krishna P (2009) Brassinosteroid: a biotechnological target for enhancing crop yield and stress tolerance. N Biotechnol 26: 131-136

Draper J, Mur LA, Jenkins G, Ghosh-Biswas GC, Bablak P, Hasterok R, Routledge AP (2001) Brachypodium distachyon. A new model system for functional genomics in grasses. Plant Physiol 127: 1539-1555

Duan K, Li L, Hu P, Xu SP, Xu ZH, Xue HW (2006) A brassinolide-suppressed rice MADS-box transcription factor, OsMDP1, has a negative regulatory role in BR signaling. Plant J 47: 519-531

Eggermont K, Goderis IJ, Broekaert WF (1996) High-throughput RNA extraction from plant samples based on homogenisation by reciprocal shaking in the presence of a mixture of sand and glass beads. Plant Mol Biol Report 14: 273-279

Fabregas N, Cano-Delgado AI (2014) Turning on the microscope turret: a new view for the study of brassinosteroid signaling in plant development. Physiol Plant 151: 172-183

Fabregas N, Li N, Boeren S, Nash TE, Goshe MB, Clouse SD, de Vries S, Cano-Delgado AI (2013) The brassinosteroid insensitive1-like3 signalosome complex regulates Arabidopsis root development. Plant Cell 25: 3377-3388

Feng Y, Yin Y, Fei S (2015) Down-regulation of BdBRI1, a putative brassinosteroid receptor gene produces a dwarf phenotype with enhanced drought tolerance in Brachypodium distachyon. Plant Sci 234: 163-173

Frey A, Di Canzio J, Zurakowski D (1998) A statistically defined endpoint titer determination method for immunoassays. Journal of immunological methods 221: 35-41

Friedrichsen DM, Nemhauser J, Muramitsu T, Maloof JN, Alonso J, Ecker JR, Furuya M, Chory J (2002) Three redundant brassinosteroid early response genes encode putative bHLH transcription factors required for normal growth. Genetics 162: 1445-1456

Fujioka S, Sakurai A (1997) Brassinosteroids. Nat Prod Rep 14: 1-10

Fujioka S, Yokota T (2003) Biosynthesis and metabolism of brassinosteroids. Annu Rev Plant Biol 54: 137-164

Fukuda H (2004) Signals that control plant vascular cell differentiation. Nat Rev Mol Cell Biol 5: 379-391

Gachotte D, Meens R, Benveniste P (1995) An Arabidopsis Mutant Deficient in Sterol Biosynthesis - Heterologous Complementation by Erg-3 Encoding a Delta(7)-Sterol-C-5-Desaturase from Yeast. Plant J 8: 407-416

Gampala SS, Kim TW, He JX, Tang W, Deng Z, Bai MY, Guan S, Lalonde S, Sun Y, Gendron JM, Chen H, Shibagaki N, Ferl RJ, Ehrhardt D, Chong K,

Burlingame AL, Wang ZY (2007) An essential role for 14-3-3 proteins in brassinosteroid signal transduction in Arabidopsis. Dev Cell 13: 177-189
Girin T, David LC, Chardin C, Sibout R, Krapp A, Ferrario-Mery S, Daniel-Vedele F (2014) Brachypodium: a promising hub between model species and cereals. J Exp Bot 65: 5683-5696
Gonzalez-Garcia MP, Vilarrasa-Blasi J, Zhiponova M, Divol F, Mora-Garcia S, Russinova E, Cano-Delgado AI (2011) Brassinosteroids control meristem size by promoting cell cycle progression in Arabidopsis roots. Development 138: 849-859
Gonzalez N, De Bodt S, Sulpice R, Jikumaru Y, Chae E, Dhondt S, Van Daele T, De Milde L, Weigel D, Kamiya Y, Stitt M, Beemster GT, Inze D (2010) Increased leaf size: different means to an end. Plant Physiol 153: 1261-1279
Grove MD, Spencer GF, Rohwedder WK, Mandava N, Worley JF, Warthen JD, Steffens GL, Flippenanderson JL, Cook JC (1979) Brassinolide, a Plant Growth-Promoting Steroid Isolated from Brassica-Napus Pollen. Nature 281: 216-217
Gruszka D, Szarejko I, Maluszynski M (2011) New allele of HvBRI1 gene encoding brassinosteroid receptor in barley. J Appl Genet 52: 257-268
Guo J, Song J, Wang F, Zhang XS (2007) Genome-wide identification and expression analysis of rice cell cycle genes. Plant Mol Biol 64: 349-360
Hacham Y, Holland N, Butterfield C, Ubeda-Tomas S, Bennett MJ, Chory J, Savaldi-Goldstein S (2011) Brassinosteroid perception in the epidermis controls root meristem size. Development 138: 839-848
Hartwig T, Chuck GS, Fujioka S, Klempien A, Weizbauer R, Potluri DP, Choe S, Johal GS, Schulz B (2011) Brassinosteroid control of sex determination in maize. Proc Natl Acad Sci U S A 108: 19814-19819
Hartwig T, Corvalan C, Best NB, Budka JS, Zhu JY, Choe S, Schulz B (2012) Propiconazole is a specific and accessible brassinosteroid (BR) biosynthesis inhibitor for Arabidopsis and maize. PLoS One 7: e36625
Hategan L, Godza B, Szekeres M (2011) Regulation of brassinosteroid metabolism, In Hayat S, Ahmad A eds, Brassinosteroids: A Class of Plant Hormone, Ed, Vol Springer Netherlands, Dordrecht pp 57-81
Hayat S, Ahmad A (2003) Brassinosteroids : bioactivity and crop productivity, Ed, Vol Kluwer Academic, Dordrecht ; Boston
He JX, Fujioka S, Li TC, Kang SG, Seto H, Takatsuto S, Yoshida S, Jang JC (2003) Sterols regulate development and gene expression in Arabidopsis. Plant Physiology 131: 1258-1269
He JX, Gendron JM, Sun Y, Gampala SS, Gendron N, Sun CQ, Wang ZY (2005) BZR1 is a transcriptional repressor with dual roles in brassinosteroid homeostasis and growth responses. Science 307: 1634-1638
He JX, Gendron JM, Yang Y, Li J, Wang ZY (2002) The GSK3-like kinase BIN2 phosphorylates and destabilizes BZR1, a positive regulator of the

brassinosteroid signaling pathway in Arabidopsis. Proc Natl Acad Sci U S A 99: 10185-10190

Hedden P, Kamiya Y (1997) GIBBERELLIN BIOSYNTHESIS: Enzymes, Genes and Their Regulation. Annu Rev Plant Physiol Plant Mol Biol 48: 431-460

Heyman J, Cools T, Vandenbussche F, Heyndrickx KS, Van Leene J, Vercauteren I, Vanderauwera S, Vandepoele K, De Jaeger G, Van Der Straeten D, De Veylder L (2013) ERF115 controls root quiescent center cell division and stem cell replenishment. Science 342: 860-863

Hong SY, Lee S, Seo PJ, Yang MS, Park CM (2010) Identification and molecular characterization of a Brachypodium distachyon GIGANTEA gene: functional conservation in monocot and dicot plants. Plant Mol Biol 72: 485-497

Hong Z, Ueguchi-Tanaka M, Fujioka S, Takatsuto S, Yoshida S, Hasegawa Y, Ashikari M, Kitano H, Matsuoka M (2005) The Rice brassinosteroid-deficient dwarf2 mutant, defective in the rice homolog of Arabidopsis DIMINUTO/DWARF1, is rescued by the endogenously accumulated alternative bioactive brassinosteroid, dolichosterone. Plant Cell 17: 2243-2254

Hong Z, Ueguchi-Tanaka M, Matsuoka M (2004) Brassinosteroids and rice architecture. J Pestic Sci 29: 184-188

Hong Z, Ueguchi-Tanaka M, Shimizu-Sato S, Inukai Y, Fujioka S, Shimada Y, Takatsuto S, Agetsuma M, Yoshida S, Watanabe Y, Uozu S, Kitano H, Ashikari M, Matsuoka M (2002) Loss-of-function of a rice brassinosteroid biosynthetic enzyme, C-6 oxidase, prevents the organized arrangement and polar elongation of cells in the leaves and stem. Plant J 32: 495-508

Hong Z, Ueguchi-Tanaka M, Umemura K, Uozu S, Fujioka S, Takatsuto S, Yoshida S, Ashikari M, Kitano H, Matsuoka M (2003) A rice brassinosteroid-deficient mutant, ebisu dwarf (d2), is caused by a loss of function of a new member of cytochrome P450. Plant Cell 15: 2900-2910

Hu X, Qian Q, Xu T, Zhang Y, Dong G, Gao T, Xie Q, Xue Y (2013) The U-box E3 ubiquitin ligase TUD1 functions with a heterotrimeric G alpha subunit to regulate Brassinosteroid-mediated growth in rice. PLoS Genet 9: e1003391

Hu Y, Bao F, Li J (2000) Promotive effect of brassinosteroids on cell division involves a distinct CycD3-induction pathway in Arabidopsis. Plant J 24: 693-701

International Rice Genome Sequencing P (2005) The map-based sequence of the rice genome. Nature 436: 793-800

Inze D, De Veylder L (2006) Cell cycle regulation in plant development. Annu Rev Genet 40: 77-105

Iwahori S, Tominaga S, Higuchi S (1990) Retardation of Abscission of Citrus Leaf and Fruitlet Explants by Brassinolide. Plant Growth Regul 9: 119-125

Iwasaki T, Shibaoka H (1991) Brassinosteroids Act as Regulators of Tracheary-Element Differentiation in Isolated Zinnia Mesophyll-Cells. Plant Cell Physiol 32: 1007-1014

Je BI, Han CD (2010) Brassinosteroid homeostasis via coordinate regulation of signaling and synthetic pathways. Plant Signal Behav 5: 1440-1441

Je BI, Piao HL, Park SJ, Park SH, Kim CM, Xuan YH, Park SH, Huang J, Do Choi Y, An G, Wong HL, Fujioka S, Kim MC, Shimamoto K, Han CD (2010) RAV-Like1 maintains brassinosteroid homeostasis via the coordinated activation of BRI1 and biosynthetic genes in rice. Plant Cell 22: 1777-1791

Jeong DH, An S, Kang HG, Moon S, Han JJ, Park S, Lee HS, An K, An G (2002) T-DNA insertional mutagenesis for activation tagging in rice. Plant Physiol 130: 1636-1644

Jeong DH, An S, Park S, Kang HG, Park GG, Kim SR, Sim J, Kim YO, Kim MK, Kim SR, Kim J, Shin M, Jung M, An G (2006) Generation of a flanking sequence-tag database for activation-tagging lines in japonica rice. Plant J 45: 123-132

Jiang Y, Bao L, Jeong SY, Kim SK, Xu C, Li X, Zhang Q (2012) XIAO is involved in the control of organ size by contributing to the regulation of signaling and homeostasis of brassinosteroids and cell cycling in rice. Plant J 70: 398-408

Kang JG, Yun J, Kim DH, Chung KS, Fujioka S, Kim JI, Dae HW, Yoshida S, Takatsuto S, Song PS, Park CM (2001) Light and brassinosteroid signals are integrated via a dark-induced small G protein in etiolated seedling growth. Cell 105: 625-636

Kauschmann A, Jessop A, Koncz C, Szekeres M, Willmitzer L, Altmann T (1996) Genetic evidence for an essential role of brassinosteroids in plant development. Plant J 9: 701-713

Khan M, Rozhon W, Bigeard J, Pflieger D, Husar S, Pitzschke A, Teige M, Jonak C, Hirt H, Poppenberger B (2013) Brassinosteroid-regulated GSK3/Shaggy-like kinases phosphorylate mitogen-activated protein (MAP) kinase kinases, which control stomata development in Arabidopsis thaliana. J Biol Chem 288: 7519-7527

Kim B, Fujioka S, Kwon M, Jeon J, Choe S (2013) Arabidopsis brassinosteroid-overproducing gulliver3-D/dwarf4-D mutants exhibit altered responses to jasmonic acid and pathogen. Plant Cell Rep 32: 1139-1149

Kim B, Jeong YJ, Corvalan C, Fujioka S, Cho S, Park T, Choe S (2014) Darkness and gulliver2/phyB mutation decrease the abundance of phosphorylated BZR1 to activate brassinosteroid signaling in Arabidopsis. Plant J 77: 737-747

Kim B, Kim G, Fujioka S, Takatsuto S, Choe S (2012) Overexpression of 3beta-hydroxysteroid dehydrogenases/C-4 decarboxylases causes growth defects possibly due to abnormal auxin transport in arabidopsis. Molecules and Cells 34: 77-84

Kim B, Kwon M, Jeon J, Schulz B, Corvalán C, Jeong YJ, Choe S (2014) The Arabidopsis *gulliver2*/*phyB* Mutant Exhibits Reduced Sensitivity to Brassinazole. J Plant Biol 57: 20-27

Kim BK, Fujioka S, Takatsuto S, Tsujimoto M, Choe S (2008) Castasterone is a likely end product of brassinosteroid biosynthetic pathway in rice. Biochem Biophys Res Commun 374: 614-619

Kim HB, Kwon M, Ryu H, Fujioka S, Takatsuto S, Yoshida S, An CS, Lee I, Hwang I, Choe S (2006) The regulation of *DWARF4* expression is likely a critical mechanism in maintaining the homeostasis of bioactive brassinosteroids in Arabidopsis. Plant Physiol 140: 548-557

Kim TW, Guan S, Sun Y, Deng Z, Tang W, Shang JX, Burlingame AL, Wang ZY (2009) Brassinosteroid signal transduction from cell-surface receptor kinases to nuclear transcription factors. Nat Cell Biol 11: 1254-1260

Kim TW, Michniewicz M, Bergmann DC, Wang ZY (2012) Brassinosteroid regulates stomatal development by GSK3-mediated inhibition of a MAPK pathway. Nature 482: 419-422

Kim TW, Wang ZY (2010) Brassinosteroid signal transduction from receptor kinases to transcription factors. Annu Rev Plant Biol 61: 681-704

Kim YS, Kim TW, Kim SK (2005) Brassinosteroids are inherently biosynthesized in the primary roots of maize, Zea mays L. Phytochemistry 66: 1000-1006

Kir G, Ye H, Nelissen H, Neelakandan AK, Kusnandar AS, Luo A, Inze D, Sylvester AW, Yin Y, Becraft PW (2015) RNA Interference Knockdown of BRASSINOSTEROID INSENSITIVE1 in Maize Reveals Novel Functions for Brassinosteroid Signaling in Controlling Plant Architecture. Plant Physiol 169: 826-839

Kleber-Janke T, Becker WM (2000) Use of modified BL21(DE3) Escherichia coli cells for high-level expression of recombinant peanut allergens affected by poor codon usage. Protein Expr Purif 19: 419-424

Koh S, Lee SC, Kim MK, Koh JH, Lee S, An G, Choe S, Kim SR (2007) T-DNA tagged knockout mutation of rice OsGSK1, an orthologue of Arabidopsis BIN2, with enhanced tolerance to various abiotic stresses. Plant Mol Biol 65: 453-466

Kosugi S, Ohashi Y (2002) Interaction of the Arabidopsis E2F and DP proteins confers their concomitant nuclear translocation and transactivation. Plant Physiology 128: 833-843

Kwon M, Choe S (2005) Brassinosteroid biosynthesis and dwarf mutants. J Plant Biol 48: 1-15

Li D, Wang L, Wang M, Xu YY, Luo W, Liu YJ, Xu ZH, Li J, Chong K (2009) Engineering OsBAK1 gene as a molecular tool to improve rice architecture for high yield. Plant Biotechnol J 7: 791-806

Li H, Jiang L, Youn JH, Sun W, Cheng Z, Jin T, Ma X, Guo X, Wang J, Zhang X, Wu F, Wu C, Kim SK, Wan J (2013) A comprehensive genetic study

reveals a crucial role of CYP90D2/D2 in regulating plant architecture in rice (Oryza sativa). New Phytol 200: 1076-1088
Li J, Jin H (2007) Regulation of brassinosteroid signaling. Trends Plant Sci 12: 37-41
Li J, Nam KH (2002) Regulation of brassinosteroid signaling by a GSK3/SHAGGY-like kinase. Science 295: 1299-1301
Li J, Wen J, Lease KA, Doke JT, Tax FE, Walker JC (2002) BAK1, an Arabidopsis LRR receptor-like protein kinase, interacts with BRI1 and modulates brassinosteroid signaling. Cell 110: 213-222
Li JM, Nagpal P, Vitart V, McMorris TC, Chory J (1996) A role for brassinosteroids in light-dependent development of Arabidopsis. Science 272: 398-401
Li L, Deng XW (2005) It runs in the family: regulation of brassinosteroid signaling by the BZR1-BES1 class of transcription factors. Trends Plant Sci 10: 266-268
Li L, Yu X, Thompson A, Guo M, Yoshida S, Asami T, Chory J, Yin Y (2009) Arabidopsis MYB30 is a direct target of BES1 and cooperates with BES1 to regulate brassinosteroid-induced gene expression. Plant J 58: 275-286
Li XJ, Chen XJ, Guo X, Yin LL, Ahammed GJ, Xu CJ, Chen KS, Liu CC, Xia XJ, Shi K, Zhou J, Zhou YH, Yu JQ (2016) DWARF overexpression induces alteration in phytohormone homeostasis, development, architecture and carotenoid accumulation in tomato. Plant Biotechnol J 14: 1021-1033
Li ZH, Zlabek V, Velisek J, Grabic R, Machova J, Kolarova J, Li P, Randak T (2013) Multiple Biomarkers Responses in Juvenile Rainbow Trout, Oncorhynchus mykiss, After Acute Exposure to a Fungicide Propiconazole. Environ Toxicol 28: 119-126
Liu K, Goodman M, Muse S, Smith JS, Buckler E, Doebley J (2003) Genetic structure and diversity among maize inbred lines as inferred from DNA microsatellites. Genetics 165: 2117-2128
Liu T, Zhang J, Wang M, Wang Z, Li G, Qu L, Wang G (2007) Expression and functional analysis of ZmDWF4, an ortholog of Arabidopsis DWF4 from maize (Zea mays L.). Plant Cell Rep 26: 2091-2099
Liu TS, Zhang JP, Wang MY, Wang ZY, Li GF, Qu L, Wang GY (2007) Expression and functional analysis of ZmDWF4, an ortholog of Arabidopsis DWF4 from maize (Zea mays L.). Plant Cell Rep 26: 2091-2099
Magyar Z, Atanassova A, De Veylder L, Rombauts S, Inze D (2000) Characterization of two distinct DP-related genes from Arabidopsis thaliana. FEBS Lett 486: 79-87
Maharjan PM, Choe S (2011) High Temperature Stimulates *DWARF4* (*DWF4*) Expression to Increase Hypocotyl Elongation in Arabidopsis. J Plant Biol 54: 425-429

Maharjan PM, Schulz B, Choe S (2011) BIN2/DWF12 Antagonistically Transduces Brassinosteroid and Auxin Signals in the Roots of Arabidopsis. J Plant Biol 54: 126-134
Makarevitch I, Thompson A, Muehlbauer GJ, Springer NM (2012) Brd1 gene in maize encodes a brassinosteroid C-6 oxidase. PLoS One 7: e30798
Marcinkowska E, Wiedlocha A (2002) Steroid signal transduction activated at the cell membrane: from plants to animals. Acta Biochim Pol 49: 735-745
Min YK, Asami T, Fujioka S, Murofushi N, Yamaguchi I, Yoshida S (1999) New lead compounds for brassinosteroid biosynthesis inhibitors. Bioorg Med Chem Lett 9: 425-430
Mizutani M, Ohta D (2010) Diversification of P450 genes during land plant evolution. Annu Rev Plant Biol 61: 291-315
Mora-Garcia S, Vert G, Yin Y, Cano-Delgado A, Cheong H, Chory J (2004) Nuclear protein phosphatases with Kelch-repeat domains modulate the response to brassinosteroids in Arabidopsis. Genes Dev 18: 448-460
Morinaka Y, Sakamoto T, Inukai Y, Agetsuma M, Kitano H, Ashikari M, Matsuoka M (2006) Morphological alteration caused by brassinosteroid insensitivity increases the biomass and grain production of rice. Plant Physiol 141: 924-931
Murchie EH, Chen Y, Hubbart S, Peng S, Horton P (1999) Interactions between senescence and leaf orientation determine in situ patterns of photosynthesis and photoinhibition in field-grown rice. Plant Physiol 119: 553-564
Nakagawa H, Tanaka A, Tanabata T, Ohtake M, Fujioka S, Nakamura H, Ichikawa H, Mori M (2012) Short grain1 decreases organ elongation and brassinosteroid response in rice. Plant Physiol 158: 1208-1219
Nakamura A, Fujioka S, Sunohara H, Kamiya N, Hong Z, Inukai Y, Miura K, Takatsuto S, Yoshida S, Ueguchi-Tanaka M, Hasegawa Y, Kitano H, Matsuoka M (2006) The role of OsBRI1 and its homologous genes, OsBRL1 and OsBRL3, in rice. Plant Physiol 140: 580-590
Nakaya M, Tsukaya H, Murakami N, Kato M (2002) Brassinosteroids control the proliferation of leaf cells of Arabidopsis thaliana. Plant Cell Physiol 43: 239-244
Neff MM, Nguyen SM, Malancharuvil EJ, Fujioka S, Noguchi T, Seto H, Tsubuki M, Honda T, Takatsuto S, Yoshida S, Chory J (1999) BAS1: A gene regulating brassinosteroid levels and light responsiveness in Arabidopsis. Proc Natl Acad Sci U S A 96: 15316-15323
Noguchi T, Fujioka S, Takatsuto S, Sakurai A, Yoshida S, Li J, Chory J (1999) Arabidopsis det2 is defective in the conversion of (24R)-24-methylcholest-4-En-3-one to (24R)-24-methyl-5alpha-cholestan-3-one in brassinosteroid biosynthesis. Plant Physiol 120: 833-840
Oh E, Zhu JY, Wang ZY (2012) Interaction between BZR1 and PIF4 integrates brassinosteroid and environmental responses. Nat Cell Biol 14: 802-809

Oki K, Inaba N, Kitagawa K, Fujioka S, Kitano H, Fujisawa Y, Kato H, Iwasaki Y (2009) Function of the alpha subunit of rice heterotrimeric G protein in brassinosteroid signaling. Plant Cell Physiol 50: 161-172

Orlova I, Nagegowda DA, Kish CM, Gutensohn M, Maeda H, Varbanova M, Fridman E, Yamaguchi S, Hanada A, Kamiya Y, Krichevsky A, Citovsky V, Pichersky E, Dudareva N (2009) The small subunit of snapdragon geranyl diphosphate synthase modifies the chain length specificity of tobacco geranylgeranyl diphosphate synthase in planta. Plant Cell 21: 4002-4017

Peng P, Yan Z, Zhu Y, Li J (2008) Regulation of the Arabidopsis GSK3-like Kinase BRASSINOSTEROID-INSENSITIVE 2 through Proteasome-Mediated Protein Degradation. Mol Plant 1: 338-346

Rademacher W (2000) GROWTH RETARDANTS: Effects on Gibberellin Biosynthesis and Other Metabolic Pathways. Annu Rev Plant Physiol Plant Mol Biol 51: 501-531

Raikhel N, Pirrung M (2005) Adding precision tools to the plant biologists' toolbox with chemical genomics. Plant Physiol 138: 563-564

Ramirez-Parra E, Gutierrez C (2000) Characterization of wheat DP, a heterodimerization partner of the plant E2F transcription factor which stimulates E2F-DNA binding. FEBS Lett 486: 73-78

Ramirez-Parra E, Lopez-Matas MA, Frundt C, Gutierrez C (2004) Role of an atypical E2F transcription factor in the control of Arabidopsis cell growth and differentiation. Plant Cell 16: 2350-2363

Ryu H, Kim K, Cho H, Park J, Choe S, Hwang I (2007) Nucleocytoplasmic shuttling of BZR1mediated by phosphorylation is essential in Arabidopsis brassinosteroid signaling. Plant Cell 17: 2749-2762

Sahni S, Prasad BD, Liu Q, Grbic V, Sharpe A, Singh SP, Krishna P (2016) Overexpression of the brassinosteroid biosynthetic gene DWF4 in Brassica napus simultaneously increases seed yield and stress tolerance. Sci Rep 6: 28298

Sakamoto T (2006) Phytohormones and rice crop yield: strategies and opportunities for genetic improvement. Transgenic Res 15: 399-404

Sakamoto T, Morinaka Y, Ohnishi T, Sunohara H, Fujioka S, Ueguchi-Tanaka M, Mizutani M, Sakata K, Takatsuto S, Yoshida S, Tanaka H, Kitano H, Matsuoka M (2006) Erect leaves caused by brassinosteroid deficiency increase biomass production and grain yield in rice. Nat Biotechnol 24: 105-109

Sala C, Sala F (1985) Effect of brassinosteroid on cell division and enlargement in cultured carrot (Daucus carota L.) cells. Plant Cell Rep 4: 144-147

Schenk PM, Baumann S, Mattes R, Steinbiss HH (1995) Improved high-level expression system for eukaryotic genes in Escherichia coli using T7 RNA polymerase and rare ArgtRNAs. Biotechniques 19: 196-198, 200

Schnabel G, Dait Q, Paradkar MR (2003) Cloning and expression analysis of the ATP-binding cassette transporter gene MFABC1 and the alternative

oxidase gene MfAOX1 from Monilinia fructicola. Pest Manag Sci 59: 1143-1151
Scofield S, Jones A, Murray JA (2014) The plant cell cycle in context. J Exp Bot 65: 2557-2562
Sekimata K, Han SY, Yoneyama K, Takeuchi Y, Yoshida S, Asami T (2002) A specific and potent inhibitor of brassinosteroid biosynthesis possessing a dioxolane ring. J Agric Food Chem 50: 3486-3490
Sekimata K, Kimura T, Kaneko I, Nakano T, Yoneyama K, Takeuchi Y, Yoshida S, Asami T (2001) A specific brassinosteroid biosynthesis inhibitor, Brz2001: evaluation of its effects on Arabidopsis, cress, tobacco, and rice. Planta 213: 716-721
Sekine M, Ito M, Uemukai K, Maeda Y, Nakagami H, Shinmyo A (1999) Isolation and characterization of the E2F-like gene in plants. FEBS Lett 460: 117-122
Singh AP, Savaldi-Goldstein S (2015) Growth control: brassinosteroid activity gets context. J Exp Bot 66: 1123-1132
Song L, Zhou XY, Li L, Xue LJ, Yang X, Xue HW (2009) Genome-wide analysis revealed the complex regulatory network of brassinosteroid effects in photomorphogenesis. Mol Plant 2: 755-772
Steber CM, McCourt P (2001) A role for brassinosteroids in germination in Arabidopsis. Plant Physiol 125: 763-769
Sun S, Chen D, Li X, Qiao S, Shi C, Li C, Shen H, Wang X (2015) Brassinosteroid signaling regulates leaf erectness in Oryza sativa via the control of a specific U-type cyclin and cell proliferation. Dev Cell 34: 220-228
Sun Y, Fan XY, Cao DM, Tang W, He K, Zhu JY, He JX, Bai MY, Zhu S, Oh E, Patil S, Kim TW, Ji H, Wong WH, Rhee SY, Wang ZY (2010) Integration of brassinosteroid signal transduction with the transcription network for plant growth regulation in Arabidopsis. Dev Cell 19: 765-777
Symons GM, Ross JJ, Jager CE, Reid JB (2008) Brassinosteroid transport. J Exp Bot 59: 17-24
Szekeres M, Nemeth K, Koncz-Kalman Z, Mathur J, Kauschmann A, Altmann T, Redei GP, Nagy F, Schell J, Koncz C (1996) Brassinosteroids rescue the deficiency of CYP90, a cytochrome P450, controlling cell elongation and de-etiolation in Arabidopsis. Cell 85: 171-182
Tanabe S, Ashikari M, Fujioka S, Takatsuto S, Yoshida S, Yano M, Yoshimura A, Kitano H, Matsuoka M, Fujisawa Y, Kato H, Iwasaki Y (2005) A novel cytochrome P450 is implicated in brassinosteroid biosynthesis via the characterization of a rice dwarf mutant, dwarf11, with reduced seed length. Plant Cell 17: 776-790
Tanaka A, Nakagawa H, Tomita C, Shimatani Z, Ohtake M, Nomura T, Jiang CJ, Dubouzet JG, Kikuchi S, Sekimoto H, Yokota T, Asami T, Kamakura T, Mori M (2009) BRASSINOSTEROID UPREGULATED1, encoding a helix-loop-helix protein, is a novel gene involved in brassinosteroid

signaling and controls bending of the lamina joint in rice. Plant Physiol 151: 669-680
Tang W, Yuan M, Wang R, Yang Y, Wang C, Oses-Prieto JA, Kim TW, Zhou HW, Deng Z, Gampala SS, Gendron JM, Jonassen EM, Lillo C, DeLong A, Burlingame AL, Sun Y, Wang ZY (2011) PP2A activates brassinosteroid-responsive gene expression and plant growth by dephosphorylating BZR1. Nat Cell Biol 13: 124-131
Tao YZ, Zheng J, Xu ZM, Zhang XH, Zhang K, Wang GY (2004) Functional analysis of ZmDWF1, a maize homolog of the Arabidopsis brassinosteroids biosynthetic DWF1/DIM gene. Plant Science 167: 743-751
Thole V, Peraldi A, Worland B, Nicholson P, Doonan JH, Vain P (2012) T-DNA mutagenesis in Brachypodium distachyon. J Exp Bot 63: 567-576
Thorstensen CW, Lode O (2001) Laboratory degradation studies of bentazone, dichlorprop, MCPA, and propiconazole in Norwegian soils. J Environ Qual 30: 947-953
Tong H, Chu C (2012) Brassinosteroid signaling and application in rice. J Genet Genomics 39: 3-9
Tong H, Jin Y, Liu W, Li F, Fang J, Yin Y, Qian Q, Zhu L, Chu C (2009) DWARF AND LOW-TILLERING, a new member of the GRAS family, plays positive roles in brassinosteroid signaling in rice. Plant J 58: 803-816
Tong H, Liu L, Jin Y, Du L, Yin Y, Qian Q, Zhu L, Chu C (2012) DWARF AND LOW-TILLERING acts as a direct downstream target of a GSK3/SHAGGY-like kinase to mediate brassinosteroid responses in rice. Plant Cell 24: 2562-2577
Vandepoele K, Vlieghe K, Florquin K, Hennig L, Beemster GTS, Gruissem W, Van De Peer Y, Inze D, De Veylder L (2005) Genome-wide identification of potential plant E2F target genes. Plant Physiology 139: 316-328
Verrier PJ, Bird D, Burla B, Dassa E, Forestier C, Geisler M, Klein M, Kolukisaoglu U, Lee Y, Martinoia E, Murphy A, Rea PA, Samuels L, Schulz B, Spalding EJ, Yazaki K, Theodoulou FL (2008) Plant ABC proteins--a unified nomenclature and updated inventory. Trends Plant Sci 13: 151-159
Vert G, Nemhauser J, Geldner N, Hong F, Chory J (2005) Molecular mechanisms of steroid hormone signaling in plants. Annu Rev Cell Dev Biol 21: 177-201
Vilarrasa-Blasi J, Gonzalez-Garcia MP, Frigola D, Fabregas N, Alexiou KG, Lopez-Bigas N, Rivas S, Jauneau A, Lohmann JU, Benfey PN, Ibanes M, Cano-Delgado AI (2014) Regulation of plant stem cell quiescence by a brassinosteroid signaling module. Dev Cell 30: 36-47
Wada K, Marumo S, Abe H, Morishita T, Nakamura K, Uchiyama M, Mori K (1984) A Rice Lamina Inclination Test - a Micro-Quantitative Bioassay for Brassinosteroids. Agric Biol Chem 48: 719-726

Wada K, Marumo S, Ikekawa N, Morisaki M, Mori K (1981) Brassinolide and Homobrassinolide Promotion of Lamina Inclination of Rice Seedlings. Plant Cell Physiol 22: 323-325

Wan S, Wu J, Zhang Z, Sun X, Lv Y, Gao C, Ning Y, Ma J, Guo Y, Zhang Q, Zheng X, Zhang C, Ma Z, Lu T (2009) Activation tagging, an efficient tool for functional analysis of the rice genome. Plant Mol Biol 69: 69-80

Wang L, Xu YY, Ma QB, Li D, Xu ZH, Chong K (2006) Heterotrimeric G protein alpha subunit is involved in rice brassinosteroid response. Cell Res 16: 916-922

Wang X, Chory J (2006) Brassinosteroids regulate dissociation of BKI1, a negative regulator of BRI1 signaling, from the plasma membrane. Science 313: 1118-1122

Wang X, Kota U, He K, Blackburn K, Li J, Goshe MB, Huber SC, Clouse SD (2008) Sequential transphosphorylation of the BRI1/BAK1 receptor kinase complex impacts early events in brassinosteroid signaling. Dev Cell 15: 220-235

Wang ZY, Nakano T, Gendron J, He J, Chen M, Vafeados D, Yang Y, Fujioka S, Yoshida S, Asami T, Chory J (2002) Nuclear-localized BZR1 mediates brassinosteroid-induced growth and feedback suppression of brassinosteroid biosynthesis. Dev Cell 2: 505-513

Wei L, Gu L, Song X, Cui X, Lu Z, Zhou M, Wang L, Hu F, Zhai J, Meyers BC, Cao X (2014) Dicer-like 3 produces transposable element-associated 24-nt siRNAs that control agricultural traits in rice. Proc Natl Acad Sci U S A 111: 3877-3882

Wiggins TE, Baldwin BC (1984) Binding of Azole Fungicides Related to Diclobutrazol to Cytochrome-P-450. Pestic Sci 15: 206-209

Wu CY, Trieu A, Radhakrishnan P, Kwok SF, Harris S, Zhang K, Wang J, Wan J, Zhai H, Takatsuto S, Matsumoto S, Fujioka S, Feldmann KA, Pennell RI (2008) Brassinosteroids regulate grain filling in rice. Plant Cell 20: 2130-2145

Xu Y, Zhang X, Li Q, Cheng Z, Lou H, Ge L, An H (2015) BdBRD1, a brassinosteroid C-6 oxidase homolog in Brachypodium distachyon L., is required for multiple organ development. Plant Physiol Biochem 86: 91-99

Xu YL, Gage DA, Zeevaart JA (1997) Gibberellins and stem growth in Arabidopsis thaliana. Effects of photoperiod on expression of the GA4 and GA5 loci. Plant Physiol 114: 1471-1476

Xu YL, Li L, Gage DA, Zeevaart JA (1999) Feedback regulation of GA5 expression and metabolic engineering of gibberellin levels in Arabidopsis. Plant Cell 11: 927-936

Yamamoto R, Demura T, Fukuda H (1997) Brassinosteroids induce entry into the final stage of tracheary element differentiation in cultured Zinnia cells. Plant Cell Physiol 38: 980-983

Yamamuro C, Ihara Y, Wu X, Noguchi T, Fujioka S, Takatsuto S, Ashikari M, Kitano H, Matsuoka M (2000) Loss of function of a rice brassinosteroid

insensitive1 homolog prevents internode elongation and bending of the lamina joint. Plant Cell 12: 1591-1606
Yang C-J, Zhang C, Lu Y-N, Jin J-Q, Wang X-L (2011) The Mechanisms of Brassinosteroids' Action: From Signal Transduction to Plant Development. Molecular Plant 4: 588-600
Yang XC, Hwa CM (2008) Genetic modification of plant architecture and variety improvement in rice. Heredity (Edinb) 101: 396-404
Yang Y, Dai L, Xia H, Zhu K, Liu H, Chen K (2013) Protein profile of rice (Oryza sativa) seeds. Genet Mol Biol 36: 87-92
Yin Y, Vafeados D, Tao Y, Yoshida S, Asami T, Chory J (2005) A new class of transcription factors mediates brassinosteroid-regulated gene expression in Arabidopsis. Cell 120: 249-259
Yin Y, Wang ZY, Mora-Garcia S, Li J, Yoshida S, Asami T, Chory J (2002) BES1 accumulates in the nucleus in response to brassinosteroids to regulate gene expression and promote stem elongation. Cell 109: 181-191
Yoshida Y, Aoyama Y (1991) Sterol 14-Alpha-Demethylase and Its Inhibition - Structural Considerations on Interaction of Azole Antifungal Agents with Ianosterol 14-Alpha-Demethylase (P-450[14dm]) of Yeast. Biochem Soc Trans 19: 778-782
Yoshizumi T, Nagata N, Shimada H, Matsui M (1999) An Arabidopsis cell cycle -dependent kinase-related gene, CDC2b, plays a role in regulating seedling growth in darkness. Plant Cell 11: 1883-1896
Yu X, Li L, Guo M, Chory J, Yin Y (2008) Modulation of brassinosteroid-regulated gene expression by Jumonji domain-containing proteins ELF6 and REF6 in Arabidopsis. Proc Natl Acad Sci U S A 105: 7618-7623
Yu X, Li L, Zola J, Aluru M, Ye H, Foudree A, Guo H, Anderson S, Aluru S, Liu P, Rodermel S, Yin Y (2011) A brassinosteroid transcriptional network revealed by genome-wide identification of BESI target genes in Arabidopsis thaliana. Plant J 65: 634-646
Zhang C, Bai MY, Chong K (2014) Brassinosteroid-mediated regulation of agronomic traits in rice. Plant Cell Rep 33: 683-696
Zhang C, Xu Y, Guo S, Zhu J, Huan Q, Liu H, Wang L, Luo G, Wang X, Chong K (2012) Dynamics of brassinosteroid response modulated by negative regulator LIC in rice. PLoS Genet 8: e1002686
Zhang G, Song X, Guo H, Wu Y, Chen X, Fang R (2016) A Small G Protein as a Novel Component of the Rice Brassinosteroid Signal Transduction. Mol Plant 9: 1260-1271
Zhang LY, Bai MY, Wu J, Zhu JY, Wang H, Zhang Z, Wang W, Sun Y, Zhao J, Sun X, Yang H, Xu Y, Kim SH, Fujioka S, Lin WH, Chong K, Lu T, Wang ZY (2009) Antagonistic HLH/bHLH Transcription Factors Mediate Brassinosteroid Regulation of Cell Elongation and Plant Development in Rice and Arabidopsis. Plant Cell 21: 3767-3780
Zhang YC, Yu Y, Wang CY, Li ZY, Liu Q, Xu J, Liao JY, Wang XJ, Qu LH, Chen F, Xin P, Yan C, Chu J, Li HQ, Chen YQ (2013) Overexpression of

microRNA OsmiR397 improves rice yield by increasing grain size and promoting panicle branching. Nat Biotechnol 31: 848-852

Zhao J, Peng P, Schmitz RJ, Decker AD, Tax FE, Li J (2002) Two putative BIN2 substrates are nuclear components of brassinosteroid signaling. Plant Physiol 130: 1221-1229

Zhao J, Wu C, Yuan S, Yin L, Sun W, Zhao Q, Zhao B, Li X (2013) Kinase activity of OsBRI1 is essential for brassinosteroids to regulate rice growth and development. Plant Sci 199-200: 113-120

Zhiponova MK, Vanhoutte I, Boudolf V, Betti C, Dhondt S, Coppens F, Mylle E, Maes S, Gonzalez-Garcia MP, Cano-Delgado AI, Inze D, Beemster GTS, De Veylder L, Russinova E (2013) Brassinosteroid production and signaling differentially control cell division and expansion in the leaf. New Phytol 197: 490-502

Zimmermann P, Hirsch-Hoffmann M, Hennig L, Gruissem W (2004) GENEVESTIGATOR. Arabidopsis microarray database and analysis toolbox. Plant Physiol 136: 2621-2632

ABSTRACT IN KOREAN

브라시노스테로이드 (Brassinosteroids; BRs)는 식물구조형성과 작물생산에 중요한 역할을 하는 식물생장촉진 호르몬으로 농업적으로 큰 관심을 받고있는 호르몬이다. BR 의 정확한 구성요소와 기작은 주로 쌍자엽 식물인 애기장대 (*Arabidopsis thaliana*)를 모델로 사용하여 주요 기능들이 밝혀졌지만, 정작 이 호르몬이 단자엽 식물과 쌍자엽 식물에서 차이점을 가진다는 흥미로운 연구 결과는 벼 (*Oryza sativa*)와 같은 단자엽 식물의 연구가 증가함에 따라 알려졌다. 이러한 사실은 새로은 유전자원들의 발굴 및 연구방법들의 발달에 기초하여 단자엽 식물에서의 BR 에 대한 연구가 본격적으로 시작되었다.

본 연구는 벼 또는 식용장물과 같은 농업경제에 중요한 식물을 통해 아직 알려지지 않은 단자엽에서의 BR 의 기작을 밝히려 연구를 시작하였다. 우선 본 연구를 위해 사용한 BR 억제제인 프로피코나졸 (Propiconazole; Pcz)이 단자엽 식물이 재배되는 필드에서 활용가는하물 보였다. 우선 옥수수, 벼, 브라키포디움과 같은 단자엽 식물에 Pcz 처리를 하였을 때 BR 결핍 돌연변이와 같은 표현형을 관찰하여 Pcz 의 사용이 유효함을 확인하였다. Pcz, 유전체적 그리고 유전학적 도구를 사용하여 잔디의 모델식물인 *Brachypodium distachyon* 의 BR 에 대한 반응을 규명하였고, BR 신호 (*BIN2*) 및 BR 생합성 (*DWF4*, *CPD* 및 *BR6OX2*)경로로부터 몇몇

상동유전자를 발견하였다. 또한, Pcz 를 사용하여 BR 반응에서의 새로운 요소를 발굴하기 위해 벼에서 T-DNA 돌연변이 개체군을 선별하였다. 선별된 돌연별이 개체들과 야생형을 비교했을 때 BR 에 대한 민감도 증가와 곡물 수확량 증가와 같은 다양한 BR 관련 표현형을 나타내는 *Pcz 내성 1* (*pzr1-D*)종을 발견하여 분석하였다. 돌연변이에 의해 영향을 받는 유전자는 E2F 와 이합체화하여 세포분열에 관여하는 단백질의 전사를 조절하는 전사인자로서 애기장대 DPb 에 대한 벼의 병렬상동 유전자 임이 밝혀졌다. T-DNA 활성 표지에 의한 *PZR1* 전사체 수준의 발현 증가는 *PZR1* 과발현 돌연변이체들의 분얼, 이삭 그리고 이삭가지의 개수를 증가시켰으며, 결과적으로 야생형 보다 많은 곡물 생산가능성을 보였다. 한편, 전체 전사체 분석결과와 돌연변이체 표현형 분석 결과는 세포주기와 BR 신호가 PZR1 을 통해 상호연관되어 있다는 증거를 제시하였다. 마지막으로 본 연구는 BR 관련 경로의 연구를 위한 또 다른 도구로서, 핵심 전사인자이며 BR 신호 조절의 양성 조절자인 BZR1 에 특이적인 항체인 anti BZR1 을 개발하고 시범사용을 수행하였다. Anti-BZR1 항체는 애기장대, 벼, 강아지풀 및 수수에서의 BZR1 병렬상동 단백질의 BZR1 의 활성 탈인산화 및 비활성 인산화 형태를 감지 할 수 있었으며, 이 항체는 BZR1 관련 기작, 특히 단백질간 상호작용 및 식물 신호전달 경로간의 상호간섭에 대한 기작을 규명하는데 유용한 단백실 마커로 활용 가능함을 체시하였다.

주요어: 브라시노스테로이드, 단자엽 식물, 식물구조형성, 작물생산, 세포주기

학번: 2010-24008